Teknik Dergi
Technical Journal

TEKNİK DERGİ PUBLICATION PRINCIPLES

Teknik Dergi is a scientific and technical journal indexed by the Science Citation Index Expanded. Annually six issues are published, three in Turkish in the months of January, May and September, three in English in March, July and November. Its main principles of publication are summarized below:

1. Articles reporting original scientific research and those reflecting interesting engineering applications are accepted for publication. To be classified as original, the work should either produce new scientific knowledge or add a genuinely new dimension to the existing knowledge or develop a totally new method or substantially improve an existing method.

2. Articles reporting preliminary results of scientific studies and those which do not qualify as full articles but provide useful information for the reader can be considered for publication as technical notes.

3. Discussions received from the readers of the published articles within three months from publication are reviewed by the Editorial Board and then published together with the closing remarks of the author.

4. Manuscripts submitted for publication are evaluated by two or three reviewers unknown to the authors. In the light of their reports, final decision to accept or decline is taken by the Editorial Board. General policy of the Board is to get the insufficient manuscripts improved in line with the reviewers' proposals. Articles that fail to reach the desired level are declined. Reasons behind decisions are not declared.

5. A signed statement is taken from the authors, declaring that the article has not been published as a "journal article or book chapter". In case the Editorial Board is in the opinion that the article has already been published elsewhere with minor changes or suspects plagiarism or a similar violation of ethics, then not only that article, but none of the articles of the same authors are published.

6. Papers reporting works presented as conference papers and developed further may be considered for publication. The conference it was presented to is given as a footnote in the first page.

7. Additionally, a document signed by all authors, transferring the copyright to UCTEA Chamber of Civil Engineers is submitted together with the manuscript.

Teknik Dergi
Technical Journal

Reviewers:

This list is renewed each year and includes reviewers who served in the last two years of publication.

UCTEA Turkish Chamber of Civil Engineers

Teknik Dergi

Volume: 33   Issue: 2   March 2022

CONTENTS

OBITUARY – Prof. Dr. M. SÜHEYL AKMAN

It is with sorrow that we announce the passing of our dear friend and colleague Prof. Dr. M. Süheyl Akman on February 6, 2022.

Prof. Akman served in the Editorial Board of Teknik Dergi for nearly twenty years and took place in the Teknik Dergi Advisory Board established in 2021. Furthermore, he served as a reviewer for a countless number of manuscripts considered for publication.

Prof. Akman was born on March 15, 1930 in İstanbul. After completing his background education in Galatasaray Lycée, he studied civil engineering in İstanbul Technical University and graduated in 1955. Following a period of engineering practice at the Ministry of Development and Housing, he joined İstanbul Technical University in 1961 as an assistant in the Chair of Materials of Construction. During his academic career in this chair, he received his PhD in 1967, became associate professor in 1972 and full professor in 1979 and was retired in 1997. In the meantime, he carried out post-doctoral research at EPFL, the Swiss Federal Institute of Technology in Lausanne (1968-70). During his long term membership of RILEM, The International Union of Laboratories and Experts in Construction Materials, Systems and Structures, he participated in the activities of three technical committees and was presented a "Recognition" appreciating his contributions (1979-97).

Prof. Akman authored ten books/lecture notes in the areas of materials of construction, testing techniques and repair & strengthening besides numerous technical papers he published.

Besides teaching, Prof. Akman assumed responsibility in a variety of administrative and organisational activities. He served as a member of the Construction Technology Research Group of TUBİTAK (1994-2002); as the Scientific Committee Chair for numerous National Concrete Congresses organised by the Turkish Chamber of Civil Engineers (1989-2007); as a Civil Engineering Faculty Executive Board member, İstanbul Technical University (1972-79); as an Editorial Board member, İstanbul Technical University Journal (1981-93).

Prof. Akman was a very fine gentleman reflecting traditional İstanbul manners. He used to draw the attention by his politeness and elegance. His reliable and industrious character and his refined sense of humour made collaboration with him both productive and enjoyable. In his paper reviews, he was patient, meticulous and above all very constructive; he almost never rejected a paper without giving the author a chance to improve the manuscript; he acted as a dissertation supervisor rather than a critical reviewer.

The Editorial Board acknowledge the invaluable contributions of Prof. Dr. M. Süheyl Akman to IMO Teknik Dergi and wish to extend their sincerest condolences to his family.

Prof. Tuğrul Tankut
On behalf of the Editorial Board

A Calibration Technique for Bi-axial Shake Tables with Stepper Motor

Erdem DAMCI[1]
Çağla ŞEKERCI[2]
Yener TAŞKIN[3]
Koray GÜRKAN[4]

ABSTRACT

Shaking tables are frequently used to determine the dynamic behavior of structures in the laboratory environment. In order to obtain realistic results in experimental studies, table response and performance should be consistent with the desired motion. In this multidisciplinary study, an application of a new method for determining and calibrating the mechanical response of a developed bi-axial displacement controlled shake table according to the desired motion data is presented. The bi-axial shake table's electro-mechanical components consist of stepper motors, ball screw sets, linear ball bearings, and linear potentiometers positioned on both axes for displacement measurements. For the control and data acquisition (DAQ) unit of the shake table, an open-source electronic prototyping platform Arduino was used. From several experimental results, it was seen that, with the presented calibration method, harmonic and earthquake simulations could be achieved with a relative root mean square error (relative RMS error) of less than 5% for desired displacement-time histories.

Keywords: Shaking table, calibration, Arduino, stepper motor, ball screw set, linear ball bearing, linear potentiometer.

---

1 Istanbul University - Cerrahpasa, Department of Civil Engineering, Istanbul, Turkey
  edamci@iuc.edu.tr - https://orcid.org/0000-0003-2295-1686

2 Dogus University, Department of Civil Engineering, Istanbul, Turkey
  csekerci@dogus.edu.tr - https://orcid.org/0000-0001-7070-1804

3 Istanbul University - Cerrahpasa, Department of Mechanical Engineering, Istanbul, Turkey
  ytaskin@iuc.edu.tr - https://orcid.org/0000-0003-1923-2672

4 Istanbul University - Cerrahpasa, Department of Electrical & Electronics Engineering, Istanbul, Turkey
  kgurkan@iuc.edu.tr - https://orcid.org/0000-0003-2283-8173

1. INTRODUCTION

In the field of civil engineering, the dynamic effects such as earthquakes on buildings are among the foremost research topics. The number of laboratories capable of conducting experiments by simulating earthquake records on real structures is limited worldwide and it requires high investment budgets to examine the effects of earthquakes on structures. However, shake tables are widely used to investigate dynamic behaviors through smaller scale models and smaller loading areas. On such shaking tables using scaled structure models, records from earthquakes or synthetically produced earthquake signals can be simulated as 1/1 or scaled, and many academic studies examining the effects of these earthquakes on buildings exist in the literature [1, 2]. However, shaking tables are often used to verify or compare numerical analyses on complex or simplified structures under harmonic loading and earthquake loading. The accuracy of the table performance and the monitoring system is also essential, in addition to the fact that the model to be placed on the shake table should be compatible with the numerical analysis model. Therefore, in experimental studies, the table response and the target motion should be in harmony to ensure that the results are as close to reality as possible. For this purpose, before the experimental studies on the structural model, the demand-response relationship should be determined, and the calibration of the shake table to be used should be checked or performed if required.

In this context, there are many studies in the literature aimed at improving table performance. Kuehn et al. [3] developed a computer-based control system to improve the data acquisition characteristics of a small shaking table and showed that the data obtained by monitoring the system and the desired seismic motion were the same. Nakata [4], on the other hand, mentioned a monitoring system that would provide acceleration control and system stability by using a feedback system and confirmed its reproducibility with experiments on a single axis shaking table. Luco et al. [5] studied the performance of the acceleration tracking of a uniaxial shaking table and proposed improvements to the instrument by performing harmonic scanning for different amplitudes and frequencies. Yang et al. [6], in their study on the acceleration, velocity, and displacement control of a high-performance shaking table to investigate nonlinear behavior in the system. In addition to the studies on increasing the performance of the table and monitoring system, there are also studies examining small scale models placed on shaking tables. Saranik et al. [7] examined non-elastic behavior and changes in modal parameters of a two-layer steel frame with bolted joints under dynamic effects and compared them with numerical analysis results. Zhang et al. [8] compared the numerical of a shear frame by performing a shaking table and real-time hybrid simulation. Altunışık et al. [9] determined the dynamic characteristics and dynamic behavior of the shaking table experiments by forming a model containing a calibrated liquid column damper. Alemdar [10] compared the deformation results obtained by both shaking table experiments and finite element analyses under bi-axial earthquake loads of reinforced concrete bridge columns and examined the plastic deformations. Ashasi-Sorkhabi et al. [11] investigated the accuracy of a Quanser shake table with real-time hybrid simulation using the response from a spring-mass oscillator and tuned liquid damper system. Najafi and Spencer [12] developed the modified model-based controllers' method in their studies, and with this method, they investigated the accuracy of a single-axis Quanser shake table and determined the error rates with different methods and compared the methods. Damcı and Şekerci [13] developed a single axis, 500x500 mm^2 shake table controlled by Arduino microcontroller platforms and

driven by a stepper motor. The control algorithm, calibration method, and performance investigation of the shake table were given in detail.

In this study, an application of the calibration method given by Damcı and Şekerci [13] is introduced for the new bi-axial shake table SARSAR (Figure 1), which is placed in Structures and Mechanics Laboratory at Istanbul University-Cerrahpasa in Buyukcekmece campus, is presented. There are considerable differences compared to the previous study [13]. This study is a further application of the method for a larger bi-axial shake table with higher payloads up to 600 kg. The main contribution is to apply and validate the calibration method to a bi-axial shake table which is an open-loop displacement controlled earthquake and harmonic motion simulator, developed within the scope of a TUBITAK project. Apart from the number of axes used in both shake tables, the dimensions and capacities are also different from each other. Operational payload and bandwidth have in particular been improved in the present study. It was shown that the method could be used for larger shake tables with different electro-mechanical configurations. Numerous experimental investigations are carried out for the calibration process and its validation with the help of relative root mean square error (relative RMS error) calculations and newly-added synchronization subspace plots (SSP) to find the shake table's frequency response and earthquake simulation performance. Also, comparisons of desired and achieved frequency contents and acceleration response spectra are given for the demonstration of earthquake performance. From an engineering perspective in civil engineering, it was shown that the shake table's performance is at the desired level with a relative RMS error of about 5%.

2. MATERIALS ANS METHODS

2.1. Specifications of Developed Shaking Table

In the developed bi-axial shaking table, the ability to move along each axis is obtained by forming two planes arranged on top of each other such that each axis forms a plane. The lower plane *x*, upper plane constitutes the movement in the *y*-axis shown in Figure 1. The top plane with a loading area has a dimension of 1000 mm x1000 mm and moves in the *y*-axis. The center plate on which this plane sits is 1000 mm x1100 mm and provides movement in the *x*-axis. The table dimensions that consist of the fixed bottom plane are 1000 mm x1300 mm. Both axes have a displacement capability of ±150 mm. A total of 4 limit switches are installed to ensure the table's safety against the possibility of exceeding the maximum displacement limits in the *x* and *y* directions. The table movement is automatically stopped when any limit switch is opened. Linear motion on both axes is provided by actuators consisting of a stepper motor with a capacity of 12 N.m and a 2020 precision ball screw with a pitch of 20 mm. The 2-phase hybrid stepper motors, which complete one turn in 200 steps, are controlled by digital drivers that can provide continuous high current. The digital drivers are set to 400 steps/revolution to increase motion resolution. Therefore, the motion resolution of the shake table on each axis corresponds to Δs= 20/400= 0.05 mm. The general view of the table is given in Figure 1. The technical specifications of the shake table developed within the scope of this and preceding [13] studies are summarized in Table 1.

Figure 1 - Bi-axial shake table SARSAR

Table 1 - Technical specifications of the shake tables for present and previous [13] studies

	Present Study	Previous Study [13]
Parameter	Value	Value
Degrees of freedom	Two	One
Moving top plate dimensions (*y*-axis)	1000x1000 mm^2	500x500 mm^2
Operational payload	500 kg	200 kg
Maximum motor torque	12 N.m	8.5 N.m
Stroke	±150 mm	±75 mm
Motion resolution	50 μm/step	25 μm/step
Peak velocity	700 mm/s	350 mm/s
Peak acceleration (bare table)	1.35g @ ±1 mm in *x*-axis 1.95g @ ±1 mm in *y*-axis	1.5g @ ±1 mm
Peak acceleration (600 kg payload)	0.28g @ ±1 mm in *x*-axis 0.30g @ ±1 mm in *y*-axis	-
Operational bandwidth	30 Hz	17 Hz
Self-weight	350 kg	50 kg

The control and data acquisition unit of the shake table consists of commercialoff-the-shelf Arduino development boards. The motion signal to be sent to the stepper motor drivers is realized using two Arduino DUE boards. Each board uses a 32-bit ARM-Cortex processor with a clock speed of 84 MHz and 512 KB flash memory. An Arduino MEGA development board is also used to measure the response of the table to the sent motion signal. It is a development board with an 8-bit ATMEGA256 flash microcontroller running at 16 MHz with a 256 KB flash memory. The displacement of the table on both axes is measured using two linear potentiometers with a 350 mm stroke, which were placed between the moving plates of the table. Analog signals of the potentiometers digitized by Arduino MEGA's analog-to-digital-converter (ADC) with 10-bit resolution and converted to the corresponding displacement.

2.2. Method for Calibrating the Shaking Table

Bi-axial harmonic motion and strong ground motion can be simulated with the shaking table. In order to obtain the correct response of the scaled model placed on the table, the simulated motion must be performed with minimum error. For this purpose, in harmonic motion, frequency scanning was performed for different amplitudes, and the desired amplitude and frequencies were compared with the measured amplitude and frequencies. The dominant frequency was determined by calculating the power spectrum of the measured displacement signal, and the shake table was calibrated via the difference between the desired frequencies. The difference between these frequencies, representing the total delay for a single cycle, can be obtained by Eq. (1). The latency corresponds to a single step for the desired motion and is calculated by dividing the number of steps required for a period of harmonic motion using this obtained delay. Where f_d represents the desired (demand) frequency, f_a is the achieved (response) frequency, and A represents the amplitude of the harmonic motion, and ltc_f represents the calculated latency per step [13].

$$ltc_f = \left(\frac{1}{f_a} - \frac{1}{f_d} \right) \times \frac{\Delta s}{4A} \tag{1}$$

Control signals to drive the shake table were calibrated according to the latency values obtained by Equation (1) and were replaced in the controlling software and using the displacement recordings. The table response was rechecked with Eq. (1) to ensure that the calibration process is successful [13].

3. RESULTS

3.1. Calibration under Harmonic Motion

Calibration of the table is provided with the latency values obtained as a result of harmonic scanning for different amplitudes and frequencies with the help of the Equation (1) for each axis individually. Displacement-time data measured from potentiometers on the table using the data acquisition unit were used to determine the delay values. In order to determine the difference between the demand signal and the response signal and obtain the latency values,

the demand and response frequencies were evaluated by calculating the power spectra using a code developed in Matlab environment [14]. The similarity of the two signals was also analyzed by the cross-correlation method.

Latency values obtained for various frequency-amplitude responses by numerous experimental studies conducted in this way are given in Table 2 and Table 3 for *x* and *y* axes, respectively. The main reasons for the differences in latency values observed on each axis are caused by small variations of the electro-mechanical parameters of the system, such as motor coil resistance and inductance, flux density of permanent magnets of the motor, switching behavior of Arduino boards and micro-stepping drivers. The (-) sign for upper frequencies in Table 2 indicates that the table payload limits are exceeded and cannot achieve these frequencies due to the mass of the bare table's moving parts placed on the *x*-axis. Although the table can reach high frequencies at low amplitudes (22Hz @ ± 1mm), the maximum frequency at large amplitudes can be 1 Hz. For intermediate values not given in Table 2 and Table 3, linear interpolation can be used to calculate latency values. The frequency responses of the bare table at 0.5 and 0.75 Hz for the maximum displacement ±150 mm on the *y*-axis are given in Figures 2 and 3, respectively. For example, for the experiments carried out under load, a mass of 600 kg is placed on the table (Figure 4), and the target frequency is taken as 0.53 Hz. In Table 3, the linear interpolation between the values given for 7.37 μs at 0.5 Hz and 7.21 μs at 0.75 Hz for 150 mm was calculated, and the delay value was obtained as 7.35 μs. The recording with the motion signal generated using this latency value is given in Figure 5. The table response to the demand frequency of 0.53 Hz was calculated as 0.53036. As can be seen, the difference is 0.07%, and the delay is calculated as -106 ns after calibration.

Table 2 - Latencies at different frequency and amplitudes for calibration of x-axis (μs)

Frequency [Hz]	Amplitude [mm] (x-axis)															
	5	10	20	30	40	50	60	70	80	90	100	110	120	130	140	150
0.5	6.67	8.21	7.86	7.58	7.59	7.60	7.86	7.42	7.28	7.28	7.42	7.77	7.26	7.24	7.24	7.36
0.75	7.14	7.74	7.62	7.31	7.50	7.50	7.42	7.77	7.78	7.74	7.19	7.73	7.20	7.37	7.20	7.21
1	6.67	7.14	7.50	7.78	7.41	7.74	7.18	7.21	7.22	7.33	7.23	-	-	-	-	-
1.5	6.19	6.68	7.22	7.30	7.23	7.33	7.36	7.19	-	-	-					
2	6.90	6.85	7.28	7.22	7.21	-	-	-								
2.5	6.43	6.80	7.20	7.26	-											
3	6.97	7.38	7.62	-												
4	7.14	7.02	-													
5	6.67	7.62														
6	7.46	-														
7	7.35															
8	-															

The same process for the specified frequency at 150 mm amplitude of 0.53 Hz is calculated via Table 3 for the desired latency value, where 7.82 μs for 0.5 Hz and 7.75 μs latency for 0.75 Hz were given for 110 mm amplitude. Linear interpolation was performed using these values, and the delay value was obtained as 7.78 μs for 0.65 Hz. As a result of the

measurements taken by the calibration process, the table response for the target/demand frequency of 0.65 Hz was obtained 0.65003 Hz. The difference between demand and response frequencies was found to be 0.005%. Therefore, the latency of calibrated harmonic motion was determined as -9.16 ns, as shown in Figure 6. The displacement error in the time domain for achieved vs. desired harmonic motions are shown in Figure 7 for un-calibrated and calibrated cases using synchronization subspace plots (SSP). In Figure 7a, the effect of cumulative latency, which increases the magnitude of total delay, can be seen clearly. Using the appropriate latency value for calibrating the motion signal data, the effect of cumulative latency that causes the total delay was minimized, where the synchronization plot in Figure 7b, nearly shows an overlapped position compared to ideal SSP line which has a slope of 45°.

Table 3 - Latencies at different frequency and amplitudes for calibration of y-axis (µs)

	Amplitude [mm] (*y*-axis)															
	5	10	20	30	40	50	60	70	80	90	100	110	120	130	140	150
0.5	8.81	8.57	8.15	7.86	7.59	7.69	8.00	7.50	7.35	7.30	7.45	7.82	7.31	7.27	7.26	7.37
0.75	8.33	8.57	7.86	7.51	7.56	7.45	7.46	7.82	7.81	7.77	7.21	7.75	7.20	7.37	7.20	7.21
1	7.14	7.98	7.62	7.90	7.41	7.79	7.28	7.25	7.22	7.33	7.23	7.18	7.19	9.06	7.34	7.32
1.5	9.05	7.29	7.46	7.38	7.23	7.33	7.40	7.19	7.35	7.32	7.31					
2	8.33	7.58	7.40	7.22	7.21	7.41	9.28	7.30								
2.5	7.86	7.28	7.32	7.26	7.35											
3	7.45	7.62	7.62	7.30												
4	7.14	7.26	7.68													
5	8.10	7.86														
6	7.46	7.26														
7	7.35															
8	6.85															
9	7.06															

(Frequency [Hz] — row labels)

Figure 2 – Un-calibrated results for 150 mm amplitude at 0.5 Hz for the bare table

Figure 3 – Un-calibrated results for 150 mm amplitude at 0.75 Hz for the bare table

Figure 4 - A photo from the tests performed under 600 kg lumped mass
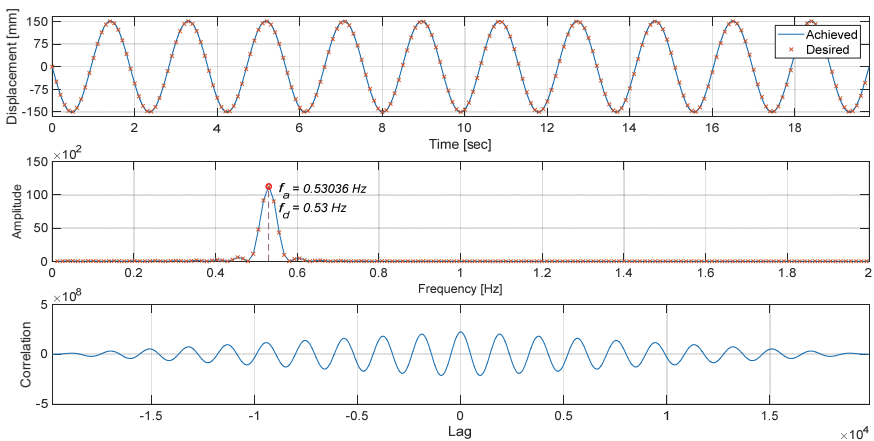
Figure 5 - Results after calibration for 150 mm amplitude at 0.53 Hz under 600 kg lumped mass
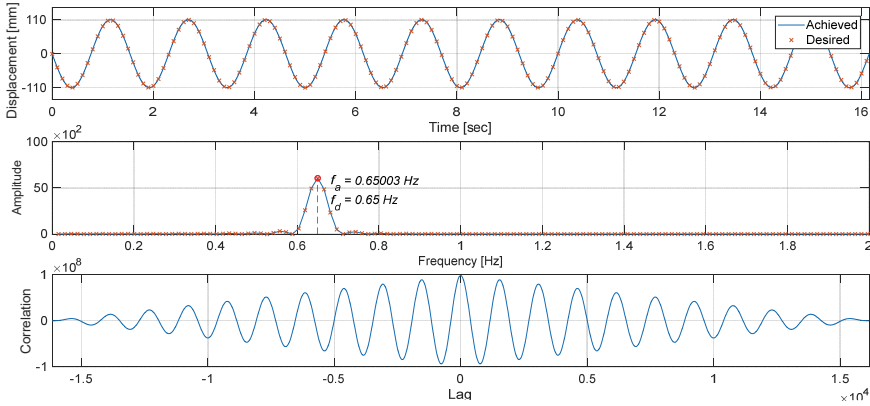
Figure 6 - Results after calibration for 110 mm amplitude at 0.65 Hz under 600 kg lumped mass

| (a) | (b) |
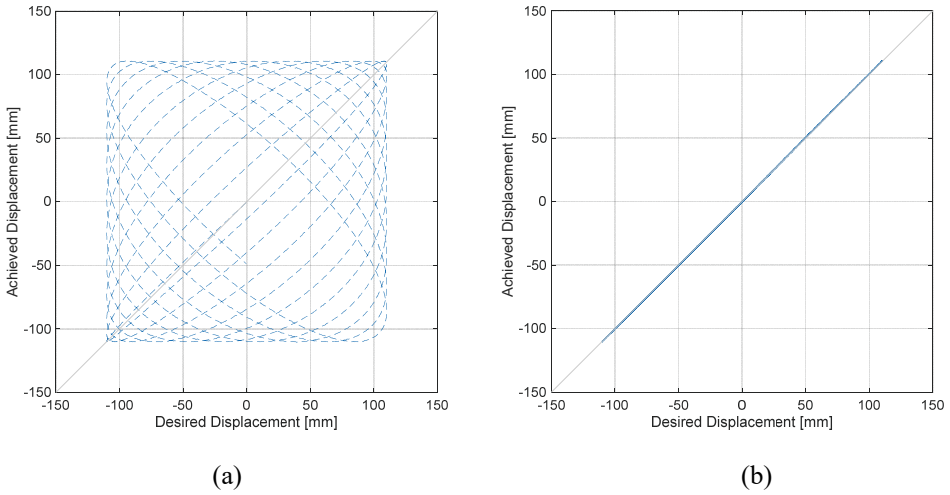
Figure 7 - Synchronization subspace plots (SSP) for 110 mm amplitude at 0.65 Hz under 600 kg lumped mass: (a) Un-calibrated (ε_{rel} = 128.05%), (b) Calibrated (ε_{rel} = 0.52%).

3.2. Use of Calibration in Earthquake Simulation

As a result of the calibration process performed under harmonic motion providing sufficient accuracy, an average delay value was chosen by considering these calibration values in earthquake simulation because of the variable frequency content of the earthquake. As can be seen in Tables 2 and 3, latencies vary between 6-9 µs. In this study, the latency value for earthquake simulations was selected as 8 µs. In this case, the simulated ground motion was compared with scaled ground motion as a result of simultaneous measurements taken from both axes via linear potentiometers. From the PEER strong ground motion database [15], the

1999 Chi-Chi earthquake was selected for simulation, and the test was carried out under 240 kg payload for the latency value of 8 μs. In Figures 8 and 9, the plotted graphs of the desired and achieved motions of the *x* and *y* components of the 1/3 scale Chi-Chi earthquake and their cross-correlation are given. Displacement records taken in 1/3 scale Chi-Chi Earthquake simulation are evaluated using the relative RMS error, ε_{rel} with Eq. (2). The errors calculated between the desired (x_d) and the measured (x_a) displacements are $\varepsilon_{rel} = 4.05\%$ for the *x*-axis and $\varepsilon_{rel} = 3.41\%$ for the *y*-axis. The error was seen to be less than 5% and found to be within the acceptable range. This approach's accuracy is also shown in Figure 10 by SSP graphs, where the relationship between the desired vs. achieved earthquake motion is nearly overlapped on the 45° reference line, indicating minimum delays.

$$\varepsilon_{rel} = \frac{\sqrt{(1/N)\Sigma_{n=1}^{N}(x_a[n] - x_d[n])^2}}{\sqrt{(1/N)\Sigma_{n=1}^{N}(x_d[n])^2}} \times 100 \qquad (2)$$

As a further example, simulations were performed for the 1999 Düzce earthquake on both the bare and loaded shake table. Figures 11 and 12 show the comparison between the desired and measured displacement records for the *x*-axis and the *y*-axis, respectively. Using Eq. (2), relative RMS error was calculated as $\varepsilon_{rel} = 3.30\%$ for the *x*-axis and $\varepsilon_{rel} = 3.31\%$ for the *y*-axis. Figure 13 shows that the relationship between the desired and achieved earthquake motion is of sufficient accuracy with SSP graphics. During this simulation, accelerations were recorded by the aid of a low-cost 3-axis acceleration sensor (MPU6050) mounted on the table. Comparative graphs of the acceleration recordings, the FFT spectrums, and acceleration response spectra obtained from the desired and measured acceleration data are given in Figures 14 and 15 for the *x* and *y*-axis, respectively. The 4th degree Butterworth low pass filter was applied to the acceleration recordings where the upper cut-off frequency was set to 21 Hz. The damping rate was taken as 5% for the acceleration response spectrum graph. By using Equation (3) for the desired ($\ddot{x}_d$) and achieved ($\ddot{x}_a$) acceleration records, relative RMS errors are calculated as $\varepsilon_{rel} = 21.84\%$ for the *x*-axis and $\varepsilon_{rel} = 31.96\%$ for the *y*-axis. It was seen that the results obtained from the acceleration records coincide with the characteristic of the desired acceleration record.

$$\varepsilon_{rel} = \frac{\sqrt{(1/N)\Sigma_{n=1}^{N}(\ddot{x}_a[n] - \ddot{x}_d[n])^2}}{\sqrt{(1/N)\Sigma_{n=1}^{N}(\ddot{x}_d[n])^2}} \times 100 \qquad (3)$$

Another example of the experiments performed on the loaded shake table after the experiments on the bare table is the 1/15 scale 1999 Düzce earthquake. It was estimated that the desired strong ground motion could be performed on both axes under 360 kg payloads for this scale, with the methodology given by Damcı and Şekerci [13]. Figure 16 and Figure 17 show the comparison of the displacement records taken for the *x* and *y* axes, respectively. As a result of the calculations carried out for the desired (x_d) and achieved (x_a) displacement records, using Eq. (2), the relative RMS errors obtained on both axes were $\varepsilon_{rel} = 2.06\%$ for the *x*-axis and $\varepsilon_{rel} = 5.64\%$ for the *y*-axis. Figure 18 shows that the relationship between the desired and achieved earthquake motion is of sufficient accuracy with SSP graphics.
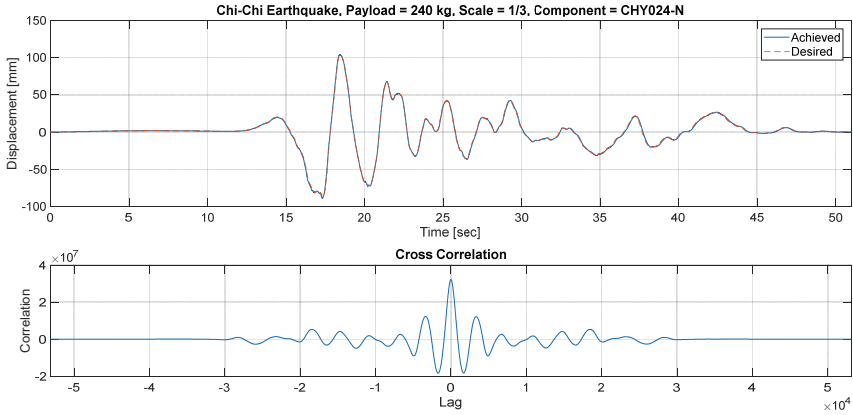
Figure 8 - Comparison of desired and achieved strong ground motion simulation at x-axis for 1/3 scale Chi-Chi earthquake under 240 kg payload
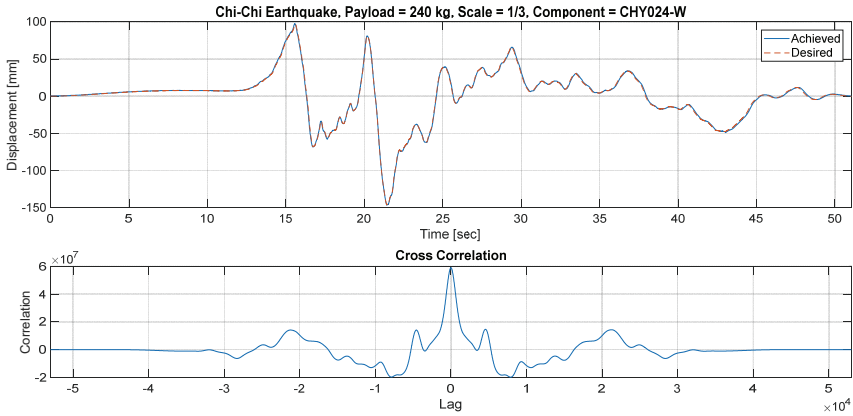
Figure 9 - Comparison of desired and achieved strong ground motion simulation at y-axis for 1/3 scale Chi-Chi earthquake under 240 kg payload

(a)   (b)
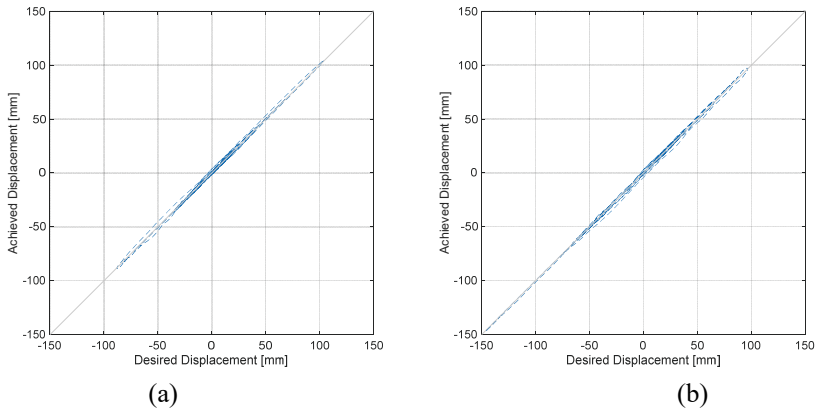
Figure 10 - Synchronization subspace plots (SSP) for 1/3 scale Chi-Chi earthquake: (a) x-axis (ε_{rel} = 4.05%), (b) y-axis (ε_{rel} = 3.41%).
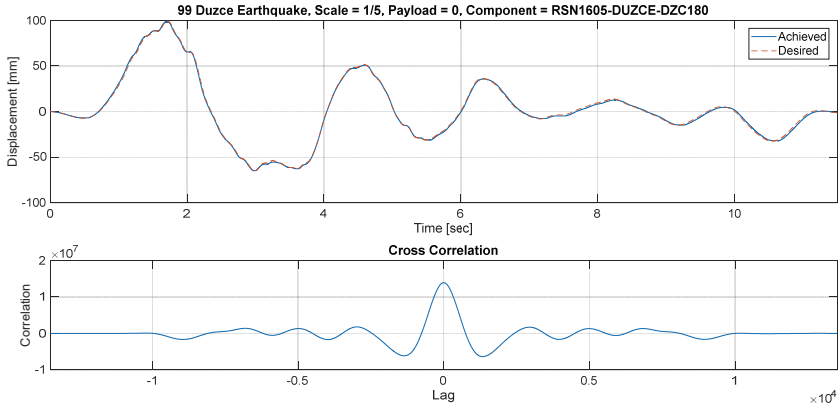
Figure 11 - Comparison of desired and achieved strong ground motion simulation at x-axis for 1/5 scale Düzce earthquake for the bare table (payload=0)
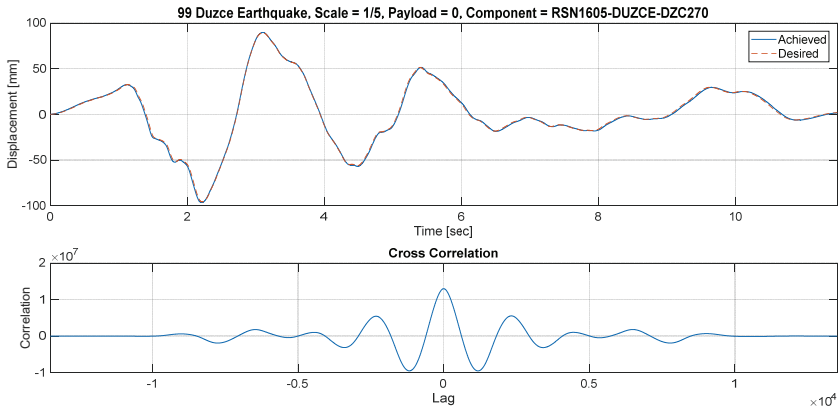
Figure 12 - Comparison of desired and achieved strong ground motion simulation at y-axis for 1/5 scale Düzce earthquake for the bare table (payload=0)

(a)   (b)
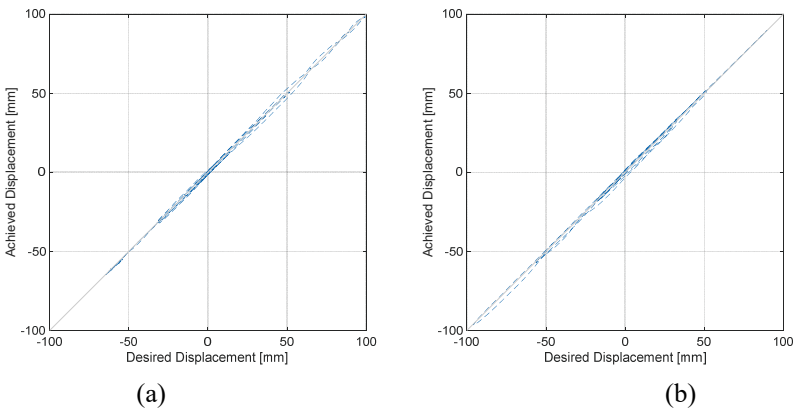
Figure 13 - Synchronization subspace plots (SSP) for 1/5 scale Düzce earthquake: (a) x-axis (ε_{rel} = 3.30%), (b) y-axis (ε_{rel} = 3.31%).
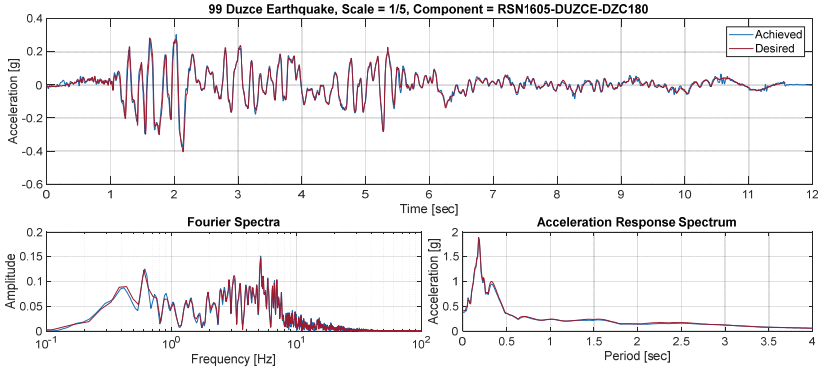
Figure 14 - Comparison of desired and achieved accelerations of 1/5 scale Düzce earthquake simulation at the x-axis, their frequency content and acceleration response spectra for the bare table
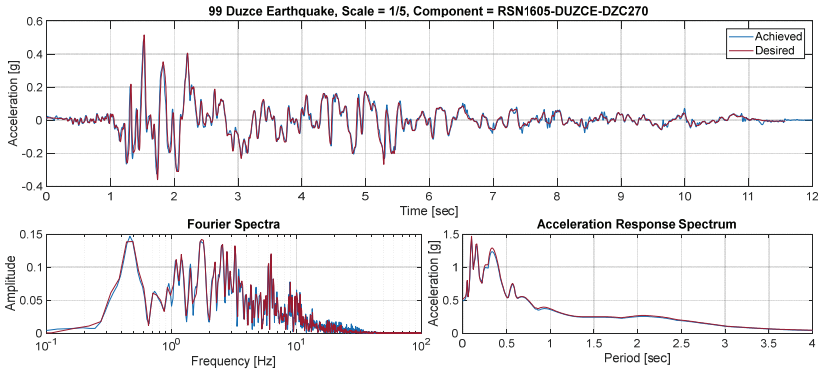
Figure 15 - Comparison of desired and achieved accelerations of 1/5 scale Düzce earthquake simulation at the y-axis, their frequency content and acceleration response spectra for the bare table
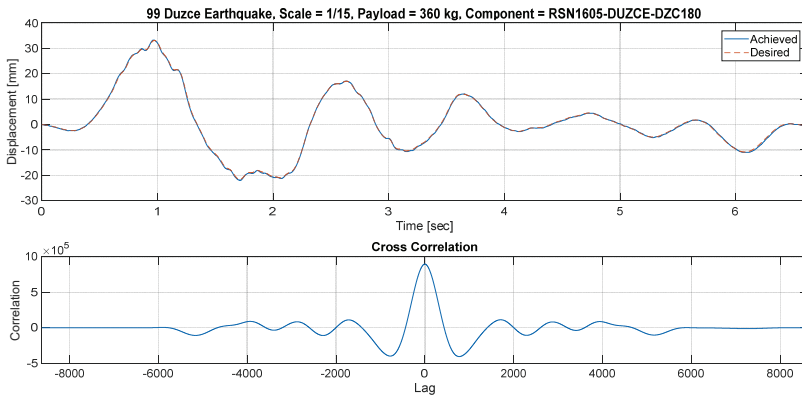
Figure 16 - Comparison of desired and achieved strong ground motion simulation at x-axis for 1/15 scale Düzce earthquake for 360 kg payload
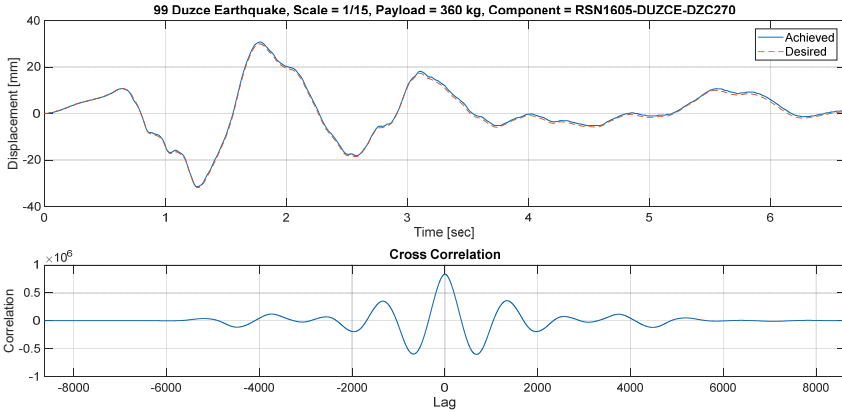
Figure 17 - Comparison of desired and achieved strong ground motion simulation at y-axis for 1/15 scale Düzce earthquake for 360 kg payload

(a) (b)
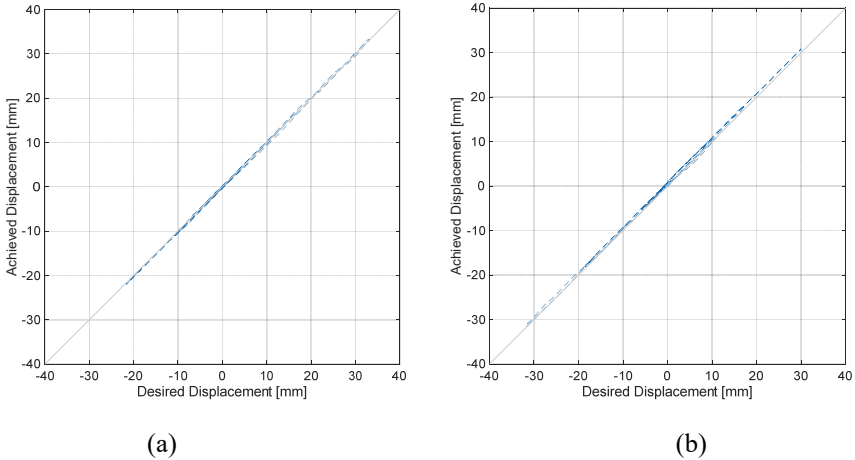
Figure 18 - Synchronization subspace plots (SSP) for 1/15 scale Düzce earthquake: (a) x-axis ($\varepsilon_{rel} = 2.06\%$), (b) y-axis ($\varepsilon_{rel} = 5.64\%$).

4. CONCLUSIONS

In the experiments to be performed with the shake table developed in this study, a technique for calibrating the table is presented to determine the table performance accurately and perform the simulations with minimum errors. For this purpose, 350 mm linear potentiometric rulers placed between the table plates were used, and the table was calibrated using displacement records taken from these rulers. Due to the 10-bit ADC resolution of the Arduino MEGA development board, which forms the data acquisition unit, the sensitivity of reading signals from the linear potentiometer is 0.342 mm. This resolution is insufficient for tracking small-amplitude harmonic motions but provides sufficient resolution for the table's maximum displacement capacity of ± 150 mm. In order to drive the shake table accurately

Erdem DAMCI, Çağla ŞEKERCI, Yener TAŞKIN, Koray GÜRKAN

for the desired motion information, many measurements were taken by frequency scanning for different harmonic motion simulations, and calibration tables were obtained from the experimental results for *x* and *y* axes. The corrections were made with the help of software developed by open-loop control technique using these results. Besides, the effect of calibration on bi-axial earthquake simulation was examined, and it was found that the presented calibration technique was able to simulate the desired strong ground motion with a relative RMS error of about 5%, under repeated trials. With these satisfactory results, the shake table SARSAR can be used for future research projects to investigate structural behavior under simulated bi-axial earthquake excitations.

Symbols

A	Amplitude of the harmonic motion
f_a	Achieved (response) frequency
f_d	Desired (demand) frequency
ltc_f	Latency per step
N	Number of samples
x_a	Achieved (measured) displacement
x_d	Desired displacement
$\ddot{x}_a$	Achieved (measured) acceleration
$\ddot{x}_d$	Desired acceleration
Δs	Unit displacement of the actuator assembly for a single step
ε_{rel}	Relative root mean square error

Acknowledgment

References

[1] O. Ozcelik, J.E. Luco, J.P. Conte, Identification of the mechanical subsystem of the NEES-UCSD shake table by a least-squares approach, *Journal of Engineering Mechanics*, 134(2008)23–34. https://doi.org/10.1061/(ASCE)0733-9399(2008)134:1(23)

[2] S.E. Kim, D.H. Lee, C. Ngo-Huu, Shaking table tests of a two story unbraced steel frame. *Journal of Constructional Steel Research*, 63 (2007) 412–421. https://doi.org/10.1016/j.jcsr.2006.04.009

[3]   J. Kuehn, D. Epp, W. N. Patten, High-fidelity control of a seismic shake table, *Earthquake Engineering and Structural Dynamics*, 28 (1999) 1235–1254. https://doi.org/10.1002/(SICI)1096-9845(199911)28:11<1235::AID-EQE864>3.0.CO;2-H

[4]   N. Nakata, Acceleration trajectory tracking control for earthquake simulators, *Engineering Structures*, 32 (2010) 2229–2236. https://doi.org/10.1016/j.engstruct.2010.03.025

[5]   J. E. Luco, O. Ozcelik, J. P. Conte, Acceleration Tracking Performance of the UCSD-NEES Shake Table. *Journal of Structural Engineering*, 136 (2010) 481–490. https://doi.org/10.1061/(ASCE)ST.1943-541X.0000137

[6]   T. Y. Yang, K. Li, J. Y. Lin, Y. Li, D. P. Tung, Development of high-performance shake tables using the hierarchical control strategy and nonlinear control techniques, *Earthquake Engineering & Structural Dynamics*, 44 (2015) 1717–1728. https://doi.org/10.1002/eqe.2551

[7]   M. Saranik, D. Lenoir, L. Jézéquel, Shaking table test and numerical damage behaviour analysis of a steel portal frame with bolted connections, *Computers and Structures*, 112–113 (2012) 327–341. https://doi.org/10.1016/j.compstruc.2012.07.009

[8]   R. Zhang, P. V. Lauenstein, B. M. Phillips, Real-time hybrid simulation of a shear building with a uni-axial shake table, *Engineering Structures*, 119 (2016) 217–229. https://doi.org/10.1016/j.engstruct.2016.04.022.

[9]   A. C. Altunisik, A. Yetisken, V. Kahya, Experimental study on control performance of tuned liquid column dampers considering different excitation directions, *Mechanical Systems and Signal Processing*, 102 (2018) 59–71. https://doi.org/10.1016/j.ymssp.2017.09.021

[10]   Z. Fırat Alemdar, Betonarme Köprü Kolonlarında Plastik Mafsal Bölgelerinin Modellenmesi, *İMO Teknik Dergi*, 444 (2015) 7279-7286.

[11]   A. Ashasi-Sorkhabi, H. Malekghasemi, O. Mercan, Implementation and verification of real-time hybrid simulation (RTHS) using a shake table for research and education, *Journal of Vibration and Control*, 21(8) (2015) 1459–1472. DOI: 10.1177/1077546313498616

[12]   A. Najafi, B. F. Spencer Jr, Modified model-based control of shake tables for online acceleration tracking, *Earthquake Engng Struct Dyn.,* (2020) 1–17. DOI: 10.1002/eqe.3326

[13]   E. Damcı, Ç. Şekerci, Development of a Low-Cost Single-Axis Shake Table Based on Arduino. Experimental Techniques, 43 (2019) 179-198. https://doi.org/10.1007/s40799-018-0287-5

[14]   MATLAB version R2017b, 2017, computer program, The MathWorks Inc., Natick, Massachusetts.

[15]   PEER Ground Motion Database - PEER Center. http://ngawest2.berkeley.edu/ (Accessed, 15th November 2018).

The Effects of Iraq Natural Asphalt on Mechanical Properties of Bituminous Hot Mixtures

Yunus ERKUŞ[1]
Baha Vural KÖK[2]
Mehmet YILMAZ[3]

ABSTRACT

The increasing rate of traffic every day requires the roads to be made more stable. To improve the low and high temperature properties of the bituminous mixtures forming the coating layer of the flexible pavements, the binder in the mixture is often modified with various polymers. The most commonly used polymer in the modification is styrene-butadiene-styrene (SBS). However, SBS, which is very successful in improving the mechanical properties of the mixtures, is expensive and has brought the search for cheaper alternative additives. In this context, natural asphalts (NA) which are not subjected to any processes are used as additive. In this study, natural asphalt obtained from Zaho region of Iraq was used in 20%, 35% and 50% of bitumen modification by weight. The mechanical properties of mixtures prepared with different amount of NA modified bitumen were compared with 4% SBS modified bituminous mixtures. As a result, NA modification significantly improved the properties of bituminous mixtures. In particular, above 35% NA, the mixtures exhibited a superior performance by significantly resisting the effect of repeated loads. It was found that an average of 17.3% NA modification exhibited similar behaviour with 4% SBS modification and provided significant economic savings.

Keywords: Natural asphalt, SBS, modification, mechanical properties, mixture.

1. INTRODUCTION

Natural asphalts are solid or semi-solid materials composed of hydrocarbons and aromatic molecules. Natural asphalts generally consist carbon, hydrogen, nitrogen, oxygen, sulphur as well as a small amount of iron, nickel and vanadium [1]. Gilsonite, Trinidad Lake and rock

asphalt in America and Iran are the most common types of natural asphalt used as a part of original bitumen. Trinidad Lake Asphalt (TLA), mainly consists of asphalt and mineral matter, different from petroleum asphalt. Although the chemical composition of the asphalt part of TLA is similar to that of petroleum asphalt, it cannot be used as a binder alone in asphalt mixtures because it is very hard due to its high mineral and asphaltene content [2]. Xu et al. investigated the properties of Trinidad Lake Asphalt and SBS modified asphalt mixtures. In the light of experimental data, it was found that TLA and SBS increased the fracture resistance of asphalt. It was also determined that TLA and SBS improve aging resistance and service life of asphalt [3]. Gilsonite is usually located parallel to each other in the form of vertical veins in the depths. The mass gilsonite is a natural asphalt with a rather shiny, black color, notched rupture surface, similar to obsidian mineral. It can be easily crushed due to its fragile structure. The specific gravity of gilsonite is between 1.03 and 1.10. It melts between 120°C and 175°C. The penetration value of gilsonite is 0. Gilsonite is characterized by its high asphaltene properties, high solubility in organic solvents, high molecular weight and high nitrogen content. Jahanian et al. modified the mixtures by adding 0, 2, 4, 6, 8, 10% gilsonite by weight of the bitumen. It was found that Marshall stability and stiffness modulus parameters of gilsonite modified mixtures increased significantly. In addition, the increase in flow number obtained from the dynamic creep test is indicative of an increase in the rutting resistance [4]. It was determined that the penetration value of the gilsonite modified binders decreased and the softening point value increased. Gilsonite significantly increased the stability and rutting resistance of bituminous hot mixtures prepared with modified binders containing 4% and 8% gilsonite. According to indirect tensile stiffness modulus test, the rigidity of gilsonite modified hot mixtures increased at 25°C while the gilsonite did not have a significant effect at 35°C and 45°C [5]. Babagoli et al. have investigated the effects of gilsonite on the performance of stone mastic asphalt mixtures. Gilsonite was added to the binders at 5%, 10% and 15% by weight of bitumen. According to the test results, gilsonite reduced the penetration of the binders and increased the softening point. Ductility values decreased while viscosity values increased with the increasing rate of gilsonite. Marshall stability of gilsonite modified mixtures increased while creep values decreased. Mixtures containing 10% gilsonite gave the highest elastic modulus values. The tensile stress values of mixtures containing 15% gilsonite were higher than those of other mixtures. In addition, it was found that gilsonite-containing mixtures had greater resistance to moisture damage. Finally, it was observed that gilsonite modified mixtures gave a lower rutting depth [6]. It was determined that the addition of 18 wt % American gilsonite to PG 58-18 pure binder resulted in PG 76-16 and also gives lower mixing-compaction temperature compared to 5% SBS modification [7]. Rock asphalt is a type of natural asphalt that passes through the oiling process following the division of rocks from the cracks. Rock asphalt is transformed for millions of years due to heat, pressure, oxidation and mineral precipitation. Rock asphalt is environmentally friendly, does not need chemical processing and is a highly compatible building material with bitumen. When used in modified binders, it increases the high temperature strength, water resistance and durability. Li et al. have investigated the potential impact of different types of rock asphalt on the performance of asphalt composites. It was determined that rock asphalt admixture increased the rigidity but reduced the low temperature performance [8]. Yilmaz and Celoglu investigated the effect of three different natural asphalts (Trinidad Lake Asphalt, Iranian gilsonite and American gilsonite) and styrene-butadiene-styrene (SBS) additives on the performance of bituminous hot mixtures. The mixtures prepared with 10% American gilsonite, 9.5% Iranian gilsonite, 60% Trinidad

Lake Asphalt and 3.8% SBS modified binders at the same performance grade (PG-70-34) were compared with control mixtures prepared by pure bitumen (PG 58-34). Indirect tensile strength (ITS) and Marshall stability values of the mixtures prepared with TLA were found to be the highest. The mixtures prepared with 9.5% Iranian gilsonite and 3.8% SBS had the highest resistance to moisture damage. The mixtures prepared with 60% TLA had the highest hardness and the longest fatigue life [9]. It has been determined that the fatigue life, rutting resistance and high temperature performances of bituminous hot mixtures prepared with gilsonite modified binders have increased [10, 11]. Hot bituminous mixtures prepared by natural asphalt which consists of 17% asphalt fraction and 83% mineral fraction was found to have higher stiffness modulus and also resistance to permanent deformation compared to control mixtures [12]. It was concluded that the use of gilsonite is useful for constructing asphalt mixture with harder bitumen to have more rutting resistance and better load distribution within structure and as a result less stresses in pavement structure [13]. Studies showed the improvement in high temperature and temperature sensitivity performance with addition of rock asphalt [14, 15]. Li et al. reported that the America rock asphalt can increase the surface free energy of asphalt, thus results in a better moisture damage resistance [16]. It was reported that the moisture damage resistance, tensile strength and fatigue performance of petroleum mixture were enhanced as well with the addition of rock asphalt from Xinjiang, China. However, the low temperature performance was slightly sacrificed after the modification of rock asphalt [17].

Recently, SBS modified bitumen was widely used in hot bituminous mixtures. The studies showed the achievement of these additive on improving the rheological properties of bitumen [18-20] and mechanical properties of asphalt mixtures [21, 22]. The improved rheological properties result in viscoelastic behaviour over a wider temperature range. The enhanced viscoelasticity also induces longer fatigue life and less rutting potential. Some co-additives are also used besides the SBS in order to enhance the efficiency in terms of storage stability and aging properties [23, 24]. The main drawback of the SBS modification such as the limited production and high cost of the additive has motivated the researchers to explore alternative additives without sacrificing the performance.

In this study Iraq gilsonite which is a type of natural asphalt and 20% cheaper than original refinery bitumen was used as a modifier to improve the mechanical properties of mixtures. The mechanical properties of the natural asphalt modified mixtures were compared to those of the SBS modified mixtures.

2. MATERİALS AND METHOD

B 160/220 grade bitumen, which is obtained from TÜPRAŞ Batman refinery, was used as pure binder. Natural asphalt (NA) was provided from Zaho region of Iraq. The elemental analyses of the base and natural asphalt are given in Table 1. Natural asphalt was added as an additive to pure bitumen by 20%, 35% and 50% by weight of bitumen. To evaluate the performance of natural asphalt modified bituminous mixtures, the mechanical properties of the bituminous mixtures prepared by SBS (KRATON D 1101) produced by Shell Bitumen were also investigated. Kraton D-1101 is a linear triblock copolymer in powder form that consists of 31/69 styrene/rubber ratio. It has 4600 psi tensile strength and 880% elongation at break. SBS was used at 4% by weight of the binder. Bituminous mixtures produced with

20%, 35%, 50% natural asphalt modified binder are shown as 20NA, 35NA and 50NA respectively, and bituminous mixtures produced with 4% SBS modified binder are shown as 4SBS. Fig. 1 shows the natural asphalt and SBS.

Table 1 - Elemental analysis of base and natural asphalt.

	C(%)	H(%)	N(%)	S(%)	Solubility in TCE (%)
Base bitumen	82.38	8.96	0.604	7.227	99.21
Natural asphalt	81.52	10.82	0.455	5.914	97.95

Natural Asphalt (NA)   Styrene-butadine-styrene (SBS

Fig. 1 - Iraq natural asphalt and SBS

Fig.2 - High shear mixer

In the bitumen modification, different contents of natural asphalt and SBS were gradually added to the pure bitumen and mixed with a four-bladed mixer at 1000 rpm for 1 hour at a constant temperature of 170ºC. The total amount of binder in the container was adjusted to be 500 g for each batch. An insulated container (Fig.2) was used during the modification. The heater plate has a thermostat which is submerged into bitumen throughout a channel on the top of the cap. The temperature was kept constant and excessive aging during the mixing was avoided thanks to insulated container with closed cap and thermostat-controlled heating plate. The pure binder, which does not contain any additives, has been subjected to the same mixing process so that the aging effect occurring during the modified bitumen preparation was eliminated. Table 2 shows the physical properties of the binders.

Table 2 - The physical properties of the binders.

Properties	Pure	20NA	35NA	50NA	4SBS
Softening point (ºC) ASTM D36	42.1	49.7	52.8	69.7	53.9
Penetration (0.1 mm) ASTM D5	206	83.2	53.6	23	101
Penetration index	1.01	-0.24	-0.12	1.01	1.86
Viscosity (cP) 135ºC /165ºC ASTM D4402	262/100	437/150	587/162	1588/325	1125/325

Mixture samples were prepared by applying 75 blows on both sides of the samples according to the Marshall Mix Design. The properties and gradation of the limestone aggregates are given in Table 3. Type-2 of the Turkey Highways Technical Specification was used as a grading. The limestone was obtained from Elazig Karayazi region. The optimum bitumen content was determined for the mixture samples prepared with pure bitumen. Modified mixtures were prepared with the same bitumen content.

The pure and modified mixtures prepared in the optimum bitumen content (5.8%), air voids (Va), voids filled with asphalt (VFA), voids in mineral aggregates (VMA), bulk specific gravity (Gmb) and the mixing-compaction temperatures are given in Table 4. The mixing-compaction temperatures of the mixtures were determined as the temperatures corresponding to the viscosity values of 170 ± 20 and 280 ± 30 cP according to the rotational viscometer test applied to the binder [25]. The modified mixtures require more mixing-compaction temperature than the pure mixture since the viscosity of the binders increases with the use of additives. However, the NA modified mixtures give lower temperatures than the 4% SBS modified mixture even at the 50% NA content. It has been found that the mixture samples comply with the specification terms of the volumetric properties.

Table 3 - Aggregate properties and gradation.

Properties		Coarse		Fine		Filler
Los Angeles abrasion (%) ASTM D131		25				
Soundness of aggregates (MgSO₄) ASTM C88		12				
Flat and elongate particles (%) BS 812		20				
Water absorption (%) ASTM C127		0.8				
Bulk specific gravity ASTM C127, C128		2.533		2.619		
Apparent specific gravity ASTM D854						2.732
Sieve size (mm)	12.5	9.5	4.75	2.00	0.425	0.180	0.075
% Passing	100	87	55	38	21	8	6

Table 4 - Volumetric properties of mixture samples.

Mixtures	Va (%)	VFA (%)	VMA (%)	Gmb	Gmm	Mixing temperature (ºC)	Compaction temperature (ºC)
Pure	3.79	75.08	15.20	2.315	2.406	144-152	130-136
20NA	4.08	73.62	15.45	2.308	2.406	158-165	144-150
35NA	3.92	74.38	15.32	2.311	2.406	161-167	149-154
50NA	4.15	73.25	15.52	2.306	2.406	176-182	165-170
4SBS	4.14	73.31	15.51	2.307	2.406	179-186	166-172

3. EXPERIMENTAL RESULTS

3.1. Marshall Stability and Flow Test

Marshall stability and flow test, which is a performance indicator of bituminous mixtures, were conducted according to ASTM D 6927 standard. Fig. 3 shows the Marshall stability of the mixtures while Fig. 4 shows the stability / flow rates of the mixtures. The values are the average of the four replicates. Stability values increase significantly with the use of NA as in previous studies using natural asphalt additives [4, 6, 9]. The addition of 20%, 35% and 50% natural asphalt increases the stability of the mixtures by 7%, 19% and 32%, compared to the pure mixture. The 4% SBS modified mixtures give only 6.7% higher stability than the pure mixtures. The same stability value as that of the 4SBS mixture can be obtained by 14% natural asphalt modification as seen in Fig. 5. The change in the stability / flow ratios, which is an indicator of the rigidity of the mixtures, showed a similar performance to that of the stability. The stiffness of the 50NA mixture is increased by 14% compared to the pure mixture.
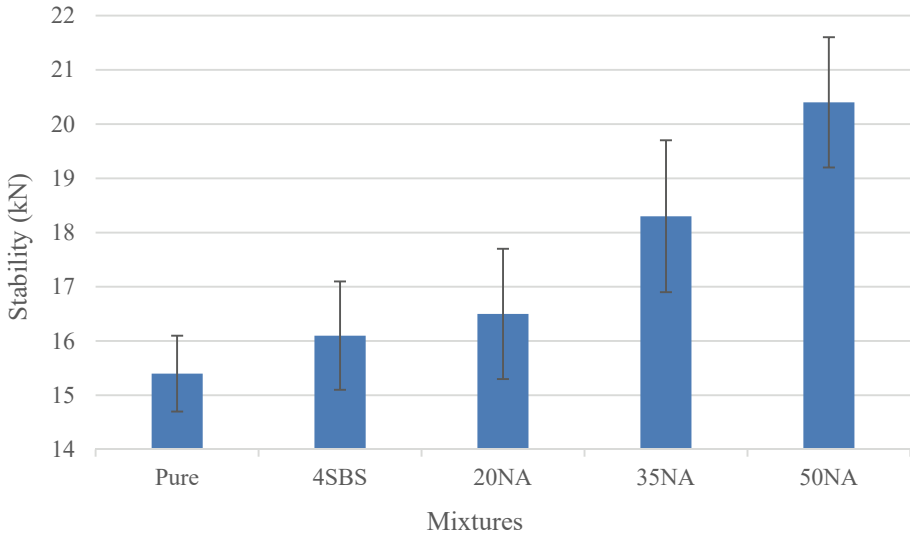
Fig. 3 - Marshall stability values of mixtures.
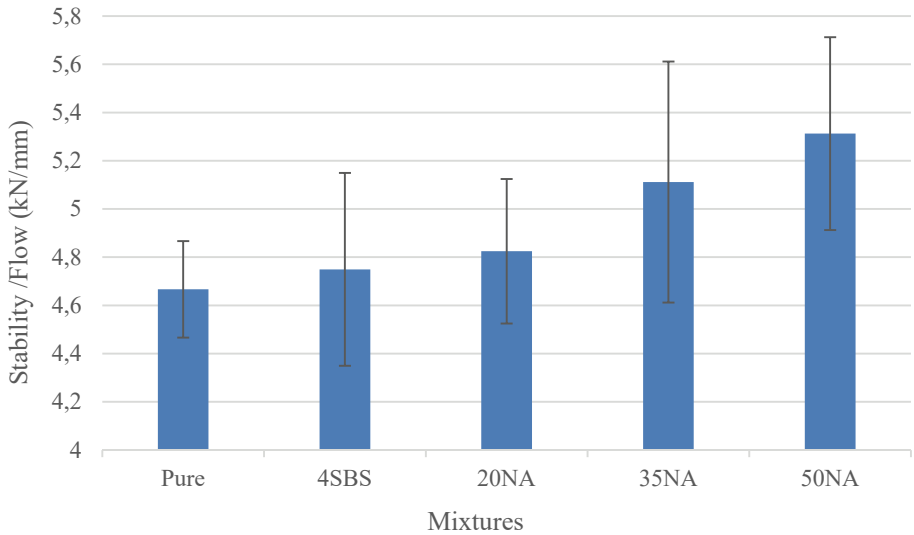
Fig. 4 - Stability / flow values of mixtures.
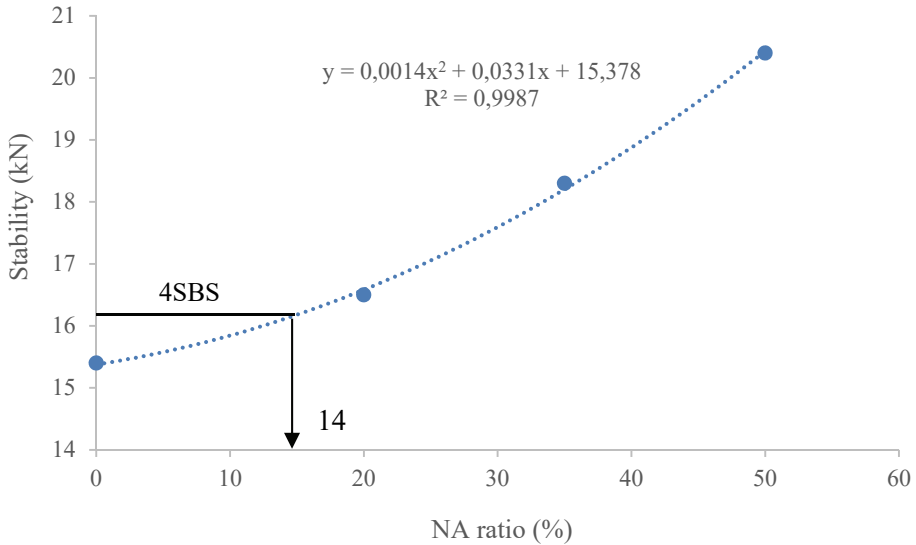
Fig. 5 - The change of the stability against NA ratio.

3.2. Indirect Tensile Strength Test

The experiment was performed using Marshall apparatus according to AASHTO T 283. The samples were wrapped in aplastic bag and placed in a 25 ºC water bath for two hours before testing. Cylindrical samples were subjected to a pressure load in the direction of the vertical diameter plane in such a way that a uniform distribution of stress was obtained. The load causing fracture was determined and ITS (kPa) values were calculated.

$$ITS = 2Pmax / \pi td \tag{1}$$

Where P is the maximum load (kN); t, the mean sample height (m); d is the sample diameter (m).

The tensile strength values of the mixtures are given in Fig. 6 sequentially. The values are the average of the four replicates. The percent increase in ITS values with natural asphalt is higher than the stability values. ITS values of 20NA, 35NA and 50NA mixtures were 64%, 97% and 180% higher than the pure mixture, respectively. It is seen that the use of natural asphalt can increase the tensile strength of the mixtures up to two times with the same trend as other studies in the literature [4, 6, 9, 12]. The 4SBS mixture has 37% higher ITS value than that of the pure mixture. The same ITS value with the 4SBS mix can be obtained by the addition of 14% NA as shown in Fig. 7. According to Marshall stability test, ITS test shows the effectiveness of additive use more clearly. The significantly higher ITS values of the NA modified mixtures compared to the pure mixture indicate that they can provide a longer service life by resisting to tensile stresses that cause crack formation.
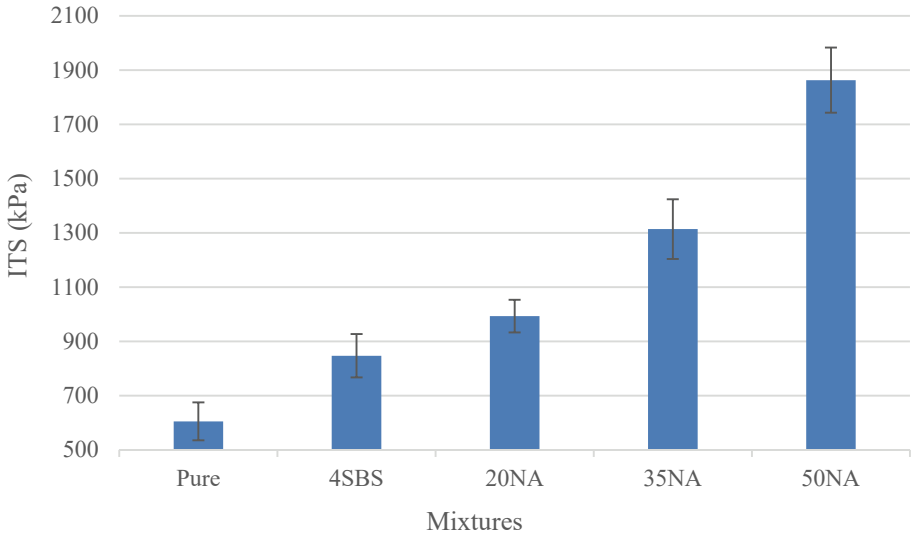
Fig. 6 - Indirect tensile strength (ITS) values of mixtures.
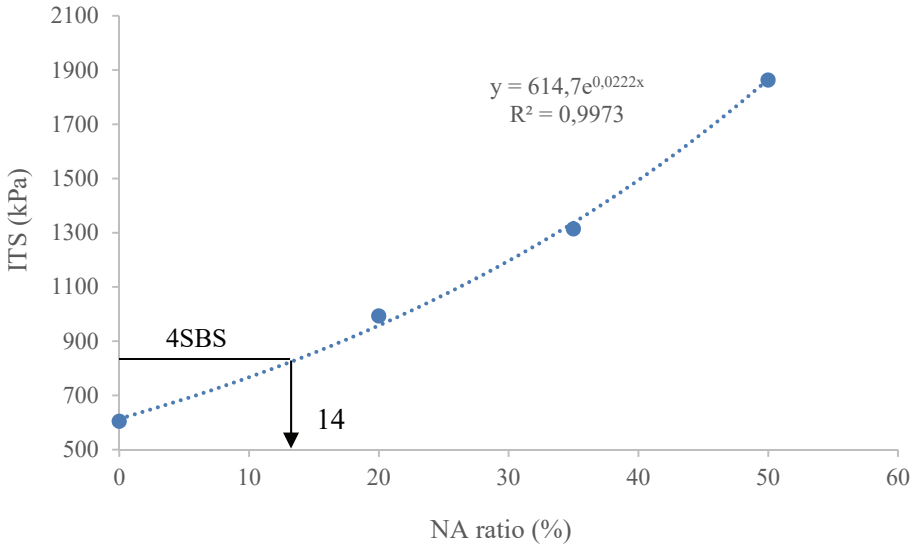
Fig. 7 - The change of ITS values against NA ratio.

3.3. Indirect Tensile Stiffness Modulus Test

The stiffness modulus, which is a measure of the load distribution capability of bituminous layers, is one of the most important performance characteristics of bituminous hot mixtures

[26]. This experiment is a non-destructive test defined by the BS DD 213 standard and the stiffness modulus (Sm, MPa) is calculated by Formula 2.

$$Sm = F(R+0.27) / LH \tag{2}$$

Where F is the maximum vertical load (N); H, mean horizontal deformation (μm) resulting from 5 repetition of loads; L, mean sample thickness (mm); R is the Poisson's ratio (0.35). The test was carried out at 25°C with deformation control. The target deformation is taken as 6 μm, the loading period is 3 seconds and the rise time is 0.124 s. Samples were stored at the test temperature for 2 hours before starting the experiment. Four samples were tested for each type of mixtures. Since the test is non-destructive, each sample was tested at three different position, hence the average of 12 value for each sample was taken into consideration.

The ITSM values of the mixtures are given in Fig. 8 with increasing order. The ITSM values of the 20NA, 35NA and 50NA mixtures were 1.80, 2.42 and 4.34 times higher than the pure mixture, respectively. Especially after 35% NA content, the increase in ITSM values of mixtures is much higher. The fact that ITSM values, which are the indicators of the load distribution capability, are significantly higher in the NA modification compared to the pure mixture means that the effect of heavy loads will be long lasting without a crack. The 4SBS mixture gave a similar performance with the 20NA mixture giving 1.7 times higher ITSM value than the pure mixture. The similar performance of the 4SBS mixture is obtained by a modification of 19% NA according to Fig. 9.
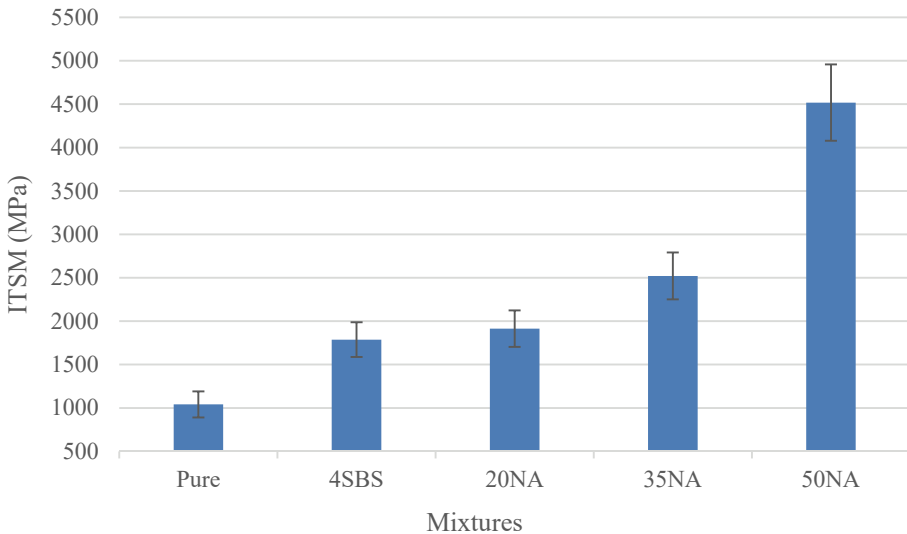
Fig. 8 - Indirect tensile strength modulus (ITSM) values of mixtures.
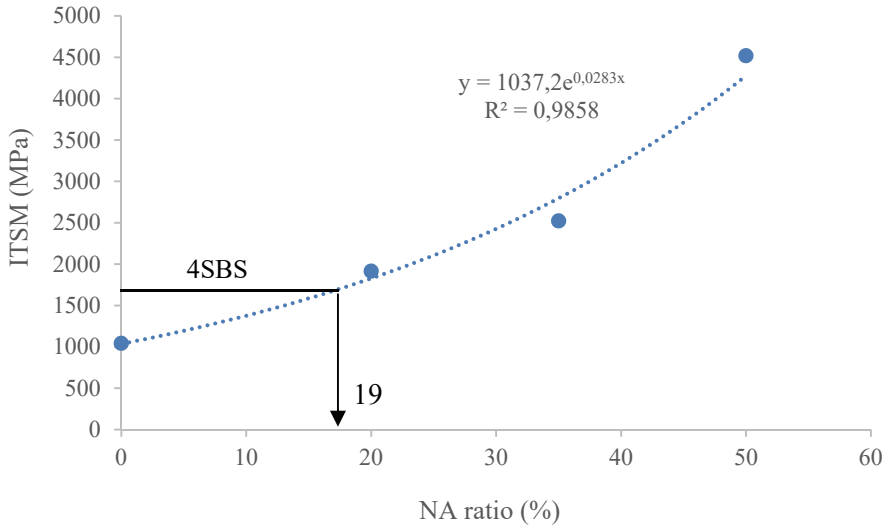
Fig. 9 - The change of ITSM values against NA ratio.

3.4. Indirect Tensile Repetitive Loading Test

Road pavements are subjected to a short-time loading on each vehicle wheel pass. This creates a very small damage that causes a decrease in the rigidity of the material. With the accumulation of these damages, the material deteriorates for a long time. Fatigue strength is the ability to resist asphalt pavement without breaking under repeated traffic loads. The test was carried out at 25ºC. Constant-stress indirect tensile-fatigue test was conducted by applying a cyclic constant load of 210 kPa for 0.1 s followed by a rest period of 1.4 s.

Samples were stored at the test temperature for 3 hours before starting the experiment. At the end of this period, the sample was placed between the loading heads, the linear variable differential transformers (LVDTs) to measure the vertical deformation were set, sample height, diameter, stress level values and loading period were entered into the computer and the experiment was started (Fig.10). The test continued until all samples were completely broken except for 50NA.

All mixtures except the 50NA mixture were broken at about 4 mm deformation. However, the 50NA mixture did not break even at 32000 load repetitions. In this load repetition, the sample was deformed 0.6 mm and no crack formation was observed. Fig. 11 shows the change in the total permanent vertical deformation of the mixture by the repetition of the load. The pure, 4SBS, 20NA and 35NA mixtures was broken in 810, 2004, 3282 and 11580 load repetitions. The 50NA mixture showed a superior performance by resisting the effect of repetitive loads for a long time. The rate of deformation increase in the load-repetition curve of the mixtures initially occurred rapidly due to the compression of the air voids in the samples and then showed a linear increase. Finally, with the beginning of the crack, it shows a rapid increase again. In the 50NA mixture, the curve is still in the linear zone at 32000 load repetition and no cracks occur. According to the number of repetition loads at the 4 mm

deformation level, the 20NA and 35NA mixtures have 4.1 and 14.5 times more load cycles than the pure mixture, respectively. The use of natural asphalt additive increased the number of load repetitions of the mixtures with the same trend as other studies in the literature [9]. The pure mixture at the deformation level of 0.7 mm, which is the biggest deformation seen by the 50NA mixture, has only 144 load repeats, so that according to this level of deformation, the 50NA mixture has 222 times greater load repeats than the pure mixture. In particular, the use of more than 20% natural asphalt increases the fatigue resistance of the mixtures considerably. The 4SBS mixture can withstand 2.5 times more load repetition than the pure mixture. The same performance with the 4SBS mixture can be obtained by 13% natural asphalt modification as seen from Fig. 12.
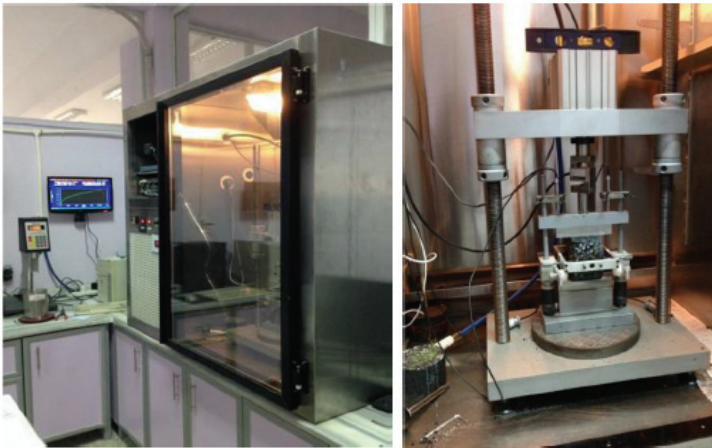
Fig.10 - Indirect tensile fatigue test equipment
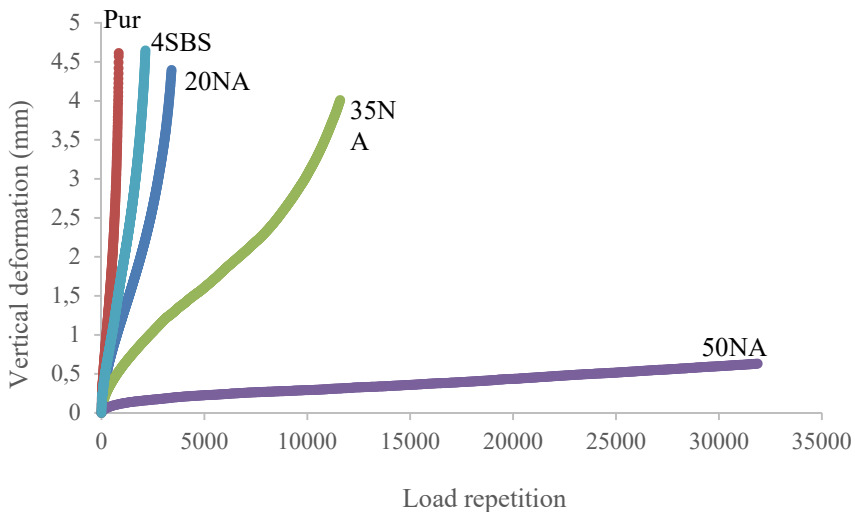
Fig. 11 - Load repetition - deformation relationship.
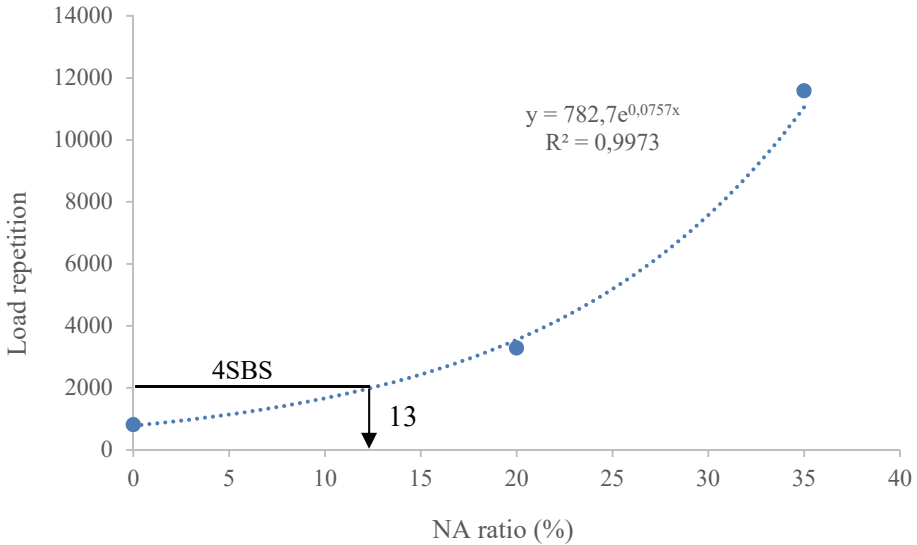
Fig. 12 - The change of load repeat against NA ratio at 4 mm deformation.

3.5. Dynamic Creep Test

The dynamic creep test is an important test used to determine the resistance of bituminous mixtures against permanent deformations and has a high correlation with the rutting resistance [27]. In the experiment, the deformations occurring together with the repetition of the load increased rapidly due to the compression of the air voids in the sample, then continued linearly in the consolidated sample and increased rapidly after the sample began to lose its integrity [28]. Creep stiffness is determined from the following formula [29].

$$E_c = \frac{\sigma}{\varepsilon_c} \tag{4}$$

Where Ec is the creep stiffness (MPa); σ is the applied dynamic stress (MPa); and ε_c is the total permanent strain. The test was carried out at a temperature of 50ºC under 0.5 MPa cycling stress. The samples were incubated at the test temperature for 3 hours before starting the experiment. In the experiment, square wave load was applied in the loading period of 1000 ms with 500 ms rest time. Samples were subjected to a conditioning static stress under 0.1 MPa for 10 minutes before starting the experiment.

In this high temperature, the resistance of the samples to the formation of permanent deformation under the influence of repeated loads was evaluated. Fig. 13 shows the variation of the total permanent strain with the repetition of loads in the mixtures. Here, as in the fatigue test, the deformation is initially linear after a rapid increase and then tends to increase rapidly again because of the loss of integrity of the mixture in the third zone. The increase in the third region is clearly seen in the pure and 20NA mixture. In the other mixtures, the test was
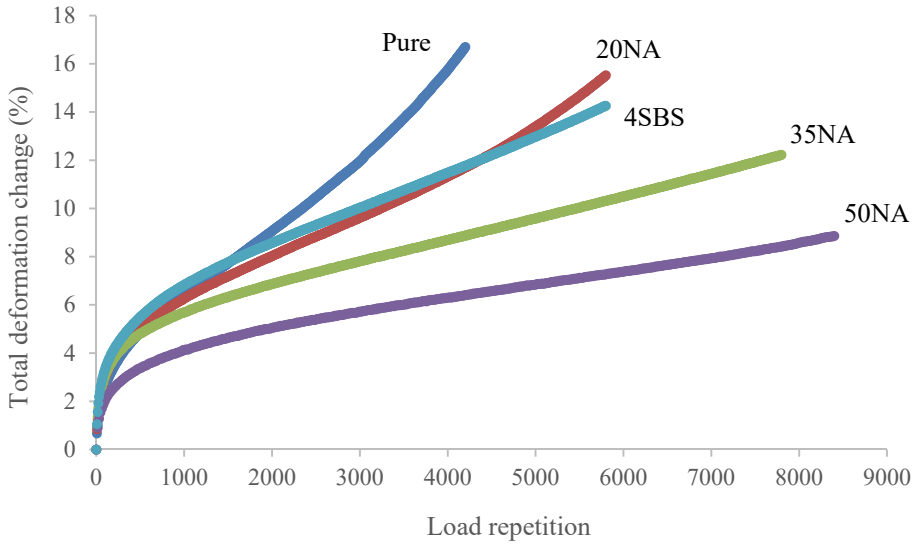
Fig. 13 - Load repetition - strain relationship.
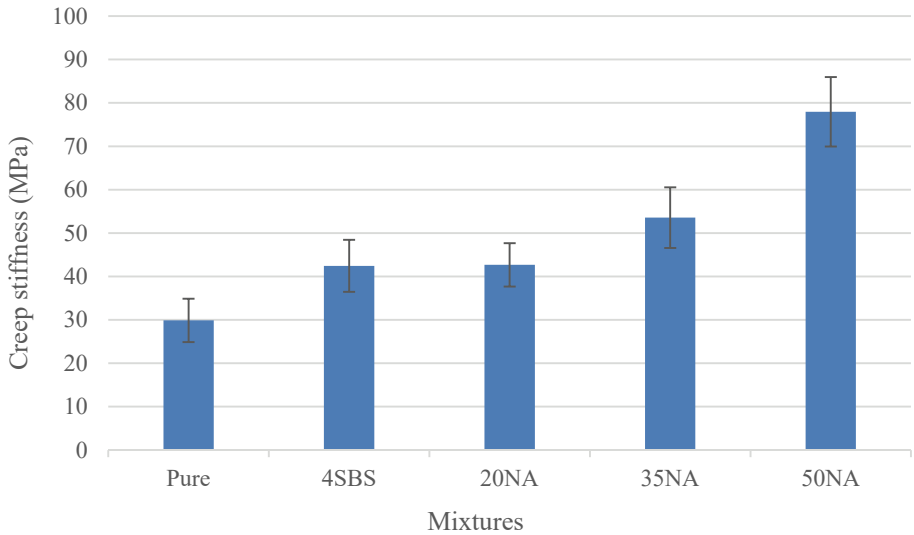
Fig. 14 - Creep stiffness values of mixtures.

terminated until the strains in the samples were passed to the third region. It is seen that 4SBS and 20NA mixtures have similar performance compared to the pure mixture until the 2000 load repetition but the pure mixture has lost its integrity after this repetition. In the pure mixture, the experiment continued until 4200 load repetitions, and the creep stiffness values at the 4200 load repeats were considered in the other mixtures. Fig. 14 shows the change of creep stiffness values. The increase in creep stiffness is evident after 20% natural asphalt content, as in other experiments. The creep stiffnesses of the 20NA, 35NA and 50NA mixtures are 1.4, 1.8 and 2.6 times higher than the pure mixture, respectively. It is clear that natural asphalt mixtures will be highly resistant to permanent deformations caused by repetitive loads at high temperature relative to the pure mixture. The 4SBS mixture gives a creep stiffness value of 1.4 times the pure mixture. The creep stiffness of the 4SBS mixture can be obtained by 22% natural asphalt modification as shown in Fig. 15. When 8% strain level at which 50NA samples reach at the end of the test is considered as a threshold value, it was determined that pure, 4SBS, 20NA, 35NA and 50NA samples have 1600, 1632, 1976, 3216 and 7136 load repetition numbers, respectively. It can be concluded that pure, 20NA and 4SBS mixtures do not behave very differently at this strain level which can be occurred at the early stage of the pavement.
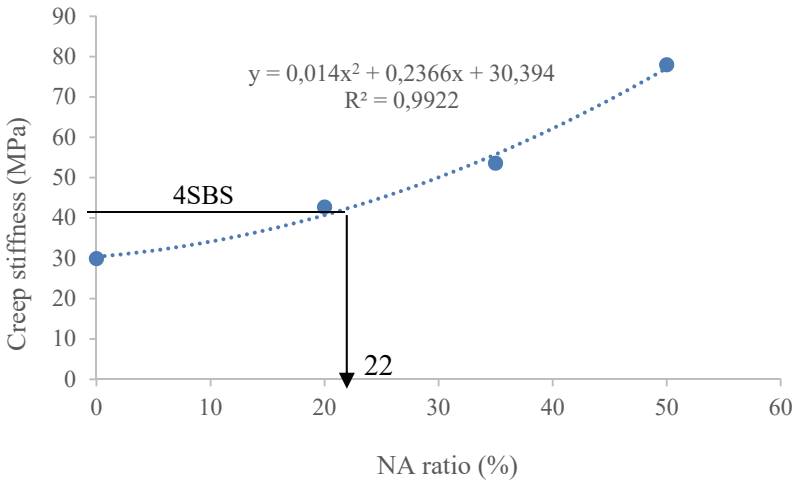
Fig. 15 - The change of creep stiffness against NA ratio at 4200 load repeats.

Table 5 - Equations used to determine the flow number of mixtures.

Mixture	Equation	R^2	FN
Pure	$y = -0.0098x^2 + 65.453x + 19095$	0.993	3339
20NA	$y = -0.0059x^2 + 63.401x + 19288$	0.997	5373
35NA	$y = -0.004x^2 + 68.604x + 20554$	0.998	8576
50NA	$y = -0.0044x^2 + 89.533x + 31903$	0.998	10174
4SBS	$y = -0.0047x^2 + 58.615x + 16550$	0.998	6235
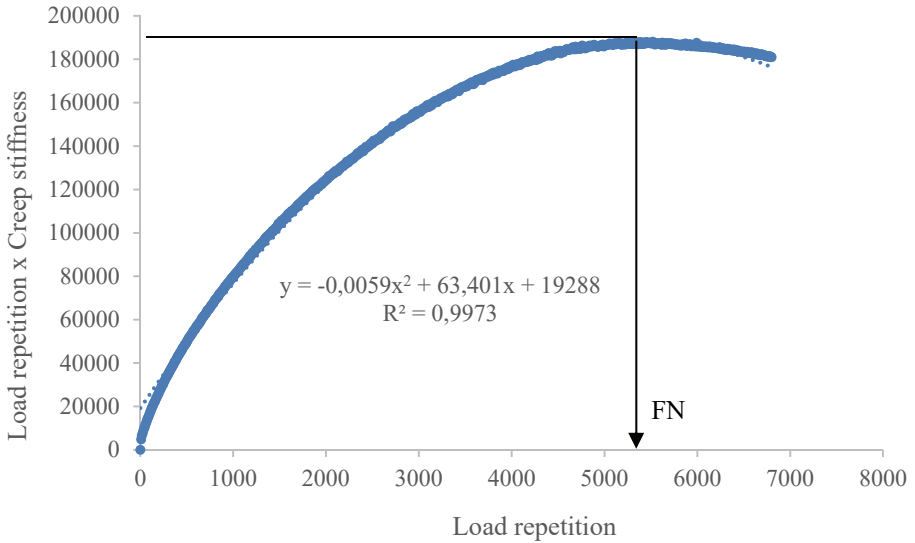
Fig. 16 - Determination of the flow number (FN).
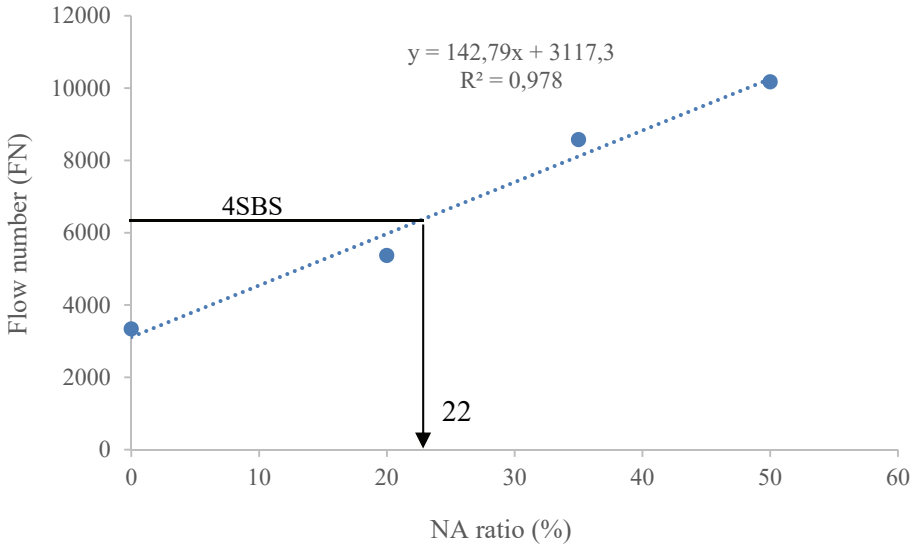
Fig. 17 - The change of the flow number against the NA ratio.

The flow number (FN), which is closely related to the rutting resistance of the mixtures, is determined as the turning point of the curve in the graph of the load repetition product creep stiffness versus load repetition [30,31]. Fig. 16 shows a graph of the 20NA mixture as an example. The second-degree parabolic equation which is adapted to the points that make up

the graph was determined and given in Table 4. The change of FN and natural asphalt content is given in Fig. 17. The flow number shows a linear increase with the increase of natural asphalt content. The flow numbers of the 20NA, 35NA and 50NA mixtures were 1.6, 2.5 and 3 times higher than the pure mixture, respectively. The flow number of 4SBS mixture is 1.9 times greater than the pure mixture. The flow number of the 4SBS mixture can be achieved by 22% natural asphalt modification as shown in Fig. 17.

4. CONCLUSION

In the study, mechanical tests were applied to bituminous mixtures prepared with binders modified by 20%, 35% and 50% Iraq natural asphalt and 4% SBS by bitumen weight and the performance of the mixtures were compared. The results are given below.

The 4SBS mixture gave only 6.7% greater stability than the pure mixture, while 20NA, 35NA and 50NA mixtures gave 7%, 19% and 32% greater stability, respectively. According to the stability / flow rates, the 50NA mixture shows 14% more rigid behaviour than the pure mixture. The stability of the 4SBS mixture is achieved by 14% NA modification.

According to the indirect tensile strength test, the 50NA mixture gave 180% higher ITS value than the pure mixture. ITS experiment, which is in static mode, emphasizes the effectiveness of additive usage according to Marshall experiment. The performance of the 4SBS mixture in terms of ITS is obtained by 14% NA modification.

ITSM values, which are a measure of the load distribution capability, were determined to increase significantly in natural asphalt modified mixtures. Especially after the 35% NA content, the increase in the ITSM values of the mixtures is much more. The performance of the 4SBS modified mixture in terms of ITSM is obtained by modification of 19% NA.

In the indirect tensile repetitive loading test, 20NA and 35NA mixtures gave 4.1 and 14.5 times more repeats than the pure mixture, respectively. 50NA modified mixture was not broken even at 32000 load repetition. At 0.7 mm deformation level, the 50NA mixture has 222 times greater load repeats than the pure mixture. The performance of the 4SBS mixture may be obtained with 13% NA modification.

The creep stiffness and flow numbers of the mixtures were determined in the dynamic creep test. Accordingly, the creep stiffness of the 20NA, 35NA and 50NA mixtures were found to be 1.4, 1.8 and 2.6 times higher than the pure mixture, respectively. According to the flow numbers, these ratios are 1.6, 2.5 and 3 times respectively. The performance of the 4SBS mixture according to both creep stiffness and flow number is achieved by 22% NA modification.

Natural asphalt modification has been found to be very successful in improving mechanical properties in static and dynamic experiments. Considering all experiments, it was determined that the 17.3% NA modification gave similar characteristics with 4% SBS modification. The use of natural asphalt, which is 20% cheaper than pure bitumen, rather than SBS, which is about 5-6 times more expensive than pure bitumen [32, 33], will provide a very significant economy without adversely affecting the overall performance.

References

[1] Meyer, R.F., De Witt W., Definition and world resources of natural bitumens. US Government Printing Office, 1990.

[2] Liao, M.C., Chen, J.S., Airey, G.D., Wang, S.J., Rheological behavior of bitumen mixed with Trinidad lake asphalt: *Construction and Building Materials*, 2014, DOI: 10.1016/j.conbuildmat.2014.05.068.

[3] Xu, S., Huang, W., Cai, F., Huang, H., Hu, C., Evaluation of properties of Trinidad Lake Asphalt and SBS-modified petroleum asphalt. *Petroleum Science and Technology*, 37(2):234-241,2019.

[4] Jahanian, H.R., Shafabakhsh, G., Divandari, H., Performance evaluation of Hot Mix Asphalt (HMA) containing bitumen modified with Gilsonite: *Construction and Building Materials*, 2017, DOI: 10.1016/j.conbuildmat.2016.11.069.

[5] Hamidi, H., Stiffness modulus and permanent deformation characteristics of asphalt mix containing gilsonite. Master's Thesis, Institute Technology Bandung, 1998.

[6] Babagoli, R., Hasaninia, M., Mohammad Namazi, N., Laboratory evaluation of the effect of gilsonite on the performance of stone matrix asphalt mixtures: *Road Materials and Pavement Design*, 2015, DOI: 10.1080/14680629.2015.1042016.

[7] Balık, G., Yılmaz, M., Kök, B.V., Alataş, T., Effects of Mixing Temperature on the Mechanical Properties of Hot Mix Asphalt: *Teknik Dergi,* 2019 (4), 9221-9241.

[8] Li, R., Wang, P., Xue, B., Pei, J., Experimental study on aging properties and modification mechanism of Trinidad lake asphalt modified bitumen: *Construction and Building Materials*, 2015, DOI: 10.1016/j.conbuildmat.2015.10.155.

[9] Yilmaz, M., Çeloğlu, M.E., Effects of SBS and different natural asphalts on the properties of bituminous binders and mixtures: *Construction and Building Materials*, 2013, DOI: 10.1016/j.conbuildmat.2013.03.036.

[10] Ameri, M., Mansourian, A., Ashani, S. S., & Yadollahi, G. (2011). Technical study on the Iranian Gilsonite as an additive for modification of asphalt binders used in pavement construction. Construction and Building Materials, 25(3), 1379-1387.

[11] Suo, Z., & Wong, W. G. (2009). Analysis of fatigue crack growth behavior in asphalt concrete material in wearing course. Construction and Building Materials, 23(1), 462-468.

[12] Kök, B. V., Yílmaz, M., Turgut, P., & Kuloğlu, N. (2012). Evaluation of the mechanical properties of natural asphalt-modified hot mixture. International journal of materials research, 103(4), 506-512.

[13] Said, S. F., & Hakim, H. (2009). Performance evaluation of fatigue cracking in flexible pavement (No. 09-0365).

[14] Zou, G., & Wu, C. (2015). Evaluation of rheological properties and field applications of Buton rock asphalt. Journal of Testing and Evaluation, 43(5), 1146-1156.

[15] Ma, F., & Zhang, C. (2013). Road performance of asphalt binder modified with natural rock asphalt. In Advanced Materials Research (Vol. 634, pp. 2729-2732). Trans Tech Publications Ltd.

[16] Li, J., Zhang, X. N., Liu, Y., & Wu, C. H. (2013). Effect of Rock Asphalt on the Surface Free Energy of Asphalt. In Advanced Materials Research (Vol. 785, pp. 963-966). Trans Tech Publications Ltd.

[17] Zhong, K., Yang, X., & Luo, S. (2017). Performance evaluation of petroleum bitumen binders and mixtures modified by natural rock asphalt from Xinjiang China. Construction and Building Materials, 154, 623-631.

[18] Tarefder, R. A., and S. S. Yousefi. 2016. "Rheological examination of aging in polymer-modified asphalt." J. Mater. Civ. Eng. 28 (2): 04015112.

[19] Airey, G. D. 2003. "Rheological properties of styrene butadiene styrene polymer modified road bitumens." Fuel 82 (14): 1709–1719.

[20] Liang, M., P. Liang, W. Fan, C. Qian, X. Xin, J. Shi, and G. Nan. 2015. "Thermo-rheological behavior and compatibility of modified asphalt with various styrene-butadiene structures in SBS copolymers." Mater. Des. 88: 177–185.

[21] Aglan, H., A. Othman, L. Figueroa, and R. Rollings. 1993. "Effect of Sytrene-butadiene-styrene block copolymer on fatigue crack propagation behavior of asphalt concrete mixtures."

[22] Ali Khodaii, Amir Mehrara, Evaluation of permanent deformation of unmodified and SBS modified asphalt mixtures using dynamic creep test, Construction and Building Materials Volume 23, Issue 7, July 2009, Pages 2586-2592

[23] Mahmoud Ameri, Mostafa Vamegh, Reza Imaninasab, Hamed Rooholamini, Effect of nanoclay on performance of neat and SBS-modified bitumen and HMA, Petroleum Science and Technology, (2016) 34:11-12, 1091-1097.

[24] Haiying Fu, Leidong Xie, Daying Dou, Linfan Li, Ming Yu, Side Yao., Storage stability and compatibility of asphalt binder modified by SBS graft copolymer, Construction and Building Materials Volume 21, Issue 7, July 2007, Pages 1528-1533

[25] Zaniewski, J.P., Pumphrey, M.E., Evaluation of Performance Graded Asphalt Binder Equipment and Testing Protocol, 2004.

[26] Zoorob, S.E., & Suparma, L.B., Laboratory design and investigation of the properties of continuously graded Asphaltic concrete containing recycled plastics aggregate replacement (Plastiphalt): *Cement and Concrete Composites*, 2000, DOI: 10.1016/S0958-9465(00)00026-3.

[27] Kaloush, K.E., Witczak, M.W., J Assoc Asphalt Paving Technology 71:278, 2002.

[28] Little, D. N., Button, J. W., Youssef, H., Development of Criteria To Evaluate Uniaxial Creep Data and Asphalt Concrete Permanent Deformation Poteittial: *Transportation Research Record: Journal of the Transportation Research Board*, 1993.

[29] Feeley, A.J. (1994). UTM-5P universal testing machine hardware reference manual Industrial Process Controls Limited Boronia Australia.

[30] Witczak, M.W., Simple performance tests for permanent deformation of hot mix asphalt. *Transportation Research Record: Journal of the Transportation Research Board,* 2007.

[31] Bausano, J., Williams, C., A new approach to calculating flow number, 2007.

[32] https://www.alibaba.com/showroom/sbs-polymer.html

[33] https://www.tupras.com.tr/bitum-fiyatlari-guncel

Preparation and Performance Testing of SBS Modified Bitumens Reinforced with Halloysite and Sepiolite Nanoclays

Dilay UNCU[1]
Ali TOPAL[2]
Mehmet Özgür SEYDİBEYOĞLU[3]

ABSTRACT

In this study, halloysite and sepiolite nanoclays were used to reinforce SBS modified bitumens. The nanoclays used are different from the materials in the literature and have properties such as easy to find, economical and available from local sources. The mixing parameters were determined before production process. The polymer additive SBS was added into base bitumen at 3% and 5%, while the nanoclay additives were added into polymer modified bitumen at 2% and 4% ratios. The morphological structures were investigated under fluorescence microscope. Physical and rheological properties of the samples were compared. The phase separation cases were investigated by storage stability test. Furthermore, rutting performance of samples was measured with zero shear viscosity (ZSV) and multi stress creep recovery (MSCR) test methods.

Keywords: Polymer modified bitumen, halloysite, sepiolite, dynamic shear rheometer, zero shear viscosity, multiple stress creep recovery.

1. INTRODUCTION

Bitumen is a mixture of aliphatic, aromatic, and naphthenic hydrocarbons and it is commonly used in construction of roads [1]. Several types of failures (rutting, fatigue cracking and thermal cracking) occur during the service life of asphalt pavements [2]. Bitumen is provided to increase the low and high temperature performance, and to provide elasticity, and to reduce permanent deformation by using various additives [3]. Modification of bitumen improves

performance properties like oxidation, aging resistance, temperature sensitivity, adhesion, durability, rutting, and fatigue resistance [4, 5, 6].

In recent years, polymers having very long chain molecules consisting of several ordered small molecules, are used for the modification of bitumen [7]. The prevalent used polymers from the group of elastomeric block copolymers [8] and Styrene-Butadiene-Styrene (SBS) belongs to this group enhances the elasticity of bitumen. However, weak compatibility between SBS and bitumen causes separations especially at high storage temperatures. Thus, when the modified bitumen is exposed to heat, ultraviolet light and oxygen, the separation becomes even worse due to the unsaturated bonds in SBS [9, 10, 11]. The search for new additives has been done to eliminate this problem. Recently, nanomaterials as new additives have been used in many engineering fields.

At least one dimension of nanomaterials is between 1 and 100 nanometers. Nanomaterials show better and varied properties according to normal sized materials by means of high surface area and their small size [12]. Significant development is obtained in mechanical, thermal and barrier properties of bitumen by addition of several nanomaterials for modification [10, 13]. Furthermore, the rutting resistance and fatigue cracking are improved by usage of nanomaterials in bitumen and bituminous mixtures according to some researches in the literature [12].

Nanomaterials are used as additives in polymer modified bitumens (PMB) and also used alone for modification. The parameters like type of nanomaterials, ratios of additives, mixing method and conditions are used in these studies vary. According to the studies, 3-6%, 2-5% and 3-7% ratios of SBS are commonly used [10, 13, 14]. When the studies are examined, it is seen that nanoclays are mostly used as nanomaterial additives and the use of montmorillonite, which belongs to smectite clay group that the distance between layers is high, is quite common among nanoclays [10, 15, 16, 17]. The reasons for preference of nanoclays are easily attainability from natural sources and being economic. The usage percentages of nanoclays are 2%, 3% and 4% in general [14, 15, 18, 19]. Nanoclay addition solves separation, storing and transportation problems with reducing the density difference between bitumen and polymer [10, 20]. In addition, it has been observed that with this modification process, there are significant improvements in the thermal, mechanical and barrier properties of bituminous binders [10, 12, 13]. The reason for this improvement is that nanomaterials show different and superior properties due to their small sizes and high surface areas compared to other normal sized materials [12].

The properties of the samples were researched by conventional methods and compared with each other. The morphological structures of modified bitumen samples were investigated under fluorescence microscope. The rheological properties were utilized by DSR. The upper critical temperatures determined according to the Superpave Performance Grading (PG) system for base and modified bitumen samples using rutting parameter ($G^*/\sin\delta$). The loading and temperature effects on the unaged and aged bitumens performance were analysed at five different temperatures from 40°C to 80°C with 10°C increment at low frequency (0.01 Hz) and high frequency (10 Hz) levels. Rutting performances of all bitumen samples were also investigated with zero shear viscosity (ZSV) and multiple stress creep recovery (MSCR) tests.

2. EXPERIMENTAL

2.1. Materials

The base bitumen with a penetration grade of 50/70 was procured from Tupras Refinery, Aliaga/Izmir. Penetration [21] softening point [22], viscosity [23], rolling thin film oven test [24] and, in addition, penetration, softening point tests after RTFOT [21, 22] were performed as conventional test methods for characterizing the properties of the base bitumen. Brookfield Viscometer was used for viscosity test results at 135°C and 165°C. The results obtained from these tests are presented in Table 1.

Table 1 - The properties of the base bitumen

Test	Specification	Results	Specification limit
Penetration (25°C; 0.1 mm)	ASTM D5	65	50-70
Softening point (°C)	ASTM D36	53.7	46-54
Viscosity at 135°C (cP)	ASTM D4402	425	-
Viscosity at 165°C (cP)	ASTM D4402	112.5	-
Rolling thin film oven test (RTFOT)	ASTM D2872		
Change of mass (%)		0.16	0.5 (max.)
Retained penetration (%)	ASTM D5	82	50 (min.)
Softening point after RTFOT (°C)	ASTM D36	58.3	48 (min.)
Flash point (°C)	ASTM D92	334	230 (min.)

Kraton® D1101 is used as a modifier of bitumen for roads. The SBS block copolymers are composed of blocks of styrene and butadiene and the properties belong to SBS in this study are seen in Table 2.

In this paper, halloysite and sepiolite were used for reinforcing PMB with a high shear mixer. These are two different Turkish natural clays that are abundant in Turkish mines and they have two different distinct shapes at the nanoscale. Sepiolite is a needle like structure that can reinforce the matrix. The other clay Halloysite is natural clay that has tubular structure at the nanoscale. The morphology is different and thus the rheology and the asphalt reinforcement are different compared to sepiolite. These two clays are close in chemical composition to layered clays like montmorillonite. In this study these two nanoclays were used as alternative additives for modification.

The above mentioned nanoclays were supplied from ESAN Company for adding into PMB and producing nanocomposites. The contents of halloysite and sepiolite nanoclays are depicted in Table 3 and 4.

Table 2 - Typical properties of Kraton® D1101 SBS [25]

Property	Test Method	Units	Typical Value
Elongation at break	ISO 37	%	880
Tensile strength	ISO 37	Mpa	33
Specific gravity	ISO 2781		0.94
Hardness, shore A(30 sec)	ISO 868	Hardness, Shore A (30 sec)	72
300% Modulus	ISO 37	MPa	2.9
Melt flow ratio, 200°C/5kg	ISO 1133	g/10 min.	<1
Bulk density	ASTM D 1895 method B	kg/dm^3	0.4

Table 3 - Chemical analysis of halloysite

Content	AZ. (Lol)	SiO_2	Al_2O_3	Fe_2O_3	TiO_2	CaO	MgO	Na_2O	K_2O
(%)	16.50 ±1.00	43.00 ±1.50	37.50 ±1.50	0.70 ±0.10	0.10 ±0.05	0.10 ±0.05	0.15 ±0.05	0.05 ±0.01	0.30 ±0.05

Table 4 - Chemical analysis of sepiolite

Content	SiO_2	Al_2O_3	Fe_2O_3	TiO_2	CaO	MgO	Na_2O	K_2O
(%)	18.45	0.84	0.218	0.029	21.64	22.27	0.13	0.11

2.2. Preparation of Samples

The samples were produced by a high shear mixer at 180°C and 2000 rpm. In this method SBS was added into the base bitumen and mixed for 15 minutes firstly. Then halloysite and sepiolite were added into the mixture and mixed for 45 minutes more. These production parameters were determined in the light of the literature as a result of viscosity measurements. 3% and 5% ratios were selected for SBS as the weight of the base bitumen according to minimum and maximum ratios in the literature [26, 27] and similarly nanoclays were used at 2% and 4%.

2.3. Test Methods

2.3.1. Conventional Bitumen Tests

The conventional bitumen tests were implemented for bitumen samples. Penetration [21], softening point [22], viscosity [23], storage stability [28], rolling thin film oven test (RTFOT)

[24], and in addition, penetration and softening point after RTFOT were applied on all samples. The results of viscosity were measured at 135°C and 165°C.

2.3.2. Morphological Structure

Fluorescent microscope was operated for investigating the morphological structure of the samples. The morphology term is used to define the properties of microstructure between bitumen and polymer [29]. Fluorescent microscopy helps to understand the morphologic structure of samples by examining the quality of the dispersion. The working principle of fluorescent microscopy is that polymers swell due to absorption of some of the components of the base bitumen under fluoresce in ultraviolet light. The bitumen phase looks dark or black and the polymer phase seems light [30]. Leica DMEP fluorescent microscope was used for investigating the images of all modified bitumen samples.

2.3.3. Rheological Test Methods

Dynamic rheological tests were applied to define the viscous and elastic behaviour of bitumen samples by using DSR. The tests were implemented with parallel plates and the diameter of plates was 25 mm with 1 mm gap. The unaged and RTFOT aged samples are subjected to DSR tests.

The viscous and elastic behaviour of bitumen as represented by the complex shear modulus (G^*), shear storage modulus (G'), shear loss modulus (G") and phase angle (δ) are measured by DSR. Rutting and fatigue behaviours are represented with G^* and δ. The $G^*/\sin\delta$ and $G^*.\sin\delta$ are defined as rutting resistance and fatigue cracking performance parameters respectively [24].

Lately, it has been stated that $G^*/\sin\delta$ parameter is not efficient and unsuccessful for predicting the rutting performance. For this reason, as an alternative to $G^*/\sin\delta$, the value of zero shear viscosity is recently used. ZSV is the viscosity measured in shear deformation, when the shear rate approaching zero [25]. In this study, determination of ZSV was performed by the implementation of creep test.

In this creep test, a constant shear strain is applied to the bitumen sample, and the exiting strain is observed for a prespecified period of time. If the stress is applied for a sufficient period, the bitumen deformation rate takes a constant value corresponding to the steady state flow of bitumen. At this stage, the viscosity is determined as the steady state viscosity or the ZSV [26]. The ZSV values have been estimated by implementation of creep test at 60°C and the test was carried out according to CEN/TS 15325 standard [27]. The creep test geometry is composed of 25 mm parallel plates. The gap between the plates is 1 mm. The value of stress is 10 Pa for base bitumen and 30 Pa for modified bitumens. Each creep test proceeds for 30 minutes. Time-creep and time-creep compliance graphs are obtained at the end of the test. When it reaches steady state, the curve of time-creep compliance becomes closer to the line. The slope of the time-creep compliance curve in the last 15 minutes (900 seconds) before removing the load is calculated by the following Eq. (1) with the average slope $\Delta t/\Delta J$ stable viscosity value is zero shear viscosity.

$$ZSV = \Delta t/\Delta J = 900/(J_f\text{-}J_{15}) \tag{1}$$

In Eq. (1) J_{15} symbolizes the compliance stated in Pa^{-1}, measured last 15 minutes before removing the loading, J_f is the compliance stated in Pa^{-1}, measured at the end of the 30 minutes. The expression 900 is indicated the time interval between the two measurements as seconds [28].

The latest development to the Superpave Performance Graded (PG) Asphalt Binder specification is the multiple stress creep and recovery (MSCR) test. DSR is used for the test and the test is applied to short term aged samples [29]. The MSCR test was performed according to ASTM D7405-08 standard [30]. 25 mm parallel plates with 1 mm gap and 60°C temperature value are used for the test. The bitumen sample is exposed to creep loading and unloading cycle of 1 s and 9 s, at 100 Pa and 3200 Pa stress levels and 10 cycles for both stress levels. Two main parameters, the non-recoverable creep compliance (J_{nr}) and percent recovery (%rec), are calculated from the test results for evaluating the rutting sensibility. The difference in J_{nr} between two stress levels is calculated to detect the stress sensibility of the sample and expressed as percentage $J_{nr,diff}$.

2.4. Result and Discussions

2.4.1. Conventional Test Results

The conventional properties of the samples are presented in Table 5. In the table, halloysite and sepiolite were shortened as "Hal" and "Sep" respectively.

The test results of conventional bitumen tests indicated that all modified samples had a remarkable decline in penetration and increment in temperature of softening point according to base bitumen. Table 5 shows decline in penetration values and an increment in softening point temperature especially for 3% SBS and nanoclay modified bitumen samples. A less decrease in penetration value is identified for 5% SBS and modified bitumen samples reinforced with nanoclay. Softening point temperatures of 5% SBS + 2% Hal and 5% SBS + 2% Sep modified bitumen are lower than 5% SBS modified bitumen, 5% SBS + 4% Hal and 5% SBS + 4% Sep modified bitumen have close values with 5% SBS modified bitumen. After short term aging, a decrease is observed in penetration values in all samples except 3% SBS + 2% Sep and 3% SBS + 4% Sep modified bitumen. In softening point temperatures after short term aging, 3% SBS and nanoclay modified bitumen samples have lower values according to 3% SBS modified sample. It is thought that nanoclays prevent aging of PMB due to complicated oxygen diffusion. In 5% SBS and nanoclay modified bitumen samples, softening point temperatures increased except 5% SBS + 2% Sep modified bitumen. It is predicted that the amount of nanoclays has been insufficient and properties of polymer has become dominant.

The flow resistances of all samples were obtained by viscosity values. The viscosity test results are lower at high temperature values because the bitumen samples became more viscous. All modified bitumen samples had high viscosity values according to the base bitumen for both temperatures. The addition of 3% SBS roughly increased the viscosity values two times and the addition of 5% SBS increased viscosity four times. The nanoclay

Table 5 - Results of the conventional bitumen tests conducted on base bitumen, polymer and nanoclay modified bitumen samples

Test	Standard	Base Bitumen	3% SBS	3% SBS+2% Hal	3% SBS+4% Hal	3% SBS+2% Sep	3% SBS+4% Sep	5% SBS	5% SBS+2% Hal	5% SBS+4% Hal	5% SBS+2% Sep	5% SBS+4% Sep
Penetration (25°C, 0.1 mm.)	ASTM D 5-06	65	59	51	50	56	53	52	51	51	49	48
Softening Point (°C)	ASTM D 36-06	53.7	57.9	58.5	57.4	56.4	56.7	77.9	73.7	77.0	72.0	77.9
Viscosity (135°C, cP)	ASTM D 4402-06	425	850	912.5	925	850	925	1563	1638	1700	1638	1725
Viscosity (165°C, cP)	ASTM D 4402-06	112.5	275	312.5	325	362.5	375	462.5	512.5	562.5	500	525
Penetration Index (PI)		0.35	1.03	0.77	0.50	0.57	0.49	4.14	3.47	3.96	3.10	3.92
After Rolling Thin Film Oven Test (RTFOT - ASTM D 2872-12)												
Change of mass (%)		0.160	0.068	0.085	0.074	0.073	0.064	0.090	0.060	0.062	0.054	0.052
Penetration (25°C, 0.1 mm.)	ASTM D 5-06	53	37	36	35	40	41	41	38	37	37	38
Retained penetration (%)		82	63	71	70	71	77	79	75	73	76	79
Softening Point (°C)	ASTM D 36-06	58.3	64.1	63.7	62.5	63.3	61.3	70	72.9	73.8	69.2	74.8
Increase/decrease in softening point (°C)		4.6	6.2	5.2	5.1	6.9	4.6	-7.9	-0.8	-3.2	-2.8	-3.1
Storage Stability Test												
Softening point (°C) Upper segment	ASTM D 36-06	-	63.8	62.4	58.6	61.1	58.2	89.6	88.5	83.9	86.6	85.8
Softening point (°C) Lower segment	ASTM D 36-06	-	56.2	60.8	57.5	60.5	58.5	62.1	61.2	68.8	74.8	64.8
Difference (°C)		-	7.6	1.6	1.1	0.6	-0.3	27.5	27.3	15.1	11.8	21

addition into the PMB also increased the viscosity values. The 3% SBS + 4% Sep has the highest viscosity for two temperatures between 3% SBS and nanoclay modified bitumens. The 5% SBS + 4% Sep has the highest viscosity at 135°C and the 5% SBS + 4% Hal has the highest viscosity at 165°C between 5% SBS and nanoclay modified bitumens. The increment in viscosity is permitted in the specification up to 3000 mPa s at 135°C. The reason of the limitation is that the too high viscosity values negatively affect the bitumen workability. When the results of the viscosity test are examined, this undesirable situation isn't occurring for any samples.

The penetration index value expresses the temperature sensitivity of the bituminous binder and there is an inverse proportion between them. Increase of penetration index is an indicator about decrease of sensitivity to temperature. Penetration Index value less than -2 indicates that bitumen is very sensitive to temperature, and the value greater than +2 indicates that it is less sensitive to temperature [38]. The penetration indexes of all modified bitumen samples increased compared to base bitumen, so their sensitivity to temperature decreased. The polymer additive is more effective in decreasing the temperature sensitivity compared to the penetration index values, and the increase in the additive ratio decreased the sensitivity.

The lower storage stability values are better and it is desirable that the difference in softening point between the upper and lower does not exceed 5°C in the specification. When the test results of the modified bitumens are examined, the storage stability values are improved by adding nanoclay into the SBS modified bitumen. Only the storage stability of the SBS modified bitumen sample was above the limit value in the 3% SBS modified group, and the addition of nanoclays reduced the storage stability values to below the limit value of 5°C. The bitumen samples containing sepiolite have lower storage stability values than the bitumen samples containing halloysite. All the samples are seen to exceed the limit value in 5% SBS modified group due to the increase in the percentage of polymer. The storage stability values worsen as the percentage of polymer increases. In the previous studies in the literature, it is found that the increase in the amount of polymer negatively affects the storage stability [39, 40, 41] and it is stated that storage stability of polymer modified asphalts depends on many factors, especially asphalt composition, polymer characteristics and content [39]. However, with the addition of nanoclay, the storage stability values did not fall below the limit value, but lower values were obtained.

2.4.2. Examination of Morphological Structure

Thin section specimens were taken after completion the production of all modified bitumens. The specimens were examined under fluorescence microscopy and the information of the additives distribution in the bitumen phase was obtained. Dispersion of thin section specimens between lame and lamella of modified bitumens containing nanoclays has become more difficult, so this situation overlaps with increasing viscosity values.

When only the polymer modified sample in Figure 1.a is examined from the 3% modified bitumen samples, it is seen that the polymers have spread to the bitumen phase but formed thin bond structures. These bonds have gained volume and have spread to more areas in the bitumen phase with the addition of nanoclays in Figure 1.b, c and d. The microscope image of 3% SBS + 4% Sep modified bitumen sample cannot be obtained because of insufficient dispersion amount, so polymers and nanoclays cannot be distinguished in the image.
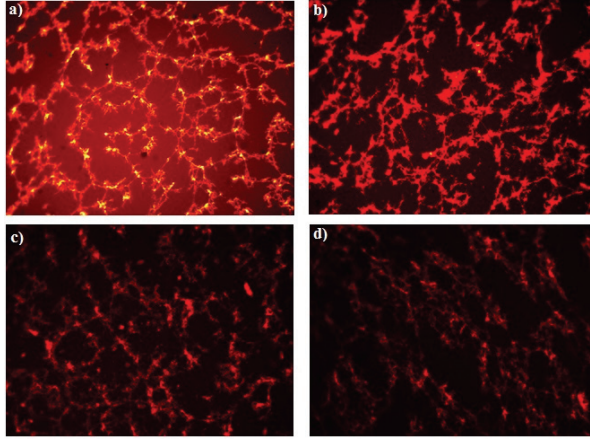
Figure 1 - Images of 3% polymer and nanoclay modified bitumen samples (10x)
(a) 3% SBS modified bitumen sample (b) 3% SBS + 2% Hal modified bitumen sample
(c) 3% SBS + 4% Hal modified bitumen sample
(d) 3% SBS + 2% Sep modified bitumen sample
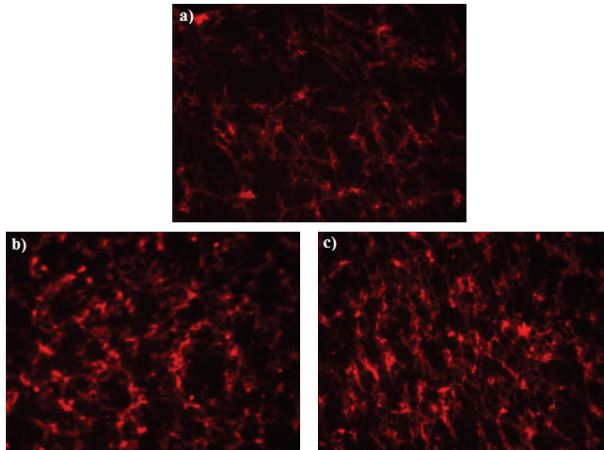
Figure 2 - Images of 5% polymer and nanoclay modified bitumen samples (10x)
(a) 5% SBS modified bitumen sample (b) 5% SBS + 2% Hal modified bitumen sample
(c) 5% SBS + 4% Hal modified bitumen sample

As seen in Figure 2.a, b and c, 5% PMB samples, more intensive bonds were formed, dispersion and occupied area of additives were increased with the usage of nanoclays in the PMB is shown by Figure 2.a, b and c. Similarly, due to the insufficient dispersion amount, the images of 5% SBS + 2% Sep and 5% SBS + 4% Sep modified bitumen samples were not obtained.

2.4.3. Dynamic Shear Test Results

Unaged and RTFOT aged bitumens were exposed to oscillatiion by DSR at 10 rad/s frequency (1.59 Hz) for determining upper critical temperature for PG system. The initial temperature values were set to 52°C and 64°C for respectively unaged and short term (RTFOT) aged bitumens with increments of 6°C. The upper critical temperatures were specified for each sample according to $G^*/\sin\delta$ results. The temperature is indicated the upper critical temperature at $G^*/\sin\delta$ is 1.0 kPa for unaged bitumen, and $G^*/\sin\delta$ is 2.2 kPa for short term aged bitumen sample [24]. The upper critical temperatures for each bitumens are seen in Table 6.

Table 6 - Determination of PG upper critical temperatures for base and modified bitumen samples

Type of Bitumen	Temperature (°C)	$G^*/\sin\delta$ (Pa)		Upper Critical Temperature
		Unaged	Aged	
Base bitumen	64	1622	4080	64-X
3% SBS	70	1784	3611	70-X
	76	931.8	2111	
3% SBS + 2% Hal	70	1834	4335	70-X
	76	892.4	2160	
3% SBS + 4% Hal	76	1059	4158	76-X
	82	562.1	2107	
3% SBS + 2% Sep	70	1877	3536	70-X
	76	986	1730	
3% SBS + 4% Sep	70	1601	4225	70-X
	76	965.8	2027	
5% SBS	76	1776	3225	76-X
	82	1184	1710	
	88	769.1	-	
5% SBS + 2% Hal	76	2018	3322	76-X
	82	1101	1767	
	88	612.8	-	
5% SBS + 4% Hal	76	2115	2613	76-X
	82	1353	1464	
	88	909.9	-	
5% SBS + 2% Sep	76	2331	3240	76-X
	82	1410	1719	
	88	904.6	-	
5% SBS + 4% Sep	76	2180	3444	76-X
	82	1410	1804.57	
	88	938.2	-	

It can be inferred from Table 6 that PG upper critical temperatures of modified bitumen samples are higher than base bitumen. The performance grades of modified bitumen samples have been risen one degree for 3% SBS modified group, and two degrees for 5% SBS modified group. The higher upper critical temperature is an indicator value of higher permanent deformation resistance.

The RTFOT aged bitumen samples were exposed to oscillation by DSR at low (0.01 Hz) and high (10 Hz) frequency levels at five temperatures ranging from 40°C to 80°C with 10°C increments. The variation of $G^*/\sin\delta$ values of base and modified bitumens at two frequency values are presented in Figure 3 and Figure 4.
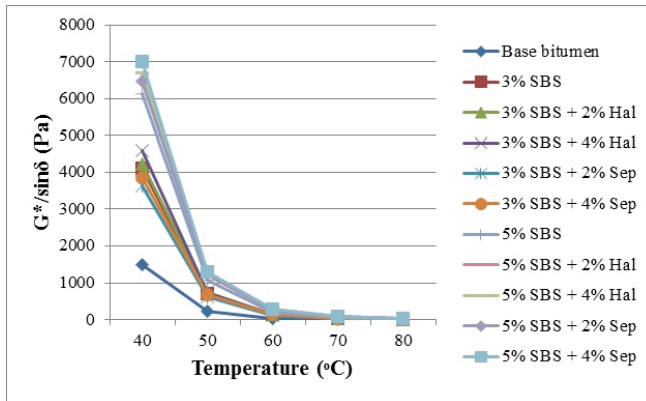
Figure 3 - $G^*/\sin\delta$ values of base and modified bitumen samples at 0.01 Hz
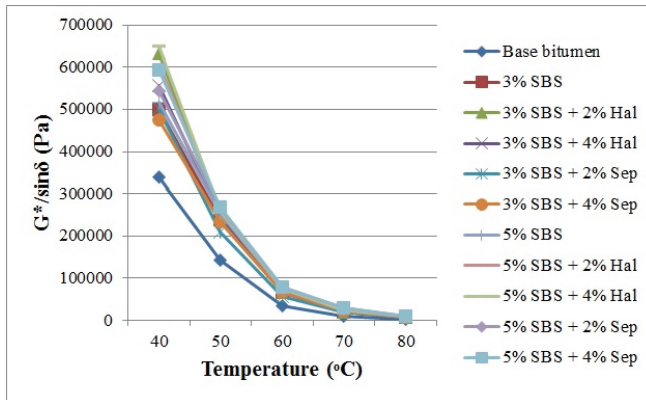
Figure 4 - $G^*/\sin\delta$ values of base and modified bitumen samples at 10 Hz

As can be seen in Fig. 3 and Fig. 4, concerning all samples, $G^*/\sin\delta$ values increase with decrease in temperature at two frequency values. The increase in $G^*/\sin\delta$ value specifies higher rutting performance. Furthermore, expectedly $G^*/\sin\delta$ values increase with increasing

frequency for all samples. This is owing to the rheological behavior of bitumen by reason of exhibiting elastic behaviour the bitumen under high frequency level or shorter loading times [42].

The rutting parameter of modified bitumen samples have been significantly increased at two different frequencies and five different temperatures according to the base bitumen. The $G^*/\sin\delta$ values improved by addition of SBS into the base bitumen, have been increased by addition of nanoclays into the PMB. This case is evidently observed on modified bitumen samples containing 5% SBS. 5% SBS + 4% Sep has the highest $G^*/\sin\delta$ value at low frequency and 5% SBS + 4% Hal has the highest $G^*/\sin\delta$ value at high frequency among the aged bitumen samples. These modified bitumen samples are the most resistant samples even as a result of expose to aging.

2.4.4. Zero Shear Viscosity Test Results

The results of ZSV for all bitumen samples obtained by DSR performed with creep mode are illustrated in Figure 5.
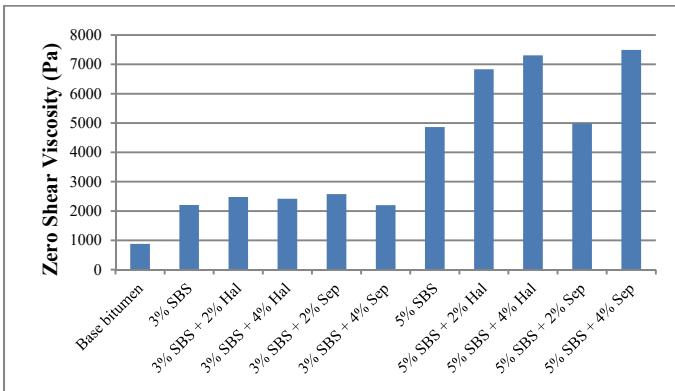
Figure 5 - ZSV values for base and modified bitumen samples

As seen in Figure 5, 5% SBS + 4% Sep sample has the highest ZSV value among the bitumen samples. As a result of the using of nanoclay in the group containing both 3% and 5% polymer additive, an increase in ZSV was observed compared to the only SBS modified bitumen. Higher ZSV values indicate higher resistance against permanent deformation during long term loading [34]. It is expected from modified bitumens that exposing the least deformation and giving the highest value of ZSV.

2.4.5. Multiple Stress Creep Recovery Test Results

The percent recovery (R), the non-recoverable compliance (J_{nr}) for 100 and 3200 Pa, stress sensibility and also the percent differences in non-recoverable compliances ($J_{nr-diff}$) of the bitumen samples are seen in Table 7.

The percentage of return of bitumen samples under a certain load has increased considerably by modifying the base bitumen. When the load on the sample was removed, it was found that the highest recovery was provided by the 5% SBS modified bitumen sample, followed by 5% SBS + 4% Sepiolite modified bitumen sample. This is thought to be due to the fact that the nanoclays do not have a flexible structure.

The higher compliance value (J_{nr}) indicates that the bitumen samples will be exposed to further deformation under a certain loading condition. Lower J_{nr} values specify lower sensibility to rutting. Base bitumen has the highest compliance value at two stress levels (100 and 3200 Pa) as expected. This shows that the base bitumen is the most susceptible bitumen type to rutting. However, 5% SBS modified bitumen sample has the lowest compliance values.

The stress sensibility of the bitumen samples was defined with the differences as percent for non-recoverable compliances ($J_{nr\text{-}diff}$). When the stress level is increased from 100 to 3200 Pa, the non-recoverable compliance value specifies the percentage of increment about J_{nr} of the sample.

Table 7 - MSCR test results for base and modified bitumen samples

Bitumen Type	R@100 Pa (%)	R@3200 Pa (%)	J_{nr}@100 Pa	J_{nr}@3200 Pa	$J_{nr\text{-}diff.}$ (%)	Stress Sensibility
Base Bitumen	6.493	3.167	1.126	1.183	5.061	0.051
3% SBS	18.044	13.474	0.461	0.499	8.104	0.081
3% SBS + 2% Hal	20.41	14.513	0.459	0.512	11.541	0.115
3% SBS + 4% Hal	18.523	14.325	0.395	0.418	5.794	0.058
3% SBS + 2% Sep	18.725	13.532	0.472	0.514	8.849	0.088
3% SBS + 4% Sep	16.834	12.467	0.496	0.534	7.751	0.078
5% SBS	45.437	41.956	0.104	0.111	6.345	0.063
5% SBS + 2% Hal	39.793	35.398	0.159	0.174	9.340	0.093
5% SBS + 4% Hal	42.017	36.705	0.16	0.181	12.509	0.125
5% SBS + 2% Sep	30.035	25.248	0.197	0.212	8.100	0.081
5% SBS + 4% Sep	49.505	40.478	0.171	0.205	19.844	0.198

It determines the sensibility against rutting when sudden loadings due to heavy traffic are implemented on pavement or extraordinary high temperatures are observed. This percent difference value is a measurement of the sensibility to the increase in the stress level; hence lower values are defined by a less stress sensible material [43, 44]. The $J_{nr\text{-}diff}$ value and stress sensibility are high for 5% SBS + 4% Sep sample, thus this modified bitumen is highly stress sensible at the stress level of 3200 Pa.

In addition, according to the MSCR test results, a new performance classification called PG Plus became a current issue. In this new classification method, the Jnr value at 3.2 kPa (3200 Pa) loading is taken into account at the temperature at which the test is performed. There are four traffic conditions according to the performance classification and named S (Standard: < 4.0 kPa^{-1} and standard traffic loading), H (Heavy: < 2.0 kPa^{-1} or slow moving traffic loading), V (Very Heavy: < 1.0 kPa^{-1} or standing traffic loading) and E (Extreme Heavy: < 0.5 kPa^{-1} ESALs and standing traffic loading) [45, 46]. PG Plus grades determined according to J_{nr} values under 3200 Pa loading obtained from MSCR test are presented in Table 8.

Table 8 - MSCR letter grades of base and modified bitumen samples

Bitumen Type	Superpave Performance Grade	J_{nr} @3200 (kPa^{-1})	PG Plus Grade
Base Bitumen	PG 64	1.183	PG 60 H
3% SBS	PG 70	0.499	PG 60 E
3% SBS + 2% Hal	PG 70	0.512	PG 60 V
3% SBS + 4% Hal	PG 70	0.418	PG 60 E
3% SBS + 2% Sep	PG 70	0.514	PG 60 V
3% SBS + 4% Sep	PG 70	0.534	PG 60 V
5% SBS	PG 76	0.111	PG 60 E
5% SBS + 2% Hal	PG 76	0.174	PG 60 E
5% SBS + 4% Hal	PG 76	0.181	PG 60 E
5% SBS + 2% Sep	PG 76	0.212	PG 60 E
5% SBS + 4% Sep	PG 76	0.205	PG 60 E

PG Plus grades increased as expected as a result of adding additives to base bitumen according to the results in Table 8. Although the class of 3% SBS modified bitumen is E, it has fallen to V class with the addition of 2% halloysite, but its values are very close to each other. The PG Plus grade rose again to E class with increase of halloysite amount and the rate

was 4%. As a result of the addition of sepiolite, there was no change in both ratios and remained constant in the V class. As a result of the 5% SBS modification, the grade rising to E class has also maintained its place with the addition of nanoclays. This MSCR letter implies that the sample can resist deformations even under extremely heavy traffic conditions.

3. CONCLUSION

As a result of the study, the conventional, rheological bitumen tests and examination of morphological structure have been utilized to evaluate the difference in the properties and performance of SBS modified bitumens containing nanoclay additives.

Conventional bitumen tests performed on two different ratios of SBS modified bitumen samples (3% and 5%) and each concentration containing 2%, 4% halloysite and sepiolite. A considerable decrease in penetration and increase in softening point temperatures of modified bitumen samples have been observed for all concentrations of additives compared to base bitumen. The decrease in penetration has been increased some more as a result of nanoclay addition into the PMB. The increase in softening point temperatures has showed a change according to the polymer ratio between PMBs containing nanoclays. The softening point temperatures have been increased for 3% SBS modified bitumen samples but have not been changed for 5% SBS modified bitumens.

It can be deduced from the viscosity test results that the addition of nanoclays increases viscosity for two temperature values. The viscosity values have been increased with increasing of nanoclay content. The storage stability results have been improved with addition of nanoclays especially in low SBS ratio. The improvement in storage stability has been reduced with increasing of SBS percentage.

The PG upper critical temperatures of modified bitumen samples are higher than base bitumen and advanced at least one degree as a result of the modification. The performance grade has increased two degrees in some modified bitumens. Higher upper critical temperature value indicates higher resistance against permanent deformation.

The results of DSR, $G^*/\sin\delta$ values have increased with an increment in frequency regarding all samples. Based on the $G^*/\sin\delta$ values at low and high frequencies, it has been seen that modification of base bitumen with SBS enhances the performance of base bitumen to rutting. Additionally, the rutting resistance of modified bitumens has been improved with using nanoclay additives in SBS modified bitumen samples.

According to ZSV results, it is deduced that increase of polymer percentage and addition of nanoclays improve rutting performance of modified bitumens.

Based on MSCR test results, especially high percentage of polymer is provided high recovery values. Besides, addition of nanoclays slightly decreases the recovery values because of low elastic behaviour of nanoclays. Bitumens have high percent recovery and low non-recoverable compliance values are more resistant to rutting under loading and unloading cycles. Otherwise the MSCR letters imply that polymer modified bitumen samples

containing nanoclays could remain resistant to deformations even under heavy and extreme heavy traffic conditions.

The results showed that nanoclays could be used as additives for improving physical and rheological properties of PMB samples. When all test results were evaluated with the limitation of storage stability results, it was seen that the addition of nanoclay in 3% SBS modified bitumens was more appropriate. This also revealed the result that determining an optimum value for the polymer ratio is very important. It is recommended that production in more detailed combinations for nanocomposites and further performance analyses are needed.

Acknowledgement

Symbols

G^* : complex shear modulus

G' : shear storage modulus

G'' : shear loss modulus

δ : phase angle

$G^*/\sin\delta$: rutting resistance parameter

$G^*.\sin\delta$: fatigue cracking performance parameter

Δt : 900 seconds time interval

ΔJ : difference between J_f and J_{15}

J_f : compliance measured at the end of the 30 minutes

J_{15} : compliance measured last 15 minutes before lifting the loading

J_{nr} : non-recoverable creep compliance

%rec : percent recovery

$J_{nr,diff}$: difference in J_{nr}

References

[1] Polacco, G., Stastna, J., Biondi, D., Zanzotto, L., Relation between polymer architecture and nonlinear viscoelastic behavior of modified asphalts, Current Opinion in Colloid & Interface Science, 11(4), 230-245, 2006.

[2] Polacco G., Kříž, P., Filippi, S., Stastna, J., Biondi, D., Zanzotto, L., Rheological properties of asphalt/SBS/clay blends, European Polymer Journal, 44(11), 3512-3521, 2008.

[3] Ahmedzade, P., Fainleib, A., Günay, T., Grigoryeva, O., Geri Dönüştürülmüş Atık Polipropilenin Bitümlü Bağlayıcılarda Kullanılması, Teknik Dergi, 456, 7497-7513, 2016.

[4] Aglan, H., Othman, A., Figueroa, L., Rollings, R., Effect of styrene-butadiene-styrene block copolymer on fatigue crack propagation behavior of asphalt concrete mixtures, Transportation Research Record, 1417, 178-86, 1993.

[5] Kumar P., Chandra S., Bose S., Strength characteristics of polymer modified mixes, International Journal of Pavement Engineering, 7(1), 63-71, 2006.

[6] Tayfur, S., Ozen, H., Aksoy, A., Investigation of rutting performance of asphalt mixtures containing polymer modifiers, Construction and Building Materials, 21(2), 328-37, 2007.

[7] Bulatović, V. O., Rek, V., Marković, K. J., Effect of polymer modifiers on the properties of bitumen, Journal of Elastomers & Plastics, 46(5), 448-469, 2014.

[8] Alatas, T., Yilmaz, M., Kuloglu, N., Cakiroglu, M., Geckil, T., Investigation of Shear Complex Modulus and Phase Angle Values of Short and Long-term Aged Polymer Modified Bitumens at Different Frequencies, KSCE Journal of Civil Engineering, 18(7), 2093-2099, 2014.

[9] Galooyak, S. S., Dabir, B., Nazarbeygi, A. E., Moeini, A., Rheological properties and storage stability of bitumen/SBS/montmorillonite composites, Construction and Building Materials, 24(3), 300-307, 2010.

[10] Golestani, B., Nejad, F. M., Galooyak, S. S., Performance evaluation of linear and nonlinear nanocomposite modified asphalts, Construction and Building Materials, 35, 197-203, 2012.

[11] Topal. A., Sureshkumar, M. S., Sengoz, B., Polacco, G., Rheology and microstructure of polymer-modified asphalt nanocomposites, International Journal of Materials Research, 103(10), 1271-1276, 2012.

[12] Yao, H., You, Z., Li, L. Goh, S. W., Lee, C. H., Yap, Y. K., Rheological properties and chemical analysis of nanoclay and carbon microfiber modified asphalt with Fourier transform infrared spectroscopy, Construction and Building Materials, 38, 327-337, 2013.

[13] Jasso, M., Bakos, D., MacLeod, D., Zanzotto, L., Preparation and properties of conventional asphalt modified by physical mixtures of linear SBS and montmorillonite clay, Construction and Building Materials, 38, 759-765, 2013.

[14] Sureshkumar, M. S., Filippi, S., Polacco, G., Kazatchkov, I., Stastna, J., Zanzotto, L., Internal structure and linear viscoelastic properties of EVA/asphalt nanocomposites, European Polymer Journal, 46, 621-633, 2010.

[15] Jasso, M., Bakos, D., Stastna, J., Zanzotto, L., Conventional asphalt modified by physical mixtures of linear SBS and montmorillonite, Applied Clay Science, 70, 37-44, 2012.

[16] Merusi, F., Giuliani, F., Polacco, G., Linear viscoelastic behaviour of asphalt binders modified with polymer/clay nanocomposites, Procedia-Social and Behavioral Sciences, 53, 335-345, 2012.

[17] Liu, G., Wu, S., Van de Ven, M., Yu, J., Molenaar, A., Structure and artificial ageing behavior of organo montmorillonite bitumen nanocomposites, Applied Clay Science, 72, 49-54, 2013.

[18] Yao, H., You, Z., Li, L., Shi, X., Goh, S.W., Mills-Beale, J., Wingard, D., Performance of asphalt binder blended with non-modified and polymer-modified nanoclay, Construction and Building Materials, 35, 159-170, 2012.

[19] You, Z., Mills-Beale, J., Foley, J. M., Roy, S., Odegard, G. M., Dai, Q., Goh, S. W., Nanoclay-modified asphalt materials: Preparation and characterization, Construction and Building Materials, 25 (2), 1072-1078, 2011.

[20] Galooyak, S. S., Dabir, B., Nazarbeygi, A. E., Moeini, A., Berahman, B., The effect of nanoclay on rheological properties and storage stability of SBS modified bitumen, Petroleum Science and Technology, 29(8), pp. 850-859, 2011.

[21] ASTM D5-06., Standard test method for penetration of bituminous materials, West Conshohocken (PA), USA: American Society for Testing and Materials, 2006.

[22] ASTM D36-06., Test method for softening point of bitumen (ring-and-ball apparatus), West Conshohocken (PA), USA: American Society for Testing and Materials, 2006.

[23] ASTM D4402-06., Standard test method for viscosity determination of asphalt at elevated temperatures using a rotational viscometer, West Conshohocken (PA), USA: American Society for Testing and Materials, 2002.

[24] ASTM D2872-12., Standard test method for effect of heat and air on a moving film of asphalt (Rolling Thin-Film Oven Test), West Conshohocken (PA), USA: American Society for Testing and Materials, 2012.

[25] Kraton® D1101 A Polymer., Data document, 2012.

[26] Şengöz, B., Topal, A., G. Işıkyakar, Morphology and image analysis of polymer modified bitumens, Construction and Building Materials, 23, 1986-1992, 2009.

[27] Topal, A., Sureshkumar, M. S., Şengöz, B., Polacco, G., Rheology and microstructure of polymer-modified asphalt nanocomposites, International Journal of Materials Research, 103, 1271-1276, 2012.

[28] EN 13399., Bitumen and bituminous binders-Determination of storage stability of modified bitumen, Avenue Marnix 17, B-1000. Brussels: European Committee for Standardization, Management Centre, 2010.

[29] Chen, J., Liao, M., Shiah, M., Asphalt modified by SBS triblock copolymer morphology and model, Journal of Materials in Civil Engineering, 14(3), 224-229, 2002.

[30] Airey, G. D., Rheological evaluation of EVA polymer modified bitumen, Journal of Construction and Building Materials, 16(8), pp. 473-487, 2002.

[31] Asphalt Institute., Superpave performance graded asphalt binder specification and testing, Third Edition, Asphalt Institute, Lexington, United States, 2003.

[32] De Visscher, J., Soenen, H., Vanelstraete, A., Redelius, P. A., Comparison of the zero shear viscosity from oscillation tests and the repeated creep test, 3rd Eurasphalt & Eurobitume Congress, Vienna, Austria, 2004.

[33] Gungor, A. G., Saglik, A., Evaluation of rutting performance of neat and modified binders using zero shear viscosity, 5th Eurasphalt & Eurobitume Congress, Istanbul, Turkey, 2012.

[34] CEN TS 15325., Bitumen and bituminous binders: Determination of zero shear viscosity (ZSV) using a shear stress rheometer in creep mode, European Committee for Standardization, Brussels, 2008.

[35] Laukkanen, O., Pellinen, T., Makowska, M., Exploring the observed rheological behavior of in-situ aged and fresh bitumen employing the colloidal model proposed for bitumen, Multi-Scale Modeling and Characterization of Infrastructure Materials, 8, 185-197, 2013.

[36] Saboo N., Kumar P., A study on creep and recovery behavior of asphalt binders, Construction and Building Materials, 96, pp. 632-640, 2015.

[37] ASTM D7405-08., Standard test method for multiple stress creep and recovery (MSCR) of asphalt binder using a dynamic shear rheometer, West Conshohocken (PA), USA: American Society for Testing and Materials, 2008.

[38] Yılmaz, M., Ahmedzade, P., Investigation of pure and SBS modified bituminous binder properties after short term ageing by using two different ageing methods, Journal of The Faculty of Engineering and Architecture of Gazi University, 23(3), 569-575, 2008.

[39] Ouyang, C., Wang, S., Zhang, Y., Zhang, Y., Thermo-rheological properties and storage stability of SEBS/kaolinite clay compound modified asphalts, European Polymer Journal, 42, 446-457, 2006.

[40] Baochang, Z., Man, X., Dewen, Z., Huixuan, Z., Baoyan, Z., The effect of styrene-butadiene-rubber/montmorillonite modification on the characteristics and properties of asphalt, Construction and Building Materials, 23, 3112-3117, 2009.

[41] Yılmaz, M., Kök, B. V., Kuloğlu, N., Alataş, T., Experimental investigation of the storage stability and rheological properties of elastomeric polymer modified bituminous binders, DEÜ Mühendislik Fakültesi Fen Ve Mühendislik Dergisi, 15(1), 67-77, 2013.

[42] Whiteoak D., Read J. M., The shell bitumen handbook, Fifth Edition, Thomas Telford Publishing, London, UK, 2003.

[43] Oner, J., Sengoz, B., Investigation of rheological effects of waxes on different bitumen sources, Road Materials and Pavement Design, 18(6), 1269-1287, 2017.

[44] Sengoz, B., Bagayogo, L., Oner, J., Topal, A., Investigation of rheological properties of transparent bitumen, Construction and Building Materials, 154, 1105-1111, 2017.

[45] Horan, B., Engineer, R.: Multiple Stress Creep Recovery (MSCR) Task Force, Asphalt Institute – Virginia Office, SEAUPG Annual Meeting, Savannah GA, 2011.

[46] Oner, J., Rheological characteristics of bitumens prepared with process oil, Gradevinar, 71(7), 559-569, 2019.

Development of an Internal Safety Evaluation Program for Ready Mixed Concrete Producers

Özge AKBOĞA KALE[1]

ABSTRACT

The aim of this study is to assist the safety specialists and departments in ready mixed concrete (RMC) industry by preparing an internal safety evaluation program (ISEP). To constitute an ISEP the 287-item control list was created and grouped as negligible, moderate, and critical. The control list was applied to thirteen RMC plants which belongs to one RMC company. It is found that even the same company cannot ensure stability in terms of OHS between its plants, none of the plants had an approved OHS policy, emergency action plan and a plant entrance OHS warning sign. OHS training was mostly missing in the plants.

Keywords: Construction industry, risk identification, control list, risk assessment, safety management system.

1. INTRODUCTION

Work-related accidents in the construction industry lead to major problems in many countries [1]. Occupational health and safety (OHS) assurance remains a major challenge because of the diverse and complex nature of this industry. In various studies, researchers have demonstrated that a high percentage of work-related injuries is attributed to construction work. [2-22]. Moreover, the construction industry ranks higher in fatal occupational injuries than in other industries [23-30]. To defuse this high percentage it is necessary to investigate every construction process (excavation works, pile driving, rough construction works, fine construction works, etc.) and sub-sectors (ready mixed concrete industry, prefabricated construction industry, brick plants, etc.) separately because production processes are unique and have differences. Therefore, potential hazards and precautions should be identified for improvement.

The construction industry's single most important material is concrete. Ready mixed concrete (RMC) industry as a producer of the primary material required for buildings and public infrastructure work is one of the most essential sub-sectors of today's construction industry with some specific advantages. Primary advantages of RMC can be listed as follows:

1 İzmir Demokrasi University, Department of Civil Engineering, Izmir, Turkey - ozge.akbogakale@idu.edu.tr - https://orcid.org/0000-0002-3848-0578

production of concrete under controlled conditions, easily placement and transportation, reduction of dust pollution, noise and air pollution, higher speed of construction, savings in labor employment, an overall reduction in cost, etc. [31]. Due to the advantages mentioned this product is increasingly being preferred, especially in modern construction, and most developed countries prefer to use RMC instead of conventional concrete production. The United States (274 million m3), Turkey (100 million m3), and Japan (84.8 million m3) are the top three largest producers according to 2018 statistics [32]. In Turkey, the second largest RMC producer, there has been tremendous growth in RMC production. RMC production was 100 million m3 with 495 RMC companies in 2018 [32].

Academic studies on RMC are abundant. Numerous studies have been conducted to develop ready mixed concrete technology, which is widely in use. However, current studies mostly focus on quality control [33-34], scheduling [35-36], waste management [37-38], delivery problems [39-40], and so on. Since safety and health is a rather new topic in RMC industry, statistical and academic studies are rarely found and limited [41]. Research studies on the subject are not abundant, not only in Turkey but also in other countries. However, when the complex and unique operating system with more component of the industry is taken into consideration, the importance of OHS emerges once again. Publications aiming to build safety awareness are still limited to guidelines and manuals printed by associations such as Occupational Safety and Health Administration (OSHA), American Concrete Pumping Association (ACPA), National Ready Mixed Concrete Association (NSCSA) [42-44]. Besides, there is a high demand for training and consultation regarding occupational safety by RMC companies.

In the interest of filling this gap, the current study has adopted the Internal Safety Evaluation Program to the ready-mixed concrete industry, which has not been applied before. The Internal Safety Evaluation Program (ISEP) provides a structured, documented method of establishing and promoting a system of continual improvement through quality and safety management. ISEP also measures performance and the effectiveness of risk control. The objective of this safety program is to correct non-conformities with risk controls within each specific department's operational processes and to improve the performance of risk controls [45]. A study on how RMC companies will conduct their ISEP will guide them and contribute to the development of OHS policies. To prepare an internal safety evaluation program, it is necessary to consider the functioning of the process in terms of occupational safety and health (OHS).

In addition, it is known that an effective occupational health and safety program contributes to quality management [46]. Total Quality is the handling and development of the management, people, work done, product and service qualities required to meet customer demands in all works performed in any enterprise within a system approach, by ensuring the participation, goals, and consensus of all employees [47]. The concept of occupational safety integrated with the principles of "Total Quality Management", together with the principles of quality and efficiency, constitutes the triple sheet leg that leads the business to success [46]. For this reason, improvement in occupational safety will also benefit total quality management. As a matter of fact, ISO 45001 Occupational Health and Safety Management System standard adopts ISO 14001 Environmental management system and ISO 9001 Quality Management system approaches. Quality assurance systems provide directive

provisions for ensuring occupational health and safety. Therefore, new programs in the field of occupational safety should be developed, considering the priorities of the industry [48].

The aim of this study is to assist the safety specialists and departments in the industry in making an assessment of the measures it adopts concerning the safety and health of its employees in all fields of its operations in the production of ready mixed concrete by preparing a comprehensive ISEP. The control list is the largest element in a company's internal safety evaluation program. When completed thoroughly, it will be used as the basis for all other areas of the program. For this reason, we investigated what should be considered for detailed ISEP of the production area of a ready mixed concrete plant and a 287-item control list was created. Afterward, the created control list was applied in 13 ready mixed concrete plants of one company. Consequently, the findings of this study will give an opportunity to provide further precautions for preventing future accidents. It is expected that the findings obtained in the study will guide the producers of the ready-mixed concrete sector, advise the occupational safety departments of the producers, inform the occupational safety experts about the sector and inspire researchers.

2. METHODS

As organizations move from the early stages to maturity, the focus turns to assuring a continuous safe operation. An Internal Safety Evaluation Program (ISEP) is the prescribed pathway for achieving this objective within a safety management system (SMS) [49]. To have a reliable safety risk assurance under SMS, internal evaluation is a very critical component. ISEP validates the processes, procedures, and controls an organization puts into place and helps ensure they are working as intended. This method also helps verify that risks have been mitigated as low as reasonably practicable [49]. Advantages of ISEP can be listed as follows: it is possible to discover and correct undetected operational risk, operational efficiencies can be promoted, risks can be mitigated to an acceptable level before an event occurs, sheds light on what is working and what is not and so on. ISEP is used in different fields such as flight safety due to its advantages.

The major objective of this study is to determine how to develop a control list for ISEP that can be used by all producers to understand and improve OHS performance in the production process. A framework for the control list should be developed according to sources of risk factors on the site. Therefore, it is necessary to consider the hazards of the complex and unique operating system (Figure 1).

Main hazards in the operation of an RMC production process can be listed as follows:; moving trucks, loaders reversing, trapping between conveyor belts in motion and head/tail drums, falls into aggregate loading hoppers, falling from the upper parts of conveyor belts, impacts from lower parts of moving conveyor belts, falling from upper levels when cleaning filters of silos, trapping, amputations by mixing mechanism, electrocution in the main fuse system, becoming trapped in compressor belts and so on. From this perspective, each stage of the production process outlined in Figure 1 should be examined in terms of OHS. This process is similar in most ready mixed concrete companies. Therefore, it can be said to reflect the general status. In addition to these mechanic hazards, preparing a control list by considering the administrative deficiencies is very important for the companies in the industry to take the necessary importance. The created control list was based on a

comprehensive literature review, legal regulations, and site visits, including mechanical hazards and safety management system principles.
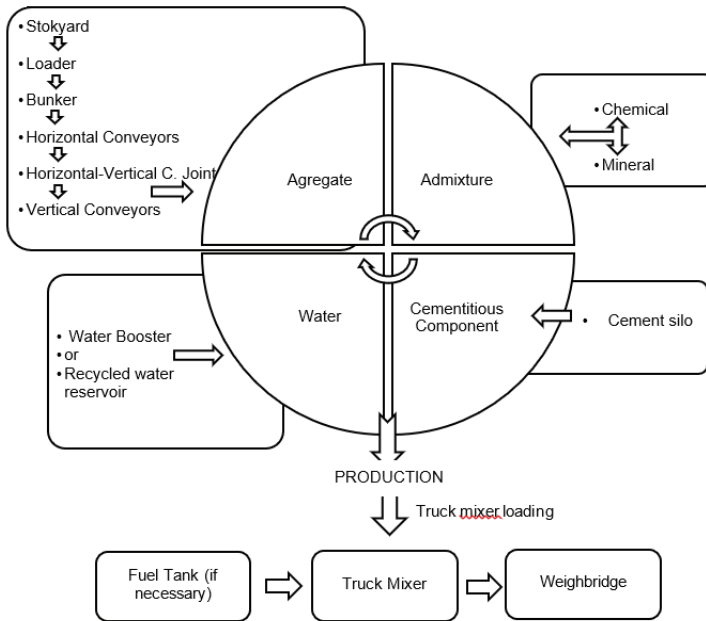
Figure 1 - Flowchart of production.

Within the scope of the created control list, questions were basically grouped under 6 sections namely general, plant, material storage and production, auxiliary facility, mobile equipment, and laboratory. Afterward, the scope of each group was determined as subsections. Within the scope of the general section, managerial OHS precautions were evaluated. Plant entrance, plant entrance OHS warning sign, on-site traffic plan, and plant lighting were investigated under the plant section. Material storage and production section mainly focused production process. Stockyard conformity, bunker conformity, horizontal conveyors, vertical conveyors, horizontal-vertical conveyor joints, mixing process, truck mixer loading, cement silo safety, silo automation, cement trailer unloading, and admixture tank were determined as subsections. Weighbridge, recycled water reservoir, compressor, water booster, generator, fuel tank, operating room, electrical panels, lightning rod, grounding, and transformer AC panel were investigated within the scope of auxiliary facilities. In addition to the production process, also truck mixers, pumps, and loader conformity were evaluated as mobile equipment. Finally, the laboratory was considered. After the process was divided into sections and subsections, a total of 287 safety risks covering the whole process were identified and listed. (Table 1).

Identified safety risk was divided into three groups as negligible, moderate, and critical and their numerical values (NV) were specified as 1, 3, and 9, respectively. The purpose of this digitization is to enable the companies to compare their plants numerically and making it

easier for them to decide where to start improving. The negligible group includes damages probably less than accident or incident levels, moderate groups covers incident to minor accident damage and critical groups include potential loss of life, accident level injury of equipment loss or damage. Since RMC production falls within the very dangerous or moderate groups of risk, critical groups constitute the majority.

Table 1 - Sections of control list.

No	Section	Subsection	List No
1	General	Managerial OHS precautions	1-22
2	Plant	Plant entrance, plant entrance OHS warning sign, on-site traffic plan, plant lighting	23-50
3	Material storage and production	Stockyard conformity, bunker conformity, horizontal conveyors, vertical conveyors, horizontal-vertical conveyor joints, mixing process, truck mixer loading, cement silo safety, silo automation, cement trailer unloading, admixture tank	51-153
4	Auxiliary facility	Weighbridge, recycled water reservoir, compressor, water booster, generator, fuel tank, operating room, electrical panels, lightning rod, grounding, transformer AC panel	154-227
5	Mobile equipment	Truck mixers, pumps, loader conformity	228-271
6	Laboratory	Laboratory	272-287

Table 2 - Properties of visited plants.

Plant no	Plant age	Number of workers	Number of trans mixers	Number of pumps
1	6 years	39	16	4
2	5 years	30	9	2
3	8 years	39	13	3
4	9 years	50	18	4
5	9 years	45	16	3
6	11 years	28	15	2
7	4 months	10	-	-
8	4 years	33	12	3
9	3 years	37	13	2
10	9 years	56	26	6
11	8 years	48	22	5
12	4 years	83	37	7
13	4 years	75	33	6

To demonstrate the applicability and the effectiveness of the created control list, it was applied to thirteen ready mixed concrete plants located in different cities of Turkey which belongs to one RMC company in 2018. The general characteristics of the ready mixed concrete plants are presented in Table 2. Site visits were conducted with the technical personnel of each plant. The visited plants were evaluated according to their current status.

Detailed control list presented in the Results section were prepared separately for each section so that it could be followed easily. In the first stage, if there is a measure taken against the risk controlled according to the created control list, it is marked as (+), if not (-). Since each safety risk was digitizing in the control list, the maximum risk score of each section was determined. For example, risk value, which is "135" in Table 3, is the score that would be obtained if no measures were taken regarding this section in the visited facility. With this approach, the risk score of each of the 13 visited facilities was determined by collecting OHS negligence. This process was repeated for each section and presented in separate tables. Finally, the sum of the deficiencies of each plant in all sections for an overall assessment was presented. The flow chart of the methodology is presented in Figure 2.
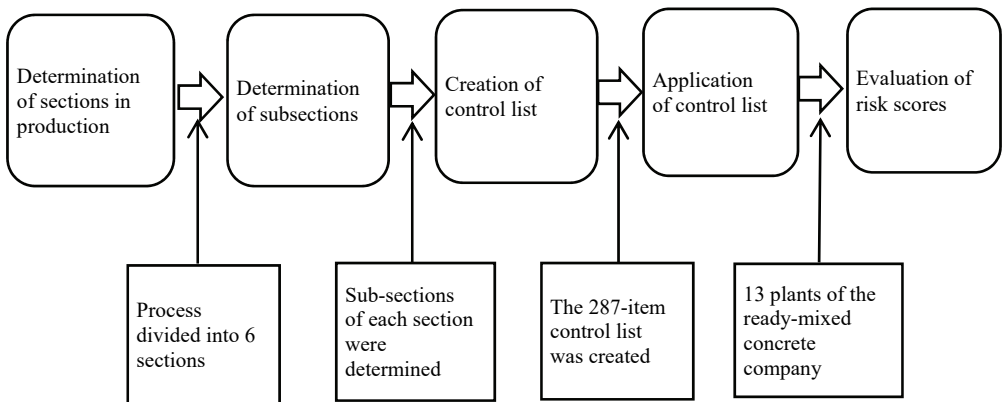
Figure 2 - Flow chart of the methodology

3. RESULTS

The plants, analyses performed, were evaluated separately for each section. The first section covers managerial OHS precautions (Table 3). The lack of managerial OHS precautions for almost all visited plants can be listed as OHS policies, reward-penalty systematics, emergency action plan (EAP), first aid instructions, fire extinguishers, OHS policy records, OHS expert, not taking into consideration near-miss reports, and the root cause analysis of previous accidents. Besides these, risk analysis, lockout – tagout system, basic OHS training, a delivery record of personal protective equipment (PPE), and accident and damage reports were mostly missing in plants.

Plant entrance, plant entrance OHS warning sign, on-site traffic plan, and plant lighting were investigated in Section 2(Table 4). The most striking point in this section is that no facility had a plant entrance OHS warning sign. In addition, only two plants had an "on-site traffic plan". Although there were deficiencies in the entrance and lighting parts of the plant, certain precautions had been taken.

Table 3 - General evaluation.

List No	MANAGERIAL OHS PRECAUTIONS	NV*	1	2	3	4	5	6	7	8	9	10	11	12	13
									PILOTED-TEST							
1	Is a risk analysis available in terms of OHS?	9	−	−	+	−	−	+	−	+	−	+	+	−	−
2	Does the company possess an approved OHS policy?	3	−	−	−	−	−	−	−	−	−	−	−	−	−
3	Is a reward & penalty audit systematic available?	3	−	−	−	−	−	−	−	−	−	−	−	−	−
4	Is a lockout tag-out system available?	9	−	−	+	+	+	−	−	−	+	−	−	+	+
5	Are the general cleaning and maintenance rules followed?	3	−	+	+	+	+	+	+	+	+	+	+	+	+
6	Is an emergency action plan (EAP) available at the plant?	9	−	−	−	−	−	−	−	−	−	−	−	−	−
7	Is the list of fire extinguishers and their places hanged visibly?	9	−	−	−	−	−	−	−	−	−	−	−	−	−
8	Is the EAP visibly displayed?	3	−	−	−	−	−	−	−	−	−	−	−	−	−
9	Are fire, earthquake, flood - with a script drills performed?	9	−	−	−	−	−	−	−	−	−	−	+	−	−
10	Are first aid instructions prepared? (teams - gathering points)	9	−	−	−	−	−	−	−	−	−	−	−	−	−
11	Do all employees (incl. Subcontractors) have basic OHS training?	3	−	+	+	−	−	−	−	−	−	−	−	+	+
12	Do all employees (incl. Subcontractors) have PPE?	9	−	+	+	+	+	+	+	+	+	+	+	+	+
13	Do all employees (incl. Subcontractors) have delivery record of PPE?	3	+	+	−	−	−	+	−	+	−	+	+	−	−
14	Do all employees (incl. Subcontractors) possess certificate of no objection from heavy and hazardous works?	9	+	+	+	+	+	+	+	+	+	+	+	−	−
15	Are periodical health examinations of all employees (incl. Subcontractors) carried out? (ears & lungs)	9	+	−	+	+	+	+	+	+	+	+	+	−	−
16	Is the OHS policy written issued to employees? Are records available?	3	−	−	−	−	−	−	−	−	−	−	−	−	−
17	Is a person available, who is responsible for OHS?	3	+	−	−	−	−	−	−	−	−	−	−	−	−
18	Do employees use their PPE for their own good and safety at the plant and working sites?	9	−	−	+	+	+	−	+	+	+	−	−	−	−
19	Are the accident and damage reports available?	3	−	+	−	−	−	+	−	+	+	+	+	−	−
20	Are near miss reports available?	3	−	−	−	−	−	−	−	−	−	−	−	−	−
21	Is an adequate organization available for delivering near-miss reports?	9	−	−	−	−	−	−	−	−	−	−	−	−	−
22	Is a root cause analysis system available and implemented?	9	−	−	−	−	−	−	−	−	−	−	−	−	−
	RISK VALUE:	135	111	105	84	87	87	99	114	90	84	99	90	111	111

*NV – Numeric Value

Table 4 - Plant evaluation.

List No	PLANT ENTRANCE	PILOTED TEST													
		NV	1	2	3	4	5	6	7	8	9	10	11	12	13
23	Is the plant entrance gateavailable?	9	+	+	+	+	+	−	−	+	+	+	+	+	+
24	Is the plant entrance door working in order?	3	+	+	+	+	+	−	−	+	+	+	+	−	−
25	Is a sign with a logo of the company on it available at the entrance?	3	+	+	+	−	−	−	−	+	−	+	+	−	−
26	Is the sign with company logo appropriately lighted?	3	+	+	−	−	−	−	−	−	−	−	−	−	−
27	Is the sign with company logo appropriately placed?	3	+	+	−	−	−	−	−	+	−	+	+	−	−
28	Are the environmental fence walls available?	9	+	+	+	+	+	−	+	+	+	+	+	+	+
29	Is the deformation of the environmental fence walls available?	3	+	+	+	−	−	−	+	+	+	+	+	−	−
30	Is there available parking area for all employees and visitors?	3	+	+	−	−	−	−	−	+	+	−	−	−	−
31	Are channel grates appropriate and clean?	3	+	+	+	−	−	−	−	+	+	+	−	−	−
	PLANT ENTRANCE OHS WARNING SIGN														
32	Is it clean?	3	−	−	−	−	−	−	−	−	−	−	−	−	−
33	Is it legible?	3	−	−	−	−	−	−	−	−	−	−	−	−	−
34	Is it appropriately located?	3	−	−	−	−	−	−	−	−	−	−	−	−	−
35	Is it appropriately lighted?	3	−	−	−	−	−	−	−	−	−	−	−	−	−
36	Is it generally fit?	3	−	−	−	−	−	−	−	−	−	−	−	−	−
	ON-SITE TRAFFIC PLAN														
37	Are main rules available?	9	−	−	−	−	−	−	−	−	−	−	−	+	+
38	Is a traffic plan (vehicle-pedestrian) available?	3	−	−	−	−	−	−	−	−	−	−	−	−	−
39	Are on site traffic signs available?	3	−	−	−	−	−	−	−	−	−	−	−	+	+
40	Is the plan actively performed?	9	−	−	−	−	−	−	−	−	−	−	−	+	+
41	Does loader comply with on-site traffic plan?	9	−	−	−	−	−	−	−	−	−	−	−	+	+
42	Do aggregate trucks comply with on-site traffic plan?	9	−	−	−	−	−	−	−	−	−	−	−	+	+
43	Do cement trailers comply with on-site traffic plan?	9	−	−	−	−	−	−	−	−	−	−	−	+	+
44	Do passenger cars (visitor-company) comply with on-site traffic plan?	9	−	−	−	−	−	−	−	−	−	−	−	+	+
45	Do truck mixers - pumps comply with on-site traffic plan?	9	−	−	−	−	−	−	−	−	−	−	−	+	+
	PLANT LIGHTING														
46	Is the plant entrance appropriately lighted?	9	+	+	+	+	+	+	+	+	+	+	+	+	+
47	Are production sites-plant discharging chute under mixer appropriately lighted?	9	+	+	+	+	+	+	+	+	+	+	+	+	+
48	Is fuel tank appropriately lighted?	9	+	−	+	−	−	−	n/a	n/a	−	−	−	−	−
49	Are stockyards appropriately lighted?	9	+	−	+	−	−	+	+	+	+	+	+	+	+
50	Are the weighing belts over the aggregate bunkers and their back areas appropriately lighted?	9	+	−	−	+	+	−	+	+	+	+	+	+	+
	RISK VALUE:	168	84	111	102	120	120	132	111	99	102	99	99	66	66

The material storage and production sections are presented in Table 5. Common lack of stockyards was warning signs and indoor stock area. Frame and cover of a manhole, bump concrete in front of the bunker and warning signs of bunker were missing. In general, the

lack of horizontal conveyors was warning signs, secured surrounding, fire extinguishers, and appropriate walking platforms and their railings. It is quite remarkable that almost in all plants vertical conveyors were not secured and there were no emergency stops. Besides, there were no warning signs. The interlock system of the mixer was not secured against dust and there were no cleaning and maintenance instructions. Common lack of truck mixer loading can be listed as; no loading indicator, no docking stop mechanism, no safe area for the operator. Common lack of cement silo safety was rubber protection under the electric panel, warning signs around the electric panel, rope grab & d-clip, bottom cap of stairs to the silo, guard chains on silo venting filters, and safety belts and appropriate working platform. The pressure gauge was missing in the silo automation of all plants. There were no warning signs around the cement trailer unloading part and no fixed support (bed) for hose clamps. Commonly, there were no instructions to follow for drivers. In general, like other parts, there were no warning signs around the electric panel of the admixture tank. Commonly, there was no rubber protection below the electric panel, or an emergency instruction, or emergency instruction.

Table 5 - Material storage and production evaluation.

No	STOCKYARD CONFORMITY	PILOTED TEST													
		NV	1	2	3	4	5	6	7	8	9	10	11	12	13
51	Are aggregate labelling signs appropriate?	9	+	+	+	+	+	−	+	+	+	−	−	−	−
52	Are closing metal sheets of stockyard appropriate?	9	+	+	+	+	+	−	+	+	+	+	+	+	+
53	Is the stockyard efficiently lighted?	9	−	−	+	−	−	+	+	+	+	+	+	+	+
54	Is the slope of the stockyard acceptable?	9	+	+	+	+	+	+	+	+	+	+	+	+	+
55	Are the guards on the way from the stockyard to the bunker suitable?	9	−	−	−	+	+	−	+	+	+	−	−	+	+
56	Is there any warning sing available? (e.g. "no trespassing")	3	−	−	−	−	−	−	−	−	−	−	−	+	+
57	Is the maneuvering area appropriate for the loader?	9	+	+	+	+	+	+	+	+	+	+	+	+	+
58	Is the working slope of the stockyard appropriate for loaders and trucks?	9	+	−	+	+	+	+	+	+	+	−	−	+	+
59	Is the dust emission levels at acceptable levels in the stockyard?	3	+	+	−	+	+	−	−	−	+	+	+	+	+
60	Is there an indoor stock area?	3	−	−	−	−	−	−	+	+	+	−	−	−	−
	BUNKER CONFORMITY														
61	Are there railings around the bunker?	3	+	+	−	+	+	+	+	+	+	+	+	−	−
62	Is there frame and cover of manhole of bunker?	3	+	−	−	−	−	−	−	−	−	−	−	+	+
63	Are the grate openings of the bunker appropriate?	9	+	+	+	+	+	−	+	+	−	−	−	−	−
64	Is an upside closing possible?	3	+	+	+	+	+	+	+	+	+	+	+	+	+
65	Is there bump barrier concrete in front of the bunker?	9	+	−	−	−	+	−	+	+	−	−	−	+	+
66	Are aggregate labelling signs of bunker divisions?	3	+	+	+	+	−	−	+	+	+	+	+	+	+
67	Is there any warning sing available?	9	−	−	−	−	−	−	−	−	−	−	−	−	−
68	Are the bunker efficiently lighted?	9	+	−	+	−	+	−	+	+	+	−	−	−	−

HORIZONTAL CONVEYORS

No	Question	W	1	2	3	4	5	6	7	8	9	10	11	12	13
69	Are power outlets protected?	9	+	+	+	+	+	+	+	−	+	+	+	+	+
70	Are walking platforms and their railings appropriate?	9	+	+	−	−	−	+	−	−	+	−	+	+	
71	Is the lighting sufficient?	9	+	+	+	+	+	−	+	+	+	+	+	+	+
72	Are the warning signs available?	3	−	−	−	−	−	−	−	−	−	−	−	−	
73	Is there cord switch?	9	+	+	+	+	+	+	+	+	+	+	−	−	+
74	Is there emergency stop?	9	+	−	−	+	+	−	−	+	+	−	−	−	+
75	Is there any platform with railings?	9	+	+	+	+	+	+	+	+	+	+	+	+	+
76	Is motor protecting casing available?	9	+	+	+	+	−	−	+	+	+	−	+	+	−
77	Is the surrounding area secured?	9	−	+	−	−	−	−	−	−	−	−	+	−	−
78	Is the underside of the conveyor regularly cleaned?	3	−	+	−	+	−	−	−	−	−	+	−	+	+
79	Are there sufficient appropriately located fire extinguishers?	9	−	−	−	−	−	−	−	−	−	−	−	−	−
80	Is the periodic check and filling of the fire extinguishers done?	9	−	−	−	−	−	−	−	−	−	−	−	−	−
81	Are there top, side and bottom protections for weighing belts available?	9	+	−	−	−	−	−	−	−	−	−	−	−	−

VERTICAL CONVEYORS

No	Question	W	1	2	3	4	5	6	7	8	9	10	11	12	13
82	Is the walkway available?	9	+		+	+	+	+	+	+	+	+	+	+	+
83	Is the railing appropriate?	9	+		−	+	+	+	+	+	+	−	+	+	+
84	Is the protecting upper cover?	3	+		+	+	+	+	+	+	+	+	+	+	+
85	Is there protection under the conveyor?	3	+		−	+	+	−	−	+	+	+	+	+	+
86	Are vertical conveyors secured? (chain)	3	−		+	−	−	−	−	−	+	−	+	−	−
87	Is there motor protecting casing available?	9	−	n/a	+	−	+	+	+	+	+	−	+	−	−
88	Does cord switch work in order?	9	−		+	+	+	+	+	+	+	+	−	+	−
89	Does emergency stop work in order?	9	−		−	−	−	−	−	−	−	+	−	−	
90	Is the lighting sufficient?	9	+		+	−	−	+	+	−	+	+	+	−	+
91	Are the warning signs?	3	−		−	−	−	−	−	−	−	−	−	−	
92	Are walking platform stairs appropriate?	9	+		+	+	−	+	+	+	+	−	+	+	+

"HORIZONTAL-VERTICAL CONVEYOR JOINTS

No	Question	W	1	2	3	4	5	6	7	8	9	10	11	12	13
93	Is there protecting upper cover available?	9	−	+	+	+	−	−	+	+	+	+	−	−	−
94	Is the surrounding secured?	9	−	+	+	+	−	−	−	−	−	+	−	−	−
95	Does cord switch work in order?	9	+	+	+	+	+	−	+	+	+	+	−	+	−
96	Does emergency stop work in order?	9	+	+	+	+	−	−	−	−	−	−	−	+	+
97	Are there warning signs available?	3	−	−	−	−	−	−	−	−	−	−	−	−	
98	Is it well-organized?	3	−	+	+	+	−	−	−	−	−	−	−	+	+

MIXING PROCESS

No	Question	W	1	2	3	4	5	6	7	8	9	10	11	12	13
99	Are power outlets protected?	9	+	+	+	+	+	+	+	−	+	+	+	+	+

#	Question	W													
100	Does emergency stop of the mixer work in order?	9	+	+	+	+	+	−	+	+	+	+	+	+	+
101	Are the railing and baseboards of the discharge platform appropriate?	9	+	−	+	−	−	−	+	+	−	+	+	−	−
102	Is the interlock system of the mixer appropriate?	9	+	+	+	−	+	−	+	+	+	+	+	+	+
103	Is the interlock system of mixer secured against dust?	3	−	−	−	−	−	−	+	−	+	+	−	−	
104	Are mixer chains, locked protecting covers of chain gear, switch available?	9	+	+	+	+	+	+	+	−	+	+	+	−	+
105	Are there cleaning and maintenance instructions for the mixer?	3	−	−	−	−	−	−	−	−	−	−	−	−	
106	Are belt and pulley protections appropriate?	9	+	+	+	+	+	+	+	+	+	−	−	−	−
	TRUCK MIXER LOADING														
107	Is there a loading indicator?	3	−	−	−	−	−	−	−	−	−	−	−	−	
108	Is there docking stop mechanism?	1	+	−	−	−	−	−	−	−	−	−	−	−	
109	Is there a safe area for the operator?	3	−	−	−	−	−	−	−	+	−	−	−	−	
110	Are the discharging chute rubbers appropriate?	1	+	+	−	+	+	+	+	+	+	−	+	+	+
111	Is the discharging unit sufficiently lighted?	9	+	+	+	+	+	+	+	+	+	+	+	+	+
112	Are there railings on the stairway to the loading platform?	9	+	+	+	+	+	+	+	+	+	−	+	+	+
113	Are covering sheets of loading unit appropriate?	3	+	+	+	+	+	+	+	+	+	+	+	+	+
114	Do the mixer caps leak cement grout?	3	+	−	−	+	+	+	+	−	+	+	+	+	+
115	Is the loading area ground appropriate?	9	−	+	−	−	−	−	+	+	−	−	−	−	−
	CEMENT SILO SAFETY														
116	Are there electric panel doors available, and in working order?	9	+	+	+	+	+	−	+	+	+	+	+	+	+
117	Is rubber protection under electric panel available?	9	−	−	−	−	−	−	−	−	+	+	−	−	
118	Are there warning signs around the electric panel?	9	+	+	−	−	−	−	+	−	−	−	−	−	
119	Are silo filters working in order?	3	+	+	−	+	+	+	+	+	+	+	+	+	+
120	Is the maintenance of silo venting filter periodically performed?	3	−	+	−	+	+	+	+	+	+	+	−	−	
121	Are there railing & baseboard on the upper platform of the silo?	9	+	+	+	+	+	+	+	+	+	−	+	+	+
122	Is there deck ladder?	9	+	+	+	+	+	+	+	+	+	+	+	+	+
123	Is there a rope grab & d-clip?	9	−	−	−	−	−	−	−	−	−	−	−	−	
124	Are there bottom cap of stairs to silo? Is it actively in order?	9	−	−	−	−	−	−	−	−	−	−	−	−	
125	Are there guard chains on silo venting filters?	9	−	−	−	−	−	−	−	−	−	−	−	−	
126	Do personnel climbing to the top of the silo have safety belt and is there an appropriate working platform?	9	+	−	−	−	−	−	−	−	−	−	−	−	
127	Is there any false loading preventive system?	3	-	−	+	+	+	−	−	−	+	−	−	−	−
128	Are silos sufficiently lighted?	9	+	+	+	+	+	+	+	+	−	+	+	−	−
129	Is there an overloading safety valve?	9	+	+	+	+	+	+	+	−	+	+	+	−	−

SILO AUTOMATION													
130 Are there pressure gauges?	3	−	−	−	−	−	−	−	−	−	−	−	−	−
131 Does maximum level indicator work in order?	3	−	+	+	+	+	−	+	+	−	+	+	+	+
132 Does electrical system work in order?	3	+	+	+	+	+	+	+	+	+	+	+	+	+
133 Is there overflow emergency siren?	3	+	+	+	+	+	−	+	−	+	+	+	+	+
CEMENT TRAILER UNLOADING													
134 Are there warning signs?	3	−	−	−	−	−	−	−	−	−	−	−	−	−
135 Is fixing support (bed) for hose clamps provided?	3	−	−	−	−	−	−	−	−	−	−	−	−	−
136 Is there flange lock system?	3	+	+	+	+	+	+	+	+	+	+	+	+	+
137 Is there cement trailer board switch lock available?	9	+	+	+	+	+	+	+	−	+	+	−	+	+
138 Is the plug-socket compatibility provided?	3	+	+	+	+	+	+	+	+	+	+	+	+	+
139 Is cement trailer unloading instructions hang?	3	−	−	+	+	+	−	−	−	+	−	−	−	−
140 Does the driver follow the instructions?	9	−	−	+	+	+	−	−	−	−	−	−	−	−
ADMIXTURE TANK													
141 Are electric panel doors available, working in order?	9	+	+	+	+	+	+	+	+	+	+	+	+	+
142 Is rubber protection below electric panel available?	9	−	−	−	−	−	−	−	−	−	+	+	−	−
143 Are there warning signs around the electric panel?	3	−	−	−	−	−	−	−	−	−	−	−	−	−
144 Are there railings on admixture tank stairs and upper platforms?	9	+	+	+	+	+	+	−	+	+	+	+	+	+
145 Are there admixture labelling signs on the tanks?	1	−	−	−	+	+	−	+	−	+	−	−	−	−
146 Are the admixture tanks sufficiently lighted?	9	+	−	+	−	−	+	−	+	+	−	+	+	+
147 Are empty tanks, barrels etc. kept under control in a suitable place?	3	−	−	−	+	−	+	−	+	+	+	−	−	+
148 Is there any leak?	9	+	+	+	+	+	+	+	−	+	−	+	+	+
149 Does the level indicator work?	1	+	+	+	+	+	+	+	+	+	+	+	+	+
150 Is there an overflow measure?	9	+	+	+	+	+	+	+	+	+	+	+	+	−
151 Is the engine under protection?	9	+	−	+	+	+	+	+	+	+	+	+	+	+
152 Is there an emergency instruction?	3	−	−	−	−	−	−	−	−	−	−	−	−	−
153 Is the MSDS (material safety data sheet) hanged?	3	−	−	−	−	−	−	−	+	−	−	−	−	−
RISK VALUE:	673	232	236	246	259	289	377	247	275	253	312	314	308	305

Weighbridge, recycled water reservoir, compressor, water booster, generator, fuel tank, operating room, electrical panels, lighting rod, grounding, and transformer AC panel were investigated in Section 4 (Table 6). In general, there were no protection sets on the weighbridge ramp and the weighbridge itself. Cleaning records and instructions of the recycled water reservoir were missing. Shield grid over the reservoir and lighting was missing and chain hoists of the submersible pumps were inappropriate mostly. In general,

maintenance and operation instruction of compressors and warning signs were not hanged. There was no rubber protection under the electrical panel and the compressor room was not sufficiently lighted. In general, the lack of water booster can be listed as, warning signs around the electrical panel, signs of booster tank room, operation and maintenance instruction and rubber protection under the electrical panel. General physical precautions of the generator were not taken in most of the plants. In addition, operation instruction of the generator was not hanged, generator maintenance reports were missing, and lighting was poor. The antistatic precaution was not available in any of the plants. Although there were deficiencies in the operating room and electrical panels, rubber protections and warning signs were missing.

Table 6 - Auxiliary facility evaluation.

No	WEIGHBRIDGE	NV	1	2	3	4	5	6	7	8	9	10	11	12	13
								PILOTED TEST							
154	Are there protection sets on weighbridge ramp?	9	−	−	−	−	−	−	−	−	−	−	−	−	−
155	Are there protection sets on weighbridge?	9	−	−	−	−	−	−	−	−	−	−	−	−	−
156	Are weighbridge bolts controlled periodically?	3	+	+	+	+	+	−	−	+	+	−	−	−	−
157	Is weighbridge lighted sufficiently?	9	+	+	−	+	+	+	−	+	+	+	+	+	+
	RECYCLED WATER RESERVOIR														
158	Is there a railing?	9	−	+	+	−	−	−	+	+	−	+	+	−	−
159	Is there shield grid over the reservoir?	9	+	−	+	−	−	−	−	+	+	−	−	−	−
160	Is it lighted?	9	+	−	−	−	−	−	−	+	−	−	−	+	+
161	Is the motor secured?	9	+	+	+	+	+	−	+	+	+	+	+	+	+
162	Are there warning signs? (reservoir depths - no walk around, etc.)	3	−	−	−	−	−	−	−	−	−	−	−	−	−
163	Are electric panel doors available, and in working order?	9	+	+	+	+	+	+	−	+	+	+	+	+	+
164	Is rubber protection under electric panel available?	9	−	−	+	−	−	−	−	−	−	+	+	−	−
165	Is the capacity of the reservoir sufficient?	1	+	+	−	+	+	+	+	+	+	−	−	+	+
166	Is there cleaning instruction of the reservoir?	1	−	−	−	−	−	−	−	−	−	−	−	−	−
167	Are there cleaning records of reservoirs?	1	−	−	−	−	−	−	−	−	−	−	−	−	−
168	Are the chain hoists of the submersible pumps appropriate?	3	−	−	−	−	−	−	−	+	−	+	+	−	−
	COMPRESSOR														
169	Are general physical precautions taken? (securing the surrounding of closed area - materials storage)	3	+	−	+	+	+	−	−	−	+	−	−	+	+
170	Are compressor belt protection, air tank safety valve, manometer appropriate?	9	+	+	+	+	+	−	+	+	+	+	+	+	+
171	Is the hydrostatic test report up to date?	9	−	+	+	−	−	−	−	+	−	+	+	−	−
172	Is the maintenance and operation instruction hanged?	3	−	−	−	−	−	−	−	+	−	−	−	−	−
173	Are the warning signs hanged? (ear protection, only authorized person)	3	−	−	−	−	−	−	−	−	−	−	−	−	−

174	Is there electrical panel covers, does it work in order?	9	+	−	+	+	+	−	+	−	+	+	+	+	+
175	Is there rubber protection below the electrical panel?	9	−	−	−	−	−	−	−	+	−	+	−	−	−
176	Is the compressor room sufficiently lighted?	9	+	−	+	−	−	−	−	−	−	−	−	−	−
WATER BOOSTER															
177	Are there electrical panel covers, doethey work in order?	9	+	+	+	+	+	+	+	+	+	−	−	+	+
178	Is there rubber protection under the electrical panel?	9	−	−	−	−	−	−	+	−	+	+	−	−	
179	Is the booster tank room sufficiently lighted?	9	+	+	+	+	+	+	+	+	+	+	+	+	+
180	Are there warning signs around electrical panel?	3	−	−	−	−	−	−	−	−	−	−	−	−	−
181	Are the signs of booster tank room sufficient?	3	−	−	−	−	−	−	−	−	−	−	−	−	−
182	Is the operation and maintenance instruction of booster tank available?	3	−	−	−	−	−	−	−	−	−	−	−	−	−
183	Are the water booster and pressured tanks in a closed room?	9	+	+	+	+	+	+	+	+	+	+	+	+	+
184	Are the physical conditions of the booster and pressured tanks room appropriate?	3	−	+	+	+	+	+	+	+	+	+	+	+	+
185	Are the fan of the motor and coupling protections appropriate?	9	+	+	+	+	+	+	+	+	+	+	+	+	+
GENERATOR															
186	Are general physical precautions taken? (securing the surrounding of closed area)	3	−	−	+	+	+	+	−	−	−	−	−	−	−
187	Is the operation instruction of the generator hanged?	3	−	−	−	+	+	+	−	−	−	−	−	−	−
188	Is there a leak or overflow in the generator fuel tank?	9	+	+	+	+	+	+	+	+	+	+	+	−	−
189	Is the periodic maintenance of fire extinguishers appropriate?	9	−	−	+	−	−	−	−	+	−	+	+	+	+
190	Are warning signs hanged? (danger; do not touch the generator; only authorized person, etc.)	3	−	−	−	−	−	−	−	−	−	−	−	−	−
191	Are there generator maintenance reports?	3	+	+	−	−	−	−	+	−	−	−	−	−	−
192	Is the generator sufficiently lighted?	9	+	−	+	−	−	+	−	+	−	−	−	−	−
FUEL TANK															
193	Is there a set to prevent vehicles from crashing into the fuel tank?	9	−	−	−	+	+	n/a	n/a	−	−	+	+	+	+
194	Are warning signs available?	3	−	−	−	+	+			+	+	−	−	+	+
195	Are operating instructions available´?	3	−	−	−	−	−			−	−	−	−	+	+
196	Is a fire extinguisher available?	9	+	−	+	−	−			−	−	+	+	−	−
197	Is there antistatic precaution?	9	−	−	−	−	−			−	−	−	−	−	−
198	Is there a fuel tank ventilation does it work in order?	3	+	+	+	+	+			+	−	−	−	+	+
199	Is the tank sufficiently lighted?	9	+	−	+	−	−			−	−	−	−	−	−
200	Is there a locking mechanism for the fuel tank and the pump, does it work in order?	9	−	−	+	−	−			+	−	−	−	+	+

OPERATING ROOM														
201	Is there emergency stop switch-marking (on-off) system?	9	+	+	+	+	+	+	+	+	+	+	+	+	+
202	Is there fire extinguisher (30 cm high; fixed; not depleted)	9	–	–	+	+	–	–	+	+	+	+	+	–	–
203	Is there an air conditionerunit?	1	+	+	+	+	+	+	+	+	+	+	+	+	+
204	Is everything well organized?	3	+	+	+	+	+	+	+	+	+	+	+	+	+
205	Is there electrical panel covers, does it work in order?	9	+	+	+	+	+	+	+	+	+	+	+	+	+
206	Is there rubber protection under the electrical panel?	9	–	–	–	–	–	–	–	–	–	–	–	–	–
207	Are there warning signs around the electrical panel?	3	–	–	+	–	–	–	–	–	–	–	–	–	–
208	Are electrical panel keys available?	9	+	+	+	+	+	–	+	+	+	+	–	+	+
209	Is the operating room sufficiently lighted?	9	+	+	+	+	+	+	+	+	+	+	+	+	+
ELECTRICAL PANELS															
210	Is grounding available?	9	+	+	+	+	+	+	+	+	+	+	+	+	+
211	Are the panel doors closed?	9	+	+	+	+	+	+	+	+	+	+	+	+	+
212	Are they locked and do only authorized personnel have the keys?	9	+	+	+	–	+	–	+	+	+	+	–	+	+
213	Is there rubber band?	9	–	–	–	–	–	–	–	–	–	–	–	–	–
214	Are warning signs hanged? (50v, danger, only electrician, etc.)	3	–	–	–	–	–	–	–	–	–	–	–	–	–
215	Are the physical conditions (height, appearance, etc.) appropriate?	9	+	+	+	–	+	+	+	+	+	+	+	+	+
LIGHTNING ROD, GROUNDING, TRANSFORMER AC PANEL															
216	Are lightning rod annual maintenance reports available?	9	+	+	+	–	–	–	+	–	–	+	+	+	+
217	Is there facility grounding?	9	+	+	+	+	+	+	+	+	+	+	+	+	+
218	Is the facility transformer mast safety lock available?	9	–	+	+	–	–	+	+	–	+	+	+	+	+
219	Is the transformer maintained (oil change)?	9	+	+	+	+	+	+	+	+	+	–	–	+	+
220	Are UPS units available? Does they work in order? Is their capacity sufficient?	9	+	+	+	+	+	+	+	+	+	+	+	+	+
221	Are the doors of transformer and ac panel locked?	9	–	+	+	–	–	+	+	+	–	–	–	+	+
222	Is the transformer and ac panel suitable for internal, external lighting?	9	+	+	–	+	+	+	–	–	+	–	–	+	+
223	Is the transformer and ac panel high enough from the ground?	9	+	+	+	+	+	+	+	+	+	+	+	+	+
224	Is there any deformation in the transformer and ac panel?	9	+	+	+	+	+	+	+	+	+	+	+	+	+
225	Is there a rubber band in front of the transformer and ac panel?	9	–	+	+	–	–	–	–	–	+	+	+	+	+

No		1	2	3	4	5	6	7	8	9	10	11	12	13
226	Are the warning signs in the transformer and ac panel sufficient?	3	−	+	+	−	−	−	−	−	−	+	+	−	−
227	Is there enough fire extinguisher in transformer? Are they appropriately located?	9	−	+	−	−	−	−	+	−	+	−	−	+	+
	RISK VALUE:	508	212	218	150	266	257	242	209	188	230	210	225	203	203

Precautions taken regarding mobile equipment were more extensive than those of other sections (Table 7). The common missing in all plants was the lack of fire extinguisher. Except for this, the truck mixers, pumps, and loaders were generally safe.

Table 7 - Mobil equipment evaluation.

No	TRUCK MIXERS	NV	PILOTED TEST												
			1	2	3	4	5	6	7	8	9	10	11	12	**13**
228	Is there a vehicle tracking system on truck mixers?	3	+	+	+	+	+	+		+	+	+	+	+	+
229	Does audible reversing device work properly?	9	−	+	+	+	+	−		+	+	−	−	+	+
230	Is there protection on upper platform of the ladder?	9	+	+	+	+	+	+		+	+	+	+	+	+
231	Do the backlights of the truck mixers work in order?	9	+	+	+	+	+	+		+	+	−	−	+	+
232	Is the ladder to driving cabin appropriate?	9	+	+	+	+	+	+		+	+	+	+	+	+
233	Is there side protection of discharge gutters?	9	+	+	+	+	+	+		+	+	+	+	+	+
234	Is there any mechanism on truck mixers to prevent overflow of concrete?	3	−	−	+	+	+	−		+	+	−	−	+	+
235	Are the headlights and taillights in working order?	9	+	+	+	+	+	+		+	+	+	+	+	+
236	Are the fire extinguishers available?	9	−	−	+	−	−	+	n/a	−	−	+	+	−	−
237	Is the rest of components of drive cab fixed inside?	3	−	−	+	+	+	+		−	+	+	+	+	+
238	Are they periodically serviced?	9	−	−	+	+	+	+		+	+	+	+	+	+
239	Are there firs aid kits in every truck mixer?	9	+	+	+	+	+	−		+	+	+	+	+	+
240	Do tachometers work in order?	3	+	+	+	+	+	+		+	+	+	+	+	+
241	Do truck mixer drivers have operating license?	3	+	−	+	+	+	+		+	+	+	−	−	−
242	Do truck mixer drivers have psycho-technical report?	9	+	+	+	+	+	+		+	+	+	+	+	+
243	Did truck mixer drivers have orientation training?	3	−	−	+	+	+	+		−	+	−	−	+	+
244	Are the headlights of working truck mixers on??	9	+	−	+	−	−	−		+	−	−	−	+	+
	PUMPS														
245	Is there a vehicle tracking system on pumps?	3	+	+	+	+	+	+		+	+	−	−	+	+
246	Is there any automatic system on pumps against rollover?	9	+	+	+	+	+	+		+	+	+	+	+	+
247	Does the audible reversing device work properly?	9	−	+	+	+	+	−		+	+	−	−	−	−
248	Do the backlights of the pumps work properly?	9	−	+	+	+	+	−	n/a	+	−	−	−	+	+
249	Is there grate on hoppers?	9	+	+	+	+	+	+		+	+	+	+	+	+
250	Are pumps periodically maintained?	9	−	−	+	+	+	+		+	+	+	+	+	+
251	Is the ladder to platform appropriate?	9	−	+	+	+	+	+		+	+	+	+	+	+

No		NV	1	2	3	4	5	6	7	8	9	10	11	12	13	14
252	Are there end hose safety straps?	9	–	+	–	+	+	+			+	+	–	–	+	+
253	Are headlights and stoplights working in order?	9	+	+	+	+	+	+			+	+	+	+	+	+
254	Is the ladder to drive cab appropriate?	9	+	+	+	+	+	+			+	+	+	+	+	+
255	Are there bump stop outriggers?	9	+	+	+	+	+	+			+	+	–	–	+	+
256	Are the fire extinguishers appropriate?	9	–	+	–	–	–	+			+	–	+	+	+	+
257	Is the rest of components of drive cab fixed inside?	3	–	+	+	+	+	–			+	+	–	–	+	+
258	Are there traffic cones available?	9	–	+	+	–	–	+			+	–	–	–	+	+
259	Do tachometers of pumps work in order?	3	+	+	+	+	+	+			+	+	+	+	+	+
260	Do operators have operating certificates?	3	+	+	+	+	+	+			+	+	+	+	+	+
261	Do pump operators have parachute type safety harness?	9	–	+	+	–	–	–			+	–	+	+	–	–
262	Do pump operators have psycho-technical report?	9	+	+	+	+	+	–			+	+	+	+	+	+
	LOADER CONFORMITY															
263	Does operator have G class driving license?	9	+	–	+	+	+	+	+		+	+	+	+	+	+
264	Does operator have heavy equipment certificate?	9	–	+	+	+	+	+	n/a		+	+	+	+	–	–
265	Does reversing warning lamp work properly?	9	–	–	+	+	+	+	+		+	+	+	+	+	+
266	Does audible reversing device work properly?	9	+	+	+	+	+	+	+		+	+	+	+	+	+
267	Are headlights-mirrors and glasses appropriate?	9	+	+	+	+	+	–			+	+	+	+	+	+
268	Is there a seatbelt?	9	+	+	+	+	+	–			+	+	+	+	+	+
269	Do loader operators have operator license?	3	–	+	–	+	+	–	+		+	+	–	–	–	–
270	Are there periodic maintenance instructions? Are they followed?	9	–	–	+	+	+	–	+		+	+	+	+	–	–
271	Are loader fire extinguishers appropriate?	9	–	–	–	–	–	–	–		–	–	–	–	–	–
	RISK VALUE:	330	150	93	30	45	45	108	–	24	63	96	96	60	60	

According to laboratory evaluation (Table 8) common missing precautions were precaution against electric shock in the cure pools, precaution against the slippery ground, precaution against free fall of concrete specimens, warning signs, instructions, and labeling, specimen tong.

Table 8 - Laboratory evaluation.

No	LABORATORY		PILOTED TEST												
		NV	1	2	3	4	5	6	7	8	9	10	11	12	13
272	Is there any precaution against electric shock in cure pools?	9	–	–	–	–	–	–	–	–	–	+	+	–	–
273	Is there a system to cover the curing pool?	3	–	+	+	–	–	–	–	+	–	+	+	–	–
274	Is there any precaution against slippery ground?	9	–	–	–	–	–	–	–	–	–	–	–	–	–
275	Is there any precaution against free fall of concrete specimens?	9	–	–	+	–	–	–	+	–	–	–	–	+	+

No	Question		1	2	3	4	5	6	7	8	9	10	11	12	13
276	Are there warning signs, instructions, and labeling?	3	−	−	+	−	−	−	−	−	−	−	−	+	+
277	Is there any tool to carry specimens from the curing pool to test machine?	9	−	−	−	+	+	−	−	−	−	−	−	+	+
278	Is there protective cap-door-cover in front of the test machine?	9	+	+	+	+	+	+	+	+	+	+	+	+	+
279	Is there warning sign on the test machine such as "only authorized persons"?	3	−	−	−	−	−	−	−	−	+	+	+	+	+
280	Is pneumatic specimen demolding system secured?	9	−	+	+	−	−	−	−	−	+	+	+	+	+
281	Are there appropriate PPE in the laboratory? (glove, glasses, mask, etc.)	9	+	+	+	+	+	+	−	+	−	+	+	+	+
282	Are there specimen tongs in the laboratory?	9	−	−	−	−	−	−	−	−	−	−	−	−	−
283	Is the drying oven instruction appropriate?	3	−	−	+	−	−	−	−	−	−	+	+	+	+
284	Is there a protective glove for drying oven?	9	−	−	−	−	−	−	−	−	−	−	−	−	−
285	Is there a kit/tool at the end of pneumatic specimen demolding hose?	9	−	+	−	+	+	−	−	−	+	+	+	+	+
286	Are there enough fire extinguishers? Are they appropriately located?	9	−	−	+	−	−	+	+	−	+	+	+	+	+
287	Is periodic maintenance of fire extinguishers properly performed?	9	−	+	+	−	−	+	+	−	+	+	+	+	+
	RISK VALUE:	120	57	30	57	84	84	84	84	99	72	48	48	39	39

Table 9 - Risk values of visited plants.

List No	Section	Total RV of Sections	1	2	3	4	5	6	7	8	9	10	11	12	13
								Risk Values of Visited Plants								
1-22	General	135	111	105	84	87	87	99	114	90	84	99	90	111	111
23-50	Plant	168	84	111	102	120	120	132	111	99	102	99	99	66	66
51-153	Mat. storage and pro.	673	232	236	246	259	289	377	247	275	253	312	314	308	305
154-227	Auxiliary facility	508	212	218	150	266	257	242	209	188	230	210	225	203	203
228-271	Mobil equipment	330	150	93	30	45	45	108	−	24	63	96	96	60	60
272-287	Laboratory	120	57	30	57	84	84	84	84	99	72	48	48	39	39
	Total	1934	846	793	669	861	882	1042	765	775	804	864	872	787	784
	%		43.74	41.00	34.59	44.52	45.60	53.88	47.69	40.07	41.57	44.67	45.09	40.69	40.54

The sum of the deficiencies of each plant in all sections for an overall assessment is presented in Table 9. According to the risk values for 13 plants, belonging to one company, the

deficiencies vary between 53.88 % to 34.59. This is a good example of the fact that even the same company cannot ensure stability in terms of OHS among its plants.

4. DISCUSSION AND CONCLUSION

The ready mixed concrete industry, commonly operating not only in Turkey but also in other countries, needs to be inspected in terms of occupational health and safety because academic studies on this subject are not abundant. This study aimed to develop a control list to be used within the scope of an internal safety evaluation program that can be used by all producers to understand and improve OHS performance in the production process. For this reason, we examined what should be considered for detailed ISEP of the production area of a ready mixed concrete plant and the 287-item control list was created. Since each safety risk was digitizing in the control list, the maximum risk score of each section was determined. Afterward, the control list thus created was applied in 13 ready mixed concrete plants of a single company. RMC companies need to benefit from a guideline when conducting their own internal evaluations to improve their occupational safety efforts and to make all their plants uniformly safe. In this respect, the study is a reliable guide for RMC manufacturers. Also, it is important to list the common deficiencies of the plants visited as follows.

- Risk analysis was missing in most of the visited plants. Besides, none of the plants had an approved OHS policy. The ready mixed concrete industry is one of the subsectors of construction that has many risks as described above. It follows that risk assessment is very important for any ready mixed concrete plant. Carrying out these assessments is the only way of ensuring that the chances of incidents occurring are reduced as much as possible, and everyone is kept safe.

- The emergency action plan was not available in any of the plants. A workplace emergency is any unforeseen situation that threatens employees, customers, or the public; disrupts or shuts down operations; or causes physical or environmental damage [50]. The purpose of an EAP is to facilitate and organize employer and employee actions during workplace emergencies [51]. Therefore, it is crucial to have EAP in plants and visibly displayed.

- OHS training was mostly missing in the plants. Sawacha et al. (1999) stated that a lack of safety training is one of the causes of accidents [52]. Researchers also indicated that safety training is the most important safety management practice in terms of safety performance components [53-55]. Adopting safety-training programs increase the awareness of workers on the subject, thereby allowing them to work safely. Therefore, producers should organize and record regular OHS training. Besides, it should be noted that keeping training up to date is just as important as taking it the first time.

- Collecting statistics on safety activities will allow a company to identify common injuries and areas that may be missing in their safety program. OSHA states that collecting near-miss reports helps to create a culture that seeks to identify and control hazards, which will reduce risks and the potential for harm [56]. In addition, reporting near miss incidents can significantly improve worker safety and enhance an organization's safety culture [57]. Near-miss reports were not available in the

visited plants. Therefore, to understand better the weaknesses in the system that resulted in the circumstances that led to the near miss, root cause analyses could not be conducted. Near miss forms to collect relevant incident data during an investigation and to learn lessons, review controls and implement change where required should be used.

- Surprisingly, no facility had a plant entrance OHS warning sign. OHS warning signs should be made mandatory at the entrance of the plant. This warning sign should symbolize the summary rules that must be observed when entering the plant (Speed limit, helmet use, etc.). Warning signs also were missing in many parts of the production process such as stockyard, bunker, horizontal conveyors, vertical conveyors, horizontal-vertical conveyor joints, cement silo, cement trailer unloading, admixture tank, compressor, generator, operating room, electrical panels. Safety signs play a large part in keeping facilities compliant and employees knowledgeable. It is critical for workers to understand the types of hazards in the workplace, the level of risk the hazard presents, and what precautions to take [58].

- Instructions mean outline or text of technical procedures. Instructions also tell someone how to do something or in which order to do something. First aid instructions, cleaning, and maintenance instructions of the mixer, emergency instruction of admixture tank, cleaning instruction of the reservoir, operation and maintenance instruction of booster tank, operating instruction of fuel tank were missing. These instructions should be prepared by the managers and actively used by workers to prevent them from potential accidents because of the described risks.

- Moving vehicles and equipment on manufacturing sites can be fatal for humans if not used correctly and safely. The layout and traffic flow of a workplace is important for keeping people and plant safe as they move around [59]. Only two plants had an "on-site traffic plan" among the visited plants. Related plans should be prepared and actively used in all RMC plants.

To sum up, risk may remain within acceptable limits within an organization to maintain OHS management applications by using an internal safety evaluation program. The risks described cannot be totally avoided, but the choice can be made so that the risk is minimized. This study is mainly concerned with the assessment of pure risk in ready mixed concrete production, where managers need to know how much risk is involved in the process to decide how to go about it. It is expected that the control list would be an effective tool of preventing and minimizing accidents of RMC industry.

In addition, the control list created within the scope of the internal safety evaluation program includes the legal obligations in the laws and standards in force. According to the risk scores obtained from the control list, it is observed that some of the measures described in the Occupational Safety Law No. 6331 of Turkey and accompanying standards were not in force at the facilities visited. For this reason, ready-mixed concrete producers will also fulfill their legal obligations in the improvement works they will make with reference to this control list.

The created control list is a guide for ready-mixed concrete companies to make their own preliminary assessments and due diligence to reach internationally accepted standards and regulations. Considering the provisions of the ISO 45001 Occupational Health and Safety Management System Standard, the created control list will be able to guide companies,

especially in Section 6.1 (Methods of identifying risks and opportunities) and Section 6.2 (OHS targets and planning to achieve them).

The employees of the ready mixed concrete industry also experience the risks that may cause occupational diseases such as noise (hearing loss), dust (respiratory system diseases), ergonomics (musculoskeletal system disorders) and so on. However, the control list presented in the study does not cover occupational diseases. In future studies, the subject can also be addressed from this aspect.

Abbreviations

ACPA - American Concrete Pumping Association

EAP - Emergency Action Plan

ISEP - Internal Safety Evaluation Program

NSCSA - National Ready Mixed Concrete Association

NV – Numeric Value

OHS - Occupational Health and Safety

OSHA - Occupational Safety and Health Administration

PPE - Personal Protective Equipment

RMC - Ready Mixed Concrete

RV - Risk Value

SMS - Safety Management System

References

[1] Unsar, S., Sut, N., General assessment of the occupational accidents that occurred in Turkey between the years 2000 and 2005. Saf Sci. 47:614–619, 2009.

[2] Hinze, J.W., Construction Safety. New Jersey: Prentice Hall Publications; 1997.

[3] Ringen, K., Seegal, J., Safety and health in construction industry. Annu Rev Public Health.16:165–188, 1995.

[4] Lım, S., Oh, A., Won, J., Chon, J., Improvement of inspection system for reduction of small-scale construction site accident in Korea. Ind Health. 56:466-474, 2018

[5] Cameron, I., Hare, B., Davies, R., Fatal and major construction accidents: a comparison between Scotland and the rest of Great Britain. Saf Sci. 46:692–708, 2008.

[6] Ale, B.J.M., Bellamy, L.J., Baksteen, H., et al., Accidents in the construction industry in the Netherlands: An analysis of accident reports using Storybuilder. Reliability Eng Syst Saf. 93:1523–1533, 2008.

[7]   Arquillos, A.L., Romero, J.C.R., Gibb, A., Analysis of construction accidents in Spain, 2003-2008. J Saf Res. 43:381–388, 2012.

[8]   Colak, B., Etiler, N., Bicer, U., Fatal occupational injuries in the construction sector in Kocaeli, Turkey, 1990-2001. Ind Health. 42:424-430, 2004.

[9]   Kartam, N.A., Flood, I., Koushki, P., Construction safety in Kuwait: issues, procedures, problems, and recommendations. Saf Sci. 36:163-184, 2000.

[10]   El-Mashaleh, M.S., Al-Smadi, B.M., Hyari, K.H., et al., Safety management in the Jordanian construction industry. Jordan J Civ Eng. 4(1):47-54, 2010.

[11]   Chong, H.Y., Low, T.S., Accidents in Malaysian Construction industry: statistical data and court cases. In J Occup Saf Ergon. 20(3):503–513, 2014.

[12]   ElSafty, A., ElSafty, A., Malek, M., Construction safety and occupational health education in Egypt, the EU, and US Firms. Open J Civ Eng. 2:174-182, 2012.

[13]   Mohammed, Y.D., Ishak, M.B., Study of fatal and non-fatal accidents in construction sector. Malaysian J Civ Eng. 25(1):106-118, 2013.

[14]   Halder, D., Rahman, F., Hossain, M., et al., Contributing factors affecting the safety in construction sites of Bangladesh. Proceedings of the International Conference on Advances in Civil, Structural and Mechanical Engineering – ACSM; 2015 Feb 21-22; Bangkok, Thailand. New York (USA): Institute of Research Engineers and Doktors; 2015.

[15]   Fabiano, B., Parentini, I., Ferraiolo, A., et al., A Century of accidents in the Italian industry: Relationship with the production cycle. Saf Sci. 2:65-74, 1995.

[16]   Tam, C.M., Zeng, S.X., Deng, Z.M., Identifying elements of poor construction safety management in China. Saf Sci. 42:569–586, 2004.

[17]   Jannadi, O.A., Bu-Khamsin, M.S., Safety factors considered by industrial contractors in Saudi Arabia. Build Environ. 37(5):539–547, 2002.

[18]   Gürcanlı, G.E., Müngen, U., Analysis of Construction Accidents in Turkey and Responsible Parties. Ind Health. 51:581-595, 2013.

[19]   Tözer, K.D., Çelik, T., Gürcanlı, G.E., Classification of Construction Accidents in Northern Part of Cyprus. Teknik Dergi. 29(2): 8295-8316, 2018.

[20]   Bilir, S., Gürcanlı, G.E., A Method for Determination of Accident Probability in Construction Industry. Teknik Dergi, 29(4): 8537-8561, 2018.

[21]   Baradan, S., Akboğa, Ö., Çetinkaya, U., Usmen, M.A., Ege Bölgesindeki İnşaat İş Kazalarının Sıklık ve Çapraz Tablolama Analizleri. Teknik Dergi. 27(1): 7345-7370, 2016.

[22]   Akboğa Kale, Ö., Baradan, S., Identifying Factors that Contribute to Severity of Construction Injuries using Logistic Regression Model. Teknik Dergi. 31(2): 9919-9940, 2020.

[23] Aksorn, T., Hadikusumo, B.H.W., The unsafe acts and the decision-to-err factors of Thai construction workers. J Constr in Developing Ctries. 12(1):1–25, 2007.

[24] Ore, T., Stout, N., Traumatic occupational fatalities in the US and Australian construction industries. Am J Ind Med. 30:202–206, 1996.

[25] Pollack, E.S., Griffin, M., Ringen, K., et al., Fatalities in the construction industry in the United States, 1992 and 1993. A J Ind Med. 30:325–330, 1996.

[26] Center for Disease Control and Prevention. Fatal occupational injuries-United States, 1980–97. Morb Mortal Wkly Rep. 50:317–320, 2001.

[27] Rodsari, B.S., Ghodsi, M., Occupational injuries in Tehran. Inj. 36:33–39, 2005.

[28] Tricco, A.C., Colantonio, A., Chipman, M., et al., Work-Related deaths and traumatic brain injury. Brain Inj. 20:719–724, 2006.

[29] Hallowell, M.R., Safety-knowledge management in American construction organizations. J Manag Eng. 28(2):203–211, 2012.

[30] Larsson, T.J., Field, B., The distribution of occupational injuries risks in the Victorian construction industry. Saf Sci. 40:439–456, 2002.

[31] Quora [Internet]: What are the advantages of ready mi concrete?; [cited 2019 Nov 3] Available from: https://www.quora.com/What-are-the-advantages-of-ready-mix-concrete

[32] Turkish Ready Mixed Concrete Association [Internet]: Statistics; [cited 2019 Nov 7] Available from: https://www.thbb.org/en/industry/statistics/

[33] Aichouni, M., On the Use of the Basic Quality Tools for the Improvement of the Construction Industry: A Case Study of a Ready Mixed Concrete Production Process. Int J Civ Environ Eng. 12(5):31-38, 2012.

[34] Sarkar, D., Bhattacharjee, B., Design and application of multivariate CUSUM for quality monitoring of ready mixed concrete. Int J Qual Eng Technol. 4(2):161–179, 2014.

[35] Naso, D., Surico, M., Turchiano, B., et al., Genetic algorithms for supply-chain scheduling: A case study in the distribution od ready mix concrete. Eur J Operational Res. 117:2069-2099, 2007.

[36] Yan, S., Lai, W., An optimal scheduling model for ready mixed concrete supply with overtime considerations. Autom Constr. 16:734-744, 2007.

[37] Sealey, B.J., Phillips, P.S., Hill, G.J., Waste management issues for the UK ready-mixed concrete industry. Resour Conservation Recycling. 32:321-331, 2001.

[38] Sandrolini, F., Franzoni, E., Waste wash water recycling in ready mixed concrete plants. Cement Concr Res. 31:485-489, 2001.

[39] Schmid, V., Doerner, K.F., Hartl, R.F., et al., Hybridization of very large neighborhood search for ready-mixed concrete delivery problems. Computers&Operations Res. 37:559-574, 2010.

[40] Graham, L.D., Forbes, D.R., Smith, S.D., Modeling the ready mixed concrete delivery system with neural networks. Autom Constr. 15:656-663, 2006.

[41] Akboğa, Ö., Baradan, S., Safety in ready mixed concrete industry: descriptive analysis of injuries and development of preventive measures. Ind Health. 55:1-13, 2017.

[42] Occupational Safety and Health Administration [Internet]: Workers Safety Series Concrete Manufacturing; [cited 2019 Nov 12]. Available from: https://www.osha.gov/Publications/concrete_manufacturing.html

[43] American Concrete Pumping Association [Internet]: Ready Mixed Safety Manual-A guide for the prevention of accidents when delivering to concrete pumps; [cited 2019 Nov 1] Available from: https://www.concretepumpers.com/sites/concretepumpers.com/files/attachments/read ymixed_safety_manual_v1.0.3_eng_rs.pdf

[44] National Ready Mixed Concrete Association [Internet]: 2017 Presidents Report [cited 2019 Oct 20] Available from: https://www.nrmca.org/downloads/Presidents_Report2017.pdf

[45] OmniSMS [Internet]: Safety Management System, Internal Evaluation Program; [cited 2019 Nov 25]. Available from: https://omnisms.aero/wp-content/uploads/2018/04/Omni-Aviation-SMS-Internal-Evaluation-Quality-Assurance-Program.pdf

[46] Yakut, A., Akbıyıklı, R., İşçi sağlığı ve güvenliği yönetimi ile toplam kalite yönetimi sistemleri veri analizi incelemesi. SAU J. Sci. 17(1):97-103, 2013.

[47] Uryan, B., Toplam Kalite Yönetimi. Mevzuat Dergisi. 55, 2002.

[48] Bektaş, Ç., İşletmede İş Sağlığı ve Güvenliği Açısından Kalite Güvence Sistemlerinin Rolü. Emek ve Toplum. 8(8): 136-157, 2019.

[49] USHST [Internet]: Internal Evaluation Program Safety Assurance Check [cited 2019 Nov 12] Available from: http://www.ihst.org/portals/54/IHST_News/2014%20IEP%20Check%20FINAL%202 .pdf

[50] THRESHOLD [Internet]: Emergency Action Plans are critical for your company; [cited 2019 Nov3]. Available from: https://www.thresholdsecurity.com/Blog/Emergency-Action-Plans-are-critical-for-your-company/

[51] OSHA [Internet]: Emergency action plan; [cited 2019 Nov 2]. Available from: https://www.osha.gov/SLTC/etools/evacuation/eap.html

[52] Sawacha, E., Naoum, S., Fong, D., Factors affecting safety performance on construction sites. Int J Proj Manage. 17:309–315, 1999.

[53] Tam, C.M., Zeng, S.X., Deng, Z.M., Identifying elements of poor construction safety management in China. Saf Sci. 42:569–586, 2004.

[54] Aksorn, T., Hadikusumo, B.H.W., Critical success factors influencing safety program performance in Thai construction projects. Saf Sci. 46(4):709–727, 2008.

[55] Mohamed, S., Safety climate in construction site environments. J Constr Eng Manage. 128(5):375–384, 2002.

[56] Safety+Health [Internet]: Reporting Near Misses; [cited 2019 Nov 10 9. Available from: https://www.safetyandhealthmagazine.com/articles/10994-reporting-near-misses

[57] Industry Safe [Internet]: Why is near miss reporting important?; [cited 2019 Nov 10] Available from: https://www.industrysafe.com/blog/why-is-near-miss-reporting-important

[58] Creative Safety Supply [Internet]: Why are safety signs important?, [cited 2019 Nov 12]. Available from: https://www.creativesafetysupply.com/qa/safety-signs/why-are-safety-signs-important

[59] Work Safe [Internet]: Traffic management in manufacturing; [cited 2019 Nov 19]. Available from: https://worksafe.govt.nz/topic-and-industry/manufacturing/traffic-management-manufacturing/

Investigation of Local Scour Hole Dimensions around Circular Bridge Piers under Steady State Conditions

Ömer Yavuz ESKİ[1]
Ayşegül ÖZGENÇ AKSOY[2]

ABSTRACT

The local scour around bridge piers is one of the main causes of bridge failures. In this study, scour hole dimensions around circular bridge piers were investigated under clear water scour conditions for various steady flow rates. The experiments were performed with four different bridge pier diameters and seven different flow rates by using uniform sediment with a median diameter of 1.63 mm and geometric standard deviation of 1.3. After each experiments the bathymetry of scour hole was determined. New empirical equations to estimate scour hole length, scour hole width and scour hole volume ($\forall$) are proposed by using experimental findings and experimental data available in the literature. The experimental results were also compared with those calculated using several empirical equations given by previous studies. Since there is a lack of data about scour hole dimensions, the experimental findings presented in this study are useful for the researchers investigating the local scour process, and have contributed to the few experimental data in the literature.

Keywords: Clear water scour, bridge piers, scour hole dimensions.

1. INTRODUCTION

Local scour around bridge piers is the one of the main reasons of the bridge failures. There are many studies related to scour depth estimation [1, 2, 3, 4, 5, 6, 7, 8, 9, 10, 11, 12, 13, 14, 15, 16, 17]. But there is still a lack of studies related to scour hole dimension estimation.

Yanmaz and Altinbilek [4] performed sets of experiments by using single cylindrical and square bridge pier models under clear water conditions with uniform bed materials. They proposed two equations to estimate the scour depth and the volume of the scour hole around the cylindrical pier.

---

1 Dokuz Eylul University, Civil Engineering Department, İzmir, Turkey - omer.yavuz.eski@hotmail.com
  https://orcid.org/0000-0002-4737-8241

2 Dokuz Eylul University, Civil Engineering Department, İzmir, Turkey - aysegul.ozgenc@deu.edu.tr
  https://orcid.org/0000-0001-8779-5499

Khwairakpam et al. [18] investigated local scour around circular bridge piers experimentally. In their study, the experiments were conducted under clear water and steady state flow conditions. On the basis of the experimental results, they proposed empirical equations to estimate scour hole depth, scour hole length, scour hole width, scour hole area and scour hole volume.

Das et al. [19] performed experiments to investigate equilibrium scour hole geometry around a circular pier. They proposed some empirical equations to predict the scour hole depth, scour hole length, scour hole width, scour hole area, and scour hole volume.

D'alessandro [20] performed experiments under clear water and steady state flow conditions with uniform bed materials to investigate local scour around circular bridge piers. He analyzed the effect of blockage on scour hole geometry in their experiments.

Hodi [21] carried out experiments to investigate scour geometry of circular bridge piers influenced by flume width in the laboratory condition. The experiments were conducted by using uniform sediment size under steady flow and clear water conditions.

Khan et al. [22] investigated local scour around various sizes and shapes bridge piers experimentally. The experiments were performed under clear water and steady state flow conditions with uniform sediment.

In this study, the shape of the scour hole around circular bridge piers was investigated under different steady state flow rate conditions by using four different bridge pier diameters. The dimension of the scour hole was determined after each experiment and new empirical equations were proposed to estimate scour hole length, scour hole width and scour hole volume ($\forall$).

2. THEORETICAL BACKGROUND

It is known that the dimension of the scour hole (scour length and scour width) is a function of equilibrium scour depth d_s [18, 19]. Thus the parameters effecting the scour hole around a bridge pier are; density of the water (ρ), dynamic viscosity of the water (μ), density of the bed material (ρ_s), median grain size of the bed material (d_{50}), pier diameter (D), approach flow depth (h), velocity of the water (V), acceleration due to gravity (g), equilibrium scour depth (d_s), and pier shape. Thus the value of the scour length can be written as

$$L_s = f_1(\rho, \mu, \rho_s, d_{50}, D, h, V, g, d_s) \qquad (1)$$

The independent parameters ρ, ρ_s and g can be combined as g' where $g' = [(\rho_s - \rho)/\rho]\, g$ [19] and under turbulent flow conditions the effect of μ can be neglected. In addition, Densimetric Froude particle number (F_d) has an important role for the scour process [10] and it is defined as $F_d = V/\sqrt{(g'd_{50})}$. The non-dimensional parameters were obtained by means of Buckingham π theorem as.

$$\frac{L_s}{D} = f_3\left(\frac{d_s}{D}, F_d\right) \qquad (2)$$

Similarly scour hole width (W_s) and scour hole volume ($\forall$) can be expressed as,

$$\frac{W_s}{D} = f_3\left(\frac{d_s}{D}, F_d\right) \tag{3}$$

$$\frac{V}{D} = f_3\left(\frac{d_s}{D}, F_d\right) \tag{4}$$

Some of the relations predicting the scour hole dimension are as follows:

Yanmaz and Altinbilek [4] suggested the following equation to estimate the volume of the scour hole.

$$V = \frac{\pi}{3\tan\phi}\left(\frac{d_s^3}{\tan\phi} + \frac{3\,d_s^2\,b}{2}\right) \tag{5}$$

where ϕ is the angle of repose of sediment.

Khwairakpam et al. [18] proposed Eq. (6), Eq. (7) and Eq. (8) to predict length, width and volume of the scour hole, respectively.

$$L_s = \left\{3.958\left(\frac{h}{D}\right) - 2.371\right\}d_s + \left\{-2.649\left(\frac{h}{D}\right) + 5.082\right\} \tag{6}$$

$$W_s = \left\{6.204\left(\frac{h}{D}\right) - 5.412\right\}d_s + \left\{-4.435\left(\frac{h}{D}\right) + 7.597\right\} \tag{7}$$

$$V_s = \left\{-1.520\left(\frac{h}{D}\right) + 3.661\right\}e^{(1.568(h/D)-0.716)d_s} \tag{8}$$

where the units of the d_s, L_s, W_s are cm and V_s is cm^3.

Das et al. [19] have given the following equations to estimate length, width and volume of the scour hole.

$$\frac{L_s}{D} = 5.065\left(\frac{d_s}{D}\right) \tag{9}$$

$$\frac{W_s}{D} = 5.576\left(\frac{d_s}{D}\right) \tag{10}$$

$$\frac{V_s}{V_c} = 0.161\,e^{\left(2.461\left(\frac{d_s}{D}\right)\right)} \tag{11}$$

where V_c is the characteristic volume of pier below the water level.

3. EXPERIMENTAL SET-UP, MEASUREMENT DEVICES AND METHOD

The scheme of the experimental set-up is given in Fig. 1. The flume is 18.6 m long, 0.80 m wide and 0.75 m high. The slope of the flume was fixed to 0.006. The bed material was uniform granular sediment with median diameter d_{50} of 1.63 mm, geometric standard deviation of 1.3 and angle of repose of sediment ϕ of 33°. Sediment layer thickness was 0.26 m. The bridge piers were located at 11.5 m from the upstream end of the flume. Before each

experiment, the flume bed was readjusted by using a system moving on the rails over the side walls along the flume. The flow rates and approach flow depths were measured by using electromagnetic flow meter and ultrasonic level sensors (ULS), respectively.

It is observed that the scour depths did not change after 320 minutes in the case of the largest flow rate and pier diameter. So the duration of the experiments was designated as 480 min which is sufficient to reach the equilibrium scour depth and scour hole dimension.

The scheme of the experimental setup is given in Figure 1.
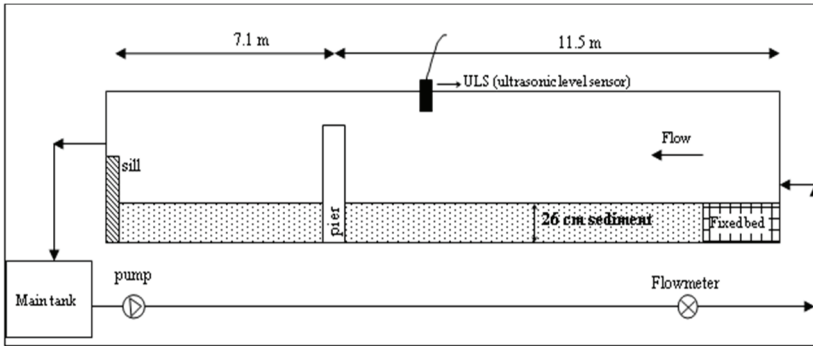
Fig. 1 - The scheme of the experimental set-up

4. EXPERIMENTAL RESULTS

28 experiments were performed by using seven different steady flow rates and four different circular bridge pier diameters.

The features of the experiments are given in Table 1 where D is pier diameter, Q is flow rate, y is approach flow depth, F_d is densimetric Froude particle number and (V/V$_c$) is flow intensity.

The critical velocity V_c is determined from the equation given below [23].

$$\frac{V_c}{u_{*c}} = 5.75 \log\left(5.53 \frac{y}{d_{50}}\right) \tag{12}$$

where u_{*c} is the critical shear velocity which can be calculated by using the following relations [7]:

$$u_{*c} = 0.0115 + 0.0125 d_{50}^{1.4} \qquad \text{for } 0.1\text{mm} < d_{50} < 1\text{mm} \tag{13}$$

$$u_{*c} = 0.0305 d_{50}^{0.5} - 0.0065 d_{50}^{-1} \qquad \text{for } 1\text{mm} < d_{50} < 100\text{mm} \tag{14}$$

In these relations u_{*c} is in m/s and the sediment size d_{50} is in mm.

Clear water scour was observed since the flow intensity parameters (V/V$_c$) are smaller than 1 during the experiments.

Table 1 - The features of the experiments

Experiment No	D (cm)	Q (l/s)	y (cm)	F_d	V/V_c
AE1	8	43	19.5	1.70	0.49
AE2	8	47	20.2	1.79	0.51
AE3	8	53	20.7	1.97	0.56
AE4	8	57	21.3	2.06	0.58
AE5	8	62	22.3	2.14	0.60
AE6	8	66	22.7	2.24	0.63
AE7	8	71	23.4	2.33	0.65
AE8	11	43	19.5	1.70	0.49
AE9	11	47	20.2	1.79	0.51
AE10	11	53	20.7	1.97	0.56
AE11	11	57	21.3	2.06	0.58
AE12	11	62	22.3	2.14	0.60
AE13	11	66	22.7	2.24	0.63
AE14	11	71	23.4	2.33	0.65
AE15	15	43	19.5	1.70	0.49
AE16	15	47	20.2	1.79	0.51
AE17	15	53	20.7	1.97	0.56
AE18	15	57	21.3	2.06	0.58
AE19	15	62	22.3	2.14	0.60
AE20	15	66	22.7	2.24	0.63
AE21	15	71	23.4	2.33	0.65
AE22	20	43	19.5	1.70	0.49
AE23	20	47	20.2	1.79	0.51
AE24	20	53	20.7	1.97	0.56
AE25	20	57	21.3	2.06	0.58
AE26	20	62	22.3	2.14	0.60
AE27	20	66	22.7	2.24	0.63
AE28	20	71	23.4	2.33	0.65

The measured parameters are given in Table 2 where d_s is equilibrium scour depth, W_s is the scour hole width, L_s is the scour hole length and ∀ is the scour hole volume.

The schematic sketch of the scour hole is given in Figure 2.
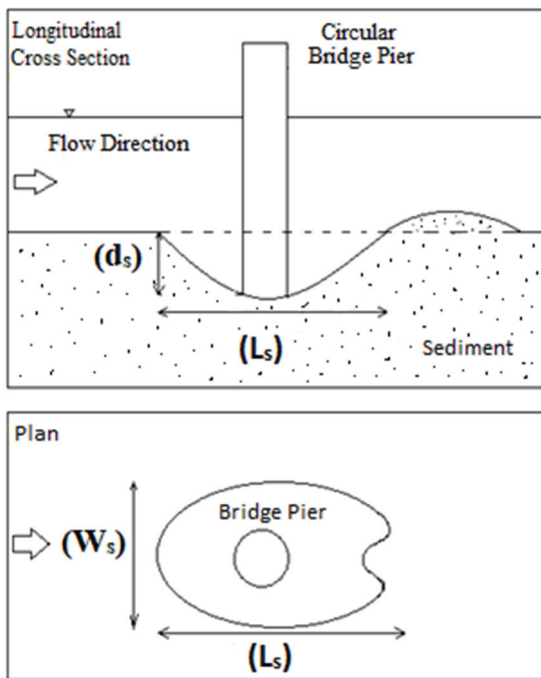
Fig. 2 - Schematic sketch of the scour hole [18]

After each experiment, the longitudinal and cross sections were measured by means of laser meter with a resolution up to 0.2 mm. A grid was determined to measure the scour hole dimensions. Each grid cell has a dimension of 2*5 cm. That means measurements were taken for every two centimeters along the flow direction and every five centimeters along the channel cross-section. The scour hole volume was calculated by means of measured data for each experiment.

The measured longitudinal and cross sections are given in Figure 3 and 4, respectively.

Table 2 - The results of the experiments

Experiment No	d_s (cm)	W_s (cm)	L_s (cm)	V (cm³)
AE1	3	29.8	21	173.56
AE2	5.5	29.6	26	664.22
AE3	8	29.6	32	1553.31
AE4	9	33.6	34	2674.39
AE5	10	39.4	38	5571.06

Table 2 - The results of the experiments (continue)

Experiment No	d_s (cm)	W_s (cm)	L_s (cm)	V (cm³)
AE6	10.2	39.8	38	5365.91
AE7	11.2	40	46	7073.01
AE8	4.7	31	28	590.04
AE9	6.7	30	32	1344.90
AE10	10.4	47.8	42	3364.78
AE11	11.3	44.4	44	4651.27
AE12	12.8	50.8	50	7372.02
AE13	13.7	59.2	54	10138.80
AE14	14.6	53	60	15721.23
AE15	4.4	33.6	36	2404.00
AE16	6.8	44.2	42	2169.93
AE17	11.9	48.6	52	6905.75
AE18	13.3	56.6	58	7775.07
AE19	15.9	62	68	15579.21
AE20	16.6	62.2	70	22329.12
AE21	18.4	69.4	84	26596.91
AE22	7.2	51.6	44	2551.91
AE23	8.7	54.6	52	3894.75
AE24	10.2	61	58	9951.24
AE25	13.8	69	70	15444.34
AE26	16.1	71.4	76	28393.91
AE27	19.2	79	88	31081.73
AE28	20.6	79.2	96	42944.73
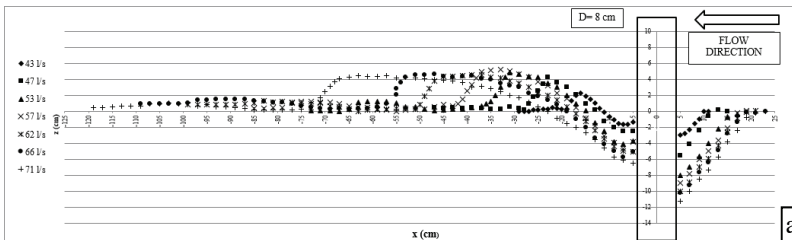
Fig 3 - The longitudinal sections measured after each experiment a) D=8 cm, b) D=11 cm, c) D=15 cm, d) D=20 cm.
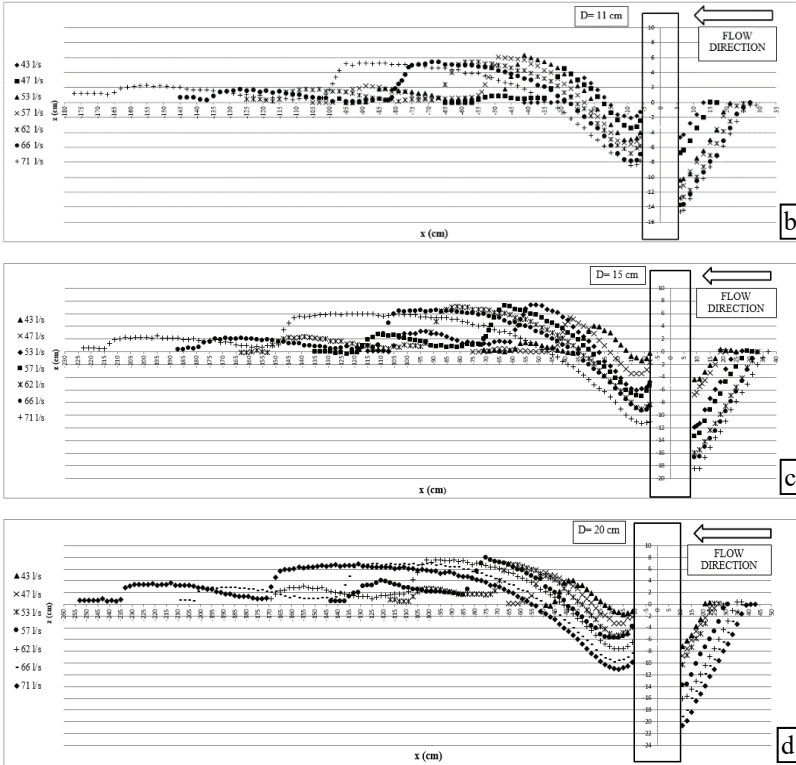
Fig 3 - The longitudinal sections measured after each experiment a) D=8 cm, b) D=11 cm, c) D=15 cm, d) D=20 cm. (continue)
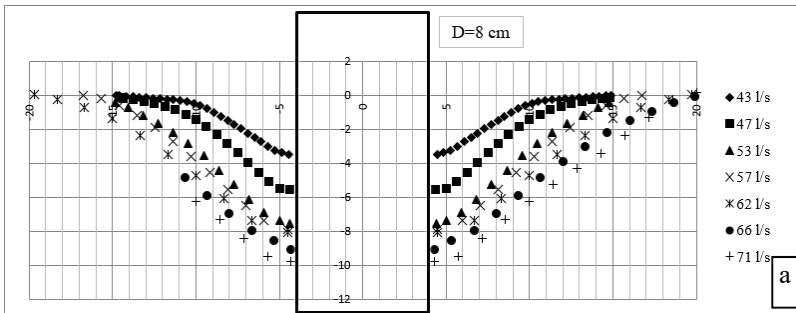
Fig 4 - The cross sections measured after each experiment a) D=8 cm, b) D=11 cm, c) D=15 cm, d) D=20 cm.
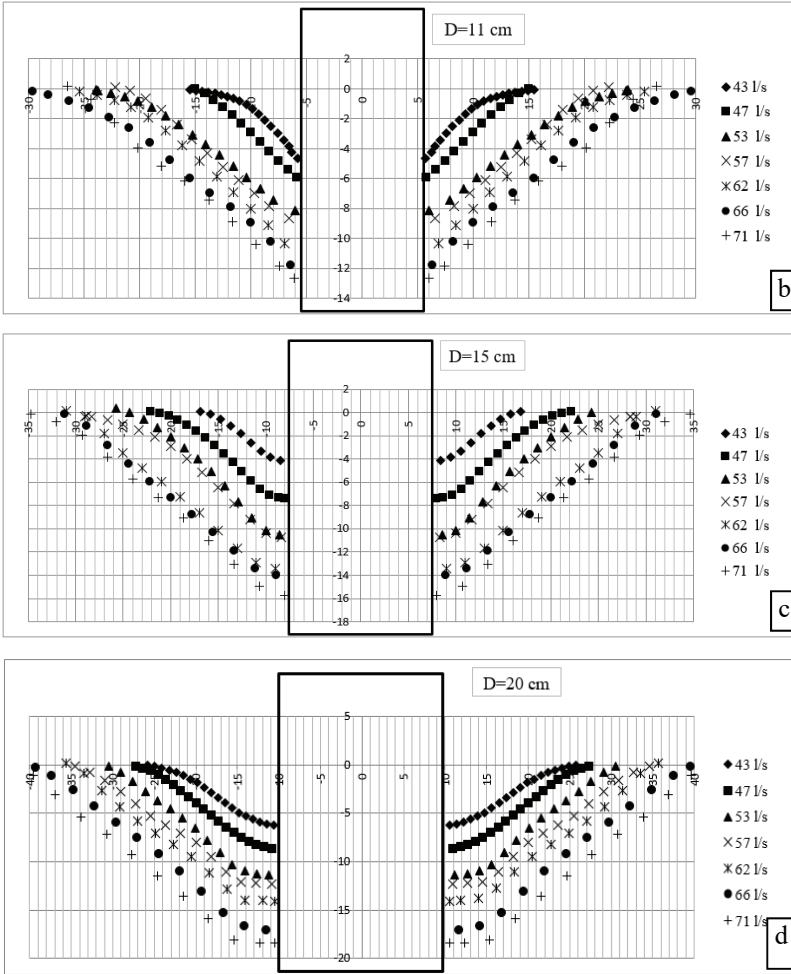
Fig 4 - The cross sections measured after each experiment a) D=8 cm, b) D=11 cm, c) D=15 cm, d) D=20 cm. (continue)

As seen from the graphs, the width and the length of the scour hole increase with the flow rate as expected. Accordingly, the volume of the scour hole increase with the flow rate. The equilibrium scour depth values increase depending on flow rate and diameter of the bridge pier. The maximum scour depth and scour hole volume were observed in the case of the largest flow rate (Q= 71 l/s) and pier diameter (D=20 cm).

28 additional experimental findings obtained by previous studies were taken into account to propose a more comprehensive and general equations. The features and the results of the additional experiments are given in Table 3 and Table 4, respectively. Only four scour hole volume data can be obtained from literature.

Table 3 - The features of the experiments obtained by previous studies ((A1-A16) D'Alessandro [20]; (B1-B4) Das et al.. [19]; (C1-C5) Hodi [21]; (D1-D3) Khan et al. [22])

Experiment No	D (cm)	y (cm)	d_{50} (mm)	F_d	V (m/s)	V/V_c
A1	3	12	0.51	2.64	0.24	0.86
A2	3	12	0.51	2.64	0.24	0.86
A3	10	12	0.51	2.64	0.24	0.86
A4	9	12	0.51	2.64	0.24	0.86
A5	8	12	0.51	2.64	0.24	0.86
A6	7	12	0.51	2.64	0.24	0.86
A7	9	12	0.51	2.64	0.24	0.86
A8	8	12	0.51	2.64	0.24	0.86
A9	7	12	0.51	2.64	0.24	0.86
A10	10	12	0.51	2.64	0.24	0.86
A11	8	12	0.51	2.64	0.24	0.86
A12	7	12	0.51	2.64	0.24	0.86
A13	9	12	0.51	2.64	0.24	0.86
A14	7	12	0.51	2.64	0.24	0.86
A15	8	12	0.51	2.64	0.24	0.86
A16	7	12	0.51	2.64	0.24	0.86
B1	11	12.5	0.825	2.14	0.247	0.682
B2	15.5	12.5	0.825	2.14	0.247	0.682
B3	13	12.5	0.825	2.14	0.247	0.682
B4	11	12.5	0.825	2.14	0.247	0.682
C1	2	10	0.85	2.1	0.25	0.76
C2	2	10	0.85	2.1	0.25	0.76
C3	3	10	0.85	2.1	0.25	0.76
C4	3	10	0.85	2.1	0.25	0.76
C5	4.5	10	0.85	2.1	0.25	0.76
D1	5	8.2	0.54	2.82	0.264	0.936
D2	4	8.2	0.54	2.82	0.264	0.936
D3	3	8.2	0.54	2.82	0.264	0.936

Table 4 - The results of the experiments obtained by previous studies ((A1-A16) D'Alessandro [20]; (B1-B4) Das et al.. [19]; (C1-C5) Hodi [21]; (D1-D3) Khan et al. [22])

Experiment No	L_s (cm)	d_s (cm)	W_s (cm)	V (cm^3)
A1	20.25	5.05	21.6	No data
A2	23.25	5.44	27.8	No data
A3	50.4	12.27	56.4	No data
A4	42.67	10.83	49	No data
A5	42.08	10.55	47.8	No data
A6	32.15	5.68	31.6	No data
A7	43.56	10.95	50.4	No data
A8	41.29	10.04	46.8	No data
A9	37.75	8.81	43.2	No data
A10	45.36	11.09	50.6	No data
A11	38.11	9.37	45.8	No data
A12	39.14	9.32	46.1	No data
A13	41.78	8.66	43.2	No data
A14	32.85	8.11	40.6	No data
A15	40.49	9.94	47.6	No data
A16	38.45	9.42	45.2	No data
B1	46	9.2	53	5835
B2	58	11.2	60	9545
B3	48	9.6	49	6842
B4	42	8.2	48	4780
C1	10.43	2.47	10	No data
C2	9.13	1.93	7	No data
C3	18.26	4.43	18.5	No data
C4	13.04	2.67	12	No data
C5	21.3	5.5	22.75	No data
D1	22.5	7	22.5	No data
D2	19	5.9	19	No data
D3	17	4.8	17	No data

New empirical relations to estimate scour hole length (L_s), scour hole width (W_s) and scour hole volume ($\forall$) were investigated by using the experimental findings obtained by present study and previous studies. The proposed relations were obtained by using the least squares method which minimizes the sum of squared residuals. Eq 15, Eq 16 and Eq 17 are proposed by using the experimental data obtained from the present study and experimental findings obtained by D'Alessandro [20], Das et al. [19], Hodi [21] and Khan et al. [22].

$$\frac{L_s}{D} = 3.39 \left(\frac{d_s}{D}\right)^{0.54} F_d^{0.32} \tag{15}$$

$$\frac{W_s}{D} = 2.1 \left(\frac{d_s}{D}\right)^{0.33} F_d^{0.91} \tag{16}$$

$$\frac{\forall}{D^3} = 0.99 \left(\frac{d_s}{D}\right)^{1.95} F_d^{1.96} \tag{17}$$

The comparison between the experimental results including the previous studies and computed values by using Eq 15, Eq 16 and Eq 17 are given in Figures 5, 6 and 7, respectively. The proposed equations were evaluated in terms of determination coefficient (R^2) and scatter index (SI). The SI indicates normalized measure of errors and lower values of SI means better model performance. These parameters are defined as follows:

$$R^2 = \left[\frac{\sum_{i=1}^{n}\left(d_{s,measured_i} - \overline{d_{s,measured}}\right)\left(d_{s,computed_i} - \overline{d_{s,computed}}\right)}{\sqrt{\sum_{i=1}^{n}\left(d_{s,measured_i} - \overline{d_{s,measured}}\right)^2 \sum_{i=1}^{n}\left(d_{s,computed_i} - \overline{d_{s,computed}}\right)^2}}\right]^2 \tag{18}$$

$$SI(\%) = \frac{\sqrt{\frac{\sum_{i=1}^{n}\left(d_{s,measured_i} - d_{s,computed_i}\right)^2}{n}}}{\overline{d_{s,measured}}} \cdot 100 \tag{19}$$

where $\overline{d_{s,measured}}$ and $\overline{d_{s,computed}}$ are the arithmetic mean of the measured and computed scour depth values, respectively.

As shown in Figures 5, 6 and 7 the predicted scour hole dimensions are in good agreement with those obtained from experiments. the determination coefficient values (R^2) were calculated as 0.98, 0.95 and 0.97 for L_s, W_s and $\forall$, respectively. That means a strong relationship exist between the calculated and measured scour hole dimensions. So, the proposed equations can predict reliable scour hole dimension values. In addition computed scatter index values (SI) support this strong relationship.

Measured experimental results were also compared with those calculated by using equations given by Yanmaz and Altınbilek [4], Khwairakpam et al. [18] and Das et al. [19]. The results are given Figures 8, 9, 10, 11, 12, 13 and 14, respectively.
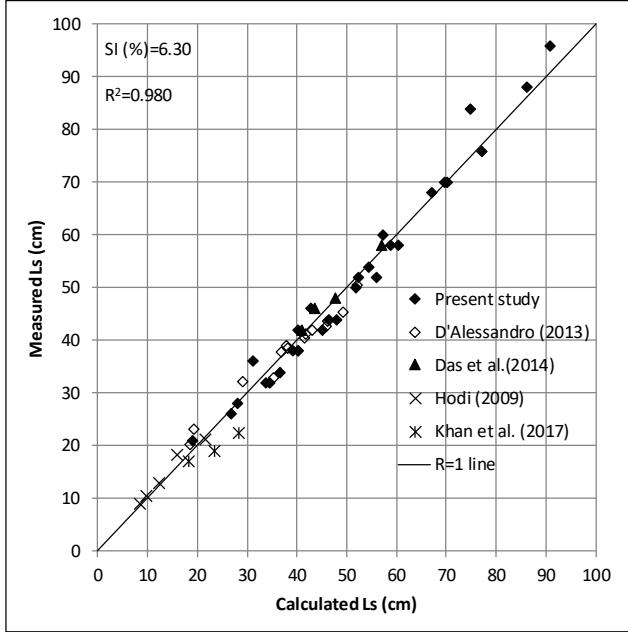
Fig. 5 - Comparison of measured and calculated L_s values obtained by proposed equation
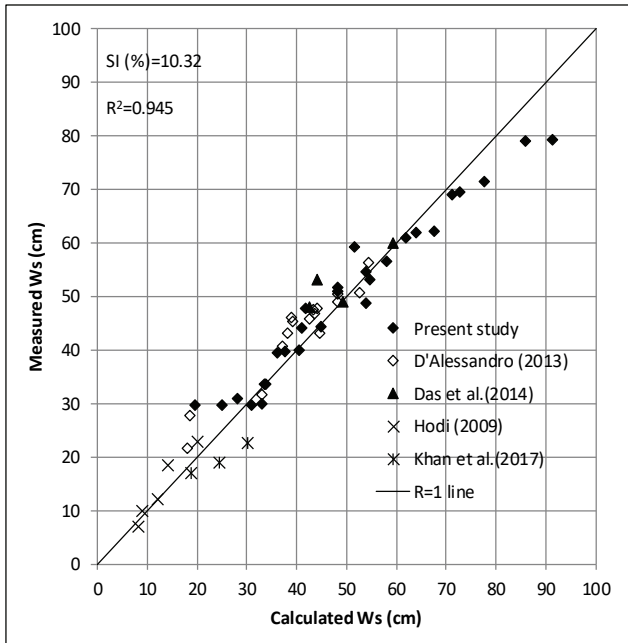

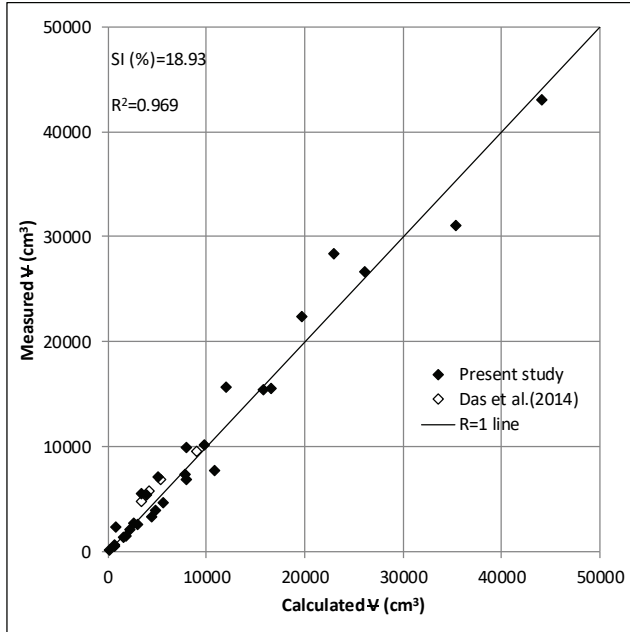*Fig. 6 - Comparison of measured and calculated W_s values obtained by proposed equation*

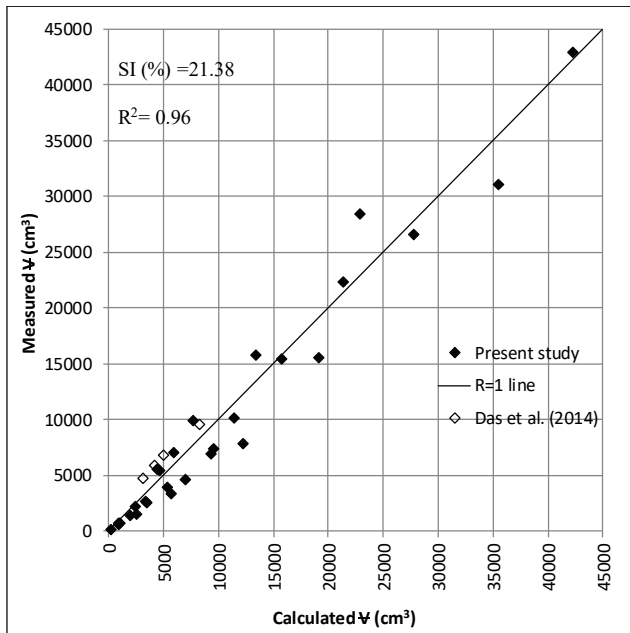*Fig. 7 - Comparison of measured and calculated ∀ values obtained by proposed equation*

Fig. 8 - Comparison of measured and calculated ∀ values obtained by Yanmaz and Altınbilek (1991) equation
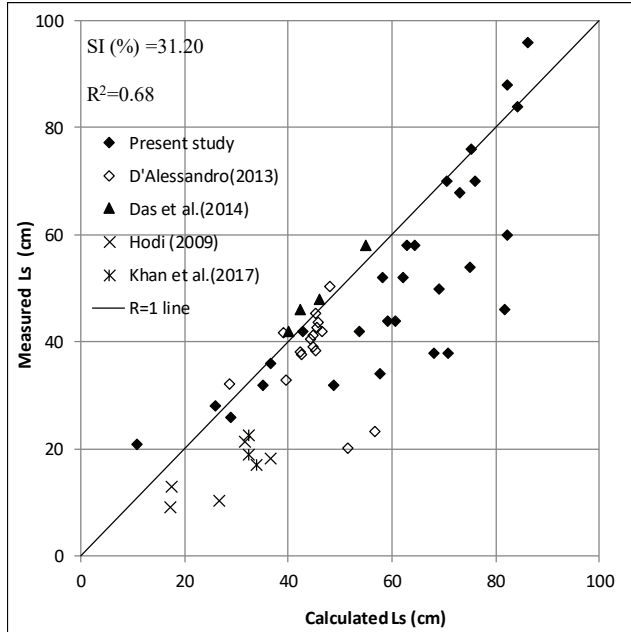
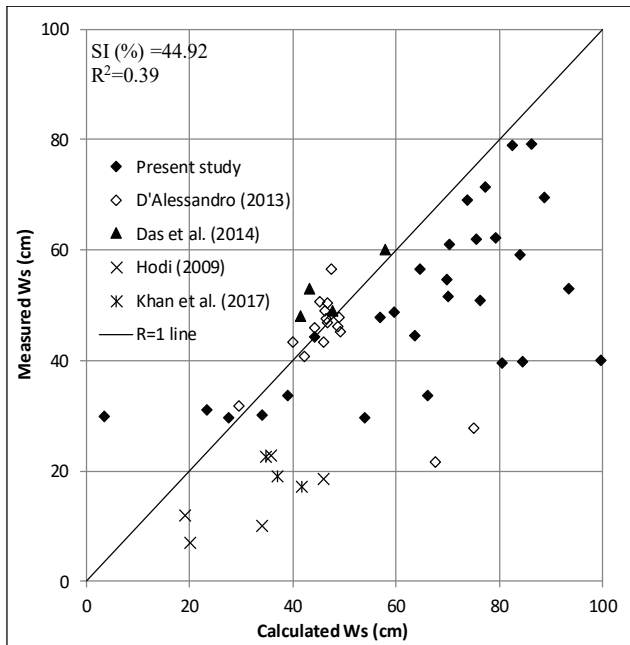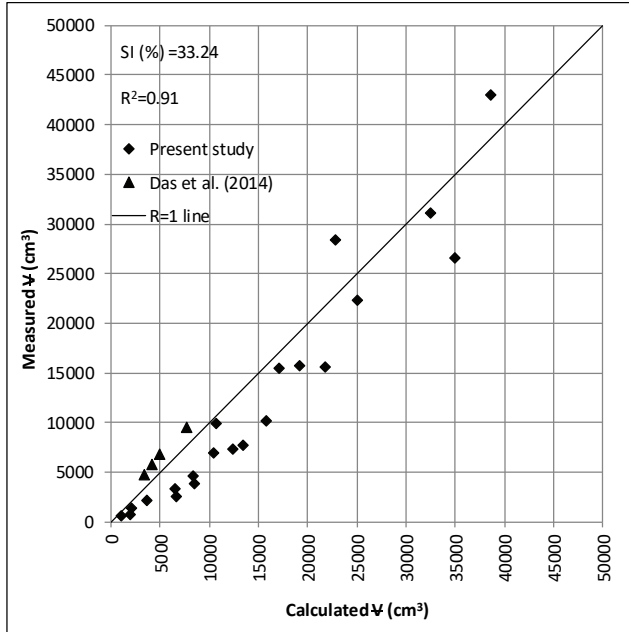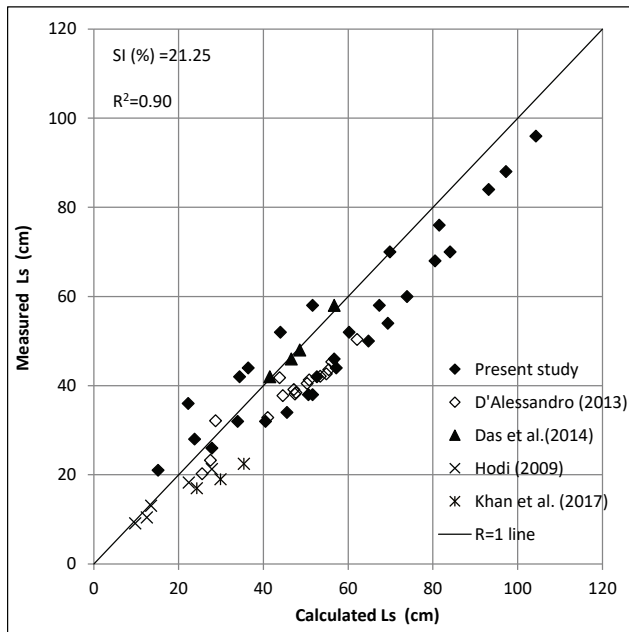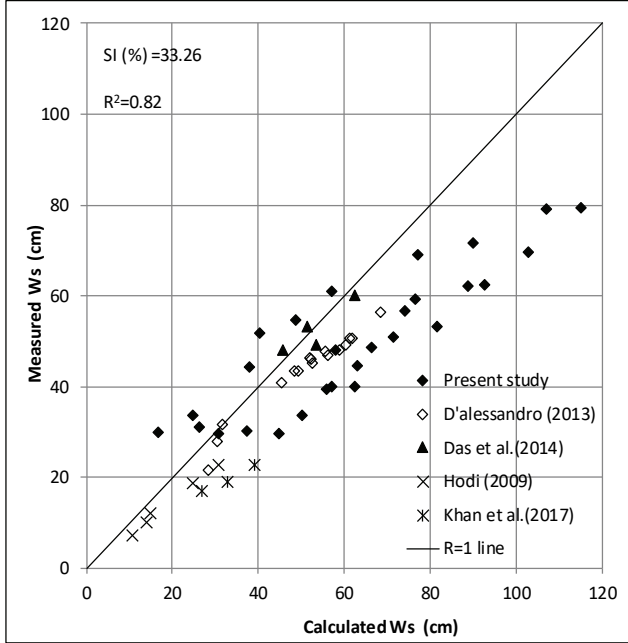*Fig. 9 - Comparison of measured and calculated L_s values obtained by Khwairakpam et al. (2012) equation*

Fig. 10 - Comparison of measured and calculated W_s values obtained by Khwairakpam et al. (2012) equation

Fig. 11 - Comparison of measured and calculated Ɐ values obtained by Khwairakpam et al. (2012) equation

Fig. 12 - Comparison of measured and calculated L_s values obtained by Das et al. (2014) equation
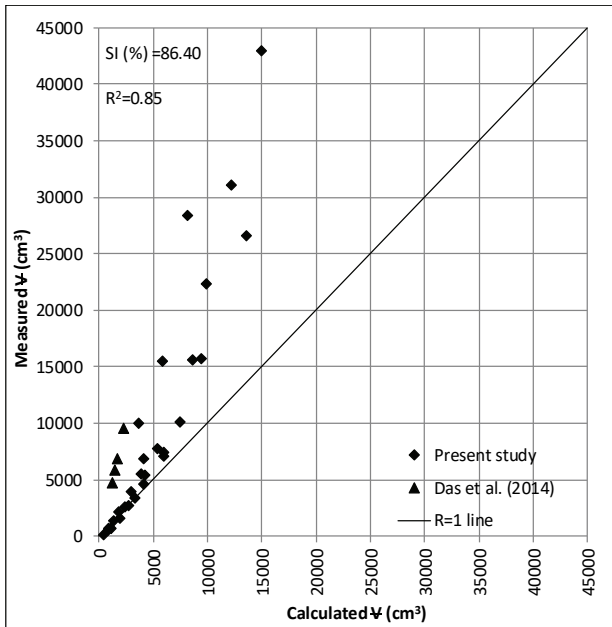
Fig. 13 - Comparison of measured and calculated W_s values obtained by Das et al. (2014) equation

Fig. 14 - Comparison of measured and calculated ∀ values obtained by Das et al. (2014) equation

According to the R^2 and SI values given in the figures, the equation proposed by Yanmaz&Altinbilek is in good agreement with experimental results obtained for volume values. The R^2 values obtained for Khwairakpam et al. equation are smaller than those obtained from other equations. The main reason could be the large number of empirical coefficients used in the equations.

Scatter index and determination coefficient values corresponding to proposed and given by other researcher's equations are given in Table 5.

Table 5 - Scatter index and determination coefficient values of various equations

	Yanmaz and Altınbilek [4]		Khwairakpam at al. [18]		Das at al. [19]		Present Equation	
	SI (%)	R^2	SI (%)	R^2	SI (%)	R^2	SI (%)	R^2
L_s	-	-	31.20	0.68	21.25	0.90	6.30	0.98
W_s	-	-	44.92	0.39	33.26	0.82	10.32	0.95
$\forall$	21.28	0.96	33.24	0.91	86.40	0.85	18.93	0.97

As shown in Table 5 the best agreement between measured and calculated parameters obtained by using present equations given in this study. The differences of the present equations are to involve the densimetric Froude particle number (F_d). According to the results it is revealed that F_d has an important role to estimate scour hole dimensions.

The statistical convenience of the proposed equations Eq 15, Eq 16 and Eq 17 were also established by applying Fisher (f) test. If the calculated f value is greater than the critical f value, then the experimental data explain the regression equation with 0.01 confidence level. To compute the f value following equation is used.

$$f = \frac{SSR/\vartheta_1}{SSE/\vartheta_2} \tag{20}$$

where SSR is the sum of squared residuals, SSE is the sum of squares for error, ϑ_1 is the number of the independent variables (k), and ϑ_2=n-k-1, (n is the number of the data). SSR and SSE can be calculated from the following equations:

$$SSR = \sum_{i=1}^{n}\left(x_i^{computed} - \overline{x_i^{measured}}\right)^2 \tag{21}$$

$$SSE = \sum_{i=1}^{n}\left(x_i^{measured} - x_i^{computed}\right)^2 \tag{22}$$

where $\overline{x_i^{measured}}$ are the arithmetic mean of the observed and computed values.

The critical value of f depends on the number of the data and selected significance level. The critical values of f for the 0.01 significance level are 5.18 for Eq 15 and Eq 16, and 5.42 for Eq 17. The f values were computed as 438, 1231 and 447 for the equations of 15, 16 and 17,

respectively. Eventually, the significance of the proposed equations Eq 15, Eq 16 and Eq 17 are demonstrated.

5. CONCLUSION

In this study, scour hole dimensions around circular bridge piers were investigated under clear water scour conditions for various steady flow rates.

Four bridge piers with different diameters and seven different flow rates were used during the experimental tests. According to the experimental findings and experimental data available in the literature, three equations were proposed to estimate scour hole length (L_s), scour hole width (W_s) and scour hole volume (V). The experimental results were also compared with those calculated using several empirical equations given by previous studies. The best fit between observed and calculated values was obtained by the proposed equation in this study. The statistical convenient of the equations were also investigated. The following conclusions were obtained according to the results of this study:

- The scour hole length, width and depth were increased with the pier diameter and mean flow velocity. The maximum scour hole occurred in the case of maximum rate of the flow and largest pier diameter used.

- The scour hole length, width and volume values were calculated by means of Equation 15, Equation 16 and Equation 17 and the results of the equations are in good agreement with experimental findings. The biggest difference of the proposed equation is that it contains the Froude particle number (F_d) which has an important role to estimate the scour hole dimensions.

- To indicate the best fit equation scatter index (SI%) values were computed for proposed and available equations given in the literature by using the observed and calculated scour hole length, width and volume values. According to the SI values it is revealed that proposed equations give the best fit between measured and calculated parameters and can be used to predict scour hole dimensions.

Since there is a lack of data about scour hole dimensions, the experimental findings are useful for the researchers investigating the scour hole dimensions and have contributed to the few experimental data in the literature.

References

[1] Laursen, E M. "Scour at bridge crossings", Bulletin No. 8, Iowa Highway Research Board, Ames, IO,1958, https://cedb.asce.org/CEDBsearch/record.jsp?dockey=0294630.

[2] Breusers, H.N.C., Nicollet, G., Shen, H.W., "Local scour around cylindrical piers", Journal of Hydraulic Resources, 15(3): 211–252, 1977, https://doi.org/10.1080/00221687709499645.

[3] Chiew, Y.M., Melville, B.W. "Local scour around bridge piers", Journal of Hydraulic Research, 25(1): 15–26, 1987, https://doi.org/10.1080/00221688709499285.

[4] Yanmaz, M., Altinbilek, H.D. "Study of time dependent local scour around bridge piers", Journal of Hydraulic Engineering, 117(10): 1247–1268, 1991, https://doi.org/10.1061/(ASCE)0733-9429(1991)117:10(1247).

[5] Kandasamy J.K., Melville B.W. "Maximum local scour depth at bridge piers and abutments", Journal of Hydraulic Research, 36(2): 183–198, 1998, https://doi.org/10.1080/00221689809498632.

[6] Kothyari, U.C., Garde, R.J., Range Raju, K.G. "Temporal variation of scour around circular bridge piers", Journal of Hydraulic Engineering, 118(8): 1091–1106, 1992 , https://doi.org/10.1061/(ASCE)0733-9429(1992)118:8(1091).

[7] Melville, B.W. "Pier and abutment scour: Integrated approach", Journal of Hydraulic Engineering, 123(2): 125–136, 1997, https://doi.org/10.1061/(ASCE)0733-9429(1997)123:2(125).

[8] Melville, B.W., Chiew, Y.M. "Time scale for local scour at bridge piers", Journal of Hydraulic Engineering, 125(1): 59–65, 1999, https://doi.org/10.1061/(ASCE)0733-9429(1999)125:1(59).

[9] Richardson, E.V., Davis, S.R. "Evaluating scour at bridges", 5th ed. Hydraulic Engineering Circular No 18, Federal Highway Administration Publication No FHWA-NHI 01-001, Washington, DC,2001, https://www.fhwa.dot.gov/engineering/hydraulics/pubs/hif12003.pdf.

[10] Oliveto, G., Hager, W.H. "Temporal evolution of clear-water pier and abutment scour", Journal of Hydraulic Engineering, 128(9): 811–820, 2002, https://doi.org/10.1061/(ASCE)0733-9429(2002)128:9(811).

[11] Mia, F., Nago, H. "Design method of time dependent local scour at circular bridge pier", Journal of Hydraulic Engineering, 129(6): 420–427, 2003, https://doi.org/10.1061/(ASCE)0733-9429(2003)129:6(420).

[12] Chang, W.Y., Lai, J.S., Yen, C.L. "Evolution of scour depth at circular bridge piers", Journal of Hydraulic Engineering, 130(9): 905–913, 2004, https://doi.org/10.1061/(ASCE)0733-9429(2004)130:9(905).

[13] Kothyari, U.C., Hager, W.H. Oliveto, G. "Generalized approach for clear-water scour at bridge foundation elements", Journal of Hydraulic Engineering, 133(11): 1229–1240, 2007, https://doi.org/10.1061/(ASCE)0733-9429(2007)133:11(1229).

[14] Sheppard, D.M., Demir, H., Melville, B. "Scour at wide piers and long skewed piers", National Cooperative Highway Research Program Report 682, Transportation Research Board, Washington, DC, 2011, https://doi.org/10.17226/14426.

[15] Ozgenc Aksoy, A., Eski, O.Y. "Experimental investigation of local scour around circular bridge piers under steady state flow conditions", Journal of the South African Institution of Civil Engineering Vol 58 No 3, pp. 21–27, 2016, http://dx.doi.org/10.17159/2309-8775/2016/v58n3a3.

[16] Yılmaz, M., Yanmaz, A.M., Köken., M., "Experimental investigation of local scour around circular bridge piers under steady state flow conditions" IMO Teknik Dergi Vol 29 No 1, pp. 8167-8184, 2018, https://doi.org/10.18400/tekderg.345263.

[17] Bor Turkmen, A., Guney, M.Ş., "Experimental Investigation of Scour Hole Characteristics for Different Shapes of Piers Caused by Flood Hydrograph Succeeding Steady Flow" IMO Teknik Dergi Vol 32 No 2, 2021, https://doi.org/10.18400/tekderg.595126.

[18] Khwairakpam, P., Ray, S. S., Das, S., Das, R., Mazumdar, A. "Scour hole characteristics around a vertical pier under clearwater scour conditions", ARPN Journal of Engineering and Applied Sciences, 7(6), 649-654, 2012, http://www.arpnjournals.com/jeas/research_papers/rp_2012/jeas_0612_704.pdf.

[19] Das, S., Das, R., Mazumdar, A. "Variations in clear water scour geometry at piers of different effective widths", Turkish Journal of Engineering & Environmental Sciences, (38), 97–111, 2014, http://doi:10.3906/muh-1308-11.

[20] D'alessandro, C. M. "Effect of blockage on circular bridge pier local scour", Master of Thesis, Department of Civil and Environmental Engineering, Windsor University, Canada, 2013, http://citeseerx.ist.psu.edu/viewdoc/download?doi=10.1.1.918.5963&rep=rep1&type=pdf.

[21] Hodi, B. S. "Effect of blockage and densimetric froude number on circular bridge pier local scour", Master of Thesis, Windsor University, Canada, 2009, https://core.ac.uk/download/pdf/72779078.pdf.

[22] Khan, M., Tufail, M., Fahad, M., Azmathullah, H.M., Aslam, M.S., Khan, F.A., Khan A. "Experimental Analysis Of Bridge Pier Scour Pattern", Journal of Engineering and Applied Sciences, Vol.36(1), 2017, https://journals.uetjournals.com/index.php/JEAS/article/view/2.

[23] Melville, B. W, and Sutherland, A. J. "Design Method for Local Scour at Bridge Piers." Journal of Hydraulic Engineering, vol. 114, no. 10, pp. 1210–1226,1988https://ascelibrary.org/doi/abs/10.1061/(ASCE)0733-9429(1988)114:10(1210)

Developing a Virtual Safety Training Tool for Scaffolding and Formwork Activities

Gokhan KAZAR[1]
Semra COMU[2]

ABSTRACT

As occupational accidents usually occur due to unsafe human behaviours in the construction industry, safety training is inevitably necessary for site personnel. On construction sites, various training methods including traditional and innovative ones, have been adopted to prevent accidents. In recent years, virtual safety training has been more prevalent because of providing highly engaging practice in a risk-free environment. Although these training tools have innumerable advantages in providing safety knowledge and awareness, they can be further improved. This study introduces a virtual safety training tool, V-SAFE.v2, to provide a more reliable and effective safety training for high-risk construction works. V-SAFE.v2 consists of three main modules; i) Training Module, ii) Testing Module 1, and iii) Testing Module 2. These modules are generated firstly to provide safety training for scaffolding and formwork activities and then to evaluate the safety performance of the trainees. An experiment was conducted with fifteen construction workers and ten engineers to measure the effectiveness of the training tool. The findings showed that V-SAFE.v2 is a reliable safety training tool for high-risk construction tasks as it supports collaboration, provides individual feedback, and repeatable practice. Also, the participants stated that V-SAFE.v2 has a great potential to reduce the falling from height accidents in the construction workplaces.

Keywords: Occupational safety, training, serious game, scaffolding, formwork.

1. INTRODUCTION

Due to the heavy work environment and complex tasks involved, construction sites have become one of the most hazardous workplaces. Statistics also show that the construction industry has the highest rate for occupational fatalities and injuries all around the world. There are approximately 60.000 occupational deaths in the construction industry every year [1]. According to the report of Bureau of Labor Statistics, while 5.5% of total workers are

1 Istanbul Gedik University, Department of Civil Engineering, Istanbul, Turkey - gokhan.kazar@gedik.edu.tr - https://orcid.org/0000-0002-8616-799X

2 Bogazici University, Department of Civil Engineering, Istanbul, Turkey - semra.comu@boun.edu.tr - https://orcid.org/0000-0001-5733-6195

employed in the construction industry, the fatality rate of construction works is approximately 20% in the U.S, which is higher than other sectors [2]. Such rates clearly show that construction sites have poor working conditions in terms of occupational safety and health. Despite giving more attention to safety issues for the last years, the number of construction accidents remains high. Therefore, there are high debates and concerns about the root causes of accidents in the construction industry. It is highly emphasized that human behaviour is one of the most important factors in occupational fatalities and injuries. Haslam et al. [3] noticed that 70% of the accidents occur due to unsafe behaviour of workers on construction sites, which shows the role of human factors in accidents. Besides, Guo and his colleagues [4] also stated that most of the accidents occurred because of inadequate safety consciousness of workers during the construction tasks. To eliminate such human-based problems, it is a well-known fact that safety training is the most efficient method. However, the effectiveness of safety training is another crucial point in the construction industry. Thus, alternative training techniques should be developed and provided to increase the reliability of safety training.

2. BACKGROUND

As known, construction works are very dangerous and carry a high risk for workers. Thus, the attitudes of workers during complex tasks might have catastrophic consequences on construction sites. In most of the previous studies, the significant correlation between unsafe human actions and construction accidents is highlighted [5-7]. For instance, Kale et al. [5] found that the factor of unsafe human activity is one of the most crucial root causes of occupational accidents in the construction industry. Moreover, the role of the human factors in construction accidents are indicated in a previous study [6]. According to the results of a previous study [7], the safety performance of the workers plays a major role in occupational accidents. In addition to unsafe human behaviour, the lack of appropriate safety training is one of the most important factors contributing to high fatality in the construction industry [9]. Previous studies in the field of construction safety emphasize that training is the most efficient human-based prevention method and should be provided to the construction workers [9-12]. Abdelhamid and Everett [9] suggest a relation between failing to identify unsafe conditions and worker training. Similarly, another research [12] found that worker actions were the main causal factor in accidents. In this context, Zhao and his colleagues [11] investigated the causes of electrocution in the U.S. construction industry. They [11] concluded that unsafe worker behaviour is the main cause of electrical fatalities and injuries. Tam and Fung [10] argue that behaviour-based safety training method has significant potential in reducing tower crane accidents. Therefore, an improperly trained worker may not be able to recognize the potential risks associated with construction works and avoid risky behaviour. Hence, more emphasis has recently been given to providing effective and adequate safety training to improve the safety performance of construction workers. Safety training methods can be grouped as i) traditional safety training programs and, ii) advanced technology-enabled safety training methods, to reduce the number of injuries and fatal accidents in construction workplaces.

2.1. Traditional Safety Training Methods

Until recently, safety training was generally provided by traditional methods in the construction industry. Zhao and Lucas [13] classified traditional safety training methods into three main categories; a) classroom training b) on-site training c) safety meetings. During classroom training, safety knowledge is just transferred only through videos, presentations, and guides. On the other hand, the employees are trained through practical applications such as the use of real tools, machines, and equipment in the on-site training method. Finally, safety meetings are held by providing presentation slides, videos, and weekly talks on safety issues encountered at construction sites [13]. Several studies provided traditional training methods to improve the safety performances of workers [14-15]. Jeschke and colleagues [14] developed a toolbox-training program aimed at improving the quality of collaboration between the project personnel on safety issues during the construction phases. The researchers used the classroom training method and 57 construction workers participated in the safety training program. A questionnaire and interview were conducted with the participants to understand the applicability of such a training method. Based on the assessments, they found that the toolbox meeting program of the trainees was beneficial and positively influenced daily work processes in terms of safety. In another study by Hinze [15], traditional safety training programs have been proposed to reduce accident rates in the construction industry. The researcher analysed major construction sites where safety training was provided based on the regulations of the Occupational Safety and Health Administration (OSHA). The results of the study show that the safety performances of large construction companies are significantly better concerning the general construction industry because of providing OSHA safety regulations [15].

On the other hand, several studies [16-17] show that traditional safety training methods are not as effective and reliable as desired. Such off-site training methods do not provide sufficient practice to experience intensively real working environments. Besides, the trainees are usually passive and bored during traditional training, which has a significant negative impact on their motivation [16]. As stated by Li et al. [18] an on-site training method could be an alternative solution to address the inefficiency of traditional safety training methods. Nevertheless, it is not widely preferred because it is time-consuming, expensive, requires special equipment, and carries real accident risks for trainees. Thus, today the majority of safety training has been delivered in classrooms through written documents, presentations, videos, and safety meetings at the construction sites. Due to the deficiencies of current safety training methods, recent studies have focused heavily on advanced technology-based safety training tools to improve the efficiency of safety training programs.

2.2. Serious Games for Advanced Technology-Enabled Safety Training

Recently, computer-based safety training tools have been more attractive in the field of construction safety to enhance the safety culture of employees. Especially those based on game-engine are more effective in developing safety knowledge and raising risk awareness due to providing interactive engagement and a risk-free environment [18]. Accordingly, construction safety training tools have been developed in recent years by using game technologies called serious games.

Serious games, a type of computer game, are designed to address real-life problems rather than entertainment goals [19]. Mertens et al. [20] stated that a serious game or game-based education integrates learning, games, and simulation components. Through the use of serious games, players can perform scenario-based tasks collaboratively and develop safety knowledge in simulated workplaces. Another advantage of serious games is that trainees can perceive the direct results of their activities on virtual platforms without experiencing their real impacts [21].

To date, serious games have been utilized for safety training in different areas such as aviation [22], medical [23], and military [24]. Also, game engine-based safety training tools have been widely utilized for construction tasks. They were developed for different application purposes including, hazard identification [25-27] delivering instructions for construction methods [28] and occupational safety training [29-30]. Pedro and his colleagues [27] introduced a game engine-based training tool that enables us to identify potential construction site hazards in a virtual environment. The training tool titled VSES consists of three different parts; a) Safety and Hazard Lecture b) Hazard Identification Game and c) Student Evaluation and Assessment modules. The first module was developed to support students to acquire safety knowledge and raise awareness of workplace hazards. The purpose of the second module is to allow virtual construction sites to be experienced and to identify the construction site risks introduced in the first module. The third module was designed to evaluate participants according to their safety performance. Fang and Teizer [29] presented a multi-user serious game that provides interactive safety training for crane operators. In this study, there are great efforts on developing an actual construction site conditions and simple game logic that can effectively train crane operators. They proposed a novel approach for crane operations to prevent accidents caused by blind points. One crane operator and a signalling person play together to lift loads safely from one place to another. The crane operator works in collaboration with the signalling player who warns the crane operator for blind points during the hoisting operation in the virtual environment.

Studies in the field of construction safety have confirmed that the usage of serious games provides important opportunities for trainees to develop safety knowledge and meet desired training objectives. Moreover, such previous initiatives prove that game-based training methods are more reliable and effective than conventional methods for construction works. However, there are still deficiencies in serious game-based training in terms of presenting all real construction site dynamics.

2.3. Scaffolding and Formwork Accidents

On construction sites, falling from height is the main cause of high fatality rates worldwide. For example, fall-related occupational deaths account for about 39% of all construction fatal accidents in the U.S [31]. This type of catastrophic accident occurs to a large extent during the use of temporary structures such as scaffolds [7, 32] and formworks [33]. Although diverse tasks are performed in the construction industry, 65% of such works are carried out by using scaffolding or such temporary structures [34]. Also, formwork is another common type of work for concrete structures. Therefore, there are many concerns about accidents related to the scaffolding [35-36] and formwork construction [37-38] to reduce accidents. Gürcanlı and Müngen [36] classified the main causes of incidences in the Turkish

construction industry. They revealed that the falls from scaffolds and roofs (54%) and falling objects (12%) were more likely to be encountered in the construction workplaces. Rubio-Romero et al. [31] investigated the safety conditions of scaffolds and evaluated 105 scaffolds installed at construction sites in Spain. The results of this study demonstrated that the general safety condition of non-standardized scaffolds is poor in terms of using anchor-tie, base plates, and walking platforms. Lopez-Arquillos et al. [38] evaluated the riskiest activities in vertical concrete formwork construction, such as columns and walls. According to the results, formwork construction, climbing ladders, and handling an object during the construction process were the highest risk activities for workers. Based on the literature review, it can be concluded that both scaffolding and formwork activities have a crucial role in common types of accidents, such as falling from a height, scaffold collapse, and falling objects. As a result, effective and reliable safety training methods are needed to prevent such accidents related to scaffolding and formwork construction.

2.4. Requirements of Safety Training Tools

Although serious games have been utilized as safety training tools in the field of construction safety, the reliability, applicability, and effectiveness of these tools can be further improved. For example, Zhou et al. [39] stated that only a few studies were conducted specifically for certain tasks such as working at height. Even though falling from height is one of the most prevalent accident types in construction sites [41], there are only a few serious game-based safety training tools that support working at height or similar construction tasks (e.g. [40,42]). Also, although many construction safety studies have concentrated on general safety training process (e.g. [30, 43]) and equipment operation (e.g. [29, 45]), the limited number of research (e.g. [27]) integrated a potential accident scenario in the game engine-based training tools.

Virtual safety training tools should enable participants to experience the consequence of their actions. When they make a mistake during the training, an accident should have occurred, which provides a more realistic experience of fatalities or injuries. Another important aspect is the collaboration between the workers during the construction activities. It is a well-known fact that the construction tasks require high interaction among the crew members. Hence, previous studies on safety training tools [18] and occupational accidents [3] recommend that future game engine-based training tools should be heavily built on collaborative tasks to improve the teamwork culture. In addition, the tools should not only focus on a sequence-based training process but also provide a behavioural improvement related to the use of Personal Protective Equipment (PPE), which is another common problem at construction sites [3]. Another key problem is that the existing game engine-based safety training tools have not been adequately tested by using actual construction workers. Zhou et al. [39] stated that user-friendly components should be embedded in training tools and easily practiced with real construction workers. These limitations indicate a high demand for multi-user, serious game-based safety training tools including accident scenarios on specific construction tasks to achieve more effective and realistic training objectives. In addition, they should be tested with real construction workers and received feedback from them about the safety training tool. For these reasons, this study aims to develop and test a serious game-based safety training tool to meet the requirements of serious games on construction safety training.

3. RESEARCH METHODOLOGY

This study introduces and tests the second version of a serious game-based safety training tool, called V-SAFE.v2, for scaffolding and formwork activities. The first version of V-SAFE was developed to simulate the tower crane operations in the construction sites [46]. In the research methodology section, the scenario development process for scaffolding and formwork tasks is initially explained, and then the general functions of the safety training tool are introduced. After that, the modules of V-SAFE.v2 are described in detail. At the end of this section, a case study is conducted to understand the effectiveness and applicability of V-SAFE.v2 with actual construction workers and engineers.

3.1. Scenario Development for Construction Tasks

The game engine-based safety training tool, V-SAFE.v2, incorporates a novel and more realistic scenario aimed at meeting the requirements of serious games for safety training. V-SAFE.v2 consists of construction activities, particularly related to scaffolding and formwork construction. For example, the scenario offers training opportunities on wearing a hardhat, using a safety harness, installation of guardrails and catwalks, and locking the pins during formwork and scaffolding construction. In general, the frequent root-causes of incidents are related to such activities at construction sites [5, 47]. Therefore, the common unsafe work systems leading to serious accidents and affecting overall construction workflow were included in a single scenario. The scenario steps in V-SAFE.v2, consisting of the H-Frame scaffolding system and the concrete column formwork, are shown in the following flow chart (Figure 1).

In the scenario, trainees are initially directed to the storage area where they can get standard PPEs such as gloves, glasses, hardhat, lanyard (Figure 2). The participants are then asked to go to the material storage area to pick up the necessary materials such as a toolbox, H-frames, base plates, plywood, pins, set of diagonal bars for scaffolding and formwork tasks. Afterward, participants perform scenario-based construction tasks during the training process. Finally, after completing all tasks, the trainees are ready to work at height (Figure 3).

3.2. System Architecture of V-SAFE.v2

V-SAFE.v2 was developed based on the Unity 3D game engine introduced by Unity Technologies. The Unity 3D game engine allows developers to create a virtual and multi-user interactive gaming platform by using appropriate 3D images, which makes it one of the most suitable environments for serious games. Moreover, SCORM is utilized to create a Learning Management System (LMS) platform in V-SAFE.v2 as it is the most widely used e-learning standard. LMS is a widely used online platform for e-learning and provides monitoring of a training or education process. Besides, Recording System (RS) is another crucial component in V-SAFE.v2. It is possible to record the safety performance of participants and publish a trainee's performance report for each construction task via LMS and RS. The recorded data on safety training performance is always available for trainers in the cloud-based platform. The LMS and RS are automatically enabled for each player when they sign in the safety training platform. V SAFE.v2 has both single-player and multiplayer

facilities, and SCORM is compatible with both single-player and multiplayer games. Therefore, it is available that all users together can receive training on a single platform (Figure 4).
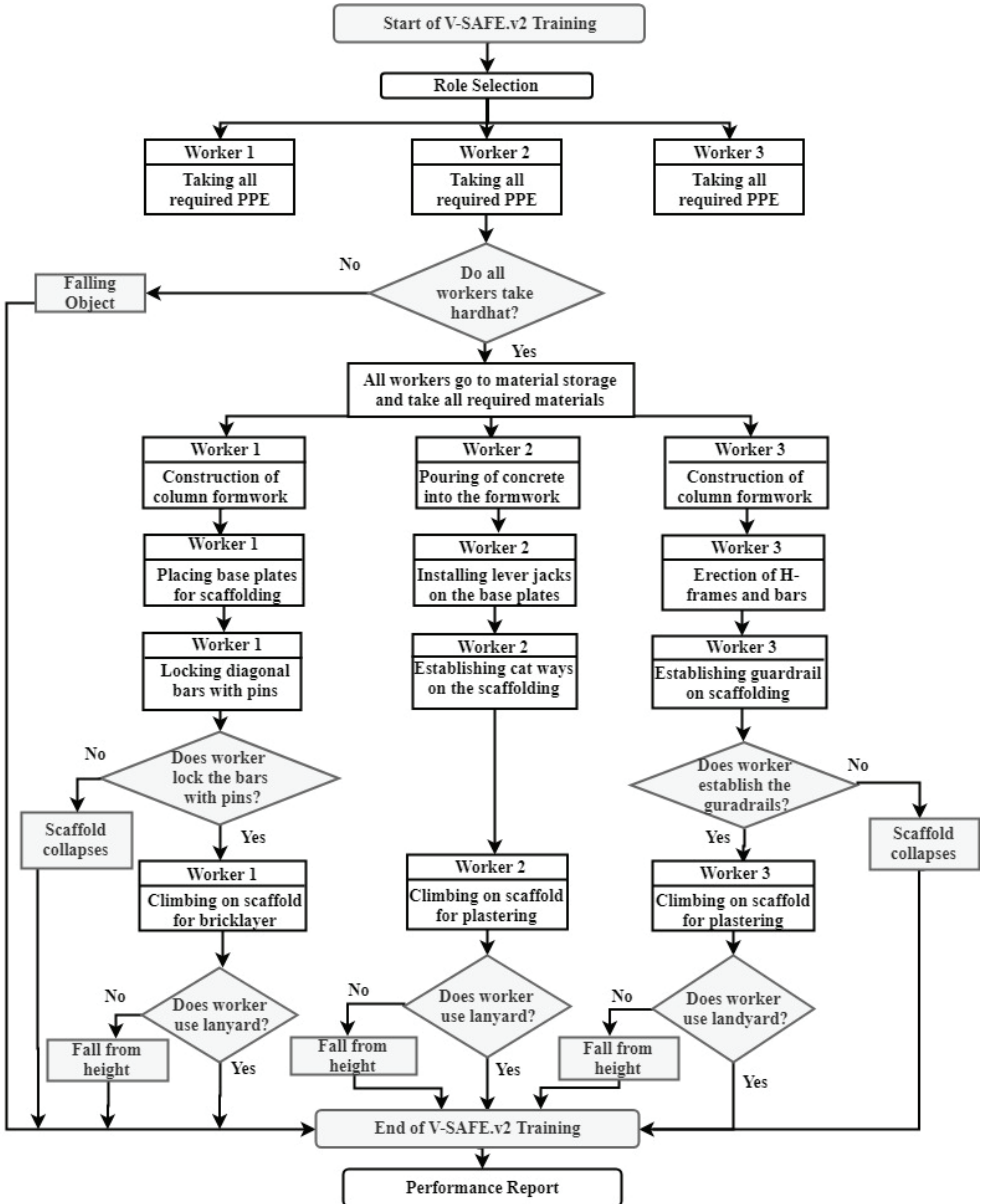

Figure 1 - Developed task workflow for V-SAFE.v2

Figure 2 - PPE store
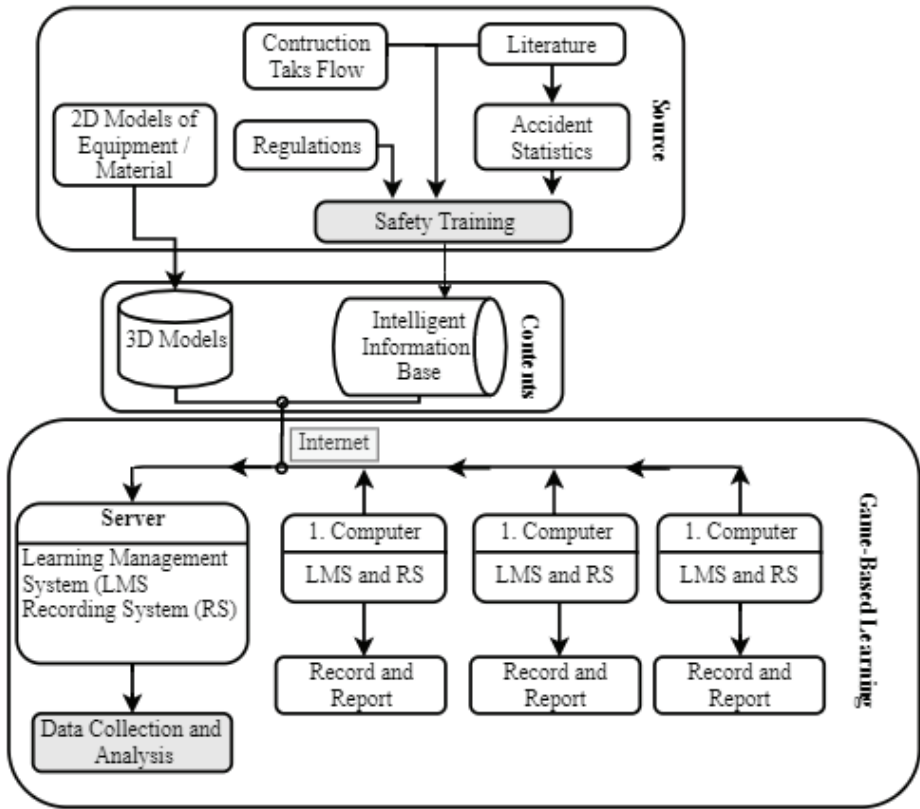

Figure 3 - Guardrails and catwalks

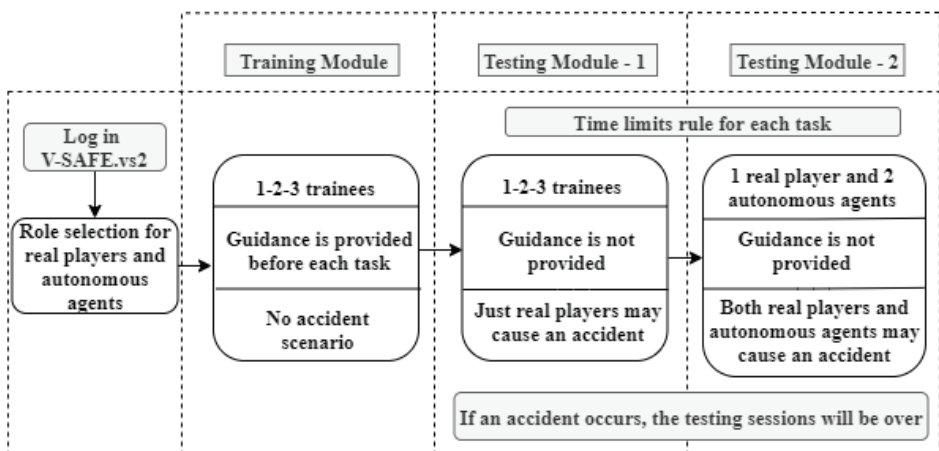*Figure 4 - System architecture of V-SAFE.v2*

Figure 5 - Modules of V-SAFE.v2

The training and testing processes of V-SAFE.v2 are designed for three users, but the number of participants can be increased. Participants are initially asked to select their roles from three different options when they start the training session. V-SAFE.v2 uses a third-person perspective to enable a better understanding of the scene. Also, the point and click mechanism is preferred to provide a more user-friendly system. Moreover, the trainees can contact each other to call for help and learn about the construction work process. The system also allows fewer than three participants to receive training. In this case, other roles are supported by autonomous agents known as a character controlled by computers. Autonomous agents can fulfil construction tasks both in compliance and non-compliance with safety rules. They are especially beneficial in providing a multi-user game environment when only a single participant receives training. In addition, such non-playable characters are also utilized in accident scenarios. V-SAFE.v2 has three different modules including; i) Training Module ii) Testing Module 1 iii) Testing Module 2, as illustrated in Figure 5.

3.2.1. Training Module

In the training module, step by step instructions for scaffolding and formwork tasks and highly engaging safety training is provided to the participants. Instructions and necessary cautionary messages on how trainees should perform each task are shown before each step. The integrated flashing objects direct trainees to the material storage or workplaces where they should go in V-SAFE.v2. They solely click on the flashing places or objects, and their avatars automatically move toward there. Besides, the trainees can walk through the virtual construction site and explore their workplaces. While three participants can receive training at the same time, only a single participant or two participants can also receive training with the support of autonomous agents.

3.2.2. Testing Module - 1

Upon successful completion of the training process, the trainees can move on to the next part, the Testing Module 1. The objective of this module is to assess the safety knowledge acquired in the Training Module and evaluate the performance of trainees without providing any guidance. In this module, the users have to make their decisions for each construction activity in 60 seconds. If the player does not act in a given time, the system accepts that the activity is not carried out, which may cause an accident based on the construction accident scenario.

In this first Testing Module, autonomous agents fulfil construction tasks in compliance with safety rules. Therefore, autonomous agents do not cause any incidence in this module, which is an important feature that allows observing only the individual performance of a real participant.

3.2.3. Testing Module - 2

Only a single trainee with two autonomous agents can carry out the tasks in the Testing Module 2. In this module, the autonomous agents could also exhibit unsafe occupational behaviour and lead to an accident identified in the scenario. Autonomous agents randomly cause an accident, according to predefined probabilities. The main purpose of this module is

to provide trainees with accident experiences that may result in fatality or injury, even if they have successfully carried out all construction tasks. Accordingly, the awareness of trainees about occupational accident risks can be increased.

3.3. Identified Accident Types in V-SAFE.v2

Although there are various activities carried out on construction sites, some of them involve risks that can lead to fatal or serious injury accidents. According to the report of BLS [48], 72% of total injuries and fatalities have occurred due to scaffold-related accidents in the US. Among these accidents, falling from height and falling objects were found to be more dangerous and more frequent than other accident types [31, 48]. Therefore, the common root causes and incidence rates of these accidents were identified and included in the construction scenario of V-SAFE.v2. For this purpose, we utilized a previous study by Whitaker et al. [47] to understand the causes of scaffold accidents. Whitaker and his colleagues [47] examined 3096 construction accident reports on scaffolding to understand the root causes of such cases. They classified the root causes of scaffold accidents as falling, collapsing, and falling objects according to the frequency of occurrence. Accident probability was calculated by dividing the number of accidents in each accident type by the total number of accidents. For instance, the absence of guardrails or edge protection systems is a common reason for the falls from height, which constitutes approximately 28% of the total scaffold-related accidents. Similarly, the failure to lock the pins to connect the H bars as the most prevalent reason causes about 30% of the scaffold collapses. Another major reason for falls at scaffolds is that workers do not usually use lanyards when working on such temporary structures. In addition, accidents when working on scaffolding are also caused by falling objects if workers do not wear a hardhat. Accidents due to falling objects account for 13% of the total scaffold related accidents (Table 1). Accordingly, if a trainee exhibits one of the unsafe behaviours, which is the main cause of an accident, the relevant accident scenario is realized according to calculated probability in V-SAFE.v2. On the other hand, the autonomous agents could randomly cause identified accidents based on the probabilities shown in Table 1.

Table 1 - Root Causes of Scaffold Accidents

Root Cause of Accident	Accident Type	Ratio
Not Wearing Hardhat	Falling Objects	13.5%
Absence of Guardrails	Fall from a Height	28.5%
Not Locking Pins	Scaffold Collapses	30.5%
Not Using Safety Harnesses	Fall from a Height	27.5%

3.4. A Case Study

To evaluate the effectiveness and applicability of the game engine based safety training tool, we tested V-SAFE.v2 with real workers and engineers. To this end, fifteen workers who work at a height in the construction sites and ten civil engineers received training in V-SAFE.v2. Since the main target of the case study is to observe the individual performance of

participants, only the Training and Testing Module-1 were applied (Figure 6). The test performance of each player was automatically scored via the LMS and provided for each trainee at the end of virtual training.

Figure 6 - Application of V-SAFE.v2 with a worker

4. RESULTS AND DISCUSSION

A total of 25 participants (15 workers and 10 engineers) attended training sessions in V-SAFE.v2. There are 13 different construction activities in the tool with certain scores according to their risk levels. For example, tasks with a high risk of accidents such as using safety harness and hardhat, and installing guardrails and pins, have higher weights for scoring (Table 2). At the end of the simulation, the total score is calculated and normalized to 100 by the LMS and presented to the players as feedback.

The participants who received safety training in V-SAFE.v2 showed high performance in the first Testing Module. Almost all of the trainees received higher than 90 points (Table 2), and the average testing score of all participants is around 97. The high-performance scores indicate easy adaptation to V-SAFE.v2. Knowing that engagement or adaptation to a game is a crucial indicator for its effectiveness (e.g. [19, 24]), we claim that V-SAFE.v2 provides effective safety training. According to the performance results, six participants forgot to lock the pins, which is a common reason for serious scaffolding accidents in real construction sites, as stated by Whitaker and colleagues [47]. Like in a real construction site, forgetting to lock the pins also leads to scaffold collapse in the virtual environment, and their training session ended (Figure 7).

It should also be emphasized that most of the real workers either do not have any computer game experience or they have very limited experience. Since the target audience of this safety training tool is real workers, especially those who erect the scaffolds and carry out formwork activities in construction sites, V-SAFE.v2 has been designed to be as user-friendly as possible using point and click function, flashing objects and guiding texts. Moreover, the participants can identify their deficiencies and weaknesses related to scaffolding and formwork construction tasks based on the provided elaborate performance report. One of the main contributions of this study is that the V-SAFE.v2 training tool has the potential to be

convenient for all users, especially construction workers who are not familiar with computer games and virtual technologies. It is emphasized by Zhou et al. [39, 49] that there is also an implementation problem of the safety training tools developed in previous studies. Thus, we propose that the easy applicability of V-SAFE.v2 overcome the implementation issue.

Table 2 - Construction Tasks in V-SAFE.v2

	Taking					Installing							Using	Total Score
	Hardhat	Safety Harness	Glass	Gloves	Tool Box	Base Plate	Jack Stand	H Bars	Diagonal Bars	Pins	Catwalk	Guardrail	Safety Harness	
Task Weights	4	1	1	1	1	1	1	1	1	4	1	4	4	
Worker 1	✓	✓	✓	✓	✓	✓	✓	✓	✓	✓	✓	✓	✓	100
Worker 2	✓	✓	✓	✓	✓	✓	✓	✓	✓	✓	✓	✓	✓	100
Worker 3	✓	✓	✓	✓	✓	✓	✓	✓	✓	✓	✓	✓	✓	100
Worker 4	✓	✓	✓	✓	✓	✓	✓	✓	✓	✗	✓	✓	✗	92
Worker 5	✓	✓	✓	✓	✓	✓	✓	✓	✓	✓	✗	✗	✗	91
Worker 6	✓	✓	✓	✓	✓	✓	✓	✓	✓	✗	✓	✓	✗	92
Worker 7	✓	✓	✓	✓	✓	✓	✓	✓	✓	✓	✓	✓	✓	100
Worker 8	✓	✓	✓	✓	✓	✓	✓	✓	✓	✗	✗	✗	✗	83
Worker 9	✓	✓	✓	✓	✓	✓	✓	✓	✓	✓	✓	✓	✓	100
Worker 10	✓	✓	✓	✓	✓	✓	✓	✓	✓	✓	✓	✓	✓	100
Worker 11	✓	✓	✓	✓	✓	✓	✓	✓	✓	✓	✓	✓	✓	100
Worker 12	✓	✓	✓	✓	✓	✓	✓	✓	✓	✓	✓	✓	✓	100
Worker 13	✓	✓	✓	✓	✓	✓	✓	✓	✓	✓	✓	✓	✓	100
Worker 14	✓	✓	✓	✓	✓	✓	✓	✓	✓	✓	✓	✓	✓	100
Worker 15	✓	✓	✓	✓	✓	✓	✓	✓	✓	✓	✓	✓	✓	100
Engineer 1	✓	✓	✓	✓	✓	✓	✓	✓	✓	✗	✓	✓	✗	92
Engineer 2	✓	✓	✓	✓	✓	✓	✓	✓	✓	✓	✓	✓	✓	100
Engineer 3	✓	✓	✓	✓	✓	✓	✓	✓	✓	✓	✓	✓	✓	100
Engineer 4	✓	✓	✓	✓	✓	✓	✓	✓	✓	✓	✓	✓	✓	100
Engineer 5	✓	✓	✓	✓	✓	✓	✓	✓	✓	✓	✓	✓	✓	100
Engineer 6	✓	✓	✓	✓	✓	✓	✓	✓	✓	✓	✓	✓	✓	100
Engineer 7	✓	✓	✓	✓	✓	✓	✓	✓	✓	✗	✓	✓	✗	92
Engineer 8	✓	✓	✓	✓	✓	✓	✓	✓	✓	✓	✓	✓	✓	100
Engineer 9	✓	✓	✓	✓	✓	✓	✓	✓	✓	✗	✓	✓	✗	92
Engineer 10	✓	✓	✓	✓	✓	✓	✓	✓	✓	✓	✓	✓	✓	100

Moreover, we also collected feedback on V-SAFE.v2 from the participants. Engineers emphasized the effectiveness of V-SAFE.v2 in terms of time and cost-benefit in creating safety awareness compared to on-site and classroom training methods. They also noticed that V-SAFE.v2 involved complex and hazardous construction tasks in a realistic scenario flow affecting the learning process. All of the participants agreed that the introduced system is capable of filling various gaps in the field of construction safety training, especially for working at heights activities and using PPE and safety harness. In addition, the workers participated in V-SAFE.vs2 training sessions stated that learning safety components via game-based safety training tools is more interactive and enjoyable compared to traditional training methods (e.g., classroom meetings, presentations, and guides). They also pointed out that such safety training tools do not require prior game or computer experience to receive training in the virtual environment since V-SAFE.vs2 has user-friendly functions such as click and point mechanism. According to the feedbacks from the workers, V-SAFE.vs2 provides invaluable opportunities to practice high-risk construction activities in a risk-free environment. As in previous studies (e.g. [18, 45, 50], V-SAFE.v2 also enables players to practice the construction tasks interactively in a risk-free environment. The serious games

allow participants to make their own decision and virtually experience the consequences of their actions as provided in this tool.

Zhou et al. [39] highlighted that effective and reliable innovative training platforms should be available especially for high-risk activities that cause catastrophic accidents. V-SAFE.v2 meets this crucial requirement by integrating scaffolding and formwork activities. In the literature, only a few studies (e.g. [51-52]) focus on the development of a serious game for the specific construction tasks which require skillful activities of labors. Moreover, few studies [27, 42] have considered integrating potential accident scenarios in the game based safety training tools. In this regard, V-SAFE.v2 has this unique Testing Module feature where the real accident scenarios take place. The use of guardrails and PPEs [3] is crucial to prevent accidents on construction sites. An effective training tool should emphasize the use of all these accident prevention elements, which are provided by V-SAFE.v2. Li and colleagues [18] stated that safety training tools should simulate the real construction site dynamics, such as the collaborative working environment. In this sense, V-SAFE.v2 offers a suitable environment for construction tasks requiring collaboration.

The autonomous agents support V-SAFE.v2, which may lead to an accident in the Testing Module 2. These non-playable characters are used in the first Testing Module to provide a multi-user game environment when only a single participant receives the safety training. In this way, it is easy to evaluate the individual performance of trainees without any external influence during the testing stage. Although a single trainee performs all the tasks correctly, he or she might be exposed to accidents due to the unsafe behaviour of the autonomous agents in the Testing Module-2.

The construction workers have the responsibility to perform the construction tasks in compliance with safety rules, not only for their safety but also for their crew. Therefore, enabling collaboration in the virtual environment is crucial even though a single participant receives training. Accordingly, they can experience the consequences of their actions for their team members as well. To give an example, a real player who forgets locking the pins to connect the H bars could result in scaffold collapse in the Testing Module 1. In such a case, all workers on the scaffold fall from a height due to the wrong action of a team member and have an accident together (Figure 7).

Figure 7 - Scaffold collapse

When the scaffold collapses, the training simulation ends, and participants are not able to complete all construction tasks. Regardless of whether the team has completed the tasks, the performance of each user is reported individually on the screen via the LMS (Figure 8). Accordingly, the trainees can see their wrong actions and their consequences. Based on their performance, a quantitative score is also calculated. All of these features are essential for providing individual feedbacks and for the trainees to retain the acquired knowledge for a long time.

Figure 8 - Performance report of one player

In this way, trainees can develop an understanding of the occupational safety culture and consciousness about accidents through a different perspective. It is also important to highlight that the scoring system of V-SAFE.v2 is quite different from other safety training tools due to the consideration of the risk levels of activities. The LMS automatically calculates the performance scores of participants and provides detailed feedback at each step in Testing Modules 1 and 2.

Although experiments have been usually conducted with students in many of the existing studies [27, 30], we have utilized real construction workers and engineers to measure the applicability of V-SAFE.v2 in this study. The main motivation behind this study is to develop a user-friendly and game engine-based safety training for the construction industry. Thus, even the construction workers who do not have any computer or gaming experience easily adopted game-based training. An advanced serious game approach, consisting of high-risk accident scenarios, multi-user interactive training platform, user-friendly properties, and performance feedback reports, can have a significant impact on reducing human-induced construction safety issues.

5. LIMITATION

Occupational safety and health issues are highly complex due to the working conditions of the construction workplaces. Such complex, hazardous and dynamic conditions of the

construction sites should be represented in the safety training tool. However, this study aims to create a road map to develop a safety training tool by using serious games, not to develop a commercial product. By using the knowledge gained through the development of V-SAFE.v2, a need-specific and more comprehensive safety training tool can be developed. In this study, we used the latest simulation technologies to understand how to design a highly engaging and effective safety training tool for scaffolding and formwork construction. Therefore, we recognize that this study has limitations, which suggest directions for further research. First of all, V-SAFE.v2 could have a more realistic visual design to represent all the construction site components. Providing real site conditions and including dynamic factors of the construction workplaces are crucial to enable more reliable safety training to the trainees. Accordingly, a more realistic visual design can help workers better visualize the hazards before facing them on site. So, more emphasis can be given to the visual design of the tool. Moreover, although the accident rates of the scenario in V-SAFE.v2 were calculated based on a previous study [47], those rates can be easily revised concerning local conditions. Therefore, in the current version of V-SAFE.v2, the weight of the accident scenarios focusing on "improper behavior of the worker" and "PPE use" can be considered as another limitation of this study. The experiments can be also carried out with a higher number of participants to statistically evaluate the effectiveness of V-SAFE.v2, which is an important research question. As future research, the effectiveness of serious game-based safety training tool should be evaluated quantitatively. Moreover, the effectiveness of the developed game-based safety training tool can be compared to traditional training methods in future studies. In addition, since V-SAFE.vs2 has the opportunity of providing safety training for three different trainees together in the same virtual environment. The impact of such interaction between participants while performing construction activities on their safety performance could be assessed in future studies.

6. CONCLUSION

Even though occupational health and safety issues are of great concern in the construction industry, the training programs are not adequate to meet the actual demands of site safety conditions. On the other hand, serious games have various benefits that have been proven to provide a realistic and effective training environment for trainees. By using game technology, it is possible to simulate high-risk construction activities in a multi-user virtual training platform. In this study, we introduced a game-engine based safety training tool called V-SAFE.v2 for scaffolding and formwork construction. The main objective of this study is to develop a more effective and reliable training environment consistent with real construction site conditions. V-SAFE.v2 consists of Training Module and Testing Modules in which the safety performance of participants is evaluated. A case study was conducted with real construction workers and site engineers to assess the effectiveness of V-SAFE.v2. The findings of the case study show that V-SAFE.v2 is effective and reliable in providing highly engaging training for high-risk construction tasks. It is also highlighted by the participants that the V-SAFE.v2 has a great potential to raise worker's awareness and prevent fatal accidents. In summary, conveniently developing safety knowledge is possible through using serious games.

Acknowledgement

<div align="center">

References

</div>

[1] ILO, Cases of Fatal Occupational Injury by Economic Activity. <https://www.ilo.org/ilostat/faces/ilostat-home/home?_adf.ctrl-state=ry1pcdok9_4&_afrLoop=4059311599607201#!> , 2019.

[2] BLS, National Census of Fatal Occupational Injuries in 2017. <https://www.bls.gov/news.release/pdf/cfoi.pdf> , 2018.

[3] Haslam, R. A., Hide, S. A., Gibb, A. G. F., Gyi, D. E., Pavitt, T., Atkinson, S., and Duff, A. R., Contributing Factors in Construction Accidents. Applied Ergonomics, 36(4), 401–415, 2005.

[4] Guo, H., Yu, Y., and Skitmore, M., Visualization Technology-Based Construction Safety Management: A Review. Automation in Construction, 73, 135–144, 2017.

[5] Kale, Ö. A., and Baradan, S., Identifying Factors that Contribute to Severity of Construction Injuries using Logistic Regression Model. Teknik Dergi, 31(2), 9919-9940, 2020.

[6] Baradan, S., Akboğa, Ö., Çetinkaya, U., and Usmen, M. A., Ege Bölgesindeki İnşaat İş Kazalarının Sıklık ve Çapraz Tablolama Analizleri. İMO Teknik Dergi, 7345(7370), 448, 2016

[7] Tözer, K. D., Çelik, T., and Gürcanlı, E., Classification of Construction Accidents in Northern Part of Cyprus. Teknik Dergi, 29(2), 8295- 8316, 2018.

[8] Uzun, İ. M., Öztürk, D., & Gürcanlı, G. E., Mimari Restorasyon ve Konservasyon Projelerinde İşçi Sağlığı ve İş Güvenliği Uygulamaları. Teknik Dergi, 31(5), 2020.

[9] Abdelhamid, T. S., and Everett, J. G., Identifying Root Causes of Construction Accidents. Journal of Construction Engineering and Management, 126(1), 52–60, 2017.

[10] Tam, V. W. Y., and Fung, I. W. H., Tower Crane Safety in the Construction Industry: A Hong Kong Study. Safety Science, 49(2), 208–215, 2011.

[11] Zhao, D., Thabet, W., McCoy, A., and Kleiner, B., Electrical Deaths in the US Construction: An Analysis of Fatality Investigations. International Journal of Injury Control and Safety Promotion, 21(3), 278–288, 2014.

[12] Winge, S., Albrechtsen, E., and Mostue, B. A., Causal Factors and Connections in Construction Accidents. Safety Science, 112, 130–141, 2019.

[13] Zhao, D., and Lucas, J., Virtual Reality Simulation for Construction Safety Promotion. International Journal of Injury Control and Safety Promotion, 22(1), 57–67, 2015.

[14] Jeschke, K. C., Kines, P., Rasmussen, L., Andersen, L. P. S., Dyreborg, J., Ajslev, J.,

Kabel, A., Jensen, E., and Andersen, L. L., Process Evaluation of A Toolbox-Training Program for Construction Foremen in Denmark. Safety Science, 94, 152–160, 2017.

[15] Hinze, J., Improving Safety Performance on Large Construction Sites. CIB Working Commission W, 99, 2003.

[16] Goldenhar, L. M., Moran, S. K., and Colligan, M., Health and Safety Training in A Sample of Open-Shop Construction Companies. Journal of Safety Research, 32(2), 237–252, 2001.

[17] Burke, M. J., Sarpy, S. A., Smith-Crowe, K., Chan-Serafin, S., Salvador, R. O., and Islam, G., Relative Effectiveness of Worker Safety and Health Training Methods. American Journal of Public Health, 96, 315-324, 2006.

[18] Li, X., Yi, W., Chi, H. L., Wang, X., and Chan, A. P. C., A Critical Review of Virtual and Augmented Reality (VR/AR) Applications in Construction Safety. Automation in Construction, 86, 150–162, 2018.

[19] Dawood, N., Miller, G., Patacas, J., and Kassem, M., Combining Serious Games and 4D Modelling for Construction Health and Safety Training. Computing in Civil and Building Engineering, 2087–2094, 2014.

[20] Martens, A., Diener, H., and Malo, S., Game-Based Learning with Computers - Learning, Simulations, and Games. Transactions on Edutainment, 172–190, 2008.

[21] Gao, Y., González, V. A., and Yiu, T. W., Serious Games vs. Traditional Tools in Construction Safety Training: A Review. Proceedings of the Joint Conference on Computing in Construction (JC3), Heraklion, Greece, 655–662, 2017.

[22] Kuindersma, E., Field, J., and Pal, J., Game-Based Training for Airline Pilots. Conference: Simulation-Based Training For The Digital Generation, London, UK, 2015

[23] Kneebone, R. L., Practice, Rehearsal, and Performance: An Approach for Simulation-Based Surgical And Procedure Training. JAMA, 302(12), 1336-1338, 2009.

[24] Mun, Y., Oprins, E., Van Den Bosch, K., Van Der Hulst, A., and Schraagen, J. M., Serious Gaming for Adaptive Decision Making of Military Personnel. Proceedings of the Human Factors and Ergonomics Society, Los Angeles, CA, 1168–1172, 2017.

[25] Sacks, R., Perlman, A., and Barak, R., Construction Safety Training Using Immersive Virtual Reality. Construction Management and Economics, 31(9), 1005–1017, 2013.

[26] Hasanzadeh, S., Esmaeili, B., and Dodd, M. D., Impact of Construction Workers' Hazard Identification Skills on Their Visual Attention. Journal of Construction Engineering and Management, 143(10): 04017070, 2017.

[27] Pedro, A., Le, Q. T., and Park, C. S., Framework for Integrating Safety into Construction Methods Education Through Interactive Virtual Reality. Journal of Professional Issues in Engineering Education and Practice, 142(2), 2015.

[28] Bosché, F., Abdel-Wahab, M., & Carozza, L., Towards A Mixed Reality System for Construction Trade Training. Journal of Computing in Civil Engineering, 30(2):

04015016, 2015

[29] Fang, Y., and Teizer, J., A Multi-User Virtual 3D Training Environment to Advance Collaboration Among Crane Operator and Ground Personnel in Blind Lifts. Computing in Civil and Building Engineering, 2014, 2071–2078, 2014.

[30] Dickinson, J. K., Woodard, P., Canas, R., Ahamed, S., and Lockston, D., Game-Based Trench Safety Education: Development and Lessons Learned. Electronic Journal of Information Technology in Construction, 16(8), 119–134, 2011.

[31] OSHA, Commonly Used Statistics: Construction's 'Fatal Four. <https://www.osha.gov/oshstats/commonstats.html> , 2017

[32] Jeong, B. Y., Occupational Deaths and Injuries in the Construction Industry. Applied Ergonomics, 29(5), 355–360, 1998.

[33] Huang, X., and Hinze, J., Analysis of Construction Worker Fall Accidents. Journal of Construction Engineering and Management, 129(3): 262–271, 2003.

[34] OSHA, Safety and Health Topics: Scaffolding. <https://www.osha.gov/SLTC/scaffolding/construction.html>, 2017.

[35] Rubio-Romero, J. C., Carmen Rubio Gámez, M., and Carrillo-Castrillo, J. A., Analysis of the Safety Conditions of Scaffolding on Construction Sites. Safety Science, 55, 160–164, 2013

[36] Gürcanli, G. E., and Müngen, U., Analysis of Construction Accidents in Turkey and Responsible Parties. Industrial Health, 51, 581–595, 2013.

[37] Hallowell, M. R., and Gambatese, J. A., Activity-Based Safety Risk Quantification for Concrete Formwork Construction. Journal of Construction Engineering and Management, 135(10): 990–998, 2013.

[38] López-Arquillos, A., Rubio-Romero, J. C., Gibb, A. G. F., and Gambatese, J. A., Safety Risk Assessment for Vertical Concrete Formwork Activities in Civil Engineering Construction. Work, 49(2), 183–192, 2014.

[39] Zhou, Z., Goh, Y. M., and Li, Q., Overview and Analysis of Safety Management Studies in the Construction Industry. Safety Science, 72, 337–350, 2015.

[40] Hsiao, H., Simeonov, P., Dotson, B., Ammons, D., Kau, T. Y., and Chiou, S., Human Responses to Augmented Virtual Scaffolding Models. Ergonomics, 48(10), 1223–1242, 2005.

[41] Bilir, S., Gürcanli, G.E., A Method For Determination of Accident Probability in Construction Industry. Teknik Dergi, DOI: 10.18400/tekderg.363613, 29 (4), 8537-8561, 2018.

[42] Le, Q. T., Pedro, A., & Park, C. S., A Social Virtual Reality Based Construction Safety Education System for Experiential Learning. Journal of Intelligent & Robotic Systems, 79(3-4), 487-506, 2015.

[43] Baradan, S., and Usmen, M. A., Comparative injury and fatality risk analysis of

building trades. J. Constr. Eng. Manage., 132(5), 533–539, 2006.

[44] Li, H., Lu, M., Hsu, S. C., Gray, M., and Huang, T., Proactive Behavior-Based Safety Management for Construction Safety Improvement. Safety Science, 75, 107–117, 2015.

[45] Guo, H., Li, H., Chan, G., and Skitmore, M., Using Game Technologies to Improve the Safety of Construction Plant Operations. Accident Analysis and Prevention, 48, 204–213, 2012.

[46] Kiral, I. A., Comu, S., and Kavaklioglu, C., Enhancing the Construction Safety Training by Using Virtual Environment: V-SAFE." 5th International/11th Construction Specialty Conference, Vancouver, British Columbia, 161–169, 2015.

[47] Whitaker, S. M., Graves, R. J., James, M., and McCann, P., Safety with Access Scaffolds: Development of A Prototype Decision Aid Based on Accident Analysis. Journal of Safety Research, 34(3), 249–261, 2003.

[48] BLS, Fatal Occupational Injuries by Event or Exposure for All Fatalities and Major Private Industry Sector. <https://www.bls.gov/iif/oshwc/cfoi/cftb0249.pdf> (June. 7, 2019), 2011.

[49] Zhou, W., Whyte, J., & Sacks, R., Construction Safety and Digital Design: A Review. Automation in Construction, 22, 102-111, 2012.

[50] Li, H., Chan, G., and Skitmore, M., Visualizing Safety Assessment by Integrating the Use of Game Technology. Automation in Construction, 22, 498–505, 2012.

[51] Li, H., Lu, M., Chan, G., and Skitmore, M., Proactive Training System for Safe and Efficient Precast Installation. Automation in Construction, 49, 163–174, 2015.

[52] Irizarry, J., & Abraham, D. M., Application of Virtual Reality Technology for the Improvement of Safety in the Steel Erection Process. Computing in Civil Engineering. 1-11, 2005.

Investigation of the Effect of Climate Change on Extreme Precipitation: Capital Ankara Case

Sertac ORUC[1]
Ismail YUCEL[2]
Aysen YILMAZ[3]

ABSTRACT

This study examines the potential impacts of climate change on extreme precipitation. Rainfall analysis with stationary and nonstationary approach for observed and future conditions is performed for (1950-2015 period) observed data of 5, 10, 15, 30 minutes and 1, 2, 3, 6 hour and projections (2015-2098 period) of 10, 15 minutes and 1, 6 hour for Ankara province, Turkey. Daily projections are disaggregated to finer scales, 5 minutes storm durations, then five minutes time series aggregated to the storm durations that are subject of interest. Nonstationary Generalized Extreme Value (GEV) models and stationary GEV models for observed and future data are obtained. Nonstationary model results are in general exhibited smaller return level values with respect to stationary model results of each storm duration for observed data driven model results. Considering the projected data driven model results; on average nonstationary models produce mostly lower return levels for mid and longer return periods for all storm durations and return periods except one hour storm duration. Depending on the models and Representative Concentration Pathways (RCP), there are different results for the future extreme rainfall input; yet all results indicate a decreasing extreme trend.

Keywords: Climate change, storm water, nonstationary, extreme rainfall.

1. INTRODUCTION

According to Intergovernmental Panel on Climate Change (IPCC) reports [1,2,3], climate change is observed in all over the world: the atmosphere and oceans are warming, volume of snow and ice covers are diminishing, sea levels are rising and weather patterns are changing.

Changes resulting from global warming may include an increase in occurrence and severity of storms and other severe weather events such as extreme rainfalls [1].

There are several studies that indicate the effect of climate change on the precipitation regimes and trends. It is a common agreement that climate change will have significant effects on the water cycle and precipitation patterns [4]. In some regions, these effects are expected to change precipitation regimes (e.g. increase in the frequency and intensity of precipitation extremes [5,6]. Extreme precipitation events (e.gfewer rainy days and more extreme rainfalls) are expected by the end of the 21st century under climate change conditions [1,7,8,9]. Seneviratne et al. [10] implies that in South East Asia, North East Europe, tropical Africa, and South America the impact of floods will increase, however these impacts will reverse in central Asia, Eastern Europe, central North America, and Anatolia regions.

Furthermore, there are studies that analyse future climate projections, try to figure out their consequences and reveal the potential change for the current conditions. For instance, Özturk et al. [11] examine the changes in seasonal precipitation and temperature of CORDEX Middle East and North Africa (MENA) and found out that warmer and drier conditions than present climate conditions are projected to occur more intensely. Furthermore, annual average precipitation will increase over the equatorial regions and decrease over the subtropical regions [12]. Another study that used multi-model ensemble of regional climate projections to estimate the climate change signal in terms of temperature and precipitation for the city of Aachen, Germany [13]. The results of the study reveal that rainfall is likely to decrease over the century and the examinations indicate longer and more frequent dry periods in the future. The Norwegian white paper on climate adaptation [14] indicates a rise of 5-30 % in annual mean precipitation by 2100 relative to the period 1961-90 and the number of days with heavy precipitation will also rise over this century.

Based on the evidence in the SREX (The Special Report on "Managing the Risks of Extreme Events and Disasters to Advance Climate Change Adaptation" of the IPCC report [15], one can say that there is significant increase in heavy precipitation events at present in more regions than there is significant decreases, but these increase and decrease show various regional and sub-regional trends [16]. Similar findings revealed by other studies; extreme weather events stated to occur more frequently and the areas that have not faced extreme events in the past started to encounter these events, both heavy rainfall increase and decrease is observed, but the areas with increasing rainfall getting larger [17, 18]. Moreover, it is found that neglecting the changing frequency may cause underestimation of extreme events [19]. Sarhadi et al. [20] show that stationary approach in frequency analyses may underestimate the magnitude (return level) of extreme precipitation events, and updated design assumption must be presented in the changing conditions.

Urban water infrastructure (e.g., sewer and stormwater management systems) and flood control structures (e.g., dams) are designed based on extreme rainfall properties and these properties are reflected as intensity-duration-frequency (IDF) curves [21,22]. The IDF curves quantify the frequency of occurrence of a storm with a specific intensity at different storm durations and it is used for many applications of urban water infrastructure design including stormwater [23]. The IDF curves are, in general, currently based on historical precipitation analysis and statistics. Infrastructure design concepts have considered stationary return levels for a long time, which assume no change to the frequency of extreme event over time however, the frequency of extremes has been changing and this change probably will

continue in the future [19]. Moreover, it is found that neglecting the changing frequency results in IDF curves that can underestimate extreme events [19,20]. Sarhadi et al. [20] introduced a fully time varying risk framework by Bayesian Markov chain Monte Carlo techniques to incorporate the effect of nonstationarities. The results demonstrate consistent results with those of Cheng and Aghakouchak [19] and show that stationary approach may underestimate the extreme precipitation events, updated design assumption must be presented in the changing conditions and nonstationary-based IDF curves must replace the stationary-based IDF curves. Hosseinzadehtalaei et al. [22] point out the changing patterns of extreme precipitation and draw attention to the current design standards based on IDF curves that assumes no temporal change.

Climate variability affects the naturel environment from two dimensions: the long-term trend of average climate variables may be altered, or fluctuations may have a wider range which results in changes in the statistical characteristics of climate variables [1,24]. Studies support that the global hydrologic cycle will be intensified due to changing climate; wet and dry extremes will be increased which result in floods and droughts [25,26,27]. However, climate change projection results from GCM/RCM couplings cannot be directly used for the hydrological impact studies since they require finer temporal resolution at hourly or less particularly for extreme events [28]. Unfortunately, reliable records are available at coarse intervals such as yearly, monthly or daily and rainfall data is generally low quality. Short interval rainfall records are limited due to the high cost and insufficiency of reliable measurement and the monitoring systems [29]. In this context, disaggregation can be employed to take the advantage of using long term data which exist in low resolution or larger time scales such as daily or above [30].

Annual count of extreme events in Turkey shows an increasing trend in 1940-2019 period according to 2019 Climate Assessment Report of State Meteorological Service [31]. During 2019 most hazardous extreme events were heavy rain/floods (36%), wind storm (27%), hail (18%), lightning (7%) and heavy snow (5%). Climate change in Turkey has been evaluated in many different studies with its different aspects. Majority of analyses that are conducted with observed and future data were focused on temperature and precipitation changes. Sensoy et al. [32] investigated the extreme climate indices in Turkey for about 109 stations and for the period from 1960 to 2010. Except Aegean and South-eastern Anatolia regions, heavy precipitation days increase in most of the stations. Furthermore, in most of the stations maximum 1-day precipitation follow an increasing trend apart from South-eastern Anatolia. In a recent study for the Rize Province in Turkey, a catchment-scale analysis of extreme rainfall events of the reference (1961–1990) and three future climate periods (2013–2039, 2040–2070, and 2071–2100) is conducted and the results projected a 30% decrease in the median value of extreme rainfall over the study region for the near future [33]. Standard duration annual maximum rainfall series with various durations and length of 14 stations up to 2010 in Turkey are used in order to capture the statistical behavior of series and it is computed that 90% of all studied annual maximum rainfall series are trendless, independent, stationary, and homogeneous. Hence, it is concluded that Intensity-Duration-Frequency (IDF) curves can be computed in the conventional way for Turkey [34]. On the other hand statistically significant increasing trends were found in Antalya Region for at least one extreme rainfall index based on frequency analysis conducted by using Generalized Pareto Distribution (GPD) for current and future periods [35]. Rainfall intensities for different return periods increased up to 23% when compared with the current period [35]. Climate change

and its urban-induced bias in different cities of Turkey were studied considering the temperature and precipitation data of stations for the period of 1950–2004 [36]. Particularly, significant warming is found in almost all of the regions for minimum temperature series and significant decreases of precipitation amounts are identified in the western parts of Turkey [36]. According to Turunçoğlu et al. [37], for the twenty first century all simulations of CMIP3 and CMIP5 agreed on a temperature increase and a precipitation decrease in Turkey.

Ankara, the Capital of Turkey has a semi-arid climate and significant influence by climate change that also has a continuous population growth and is located within Sakarya and Kızılırmak Basins. According to the results of the projections carried out in ClimaHydro Project [38] for these basins, there is a decrease tendency in the total precipitation compared to the reference period (1971-2000), and it is predicted that the basins will receive 8% and 6% respectively less rainfall compared to the reference period in 2071-2100 [38]. It is expected that rainfall decreases for this period will predominate in the southwestern and north-eastern parts of the Sakarya basin. Also, climate projections for Sakarya Basin, where Ankara is located, indicate that number of extreme wet days decrease for future periods, which will have a possible consequence of intensified precipitation [38]. Furthermore, in the last 20 years' flooding observations, heavy rainfall and flash flooding caused various damages to the property and even loss of life in the city. However, despite all these circumstances, the detailed studies that particularly focused on the status of intensity-duration and frequency of precipitation storms under changing climate have been lacking so far for Ankara, the Capital of Turkey.

In this study extreme precipitation properties through IDF curve analyses for Ankara are investigated by using observed (1950-2015) and future (2015-2098) precipitation data using 3 GCMs coupled with one RCM under two different carbon emission sceneries. Projected daily precipitation data is disaggregated to finer scales and Generalized Extreme Value (GEV) distribution is used to analyse observed and future data considering the stationary and nonstationary models, which assume changing frequency of extreme event over time. The projection results are directly used for the analyses due to the possible loss of nonstationary signal of the series. According to Aziz [39] and Aziz et al. [40], bias correction methods have a tendency to lose nonstationarity signals even though they improved the model performance substantially. After the bias-correction was applied he states that the impacts of nonstationarity were altered to opposite direction or lost. Maraun [41] also discussed the possibility of alteration of climate change trends and nonstationarity signals after bias correction. Moreover Willkofer [42] stated the poor performance of bias correction approaches with extreme values. Thus, in this study bias correction did not applied to the results of models in order to preserve nonstationary and trend directions."

The objectives of this study are to disaggregate daily future projections to finer scales, to investigate superiority of nonstationary GEV models to stationary GEV models for observed and future precipitation data, and to calculate return level values for observed and future period rainfall with stationary and nonstationary GEV models.

2. DATA AND STUDY AREA

The annual maximum precipitation data of 5, 10, 15, 30 minutes and 1, 2, 3, 6 hours duration for 1950-2015 period for Ankara province is obtained to conduct data analysis for the observation period. This data is acquired from Turkish State Meteorological Service (SMS).

The grid based data representing Ankara province were received from Turkish State Meteorological Service (SMS) where these climate projections and their performance evaluations have already been done in detail by Demircan et al. [43]. Since our aim here in this study is to look climate change impact on IDF via nonstationarity we have not focused on performance of the models which are already available in the literature.   Table 2.1 shows the location of meteorological stations and nearest projection grids to these stations as well as their altitudes. The data consists of daily projections covering 2015-2099 period however because of missing data for 2099, 2015-2098 period is used for the analyses. Also, 1971-2000 is chosen as model validation period. Daily projection results of three global climate models (GCM) coupled with regional climate model (RCM) (RegCM4) are used. These models are HadGEM2-ES, MPI-ESM-MR and GFDL-ESM2M and run under RCP 4.5 and RCP 8.5 emission scenarios. These model results were supplied by SMS.

Table 2.1 - Projection Data Stations & Grids

No	Station	Grid	Station			Grid		
			Latitude	Longitude	Altitude mt	Latitude	Longitude	Altitude mt
17129	**ETİMESGUT HAVALİMANI**	**2733**	39,9558	32,6854	806	39,9661	32,6608	1028
17131	**ANKARA GÜVERCİNLİK HAVALİMANI**	**2733**	39,9343	32,7387	820	39,9661	32,6608	1028

Rainfall/frequency analysis is conducted for daily projections of three model and two scenarios of grid no 2733 for the projection (2015-2098) period. However, daily temporal resolution from projection data is not well suited for the extreme value analysis. For instance, urban flash flooding is caused by heavy rainfalls over short durations such as in a few minutes to hours therefore it is essential to analyse extreme rainfalls for shorter durations such as sub-daily or sub-hourly. For this reason, daily RCM output data is disaggregated to finer time scales such as hourly and sub-hourly to use future projections for extreme value analysis [44]. For the disaggregation process, temporal stochastic simulation of rainfall process at high resolution, based on the Bartlett-Lewis rectangular pulse model is used [45,46].

Stationary and nonstationary rainfall return levels (in mm) for return periods 2, 5, 10, 25, 50, 100, 200 years are derived for observed (1950-2015) and projected data (2015-2098) for extreme rainfall time series of the sub-hourly and hourly annual maximum data.

Ankara is located in the northwest of Central Anatolia. The city is like a pot surrounded by four mountains of Anatolia Plateau with an altitude of 850-1000 meters. These mountains are: Karyağdı on the north, İdris on the east, Elmadağ on the south and southeast and Çal on the southwest (Figure 2.1).
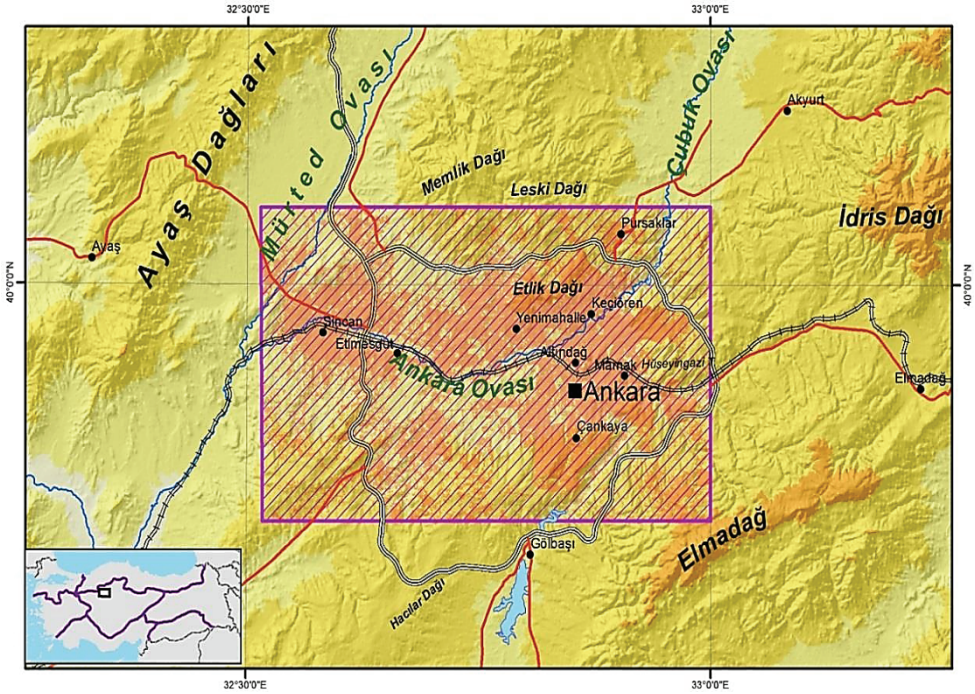
Figure 2.1 - Location of Ankara [47]

Between these mountains three rivers flow. Çubuk creek between Karyağdı and İdris mountains, Bent Stream between Elmadağ and İdris Mountains and finally İncesu creek between Elmadağ and Çal mountains; these rivers come together between Karyağdı and Çal mountains and flow into Sakarya River as Ankara stream. A population of 5.3 million people (TÜİK, 2016) are living in the capital Ankara and 88% of the population lives in the city center [48]. Ankara is generally known for its twentieth century development as the designed capital of the newly born Turkish nation-state and the city's growth at the beginning displayed a typical example of modernization efforts. The second half of the century compared to the first years, witnessed the uncontrollable expansion and transformation of the city with expanding squatter areas due to heavy migration [49].

According to Thornthwaite classification, the climate in Ankara is a second degree mesothermal semi-arid and less-humid climate with intensive water surplus in winter months. The mean temperature of Ankara and its surroundings is above 20.0°C in three months (June, July and August), it is between 10.0-20.0 °C in four months (April, May, September and October) and it is below 10.0°C in five months of the year (November, December, January, February and March). The values of some meteorological parameters for Ankara are as follow: the annual mean temperature is 11.9 °C, the mean temperature in January is 0.2 °C, the mean temperature in July is 23.5 °C, the mean annual precipitation is 387 mm, and the mean annual relative humidity is around 60. In Ankara and its surroundings, in the cold period, there are heavily cyclonic activities. As a result of this, frontal precipitation is effective in the cold period. However, in the warm period, anticyclonic conditions are

dominant. Because of this, convective precipitation occurs in the warm period, also there are big differences between day and night temperature and winter and summer temperature because of continental climate conditions [50,51].

3. METHODOLOGY

The methodology of precipitation analysis in this study consists of;

(1) Projected data is disaggregated into finest scale (5 minutes) and then it is aggregated to next analysis time scales (such as 10, 15, and 30 minutes) because each run generates rainfall depths that are independent from the other runs and subsequently the data at higher time scales may be inconsistent.

(2) Trend analysis is carried out for observed and projected data.

(3) Stationary GEV (St) models are developed; return levels are derived for desired return periods for observed and projected data.

(4) Non-stationary GEV (NSt) models are developed; return levels are derived for desired return periods for observed and projected data.

A general framework for rainfall analyses used in this study can be seen in Figure 3.1.
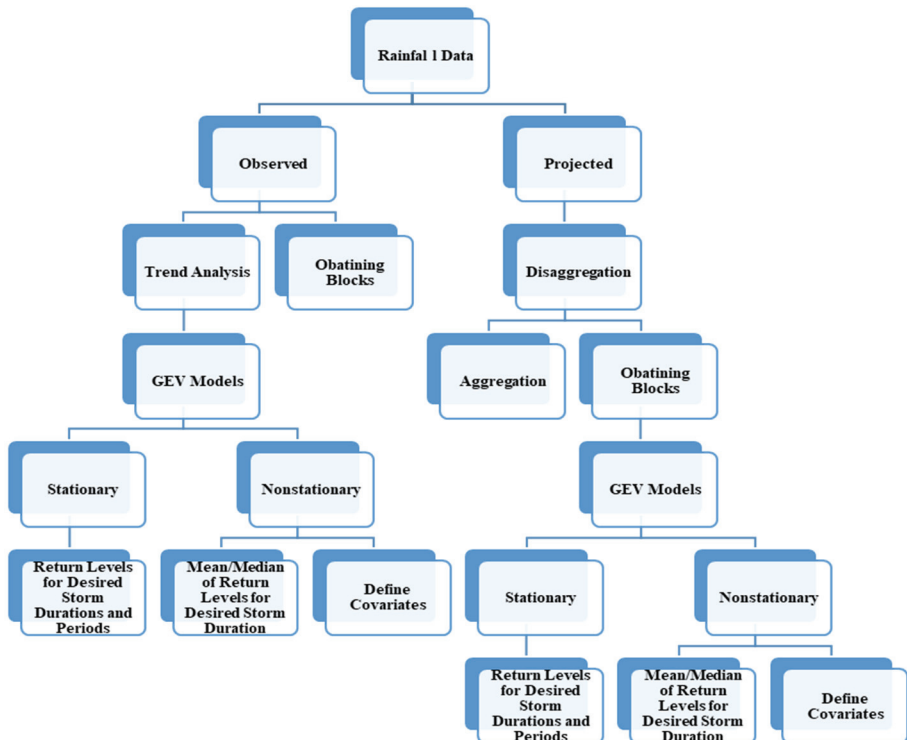

Figure 3.1 - Rainfall Data Analyses Framework

3.1. Disaggregation

Daily projected precipitation data is first disaggregated to 5 minutes duration and then for the use of GEV analyses the 5-min data is aggregated to 10, 15 minutes and 1, 6 hours storm duration. A complete software package for the temporal stochastic simulation of rainfall process at fine time scales which is developed in the R programming environment, HyetosMinute, is used to prepare daily data for extreme value analysis and used for the disaggregation process in this study. Disaggregation is based on the Bartlett-Lewis rectangular pulse model which provides temporal stochastic simulation of rainfall process at fine time scales [30, 44, 45, 46, 52].

The Bartlett–Lewis Rectangular Pulses (BLRP) model is used in many studies to disaggregate daily observed rainfall to finer scales. A member of general category of Poisson-cluster models in which rectangular pulses occur in continuous time simulates rainfall events with clusters of these rectangular pulses [28, 46, 53, 54, 55].

The initially proposed model has 5 parameters [55,56] but Random Parameter Bartlett-Lewis Rectangular Pulse Model (BLRPR) which have 6 parameters: $\{\lambda, \alpha, \nu, \kappa, \varphi, \mu X\}$, and is modified version of original model to enhance the model's flexibility in generating a greater diversity of rainfalls, is the preferred model in this study [44, 45, 53].

To calculate model parameters in disaggregation method, an enhanced version of the evolutionary annealing-simplex optimization method is used [30,57,58]. Mean, variance, covariance and probability of dry days are used as historical statistics for the objective function of the desired time scale (in this case five minutes). It is stated that the distribution of the maximum rainfall depths/heights can be better derived if the inter-annual variability of monthly statistics is incorporated in the parameter estimation process of the model. Therefore, in this study only the historical daily parameters are used for the optimization process and to make an adequate estimation every month is calculated separately and then combined by year. In the end, a set of parameters (in this case six parameters) are obtained for implementation in disaggregation.

3.2. Trend analysis

The statistical tools that provide trend tests are generally divided into two fundamental groups: Parametric and non-parametric. The non-parametric tests are said to be more appropriate to conduct trend analysis for the non-normally distributed hydro-meteorological time series data [59]. Mann-Kendall (MK) trend test is one of the non-parametric tests for trend detection and is used to detect if there is a monotonic upward or downward trend over time for precipitation in this study [60, 61, 62]. MK test is a rank-based test which has been commonly applied to hydrometeorological time series data to detect trends [19,59,63,64].

3.3. Extreme value analysis: stationary & nonstationary

Extreme value theory (EVT) is concerned with the statistical properties of the tails of distributions and provides the necessary methods to estimate the distribution of the extremes of a time series [65]. By this way quantification of the return values and return periods of extreme events become possible. EVT uses probabilistic distribution functions such as

Generalized Extreme Value (GEV) or Generalized Logistic (GL) function to annual maximum (AM) series or Generalized Pareto Distribution (GPD) function which is fitted on peak-over-threshold (POT) series [66]. GEV distribution function is used in the present study to fit the observed and future precipitation data. The methodology is widely used in engineering applications that need an assessment of extreme environmental conditions [67].

The GEV distribution function has theoretical justification for fitting to block maxima (maxima of long blocks of data, e.g., annual maximum values of daily precipitation height) of data [65,68,69]. The GEV distribution function (df) is given by (2.1).

$$G(z) = \exp[-\{1 + \xi\left(\frac{z-\mu}{\sigma}\right)\}_+^{-\frac{1}{\xi}}] \tag{2.1}$$

$\sigma > 0, -\infty < \mu, \xi < \infty$ [70].

The GEV distribution has three parameters including location (μ), scale (σ) and shape (ξ) parameters.

Equation 2.1 covers three types of df's depending on the sign of the shape parameter, ξ. The Fréchet df results from $\xi > 0$, and the Weibull df when $\xi < 0$. The Gumbel type is obtained by taking the limit as $\xi \rightarrow 0$ [71].

Yilmaz and Perera [59] indicate that Maximum Likelihood Estimation (MLE) method is a preferred method for parameter estimation of nonstationary models due to its suitability for incorporating nonstationarity into the distribution parameters as covariates. In order to obtain nonstationary models, distribution parameters are set to be a function of covariates such as time, temperature, etc. and for every value of covariate, a unique return level value is calculated. Non-stationarity can occur either as a gradual trend or a sudden shift [72]. Time (and other covariates) variant/dependent parameters are used to capture the non-stationarity of the time series [73,74]. First for the stationary cases than for the non-stationary cases, extreme value analysis is applied by using GEV models. For non-stationary case, the location parameter and/or scale parameter are set to be a function of time or other variants such as annual precipitation or temperature. Different combinations for nonstationary cases are tested and compared to find out the best fitted model among stationary and nonstationary models. In the present study, all model parameters set constant for the stationary case, and location and/or scale parameters assumed to be a function of time and/or temperature for the nonstationary case. The non-stationary models that describe each of these cases with their developed parameters are explained in Table 3.1. Several variables such as temperature, time are incorporated into non-stationary models as covariates to capture the changes in extreme precipitation characteristics. (Table 3.1.). While there are other covariates such as NAO, AO, etc., time and annual average temperature were chosen because of the widespread application of time and data availability. The covariates were restricted with these ones since amount of calculations and results increase for each time series with 3 model and 2 RCPs.

Performance of fitted models is inspected by goodness-of-fit indicators such as, Akaike Information Criterion (AIC), Bayesian Information Criterion (BIC) and Negative Log-Likelihood (NLL) [65,75,76,77,78].

Table 3.1 - Non-stationary models with time and covariate (average annual temperature) dependent location and scale parameters. The number 1 through 8 represents respectively storm duration for 5 min, 10 min, 15 min, 30 min, 1 hr, 2 hr, 3 hr, and 6 hr.

Model	Location	Scale	Shape
NStGEV1	$\mu t = \beta_0 + \beta_1 t$	σ (constant)	ξ (constant)
NStGEV2	$\mu t = \beta_0 + \beta_1 t$	$\sigma t = \beta_0 + \beta_1{}_t$	ξ (constant)
NStGEV3	μ (constant)	$\sigma t = \beta_0 + \beta_1{}_t$	ξ (constant)
NStGEV4	$\mu t = \beta_0 + \beta_1 \text{temperature}$	σ (constant)	ξ (constant)
NStGEV5	$\mu t = \beta_0 + \beta_1 t$	$\sigma t = \beta_0 + \beta_1 \exp(\text{temperature})$	ξ (constant)
NStGEV6	$\mu t = \beta_0 + \beta_1 \exp(\text{temperature})$	$\sigma t = \beta_0 + \beta_1 \exp(\text{temperature})$	ξ (constant)
NStGEV7	$\mu t = \beta_0 + \beta_1 \exp(\text{temperature})$	$\sigma t = (\text{constant})$	ξ (constant)
NStGEV8	μ (constant)	$\sigma t = \beta_0 + \beta_1 \text{temperature}$	ξ (constant)

4. RESULTS AND DISCUSSION

4.1. Climate Change and Alterations in the Precipitation Regime: Observations

4.1.1. Trend Analysis

Stationary and nonstationary models are applied to a 5-10-15-30 minutes and 1-2-3-6 hours observed (1950-2015) annual maximum storm durations for Ankara province. If a statistically significant trend in time series is detected, then it is accepted that the assumption of stationarity is violated. However, time series that did not present significant trend may also reveal superior results by nonstationary models. Visual inspection is an alternative to make rough inferences but for reliable determination, especially with complex variations and long-term series, statistical tests are needed. Figure 4.1 and Figure 4.2 demonstrate the trend for observed sub-hourly (5-10-15-30 minutes) and hourly (1-2-3-6 hours) time series of annual maximum rainfall intensities with a linear trend line between 1950-2015 period. A simple linear trend line visually indicates the downward (decreasing) trend for most of the time series.

MKtrend test is applied to time series for all storm durations and results are shown in Table 4.1. Bold ones indicate significant trend for 0.05(**) and 0.10(*) significant levels. Trends particularly in sub-hourly durations and long storm durations are largely different in terms of statistical significance but not in direction. According to MK statistics; the null hypothesis that there is no trend is rejected for the 5-10-15-30 minutes and 1 hour time series. The results suggest that there is significantly a downward monotonic trend based on 5 and 10 percent significance between 1950-2015 period.
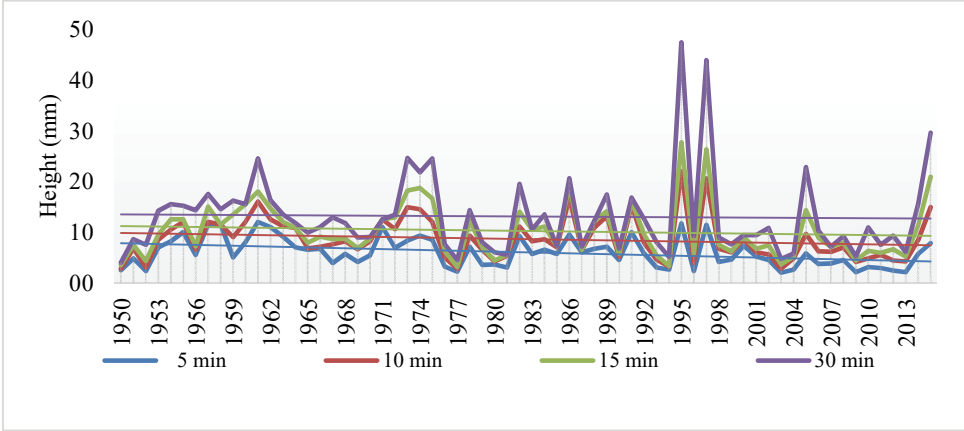
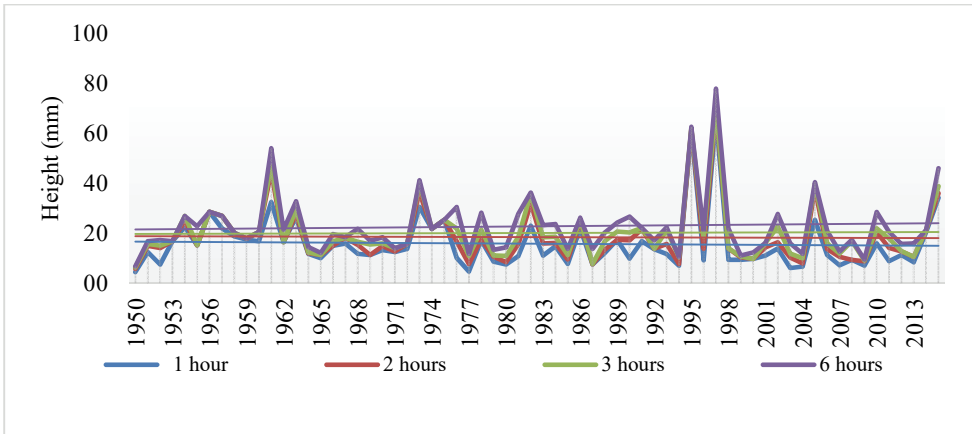*Figure 4.1 - Observed Sub-Hourly Time Series Trend*

Figure 4.2 - Observed Hourly Time Series Trend

Table 4.1 - Mann-Kendall Results for the Storm Durations

Storm Duration	MK Statistic	p-Value
5 Minutes	**tau = -0.260**	**0.0021616****
10 Minutes	**tau = -0.187**	**0.027951****
15 Minutes	**tau = -0.143**	**0.091372***
30 Minutes	**tau = -0.148**	**0.080262***
1 Hour	**tau = -0.189**	**0.025699****
2 Hour	tau = -0.136	0.10726
3 Hour	tau = -0.0565	0.50656
6 Hour	tau = -0.0266	0.75662

** -0,05 significance level, *-0,1 significance level

4.1.2. Stationarity vs Nonstationarity Analysis

Maximum precipitation and recurrence analysis rely on observation for at least 10 years of station precipitation data. SMS determines the annual maximum precipitation depths for storm durations of 5, 10, 15, 30 min, and 1, 2, 3, 4, 5, 6, 8, 12, 18, 24 hours. IDF analysis is performed for the 2, 5, 10, 25, 50 and 100-year repetition periods using the probability density functions namely; Log-Normal 2 Distribution (LN2), Log-Normal 3 Distribution (LN3), 2-parameter Gamma Distribution (G2P), Log-Pearson 3 Distribution (LP3), and Gumbel Distribution (G). The best fit among these functions is found by the Chi Square and Kolmogorov-Smirnov conformity tests. As a result, a stationary LP3 is selected as the preferred distribution for the selected station and it is based on the data from 1940-2015 period. In this study, SMS annual maximum precipitation statistics are used as reference to compare them with results obtained GEV based stationary and nonstationary analyses. This can enable us to see variations between the data officially in use and data acquired within this current study.

Table 4.2. presents the negative log-likelihood (NLL), AIC and BIC diagnostic values of stationary and best fit nonstationary models. Small negative log-likelihood and AIC/BIC values infer the superiority of the model to the other ones. Consistently, for all storm durations the proper nonstationary models provided the lower performance scores than stationary models. This implies the worthy of consideration of changing climate conditions in precipitation frequency analysis.

Table 4.2 - Stationary and Best Fit Nonstationary Model Comparison

Model	N L L	AIC	BIC	Model	N L L	AIC	BIC
StFiveMin	160	327	333	**StTenMin**	182	369	376
NStFiveMin	139	288	298	**NStTenMin**	166	342	353
StFifteenMin	194	394	401	**StThirtyMin**	210	426	432
NStFifteenMin	173	356	367	**NStThirtyMin**	190	390	401
StOneHour	222	451	457	**StTwoHours**	228	461	468
NStOneHour	201	412	423	**NStTwoHours**	205	420	431
StThreeHours	231	468	474	**StSixHours**	237	480	487
NStThreeHours	209	428	439	**NStSixHours**	216	442	452

The changes between return levels of best fit nonstationary model and stationary ones for each return period are shown in Table 4.3. Generally mean or median values are computed to simplify the results of nonstationary models because nonstationary return levels take different values for every single point of covariate.

Table 4.3 - Nonstationary GEV Best Fit Model Return Levels (mm) - Mean and Median Value Change with Respect to Stationary GEV Model Return Level Results - Observation Period

	2 year	5 year	10 year	25 year	50 year	100 year	200 year
Mean Value Change							
FiveMin	-4%	-4%	-5%	-9%	-11%	-15%	-18%
TenMin	-14%	-13%	-12%	-9%	-7%	-5%	-3%
FifteenMin	-1%	-4%	-6%	-9%	-12%	-14%	-17%
ThirtyMin	0%	-3%	-6%	-10%	-13%	-16%	-19%
OneHour	-7%	-5%	-3%	0%	3%	6%	10%
TwoHours	0%	-3%	-4%	-5%	-6%	-7%	-7%
ThreeHours	0%	-3%	-5%	-8%	-11%	-13%	-16%
SixHours	1%	-1%	-2%	-3%	-4%	-5%	-5%
Median Value Change							
FiveMin	-3%	-2%	-4%	-7%	-9%	-12%	-15%
TenMin	-13%	-12%	-10%	-7%	-4%	-2%	0%
FifteenMin	-1%	-2%	-4%	-7%	-9%	-12%	-14%
ThirtyMin	1%	-2%	-5%	-8%	-10%	-13%	-16%
OneHour	-8%	-5%	-2%	2%	5%	8%	12%
TwoHours	-1%	-2%	-3%	-4%	-4%	-5%	-5%
ThreeHours	-1%	-2%	-4%	-7%	-9%	-11%	-14%
SixHours	0%	-1%	-2%	-2%	-3%	-3%	-4%

In addition, Figure 4.3 shows return levels of stationary model, nonstationary mean and median and SMS for each storm duration from 5 min to 6 hr, respectively. By examining storm durations, it is found that the shorter the duration the larger the differences between the non-stationary and stationary extremes. In the design of storm drainage systems short durations of maximum rainfall events are mostly considered. Therefore, the use of nonstationary approach in determining the design value should be more preferable depending on safety and economical scale. For an example, for the 100-year return period, the differences between stationary and nonstationary mean (median) return level of 5 minutes and 30 minutes events are 15% (12%) and 16% (13%), while for a 6 hours storm, the difference is 5% (3%). Also, among the storm durations, only one hour time series exhibit larger values (increase) for its nonstationary model return level values, however this is not the case for shorter return periods from 2 years to 10 years.
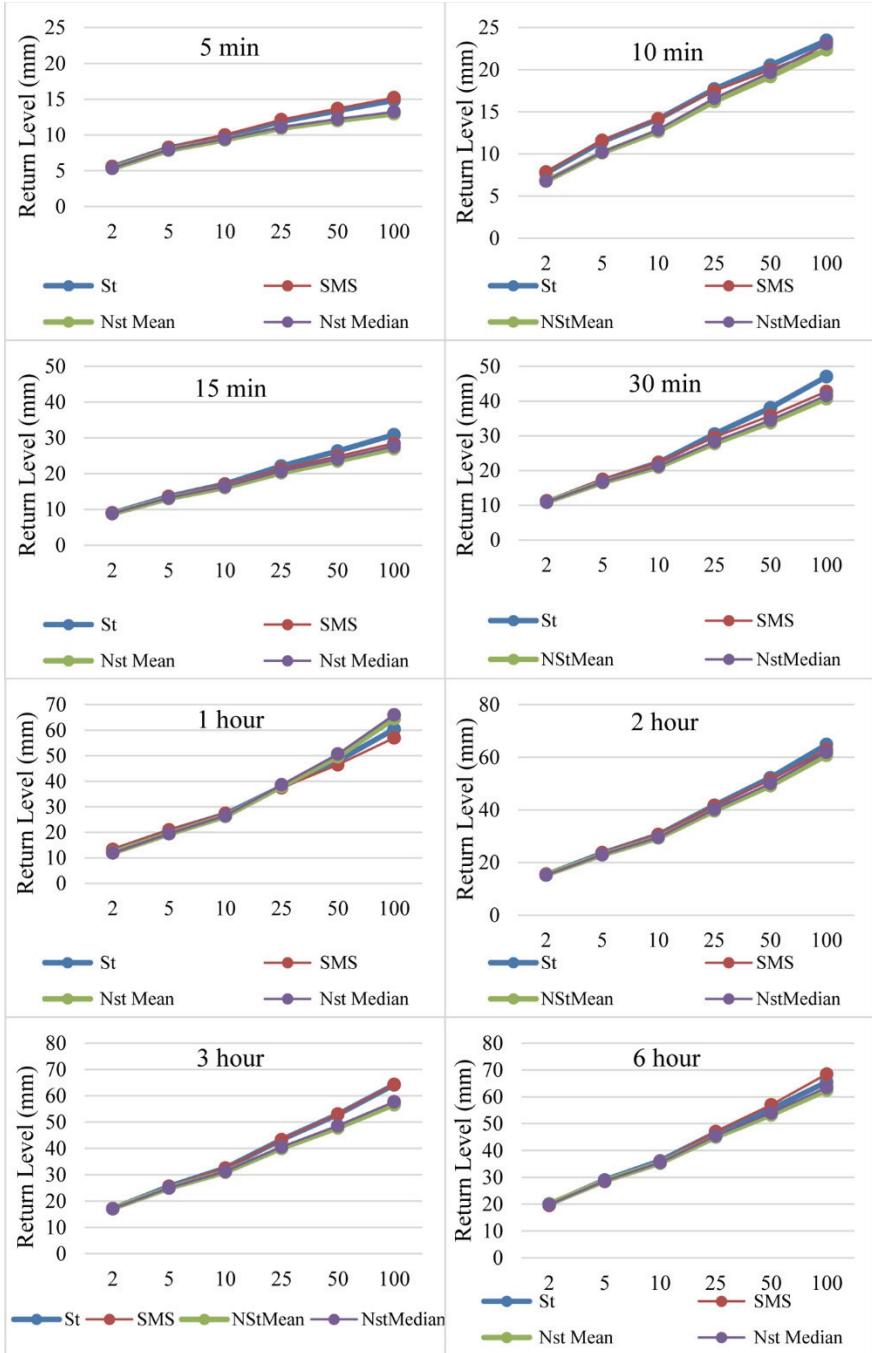
*Figure 4.3 - Stationary and best fit nonstationary model return level (mm) comparison -
Return level (mm) vs. Return period (Year)*

Differences in sub-hourly return levels between nonstationary and stationary models increase with the increasing return period, except the results from ten minutes data. While the mean (median) difference of 5-year return period is 4% (2%) for five and fifteen minutes durations, this difference reaches 11% (9%) and 12% (9%) for 50 years return period and 15% (12%) and 14% (12%) for 100 years return period. Exceptionally, ten minutes data follows the opposite direction for the alteration of nonstationary and stationary return level results with respect to storm duration, such as 14% (13%) and 12% (10%) mean (median) difference for 2 and 10 years return period and 5% (2%) for 100 years return period. It should be noted that usually the low return periods (2 to 10 years) are considered in design steps of storm drainage systems and this makes the nonstationarity more critical in controlling the uncertainty related to the determination of maximum precipitation value. The hourly time series demonstrate similar behavior to sub-hourly time series. While the negative differences from two, three- and six-hours time series are amplified with increasing return period, one-hour time series show increased return levels (positive difference) with nonstationarity after 25 years return period. SMS based stationary return levels also follow GEV based stationary levels closely and both of them provides higher return levels than nonstationary models (see Figure 4.3). The difference between the stationary and nonstationary return levels is not following a linear trend but to make a general inference sub-hourly storm durations indicate larger difference than hourly storm durations and non-stationary estimates are smaller than their corresponding stationary values. In these circumstances for a worst-case scenario it is better to use stationary return level estimates for the safety issue of a hydraulic structure. However, it will increase the cost and result in overdesign when observed data is considered. Moreover, depending on the characteristics of a time series different results can be seen; even one value can change the calculation results since every time series are evaluated independently and have its own statistical attributes. The outlier effect, distribution, parameter estimation methods, etc., all have impacts over the return level results. For instance, while observed 3 hour rainfall exceed 1 hour rainfall height, according to statistical analyses, chosen distribution, etc. a 100 year-1 hour return level result can exceed the 100 year-3 hour result; at that case distribution may change and calculations can be repeated, parameter estimation method can be changed or the highest value is taken for the calculations. Therefore, analyses and interpretation of such results need expert judgement to avoid misinterpretation.

4.2. Climate Change and Alterations in the Maximum Precipitation Events: Projections

Daily precipitation values of projection period are disaggregated to 5 minutes storm durations, then five minutes time series aggregated to the storm durations that are subject of interest such as 10 min, 15 min, 1 hour and 6 hour. Stationary and nonstationary models are applied to these projected (2015-2098) annual maximum storm durations for Ankara province. Three GCM models (MPI-ESM-MR, HADGEM2-ES, and GFDL-ESM2M) and two RCP scenario (4.5 and 8.5) for storm durations of stationary and nonstationary models are used. These driving GCM model outputs are downscaled by using the RegCM4 regional model to produce daily precipitation at 10 km.

4.2.1. Disaggregation of Daily Precipitation

The performance of the aforementioned disaggregation method has been assessed by reproducing a set of standard statistics (mean, variance, proportion of dry day, skewness, standard error and maximum value) for one hour disaggregated precipitation intensity from 24 hours precipitation data. These statistics can be compared with the same statistics obtained from hourly observed precipitation data available at the model grid location. The hourly mean statistics for January, May, June and October representing winter, spring, summer, and fall seasons, respectively are calculated for hourly and disaggregated hourly observed data and they are shown in Table 4.4. The statistics results are close to each other particularly in spring, summer and fall seasons. The higher skewness and maximum precipitation depth are observed with disaggregated data in January. However, the results indicated a good performance of the methodology in producing hourly values with their mean statistical measures (Table 4.4.). On the other hand, it must be specified the larger bias of the disaggregated data with respect to observed data for finer durations such as five minutes or ten minutes are observed. The parameters developed with observed data are used in the model to disaggregate daily precipitation of climate model outputs.

Table 4.4 - Statistical Parameters of Observed and Disaggregated Hourly Precipitation

|	January Disagg.	January Obs	May Disagg.	May Obs	June Disagg.	June Obs	October Disagg.	October Obs
Mean	0,04	0,04	0,11	0,11	0,09	0,09	0,07	0,07
Variance	0,30	0,11	0,37	0,37	0,26	0,29	0,23	0,16
Dry Day	0,98	0,95	0,90	0,90	0,91	0,93	0,95	0,93
Skewness	15,52	11,24	9,25	9,54	9,99	8,69	10,25	11,40
Std Error	0,55	0,34	0,61	0,61	0,51	0,54	0,47	0,40
Maximum	10,34	5,80	8,90	9,80	7,85	7,40	7,52	7,60

4.2.2. Trend Analysis

Figure 4.4 shows projected annual maximum rainfall intensities for storm duration of 10, 15 minutes and 1, 6 hours for three models and two RCP scenarios, between 2015-2098 periods with a linear trend line. All projections for 10 min, 15 min and 1-hr generally show decreasing tendency for their annual maximum precipitation depths according to linear regression lines. For sub-hourly durations, GFDL 8.5 and HG 8.5 are almost unresponsive to interannual changes in maximum precipitation. HG4.5, MPI4.5, and MPI8.5 are the most sensitive models to maximum precipitation changes between years for 15 min duration. Also, MPI8.5 shows higher fluctuations between years for 1-hr duration. As duration changes different responses from each model are observed.
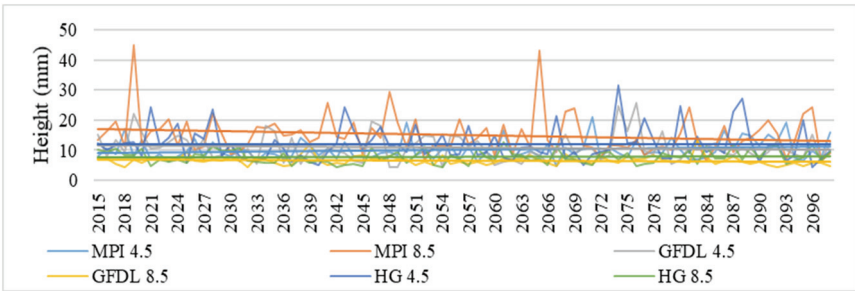
Trend test results using MK are shown in Table 4.5. The null hypothesis that there is no trend is rejected is shown with bold. The directions of trends in projections regardless of storm durations are mostly downward. The significant decreasing trends are associated with GFDL and MPI models with 8.5 RCP scenario while RCP 8.5 produces the warmest environment.
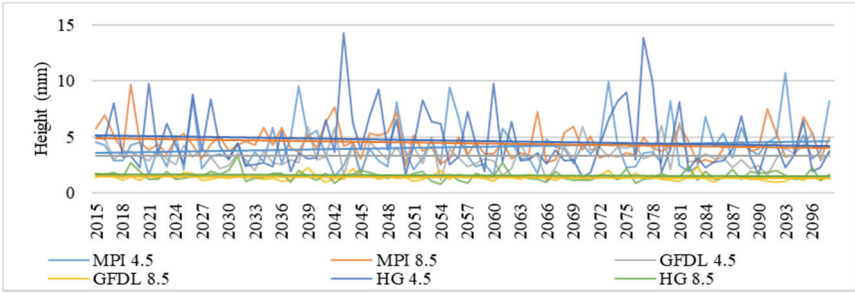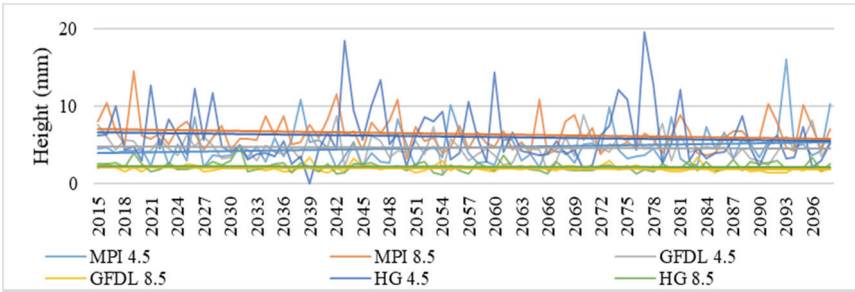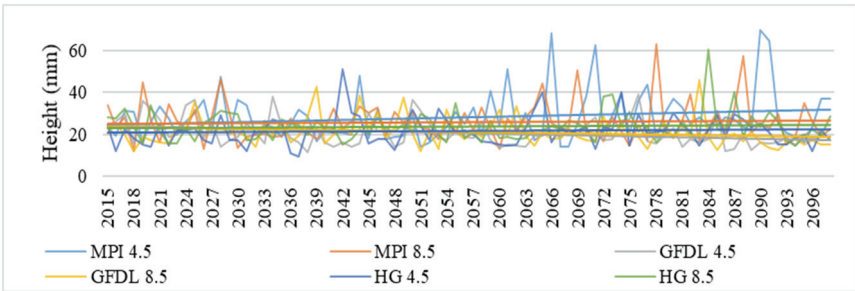
Figure 4.4 - Projected Annual Maximum-Time Series in Ankara Province for 2015-2098 period: a) Ten Minutes, b) Fifteen Minutes, c) One Hour, d) Six Hours

Moreover, increasing trends occurred only with MPI4.5 for each of storm duration. The MPI model can be sensitive to the choice of RCP scenario as it produces trend at opposite directions with different RCP. Trends in short (in particular sub-hourly) and long storm durations are largely different in terms of statistical significance and directions for model and scenario combinations.

Table 4.5 - Mann-Kendall Results for the Storm Durations of Projected Data Time Series

Storm Duration	MK Statistic	p-Value	Storm Duration	MK Statistic	p-Value
TenMinutesMPI45	0.0947	0.20374	OneHourMPI45	0.112	0.1339
TenMinutesMPI85	**-0.14**	**0.05940**	OneHourMPI85	**-0.143**	**0.05535**
TenMinutesGFDL45	-0.0175	0.8167	OneHourGFDL45	-0.0694	0.35185
TenMinutesGFDL85	-0.105	0.15966	OneHourGFDL85	**-0.141**	**0.05888**
TenMinutesHG45	-0.0967	0.19428	OneHourHG45	-0.0402	0.59128
TenMinutesHG85	-0.0531	0.47717	OneHourHG85	0.0499	0.50392
FifteenMinutesMPI45	0.0895	0.22959	SixHoursMPI45	0.0602	0.41944
FifteenMinutesMPI85	**-0.118**	**0.11235**	SixHoursMPI85	-0.0115	0.88024
FifteenMinutesGFDL45	-0.0459	0.53906	SixHoursGFDL45	**-0.173**	**0.01983**
FifteenMinutesGFDL85	**-0.122**	**0.10142**	SixHoursGFDL85	**-0.199**	**0.00759**
FifteenMinutesHG45	-0.0938	0.20789	SixHoursHG45	0.0422	0.57274
FifteenMinutesHG85	-0.0422	0.57273	SixHoursHG85	-0.0143	0.84986

4.2.3. Stationarity vs Nonstationarity Analysis

Stationary and nonstationary models are constructed for the future precipitation data and compared with each other. First nonstationary models are compared among themselves and then nonstationary model with the best fit diagnostic values is compared with stationary models. AIC, BIC and NLL values of stationary models and their corresponding best fit nonstationary ones are presented in Table 4.6. The results of best fit nonstationary models spread among the various model trials. More than 60% of constructed nonstationary models reveal best fit results for the models in which location parameter is set to a function of Temperature and exp(Temperature), and scale parameter is set to a function of exp(Temperature). Generally, best fit nonstationary models provide lower diagnostic values (at least one of three evaluation criteria) and hence they are superior comparing to stationary models.

For every model and its corresponding RCP scenarios, mean and median of best fit nonstationary return level estimate results are compared with stationary model results for all storm durations and their percent changes of these values are given in Table 4.7. For 10 min, 15 min and 1-hour durations the models with RCP 4.5 produced increased (positive change) return levels (up to 6 percent) with nonstationarity whereas the models with RCP 8.5 yielded

decreased (negative change) return levels (up to 4 percent). However, regardless of RCP scenarios almost all models (especially GFDL) released reduced (negative change) return levels with nonstationarity for 6-hour duration and such changes in return levels reached to 15 percent in maximum (based on median value). Magnitude of these changes increased with increasing return periods. The changes greater than 3 percent are highlighted in Table 4.7. GFDL and HG models with RCP 4.5 increased the return levels with nonstationarity particularly for 10 min, 15 min and 1-hour durations. The magnitude of future variations in extreme precipitation quantiles is dependent to the selection of GCMs and/or RCPs as it is also stated in Alam [79] who conducted the study of IDF curves analyses for Saskatoon, Canada, with possible climate change scenarios. Owing to semi-arid/arid climate conditions at the study location (Ankara province) Ankara is likely to encounter lower maximum precipitation depths at different frequencies in the future especially for the warmest condition (RCP 8.5) and longest duration (6-hour).

Table 4.6 - Diagnostic Values of Stationary and Best Fit Nonstationary Models of Projected Data

Model	Stationary			Best Fit Nonstationary		
	N L L	AIC	BIC	N L L	AIC	BIC
TenMinMPI45	160.49	329.98	334.27	159.58	327.15	336.88
TenMinMPI85	132.92	271.84	279.13	128.45	264.91	274.63
TenMinGFDL45	124.99	255.97	263.26	123.57	255.15	267.87
TenMinGFDL85	2.65	11.31	18.60	-1.81	6.38	18.53
TenMinHG45	181.79	369.57	376.86	180.24	368.47	378.20
TenMinHG85	43.77	93.53	100.83	43.21	94.42	104.15
FifteenMinMPI45	165.88	337.76	345.05	164.76	337.52	347.24
FifteenMinMPI85	169.16	344.31	351.61	166.22	340.43	350.16
FifteenMinGFDL45	151.40	308.81	316.10	149.05	306.10	315.83
FifteenMinGFDL85	33.81	73.61	80.91	31.63	71.25	80.98
FifteenMinHG45	203.40	412.81	420.10	201.64	411.29	421.013
FifteenMinHG85	74.74	155.48	162.78	74.03	156.06	165.78
Model	Stationary			Best Fit Nonstationary		
	N L L	AIC	BIC	N L L	AIC	BIC
OneHourMPI45	205.35	416.71	424.00	203.77	415.55	425.27
OneHourMPI85	258.91	523.82	531.11	252.66	513.33	523.05
OneHourGFDL45	235.48	476.96	484.25	234.06	476.13	485.85
OneHourGFDL85	142.67	291.34	298.63	138.44	286.87	299.03
OneHourHG45	246.33	498.66	505.95	244.51	497.02	506.74
OneHourHG85	181.81	369.61	376.91	179.66	367.33	377.05

Table 4.6 - Diagnostic Values of Stationary and Best Fit Nonstationary Models of Projected Data (continue)

Model	Stationary			Best Fit Nonstationary		
	N L L	AIC	BIC	N L L	AIC	BIC
SixHoursMPI45	303.82	613.65	620.94	302.85	613.71	623.43
SixHoursMPI85	292.30	590.61	597.90	281.20	572.41	584.56
SixHoursGFDL45	262.57	531.13	538.43	258.63	527.27	539.42
SixHoursGFDL85	261.93	529.86	537.15	252.61	515.21	527.37
SixHoursHG45	273.65	553.29	560.59	252.01	514.01	526.17
SixHoursHG85	264.12	534.24	541.53	264.08	536.17	545.89

Table 4.7 - Nonstationary Model-Stationary Model Comparison - Mean and Median Return Value Change for 2-5-10-25-50-100-200 Years Return Period with Respect to Stationary Model - Projected Data for 10 min, 15 min, 1 hour and 6 hour durations

	2	5	10	25	50	100	2	5	10	25	50	100
10 Min Model			Mean Value Change						Median Value Change			
MPI45	0%	0%	0%	0%	0%	0%	0%	0%	0%	0%	0%	0%
MPI85	0%	-1%	-1%	-2%	-2%	-2%	1%	0%	-1%	-1%	-2%	-2%
GFDL45	-1%	-1%	0%	0%	1%	1%	1%	1%	1%	1%	2%	2%
GFDL85	1%	0%	0%	-1%	-1%	-2%	2%	2%	2%	2%	2%	2%
HG45	0%	-1%	0%	1%	2%	2%	0%	-1%	0%	1%	2%	2%
HG85	0%	0%	0%	0%	0%	0%	-1%	-1%	-1%	-1%	0%	0%
15 Min Model			Mean Value Change						Median Value Change			
MPI45	0%	0%	0%	0%	1%	2%	0%	0%	0%	1%	1%	2%
MPI85	0%	-1%	-1%	-2%	-2%	-2%	1%	0%	-1%	-1%	-2%	-2%
GFDL45	-1%	-1%	-1%	0%	0%	0%	-1%	-1%	-1%	0%	0%	0%
GFDL85	0%	0%	-1%	-1%	-1%	-1%	0%	0%	0%	0%	-1%	-1%
HG45	-1%	-1%	0%	2%	**3%**	**5%**	-1%	-1%	0%	2%	**3%**	**5%**
HG85	0%	0%	0%	0%	0%	0%	-2%	-1%	-1%	-1%	-1%	0%
1 Hour Model			Mean Value Change						Median Value Change			
MPI45	-1%	-1%	-1%	-1%	-2%	-2%	-1%	-1%	-1%	-1%	-2%	-2%
MPI85	0%	-2%	-2%	-1%	-1%	0%	1%	-1%	-2%	-1%	0%	1%
GFDL45	-1%	0%	0%	1%	2%	3%	-1%	0%	0%	1%	2%	3%
GFDL85	0%	0%	-1%	-2%	**-3%**	**-3%**	2%	2%	1%	1%	0%	0%
HG45	0%	-1%	-1%	0%	0%	0%	0%	-1%	-1%	0%	0%	0%
HG85	0%	-1%	-1%	-1%	-1%	-1%	**-3%**	**-3%**	-2%	-2%	-2%	-2%
6 Hours Model			Mean Value Change						Median Value Change			
MPI45	0%	-1%	-1%	-2%	-2%	**-3%**	0%	-1%	-1%	-2%	-2%	**-3%**
MPI85	2%	2%	1%	0%	0%	-1%	2%	3%	3%	3%	3%	2%
GFDL45	1%	0%	-2%	**-5%**	**-7%**	**-10%**	1%	-1%	**-3%**	**-6%**	**-9%**	**-12%**
GFDL85	0%	-2%	**-3%**	**-5%**	**-7%**	**-9%**	1%	0%	-1%	**-3%**	**-4%**	**-5%**
HG45	0%	-1%	**-3%**	**-5%**	**-7%**	**-9%**	2%	2%	1%	-1%	-2%	**-4%**
HG85	0%	0%	0%	0%	0%	0%	0%	0%	0%	0%	0%	0%

Further the average of stationary and nonstationary model-RCP combinations of each storm duration are computed. Stationary return level averages MPI, GFDL, HG models RCP 4.5 and 8.5 results and nonstationary return level means of MPI, GFDL, HG models RCP 4.5 and 8.5 results are compared. These results are given in Figure 4.5.

It can be concluded that on average nonstationary models produce mostly lower return levels for six-hour storm duration and closer return level values for the rest of the storm duration within the same RCP scenario. Moreover RCP 8.5 model averages for all storm durations exhibit smaller values when compared with the RCP 4.5 return level values however future projections can reveal different results for different regions. While it is found that stationary return level estimates for projections reveal higher values in this study, DeGaetano et al. [80] computed future precipitation recurrence probabilities for NY State to consider the future flood risk. The study reveals that at the end of the century, NYS will face a median change of between 20 and 30% increase in one-hundred-year recurrence interval precipitation amounts.
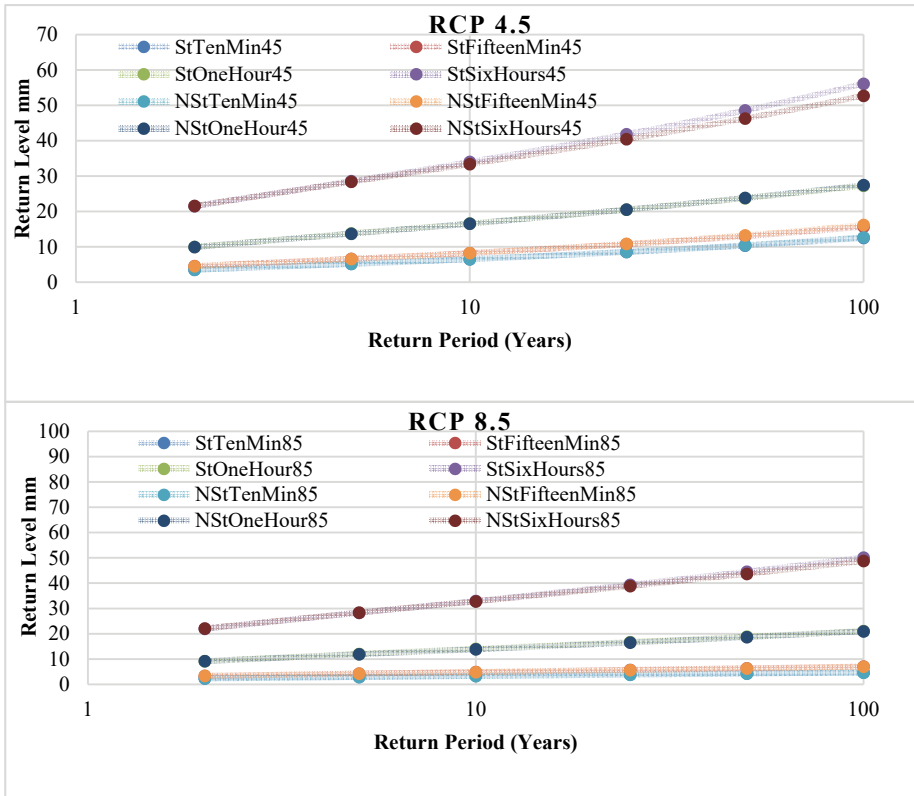
Figure 4.5 - Nonstationary Model-Stationary Model Comparison for Projected Data - Average Values

Furthermore, observation and projection period return level results are also compared in a single plot to capture and illustrate the potential temporal change. Stationary and

nonstationary return level plots of observed period, average stationary and nonstationary results of projected period and models that reveal the highest return level values among the model&RCP combinations (HG 4.5 for 10 and 15 minutes; MPI 8.5 for 1 hour and MPI 4.5 for 6 hours) of storm durations (10 minutes, 15 minutes, 1 hour, 6 hours) are presented in the Figures 4.6.
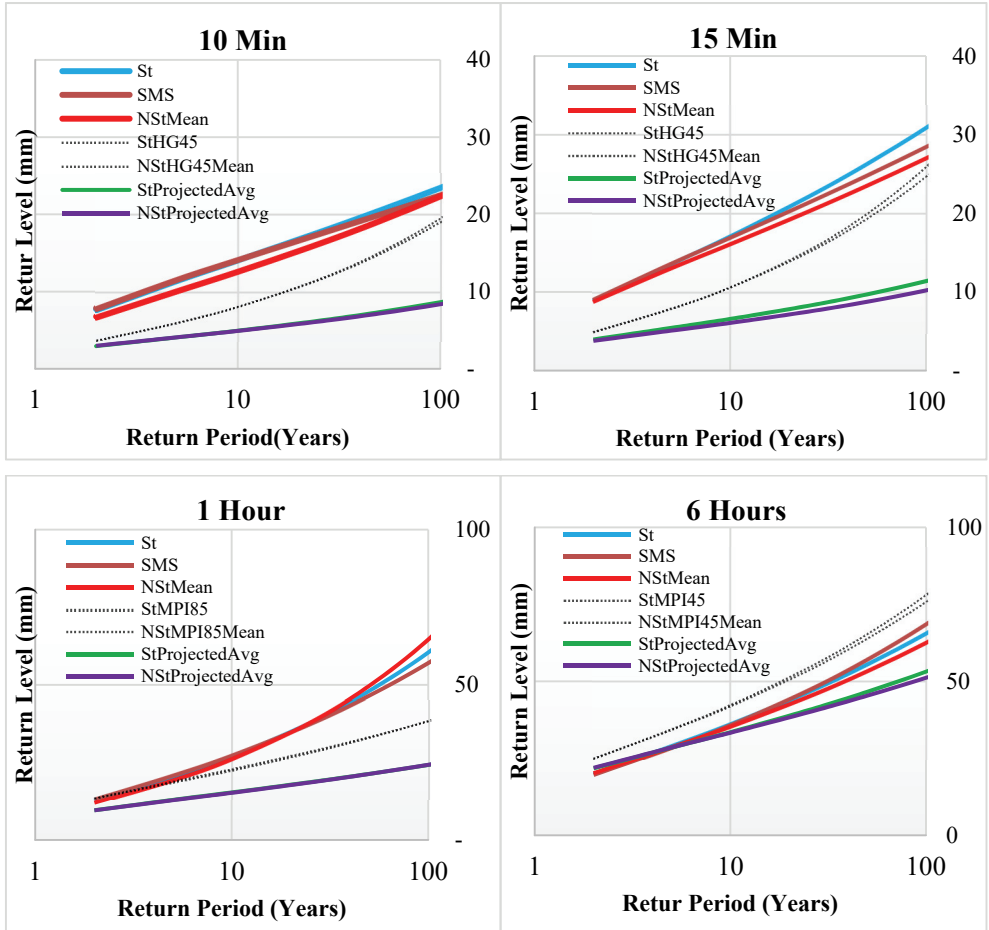
Figure 4.6 - Model Comparison – Observed Stationary and nonstationary, SMS, projected average stationary and nonstationary model results and model results with highest return level values of storm durations (10 minutes, 15 minutes, 1 hour, 6 hours)

For 10 min and 15 min storm durations in observed period, stationary return levels are higher than nonstationary levels while they are lower for 1-hour duration. In addition, for these storm durations all projected return levels with and without nonstationarity are lower than return levels in observed period. Discrepancies in return levels of observed and projected periods for these storms are significantly high which can be seen from the differences between

average values of projected period and the observed period values. However, with 6-hr duration these differences in between two periods are somewhat reduced. Even return levels of MPI with RCP 4.5 exceeded return levels calculated in historical period. Nevertheless, the maximum precipitation depths by the end of century will likely to occur with reduced magnitude comparing to the current time. In other words, the same precipitation depth in the future (by the end of century) can occur with longer return periods. With higher recurrence time and shorter storm duration this feature is more pronounced and therefore the severity of the extreme precipitation will probably be reduced in the future. Nonstationarity effect further decreases the return levels particularly for return periods greater than 10 year but it shows tendency to increase precipitation depths for sub-hourly durations even with return periods lower than 10 year. This aspect of the nonstationarity is effective in both periods.

In this study a general decrease in extreme rainfall return levels detected for the Ankara. However, for all return periods, six hours storm duration projected data driven model results do not fit the general trend. On the other hand, there are uncertainty caused by different aspects of the data and lack of practice as stated in the literature which complicate the analyses especially for future conditions. For instance Fadhel et al. [81] show that the use of different reference periods for the bias correction of RCM raise the uncertainty in the future IDF curves and emphasize the effect of the reference period on future climate projections, Kara [82] concluded that all RCMs may underestimate precipitation and Simonovic et al. [83] found that a reduction in extreme precipitation in central regions of Canada and increases in other regions based on CanESM2 results but also mentioned the GCM based uncertainty and the difference between ensemble and single model results. Moreover Arnbjerg Nielsen et al., [84] state the lack of understanding of how to quantify the impacts of climate change and the insufficiency of long-term rainfall statistics so the understanding of consequences of climate change stays limited. Haktanır and Çıtakoğlu [34] indicated that Intensity-Duration-Frequency (IDF) curves can be computed in the conventional way for Turkey which supports the findings of this study. Moreover, the future results are in line with the observed trends which indicated significant decreasing trend. On the other hand, Almazroui et al. [85] stated an average 5% increase in the rainfall intensity for semi-arid region of Turkey while Şen and Aksu [86] divided two equal halves the 7 meteorological station data of annual maximum series in İstanbul and indicated an increase of up to 30% rainfall intensity for the second period. Nevertheless, the difference between highest model results and average results for the projected data in this study indicates the unavoidable uncertainty.

5. SUMMARY AND CONCLUSIONS

In the present study, intensity-duration-frequency analysis of precipitation for the reference (1950-2015) and the future (2015-2098) conditions, which enables us to incorporate climate change and variability into the design and management of storm water drainage systems, is performed and discussed under stationary and non-stationary conditions for the capital and semi-arid climate of Ankara province in Turkey. The precipitation records of SMS of Turkey for observation period and the results of regional climate model simulations based on the HadGEM2-ES, MPI-ESM-MR and GFDL-ESM2M models with RCP4.5 and RCP8.5 scenarios for future periods have been used. Daily future precipitation projections are disaggregated to 5 minute and used for the future period analysis. The GEV frequency models for stationary and nonstationary cases during observed and projected periods are developed.

The maximum precipitation depths of all storm durations showed statistically significant decreasing trends during observed period while the models with RCP 8.5 released significant decreasing trends but the models with RCP 4.5 produced significantly increasing trends for all storm durations in projected period. Depending on the choice of emission scenarios the direction of the trend line changes from current to the future period. With more optimistic scenario (RCP 4.5) the severity of wetness increases in the future, however it is reduced and aligned with observed period when pessimistic scenario (RCP 8.5) is used. The statistical significance in precipitation change over time also inferred the existence of unavoidable nonstationarity. The stationary GEV models are capable of fitting the extreme precipitation time series of all storm durations, but the non-stationary GEV models showed advantage over the stationary models according to the diagnostic tests and values. Nonstationary model results exhibited smaller return level values with respect to stationary model results of each storm duration for the observed period. These changes reached to 15% especially for 10-15 min duration and 10-25 years return periods. These duration and frequencies are mostly considered in design of urban water drainage systems. Hence, the usage of nonstationarity approach becomes critical in application studies. Design magnitudes were lowered so that current structures do not consider nonstationarity would be overdesigned, however they will be safe for any failure. Similar reductions in return levels with nonstationarity were also obtained by models with RCP 8.5 in projected period. However, the nonstationarity models with RCP 4.5 increased the return levels in future. The negative effect of nonstationarity was the greatest for 6-hour duration regardless of any emission scenario and model.

In addition, return level values that are derived from observed data are greater than those from projected data almost for all storm duration and return period for 10-15 minutes and 1-6-hour storm duration. As the duration of storms increases projected return levels get closer to observed return levels. Future extreme precipitation depths for sub hourly storm durations are far lower than those in observed period. Therefore, the capacity of current operational storm drainage systems that were designed under stationarity will be safe enough and not create any operational difficulties in future based on the three model results used in this study. On the other hand, future projections, downscaling methods, disaggregation techniques host uncertainties that must be remembered in evaluation of the results.

Nevertheless, it should be noted that the differences in return level estimates of models support the need to update the current design parameters such as return level, return period with the most recent data and approaches. The differences also reveal the need to conduct analysis using future climate data.

References

[1]   IPCC, (2013). Climate change 2013. The Physical Science Basis. Contribution of Working Group I to the Fifth Assessment Report of the Intergovernmental Panel on Climate Change.

[2]   IPCC, (2014a). Climate change 2014. Impacts, Adaptation, and Vulnerability. Part A: Global and Sectoral Aspects. Contribution of Working Group II to the Fifth Assessment Report of the Intergovernmental Panel on Climate Change.

[3]   IPCC, (2014b). Climate change 2014. Synthesis Report. Contribution of Working Groups I, II and III to the Fifth Assessment Report of the Intergovernmental Panel on Climate Change.

[4]   Osborn, T. J., Gosling, S., Wallace, C., & Dorling, S. (2015). The Water Cycle in a Changing Climate. 7th World Water Forum. Faircount Media Group, London, 14–19.

[5]   Zhou, Q., Arnbjerg-Nielsen, K., Mikkelsen, P. S., Nielsen, S. B., & Halsnæs, K. (2012). Urban drainage design and climate change adaptation decision making. Kgs. Lyngby: DTU Environment

[6]   Papagiannaki, K., Lagouvardos, K., Kotroni, V., & Bezes, A. (2015). Flash flood occurrence and relation to the rainfall hazard in a highly urbanized area, Nat. Hazards Earth Syst. Sci., 15, 1859-1871

[7]   Willems, P. "Revision of Urban Drainage Design Rules after Assessment of Climate Change Impacts on Precipitation Extremes at Uccle, Belgium." Journal of Hydrology, vol. 496, 2013, pp. 166–177., doi:10.1016/j.jhydrol.2013.05.037.

[8]   Liew, S. C., Raghavan, S. V., & Liong, S.Y. (2014). How to construct future IDF curves, under changing climate, for sites with scarce rainfall records?. Hydrol. Process., 28, 3276–3287. doi:10.1002/hyp.9839

[9]   Pohl, B., Macron, C., & Monerie, P-A. (2017). Fewer rainy days and more extreme rainfall by the end of the century in Southern Africa. Scientific Reports, 7, 46466. doi: 10.1038/srep46466

[10]   Seneviratne, S. I., Nicholls, N., Easterling, D., Goodess, C. M., Kanae, S., & Kossin, J. (2012). Changes in climate extremes and their impacts on the natural physical environment. Cambridge University Press, Cambridge, UK, and New York, NY.

[11]   Ozturk, T., Turp, M. T., Türkeş, M., & Kurnaz, M. L. (2018). Future projections of temperature and precipitation climatology for CORDEX-MENA domain using RegCM4.4. Atmospheric Research, 206, 87-107. doi:10.1016/j.atmosres.2018.02.00

[12]   Kusunoki, S., (2017). Future changes in global precipitation projected by the atmospheric model MRI-AGCM3.2H with a 60-km size. Atmosphere, 8, 93

[13]   Buttstadt, M., & Schneider, C. (2014). Climate change signal of future climate projections for Aachen, Germany, in terms of temperature and precipitation. Mareike, 68(2), 71-83.

[14]   Meld, (2013). Climate change adaptation in Norway Meld. St. 33 (2012–2013) Report to the Storting (white paper) Recommendation of 7. May 2013 from the Ministry of the Environment, approved in the Council of State the same day. (White paper from the Stoltenberg II Government).

[15] IPCC, (2012). Managing the risks of extreme events and disasters to advance climate change adaptation. A Special Report of Working Groups I and II of the Intergovernmental Panel on Climate Change.

[16] Kundzewicz, Z. W., Kanae, S., Seneviratne, S. I., Handmer, J., Nicholls, N., Peduzzi, P., Mechler, R., Bouwer, L. M., Arnell, N., Mach, K., Muir-Wood, R. G., Robert, B., Wolfgang, K., Gerardo, B., Yasushi, H., Kiyoshi, T., & Boris, S. (2014). Flood risk and climate change: global and regional perspectives. Hydrological Sciences Journal, 59(1), 1-28. doi: 10.1080/02626667.2013.857411

[17] Li, J., Johnson, F., Evans, J., & Sharma, A. (2017). A comparison of methods to estimate future sub-daily design rainfall. Advances in Water Resources, 110. 10.1016/j.advwatres.2017.10.020.

[18] Hettiarachchi, S., Wasko, C., & Sharma, A. (2018). Increase in flood risk resulting from climate change in a developed urban watershed – the role of storm temporal patterns, Hydrol. Earth Syst. 22, 2041-2056.

[19] Cheng, L., & AghaKouchak, A. (2014). Nonstationary precipitation intensity-duration-frequency curves for infrastructure design in a changing climate. Sci. Rep. 4, 7093. doi:10.1038/srep07093

[20] Sarhadi, A., & Soulis, E. D. (2017). Time-varying extreme rainfallintensity-duration-frequency curvesin a changing climate, Geophys. Res.Lett., 44. doi:10.1002/2016GL072201

[21] Peck, A., Prodanovic, P., & Simonovic, S. P. (2012). Rainfall intensity duration frequency curves under climate change: city of London, Ontario, Canada. Can. Water Res. J., 37(3), 177–189. http://dx.doi.org/10.4296/cwrj2011-935

[22] Hosseinzadehtalaei, P., Tabari, H., & Willems, P. (2017). Precipitation intensity–duration–frequency curves for central Belgium with an ensemble of Eurocordex simulations, and associated uncertainties. Atmospheric Research, 200, 1-12. doi:10.1016/j.atmosres.2017.09.015

[23] Willems, P., Olsson, J., Arnbjerg-Nielsen, K., Beecham, S., Pathirana, A., Gregersen, I.B., Madsen, H., Nguyen, V.T.V. (2012). Impacts of climate change on rainfall extremes and urban drainage. IWA Publishing, London, UK.

[24] Yuan, X.-C., Wei, Y.-M., Wang, B., and Mi, Z. (2017). Risk management of extreme events under climate change, J. Clean. Prod., 166,1169–1174, https://doi.org/10.1016/j.jclepro.2017.07.209, 2017

[25] Yoon, J. H., Wang, S. Y., Gillies, R. R., Kravitz, B., Hipps, L., & Rasch, P. J. (2015). Increasing water cycle extremes in California and relation to ENSO cycle under global warming. Nat. Commun, 6, 8657 doi: 10.1038/ncomms9657

[26] Simonovic, S. P. (2012). Floods in a changing climate: Risk management, 194. Cambridge: Cambridge University Pres

[27] Huntington, T. G. (2006). Evidence for ıntensification of the global water cycle: review and synthesis. Journal of Hydrology, 319, 83-95. http://dx.doi.org/10.1016/j.jhydrol.2005.07.003

[28] Abdellatif, M., Atherton, W., & Alkhaddar, R. (2013). Application of the stochastic model for temporal rainfall disaggregation for hydrological studies in North Western England. Journal of Hydroinformatics, 15(2), 555-567.

[29] Harisaweni, Z., & Fadhilah, Y. (2016). The use of BLRP model for disaggregating daily rainfall affected by monsoon in Peninsular Malaysia. Sains Malaysiana, 45 (1). 87-97.

[30] Kossieris, P., Makropoulos, C., Onof, C., & Koutsoyiannis, D. (2016b). HyetosMinute, A package for temporal stochastic simulation of rainfall at fine time scales, Version 2.0.

[31] SMS, (2020). Republic of Turkey, the ministry of forestry and water affairs, state meteorological service, State of the Climate in Turkey in 2019, January 2020

[32] Sensoy, S., Türkoğlu, N., Akçakaya, A., Ulupınar, Y., Ekici, M., Demircan, M., Atay, H., Tüvan, A., & Demirbaş, H. (2013). Trends in Turkey climate indices from 1960 to 2010, 6th Atmospheric Science Symposium, 24 - 26 April 2013, ITU, Istanbul, Turkey.

[33] Danandeh Mehr, A. and Kahya, E. (2016). Climate change impacts on catchment-scale extreme rainfall variability: Case Study of Rize Province, Turkey. Journal of Hydrologic Engineering, 10.1061/(ASCE)HE.1943-5584.0001477, 05016037.

[34] Haktanir, T., & Citakoglu, H. (2014). Trend, independence, stationarity, and homogeneity tests on maximum rainfall series of standard durations recorded in Turkey. Journal of Hydrologic Engineering, 19, 9. DOI: 10.1061/(ASCE)HE.1943-5584.0000973.

[35] Yilmaz, A. G. (2015). The effects of climate change on historical and future extreme rainfall in Antalya, Turkey. Hydrological Sciences Journal, 60(12), 2148-2162. doi: 10.1080/02626667.2014.945455

[36] Tayanç, M., İm, U., Doğruel, M., & Karaca, M. (2009). Climate change in Turkey for the last half century. Climatic Change, 94, 483-502.

[37] Turunçoğlu, U. U., Türkeş, M., Bozkurt, D., Önol, B., Şen, Ö. L., & Dalfes, H. N. (2018). The Soils of Turkey. World Soils Book Series. Springer, Cham.

[38] WRP, (2016). Republic of Turkey, the ministry of forestry and water affairs, general directorate of water management. Climate Change Impacts On Water Resources Project.

[39] Aziz, R. (2018). Impacts Of Climate Nonstationarities On Hydroclimatological Variables In Turkey, PhD. Dissertation. Middle East Technical University

[40] Aziz, R.,Yucel, I., Yozgatligil, C. (2020). Nonstationarity impacts on frequency analysis of yearly and seasonal extreme temperature in Turkey. Atmospheric Research, 238, doi.org/10.1016/j.atmosres.2020.104875

[41] Maraun, D. (2016). Bias correcting climate change simulations—a critical review. Curr Clim Change Rep 2(4):211–220. doi: 10.1007/s40641-016-0050-x

[42] Willkofer, F.; Schmid, F.J.; Komischke, H.; Korck, J.; Braun, M.; Ludwig, R. The impact of bias correcting regional climate model results on hydrological indicators for Bavarian catchments. J. Hydrol. Reg. Stud. 2018, 19, 25–41

[43] Demircan, M , Gürkan, H , Eskioğlu, O , Arabacı, H , Coşkun, M . (2017). Climate Change Projections for Turkey: Three Models and Two Scenarios . Turkish Journal of Water Science and Management , 1 (1) , 22-43 . DOI: 10.31807/tjwsm.297183

[44] Kossieris, P., Makropoulos, C., Onof, C., & Koutsoyiannis, D. (2016a). A rainfall disaggregation scheme for sub-hourly time scales: Coupling a Bartlett-Lewis based model with adjusting procedures, Journal of Hydrology, 556, 980-992.

[45] Kaczmarska, J. M., Isham, V. S., & Northrop, P. (2015). Local generalised method of moments: an application to point process-based rainfall models. Environmetrics, 26, 312–325. doi: 10.1002/env.2338

[46] Ritschel, C., Ulbrich, U., Névir, P., & Rust, H. W. (2017). Precipitation extremes on multiple timescales – Bartlett–Lewis rectangular pulse model and intensity–duration–frequency curves. Hydrology and Earth System Sciences, 21(12), 6501.

[47] Yılmaz, E. (2013). Ankara Şehrinde Isı Adası Oluşumu. (Doktora Tezi), Ankara Üniversitesi, Sosyal Bilimler Enstitüsü, Ankara.

[48] Governorate of Ankara, (2018). Geography and demographics. [online] Available at: http://eng.ankara.gov.tr/geography-and-demographics. [Accessed 01 June 2018].

[49] Batuman, B. (2013). City profile: Ankara. Cities, 31. 578–590. 10.1016/j.cities.2012.05.016

[50] Sensoy, S., Turkoglu, N., Cicek I., Demircan, M., Arabacı, H., Bölük, E., 2014, Urbanization Effect on Trends of Extreme Temperature Indices in Ankara, 7th Atmospheric Science Symposium, 28-30 April 2015, İstanbul

[51] Çiçek, I., & Turkoglu, N.. (2005). Urban effects on precipitation in Ankara. Atmósfera, 18(3), 173-187.

[52] Kossieris, P., Koutsoyiannis, D., Onof, C., Tyralis, H., & Efstratiadis, A. (2012). HyetosR: An R package for temporal stochastic simulation of rainfall at fine time scales. European Geosciences Union General Assembly 2012, Geophysical Research Abstracts, Vol. 14, Vienna, 11718, European Geosciences Union.

[53] Rodriguez-Iturbe, I., Cox, D. R., & Isham, V. (1987a). Some models for rainfall based on stochastic point processes. Proceedings of the Royal Society, 410, 269–288.

[54] Rodriguez-Iturbe, I., Febres de Power, B., & Valdes, J. B. (1987b). Rectangular pulses point process models for rainfall: analysis of empirical data. Journal of Geophysical Research, 92, 9645–9656.

[55] Villani, V., Di Serafino, D., Guido, R., & Mercogliano, P. (2016). Stochastic models for the disaggregation of precipitation time series on sub-daily scale: identification of parameters by global optimization. CMCC Research Paper No. RP0256. http://dx.doi.org/10.2139/ssrn.2602889

[56] Lu, Y., & Qin, X. S. (2012). Comparison of stochastic point process models of rainfall in Singapore. Proceedings of 2012 International Conference of World Academy on Science, Engineering and Technology (WASET), 68, 1234-1238.

[57] Rozos, E., Efstratiadis, A., Nalbantis, I., & Koutsoyiannis, D. (2004).Calibration of a semi-distributed model for conjunctive simulation of surface and groundwater flows, Hydrological Sciences Journal, 49(5), 819-842.

[58] Efstratiadis, A., and D. Koutsoyiannis, An evolutionary annealing-simplex algorithm for global optimisation of water resource systems, (2002). Proceedings of the Fifth International Conference on Hydroinformatics, Cardiff, UK, 1423-1428, International Water Association, (http: //itia.ntua.gr/el/docinfo/524/)

[59] Yilmaz, A. G., & Perera, B. J. C. (2014). Extreme rainfall non-stationarity investigation and intensity-frequency-duration relationship. J. Hydrol. Eng. 19, 1160-1172. doi: 10.1061/(ASCE)HE.1943-5584.0000878

[60] Mann, H. B. (1945). Non-parametric tests against trend, Econometrica, 13,163-171.

[61] Kendall, M. G. (1975). Rank correlation methods, 4th edition, Charles Griffin, London.

[62] Gilbert, R. O. (1987). Statistical Methods for Environmental Pollution Monitoring. Wiley, NY.

[63] Onyutha, C., Tabari, H., Taye, M. T., Nyandwaro, G. N., & Willems, P. (2015). Analyses of rainfall trends in the Nile River basin. J Hydro Environ Res, 13, 36–51.

[64] Yucel, I., Güventürk, A. and Sen, O. L. (2014), Climate change impacts on snowmelt runoff for mountainous transboundary basins in eastern Turkey. Int. J. Climatol., 35: 215-228. doi:10.1002/joc.3974

[65] Umbricht, A., Fukutome, S., Liniger, M. A., Frei, C., & Appenzeller, C. (2013). Seasonal variation of daily extreme precipitation in Switzerland. Scientific Report. MeteoSwiss, 97, 122.

[66] Collet L., Beevers, L., & Prudhomme C. (2017). Assessing the impact of climate change and extreme value uncertainty to extreme flows across Great Britain. Water, 9(2),103.

[67] Coles, S. G., & Sparks, R. S. J. (2006). Extreme value methods for modelling historical series of large volcanic magnitudes. Chapter 5, Statistics in Volcanology.

[68] Wang, J., You, S., Wu, Y., Zhang, Y., & Bin, S. (2016). A method of selecting the block size of bmm for estimating extreme loads in engineering vehicles. Mathematical Problems in Engineering. 1-9. 10.1155/2016/6372197.

[69] Cai, Y., & Hames, D. (2010). Minimum sample size determination for generalized extreme value distribution,communications in statistics. Simulation and Computation, 40(1), 87-98. doi: 10.1080/03610918.2010.530368

[70] Coles, S. (2001). An Introduction to Statistical Modeling of Extreme Values, Springer, London.

[71] Gilleland, E., & Katz, R. (2016). extRemes 2.0: An Extreme Value Analysis Package in R. Journal of Statistical Software, 72(8), 1-39. doi: 10.18637/jss.v072.i08

[72] Bayazit, M. (2015). Nonstationarity of hydrological records and recent trends in trend analysis: A State-of-the-art Review. Environmental Processes, 2, 527-542.

[73] Pohlert T. (2016). Non-Parametric Trend Tests and Change-Point Detection. R package Version 0.2.0.

[74] Gül, G., Aşıkoğlu, Ö., Gül, A., Gülçem, Y. F., & Benzeden, E. (2014). Nonstationarity in flood time series. Journal of Hydrologic Engineering, 19, 1349-1360

[75] Šraj, M., Viglione, A., Parajka, J., & Blöschl, G. (2016). The influence of non-stationarity in extreme hydrological events on flood frequency estimation. Journal of Hydrology and Hydromechanics, 64, 426-437

[76] Cheng, L. (2014). Frameworks for univariate and multivariate non-stationary analysis of climatic extremes, PhD. Dissertation, UC Irvine.

[77] Wang, Y., & Liu, Q. (2006). Comparison of Akaike information criterion (AIC) and Bayesian information criterion (BIC) in selection of stock–recruitment relationships. Fish. Res. 77, 220-225.

[78] Sienz, F., Schneidereit, A., Blender, R., Fraedrich, K., & Lunkeit, F. (2010). Extreme value statistics for North Atlantic cyclones. Tellus A, 62(4), 347–360.

[79] Alam, S. (2014). Construction of the intensity-duration-frequency (idf) curves under climate change. Master of Science, University of Saskatchewan.

[80] DeGaetano, A. T., & Castellano, C. M. (2017). Future projections of extreme precipitation intensity-duration-frequency curves for climate adaptation planning in New York State. Climate Services, 5, 23-35.

[81] Fadhel, S., Rico-Ramirez, M. A., & Han, D. (2017). Uncertainty of intensity duration–frequency (IDF) curves due to varied climate baseline periods. Journal of Hydrology, 547, 600-612.

[82] Kara, F. (2014). Effects of climate change on water resources in Omerli basin. PhD. Dissertation. Middle East Technical University

[83] Simonovic, S. P., Schardong, A., & Sandink, D. (2017). Mapping extreme rainfall statistics for canada under climate change using updated intensity-duration-frequency curves. ASCE Journal of Water Resources Planning and Management, 143(3), 04016078-1 -04016078-12.

[84] Arnbjerg-Nielsen, K., Willems, P., Olsson, J., Beecham, S., Pathirana, A., Gregersen, I. B., & Nguyen, V-T. V. (2013). Impacts of climate change on rainfall extremes and urban drainage systems: A review. Water Science and Technology, 68(1), 16-28. Doi: 10.2166/wst.2013.251.

[85] Almazroui, M., Şen, Z., Mohorji, A.M. et al. Impacts of Climate Change on Water Engineering Structures in Arid Regions: Case Studies in Turkey and Saudi Arabia. Earth Syst Environ 3, 43–57 (2019). https://doi.org/10.1007/s41748-018-0082-6

[86] Şen, K , Aksu, H . (2021). İstanbul İçin Standart Süreli Gözlenen En Büyük Yağışların Eğilimleri. Teknik Dergi , 32 (1) , 1-2 . DOI: 10.18400/tekderg.647558

Effects of Gilsonite on Performance Properties of Bitumen

Perviz AHMEDZADE[1]
Omar ALQUDAH[2]
Taylan GUNAY[3]
Tacettin GECKIL[4]

ABSTRACT

The effectiveness of natural Gilsonite on the performance properties of modified bitumens was studied. Three samples having different ratios of Gilsonite that are 6%, 8% and 10% by weight of base bitumen which was PG 64-16 grade were prepared. The physical properties and storage stabilities of four samples were investigated by means of conventional tests. The short-term and long-term aging processes of bitumens were conducted with rolling thin oven and pressure aging vessel tests, respectively. Rheological properties of bitumens were examined by means of Superpave tests such as rotational viscosity, dynamic shear rheometer and bending beam rheometer. After the rheological study, the low and high temperature performance classes of bitumens were determined by the Superpave specification. The results showed that natural Gilsonite-modified bitumens provide improvement in rheological and physical properties of bitumen, and were found highly compatible with base bitumen. Gilsonite additive significantly increased stiffness and viscosity of bitumen, and improved the resistance against fatigue cracking and rutting of bitumen, without causing a reduction in thermal cracking resistance of bitumen.

Keywords: Bitumen, gilsonite, aging, rheological properties, performance grade.

1. INTRODUCTION

In the modern world, annually about 110 million metric tons of bitumen is needed. The manufacture, repair and maintenance of bituminous pavements require the large amount of

---

1 Ege University, Department of Civil Engineering, Izmir, Turkey - perviz.ahmedzade@ege.edu.tr https://orcid.org/0000-0001-8348-5901

2 German Jordanian University, Civil & Environmental Engineering Department, Madaba, Jordan - omerkudah@yahoo.com - https://orcid.org/0000-0003-1789-6749

3 Ege University, Department of Civil Engineering, Izmir, Turkey - taylan.gunay@ege.edu.tr https://orcid.org/0000-0002-2669-6320

4 Inonu University, Department of Civil Engineering, Malatya, Turkey - tacettin.geckil@inonu.edu.tr https://orcid.org/0000-0001-8070-6836

fund and energy [1]. In addition to the high cost and inadequate resources of the bitumen used in road pavements, the aging due to transportation, storage, mixing, placement on the road surface and service life on the road also causes many problems. Moreover, after the application of bitumen, hot mix asphalt (HMA) pavements are also faced with various problems during their service life [2]. As is known, the main distresses occur in flexible pavements due to traffic loading or environmental effects or other factors, such as fatigue cracking, rutting, and low-temperature cracking [3].

The bitumen plays an important role in the performance properties of HMA during service life. However, many of the distresses are related to the characteristics of bitumen used in the pavement itself. Base binder is commonly used in most countries where some defections could be occurred early stages of service life. The rheological weakness of binder is the main reason of using modifiers to enhance properties of binder, and consequently make the performance of the pavements better. By the processes of mechanical mixing or chemical reaction, polymer modified bitumens (PMBs) are produced by adding polymers into bitumens. It is necessary appropriate compatibility between bitumen and polymer to obtain the optimum properties of PMBs. Poor storage stability occurs when the compatibility is poor. Thus, the separation of polymeric and bituminous phases or inconsistent bitumen quality takes place [4].

Bitumen modifiers could be natural or artificial. Many types of modifiers were used in this field, like rubber, crumb rubber, elvaloy, polypropylene, styrene–butadiene–rubber (SBR), and styrene butadiene styrene (SBS), and ethylene vinyl acetate (EVA) [3,5,6]. It is known that modifiers vary in effectiveness, workability, performance, availability, and cost. The cost efficiency as well as the degree of compatibility of modifier with the bitumen during storing and handling have been the biggest challenges in the industry of modified bitumens. Despite the fact that there is large number of modifiers, few of them are really appropriate for modification process. There have been many attempts within this scope to solve the problem related to lack of stability in polymer-modified bitumen. For example, the recycled polymers can be exposed to irradiation to get over this problem. In this process, functional groups and new bonds are formed in polymer chain and this provides chemical bonding with bitumen by preventing phase separation. The beneficial and significant enhancement of bitumen behavior and performance was obtained by the modification of bitumen with the electron irradiated recycled low-density polyethylene (e-LDPE$_R$) [7, 8]. The compatibility between SBS-g-M grafted with vinyl monomer under x-rays irradiation and bitumen, and thus the storage stability of bitumen was improved considerably as compared with SBS modified bitumen [9].

The main purpose of bitumen modification is to improve the main quality and properties of bitumen without negatively affecting the different properties of the bitumen or mixture [10]. In recent years, natural hydrocarbon-containing additives have begun to be used to improve the performance properties of bitumen. One of these additives is known in the market as Gilsonite, which is derived from naturally occurring bitumen resources, commonly referred to as asphaltite [11,12,13,14]. Discovered in the early 1860s, Gilsonite is a resinous hydrocarbons that has been used and evaluated in a variety of industrial applications [15]. Gilsonite, a crude petroleum-based by-product, contains natural hydrocarbons with a purity of about 99%, and 57–70% of asphaltene [14,16]. It is a mineral bitumen, black and fragile, and has a structure that can easily be crushed into powder [14,17]. It is also a fast-dissolving

additive in bitumen due to its easy using and good compatibility with bitumen [18]. The favorable properties of Gilsonite make it a good alternative to other commercially produced polymers, especially at high temperatures and high traffic volumes. In various studies, Gilsonite is generally used to improve high temperature performance properties due to the hardening effect of bitumen, but the hardening that occurs can affect the low and intermediate temperature performance characteristics of bitumen [13-15,19,20,21]. The use of Gilsonite is now considered very seriously in bitumen modification when cost and time effectiveness, high performance and storage stability are taken into consideration.

In this study, the Gilsonite, a natural hydrocarbon-containing additive, was used as a modifier for bitumen to examine its impact on the physical and rheological performance properties of the road bitumens.

Generally, in the studies carried out, the Gilsonite additive was used in bitumen modification in two different ways: the addition of Gilsonite into bitumen, or the addition of Gilsonite as a filler in the aggregate mixture [14]. In previous studies, it has been reported that the use of Gilsonite in bitumen modification has increased the viscosity and softening point of bitumen but decreased its ductility and penetration [13,14,22]. In some studies, it has been reported that Gilsonite reduced the temperature sensitivity by increasing the hardness of the bitumen, but it increased its elasticity [13,23]. In many studies it has been indicated that increasing the amount of Gilsonite in the bitumen increased the high temperature performance of the bitumen, but the tendency to fatigue and low-temperature cracking increased [11,12-15,21,24]. However, Feng and Ameri have reported that the intermediate and high temperature performance of the modified bitumen with Gilsonite has improved [23]. The results of another study showed that Gilsonite, as a modifier, could be used to improve its stiffness properties and rutting resistance of mixtures used in hot climates [14]. A study, in which two different types of bitumen were used, indicate that Gilsonite improved the high temperature performances of the bitumens, but decreased the low temperature performances [17]. Similarly, Anderson et al. also noted that Gilsonite modified bitumen showed a fragile behavior at low temperatures [19]. The results of a study showed that the Gilsonite-modified bitumens serve to prevent crack formation in the coating by forming a good bond between bitumen and aggregate [25]. In another study, it was found that the storage stability of Gilsonite-modified bitumen was better than SBS modified bitumen [13]. In addition, the results of a study showed that the use of Gilsonite in appropriate amount had no negative effect on the aging process of bitumen [26]. In many studies it has been reported that HMA modified with Gilsonite had higher stability, lower permanent deformation and better fatigue and moisture resistance [10,13,15,18,23]. Additionally, it has been determined that these mixtures showed more strength under dynamic loading [15,23]. Moreover, in some studies it has been stated that Gilsonite has many economic benefits of using it in pavement design [11,13,14,15,23]. Finally, it has been suggested that Gilsonite could be used as a modifier to improve the performance properties of HMA [11,13].

This research discusses the influence of Gilsonite as a modifier in bitumen. The primary objective of this research is to characterize the physical and rheological properties of Gilsonite modified bitumen. To this end, the test results of modified binders were discussed and compared with base (unmodified) bitumen.

2. MATERIALS

2.1. Materials

The base bitumen with a PG 64-16 performance grade used in this study was supplied from Izmit refinery in Turkey. The obtained physical properties of base bitumen were given in Table 1. The modifier used was natural Gilsonite material supplied by URAN Holding Ltd. Company in Turkey. The composition and physical properties of used Gilsonite are shown in Table 2.

Table 1 - Physical properties of base bitumen (PG 64-16)

Properties	Results
Penetration (25°C, 100 gr, 5 sec) 0.1 mm	51
Softening point, °C	46.5
Elastic recovery (25°C), %	88
Flash point, °C	265
Specific gravity (25°C), gr/cm³	1.027

Table 2 - Composition and physical properties of used Gilsonite

Properties	Results
Carbon content (%)	85.22
Sulphur content (%)	3.09
Oxygen content (%)	1.49
Hydrogen content (%)	5.97
Nitrogen content (%)	0.77
Ash content (%)	2.24
Moisture content (%)	0.09
Solubility in CS2 (%)	41.74
Solubility in Toluene (%)	20.83
Softening point, °C	160-205
Specific gravity, at 25°C (gr/cm³)	1.145

2.2. Preparation of Samples

The Gilsonite-modified bitumen were prepared by blending base bitumen with Gilsonite in powder form at three different percentages (6%, 8% and 10%) of Gilsonite by total weight of bitumen. For this purpose, blending process was accomplished via a laboratory high shear mixer. After heated in oven for 90 min at 163°C, the base bitumen was poured into a

temperature-controlled container of mixer rotating 500 rpm. Subsequently the Gilsonite was slowly added into bitumen by portions within the first 15 minutes of mixing, and then the mixing rate was adjusted to 1500 rpm. This mixing process continued for another 45 min. The mixing temperature was set at 170 °C and the temperature was checked with a thermometer at every 15 minutes.

Base and Gilsonite-modified bitumens used in this study were coded as B, B+6G, B+8G and B+10G, respectively.

3. TEST METHODS

3.1. Conventional Tests

Penetration, softening and flash point, elastic recovery, and specific gravity tests were performed on both original base and modified bitumens. After the thin film oven test (RTFOT), the mass losses, retained penetrations and softening points of the bitumen were established to understand the effects of the modifier on aging. All tests were conducted according to the requirements of (TS EN 14023) standard of polymer-modified bitumens (PMBs) [27].

3.2. Storage Stability Test

In order to provide the stability and decomposition resistance of the modified bitumens during handling, mixing and in-service life, the compatibility test was also performed throughout the storage stability test according to EN 13399 standard [28].

This test was conducted as follows. A glass tube consists of three symmetrical parts, 35 mm diameter, and 180 mm height, was used and filled with about 150 g of modified bitumen. The tubes containing the modified samples were tightly closed via glass hood with two hooks. Two small springs were used to close the tube and fasten the hood with the top part of the tube in order to ensure no vaporization problem would occur during the test. After that, the tubes were placed vertically in a preheated oven in 180 °C for 72 hr. The bitumen samples stored in oven were cooled at room temperature, and then cut into three parts. To compare the top and bottom parts of samples, these two parts were tested to evaluate the storage stability by measuring their penetration, softening point [29].

3.3. Rotational Viscosity Test

The viscosities of all bitumens were determined by the rotational viscometer (RV) to ensure the workability of the modified bitumens. The rotational viscometer as compared with the capillary viscometers used in the viscosity graded method can detect the viscosity of bitumen by measuring the torque required to provide a constant rotational speed (20 RPM) of a cylindrical spindle immersed into a binder sample held at a fixed temperature [29, 30].

The tests were conducted at 135 °C and 165 °C by means of a Brookfield viscometer (DVRV-II Pro) as described in AASHTO T316 standard [31]. The mixing and compacting process temperatures of base and modified bitumens to be used in HMA were also determined. In the

calculation, the suitable ranges of viscosities corresponding to the mixing and compacting temperatures were selected as 150-190 cP and 250-310 cP, respectively. The rotational viscosity of bitumen should not exceed 3000 cP for the tests at 135 °C [32].

3.4. Aging of Bitumen

The short-term aging operations of all bitumens were conducted with the rolling thin film oven test (RTFOT) according to EN 12607-1 standard [33]. The bitumen samples were aged for 75 min in an oven at a temperature of 163 °C. After RTFOT simulating changes in the physical properties of the bitumen during mixing and construction, the bitumens were subjected to penetration and softening point tests. In addition, the mass losses of the bitumens were also determined to understand the effects of the short-term aging. The Superpave specification for RTFOT aged bitumen implies that maximum mass loss after short-term aging process should not exceed 1% by weight of bitumen; for which TS EN 14023 standard is different depending on PG grade of tested bitumen [34]. For soft bitumens the maximum limit is 1%, and for harder bitumens it is 0.8% by weight of bitumen [27]. As is known, bitumen are exposed to heat and pressure to simulate the long-term aged bitumen in field during service; the pressure aging vessel (PAV) was used to simulate in-service aging over a 7 to 10-year period [32, 35].

3.5. Rheological Characterization

The viscous and elastic behavior of bitumen was determined by the dynamic shear rheometer (DSR) at medium to high temperatures. The complex shear modulus (G^*) and phase angle (δ) were measured by subjecting a small sample of bitumen to oscillatory shear stresses as sandwiched between two parallel plates in the DSR machine in stress controlled mode at a frequency of 10 rad/s. Non-aged and RTFOT samples were tested using 25 mm diameter plates and a gap of 1 mm. After RTFOT + PAV aging, samples are tested using 8 mm diameter plates and a 2 mm thickness sample. The rutting parameters ($G^*/sin\delta$) at high temperatures of the bitumen and the fatigue parameters ($G^*sin\delta$) at the intermediate temperatures are calculated for each sample. The $G^*/sin\delta$ of original bitumen should not exceed 1 kPa, and for RTFOT aged bitumen it should not exceed 2.2 kPa. Furthermore, the $G^*sin\delta$ of RTFOT+PAV aged bitumen should not exceed 5000 kPa [32, 36].

3.6. Bending Beam Rheometer (BBR) Test

The bending beam rheometer (BBR) test is used to determine the stiffness and consistency properties of bitumen at low temperatures. The obtained parameters are considered to be indicative of the ability of the bituminous binder to resist the low temperature cracking. The BBR test is also used to determine the performance grades (PG) of the bitumens at low temperatures. Properties of bitumen at low temperatures, the creep stiffness (s) and the creep rate (*m-value*), are measured using BBR. Superpave specification entails that the creep stiffness must not exceed 300 MPa, and creep rate should not be lower than 0.300 to avoid low temperature cracking [17, 22].

4. RESULTS AND DISCUSSIONS

The criterion applied in this research to evaluate Gilsonite effects on base bitumen was at first to determine the PG grade of the bitumens, and then to compare obtained conventional tests results and rheological properties with requirements of TS EN 14023 standard of polymer-modified bitumens (PMBs) at the specified PG grade of each bitumen. To evaluate the properties of the modified bitumen according to TS EN 14023 standard, the PG grade of this bitumen must be known in advance. For this reason, the conventional test results of modified bitumens including both before and after the short-term aging were intentionally given in Table 3.

Table 3 - Evaluation of modified bitumen according to TS EN 14023 standard for (PMBs)

Tests / Binder types	B (PG 64-16)	B+6G (PG70-16)	B+8G (PG76-16)	B+10G (PG82-16)
Penetration (25°C, 100gr, 5sec), 0.1mm	51 (50-70)	30* (45-80)	28 (25-55)	22* (25-55)
Softening point, °C	46.5 (46-54)	52* (≥60)	53* (≥65)	53* (≥70)
Elastic recovery (25°C), %	-	87 (≥60)	86 (≥60)	84.5 (≥60)
Flash point, °C	250 (≥230)	255 (≥220)	255 (≥220)	260 (≥220)
Specific gravity (25°C), gr/cm³	1.027 (1.0-1.1)	1.036 (1.0-1.1)	1.039 (1.0-1.1)	1.042 (1.0-1.1)
Storage stability:				
Difference in softening point, °C	-	1.5 (≤5)	0.5 (≤5)	1.5 (≤5)
Difference in penetration, 0.1mm	-	2 (≤13)	1 (≤9)	1 (≤9)
Dynamic shear rheometer (DSR) ($G^*/sin\delta > 1kPa$) Failure temperature, (°C)	68 (≥64)	74.7 (≥70)	77 (≥76)	82 (≥82)
Rolling thin oven test (RTFOT):				
Weight loss, %	0.295 (≤0.5)	0.036 (≤1)	0.031 (≤0.8)	0.029 (≤0.8)
Change in softening point:				
Increase, °C	5.5 (≤9)	7.5 (≤8)	7.5 (≤8)	7 (≤8)
Decrease, °C	-	- (≤5)	- (≤5)	- (≤2)
Retained penetration, %	53 (≥50)	80 (≥50)	78.6 (≥45)	77.4 (≥40)

Table 3 - Evaluation of modified bitumen according to TS EN 14023 standard for (PMBs)
(continue)

Tests / Binder types	B (PG 64-16)	B+6G (PG70-16)	B+8G (PG76-16)	B+10G (PG82-16)
Dynamic shear rheometer (DSR) RTFOT aged ($G*/sin\delta$ > 2.2kPa) Failure temperature, (°C)	68.5 (≥64)	75.5 (≥70)	78.7 (≥76)	>82 (≥82)
Dynamic shear rheometer (DSR) RTFOT+PAV aged ($G*sin\delta$ <5000kPa) Failure temperature, (°C)	25 (≤31)	23.4 (≤31)	25.2 (≤34)	27.1 (≤37)
Bending beam rheometer (BBR) Stiffness (s≤300MPa, m≥0.300) Failure temperature, (°C)	-20.5 (≤-16)	-19.9 (≤-16)	-19.3 (≤-16)	-18.3 (≤-16)

( ) Requirements of binders according to standard.

* Result does not achieve the required specification.

4.1. Conventional Bitumen Tests Results

The results of penetration and softening point tests conducted on bitumens were given in Table 3. As seen in Table 3, the penetration was continuously in the decreasing trend with increasing Gilsonite additive, and therefore, B+10G had the lowest penetration with a value of 22 dmm. The softening point of the bitumen increased with increasing Gilsonite addition, confirming the results of the penetration test. These results mean a significant increase in the stiffness of the bitumen after Gilsonite addition. However, this is accompanied by a decrease in elastic recovery since bitumen becomes harder after the modification. However, Gilsonite had only a slight adverse effect on elastic properties of bitumen as the elastic recovery percentage decline to 84.5 (for B+10G) from 88 (for B). As for flash point tests, values for all the base and Gilsonite modified bitumen samples were found above the recommended minimum value of 220 ºC.

As seen from Table 3, the tests performed on aged bitumens showed that the Gilsonite additive had a relatively positive effect on the aging potential of bitumens. The mass losses of modified bitumens were still very slight and its value was in the specified standard limits. The difference between softening point before and after aging within the specification for all bitumens. Additionally, after short-term aging, the retained penetrations of B, B+8G, and B+10G after RTFOT aging were (80, 78.6, and 77.4) % of the original bitumens, respectively. This showed that as the decrease in retained penetration was very slight while Gilsonite content is increased from 6 to 10 %. This also indicated that the increase in the modifier content had a positive effect on short term aging.

4.2. Storage Stability Test Results

A long period of storage for bitumen could lead to phase separation of the bitumen and poor stability problems. This situation is a major problem in the modified bitumen industry. The

results associated with storage stability was given in Table 4. Accordingly, both the softening point and the penetration results of the bottom and top parts of the Gilsonite-modified bitumen subject to the storage stability test are very close to each other. This result can be regarded as a good indicator of the homogeneity and consistency of Gilsonite modified bitumens.

Table 4 - Storage stability test results of Gilsonite modified bitumens

Property / Bitumen types	B+6G	B+8G	B+10G
Penetration bottom part, 0.1mm	24	22	17
Penetration top part, 0.1mm	26	23	18
Difference in penetration between bottom and top part, 0.1mm	2	1	1
Softening point bottom part, °C	50.5	54	56.5
Softening point top part, °C	52	53.5	0.5
Difference in softening point between bottom and top part, °C	1.5	55	1.5

4.3. Rotational Viscosity Test Results

The rotational viscosity (RV) of the bitumen was determined at 135 and 165 °C, and the results were summarized in Table 5. The mixing and compacting temperatures and the modification indexes ($\eta_{modified} / \eta_{base}$) of all bitumens to be used in HMA were also given in Table 5. Addition of Gilsonite to base bitumen increased the viscosity at 135 °C and 165 °C. This indicates that Gilsonite modification improved the stiffness of bitumen. For instance, at the heavy modification level of 10%, the viscosity increased from 443 cP to 1122.5 cP. On the other hand, both mixing and compacting temperatures increased as the content of Gilsonite was increased.

Table 5 - Rotational viscosity test results of the base and Gilsonite modified bitumens

Binder types	Rotational viscosity (cP)		$\eta_{modified} / \eta_{base}$		Temperature range (°C)	
	135°C	165°C	135°C	165°C	Mixing	Compaction
B	443	128	1.0	1.0	157-163	145-150
B+6G	715	170	1.61	1.33	162-167	152-157
B+8G	873	208	1.97	1.63	166-171	156-161
B+10G	1122.5	255	2.53	1.99	172-177	162-167

The mixing and compacting temperatures of the bitumen were detected by means of Figure 1. The mixing and compacting temperature ranges increased from (157–163) °C and (145–150) °C for B, to (172–177) °C and (162–167) °C for B+10G, respectively. Although

the workability of modified bitumen decreased, the value of RV was less than 3000 cP and therefore still satisfied the ASTM D6373 standard criterion for bitumen workability [32, 38].
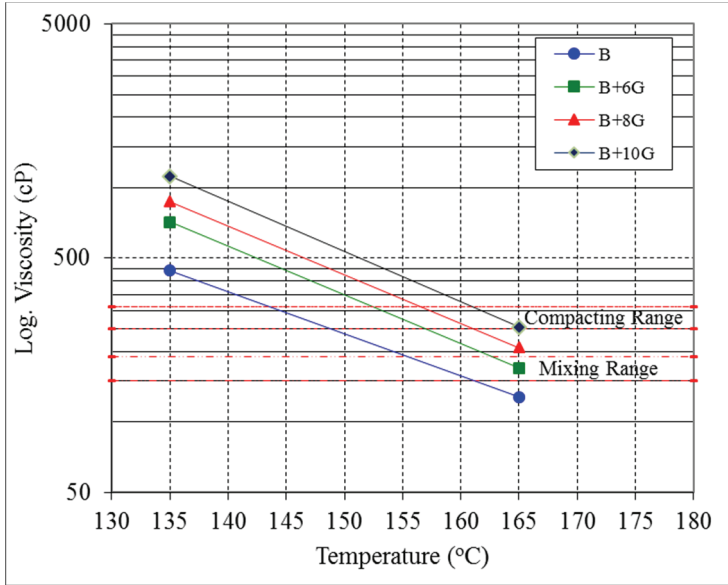
Figure 1 - Viscosity-temperature relationship for the base and Gilsonite modified bitumens

4.4. Rheological Characterization- Dynamic Shear Rheometer (DSR) Test Results

To determine the PG grade of each bitumen type and to study the effect of Gilsonite modification on rheological properties of bitumen, the DSR test was conducted. Viscoelastic parameters of all bitumens, such as complex modulus (G^*) and phase angle (δ) were obtained, and the effect of Gilsonite on G^* and δ for original and RTFOT-aged bitumens was shown in Figures 2 and 3, respectively. The rutting parameter ($G^*/sin\delta$) was calculated for each sample of base and modified bitumens and shown graphically in Figure 4.

As seen from Figure 2, the G^* parameter for original base bitumen (B) for example at 64 °C was 1.64 kPa and increased to 8.56 kPa for B+10G at the same temperature. Adding 10% of Gilsonite leads to an increase of bitumen's stiffness by 421%. It can be said that Gilsonite modification improved the stiffness of bitumen and rheological behavior especially under high temperatures.

As shown in Figure 3, the values of δ were decreased as Gilsonite content increased in original and aged bitumens. For example, δ at 64 °C for B was 87.2 and for B+10G was 78.7 of original case. This indicated that Gilsonite exhibited an improvement of elastic component of bitumen.

The bitumen used in the mixture provides its fair share of the overall resistance in the pavement in terms of permanent deformations by controlling stiffness of the mixture at high temperatures. The rutting parameters ($G^*/sin\delta$) of base and modified bitumens were found for original and RTFOT aged bitumen at high levels of temperature starting at 52 °C. While

$G*/sin\delta$ value increased, the bitumen was expected to be stiffer and as a result more rut resistant mixtures could be achieved.
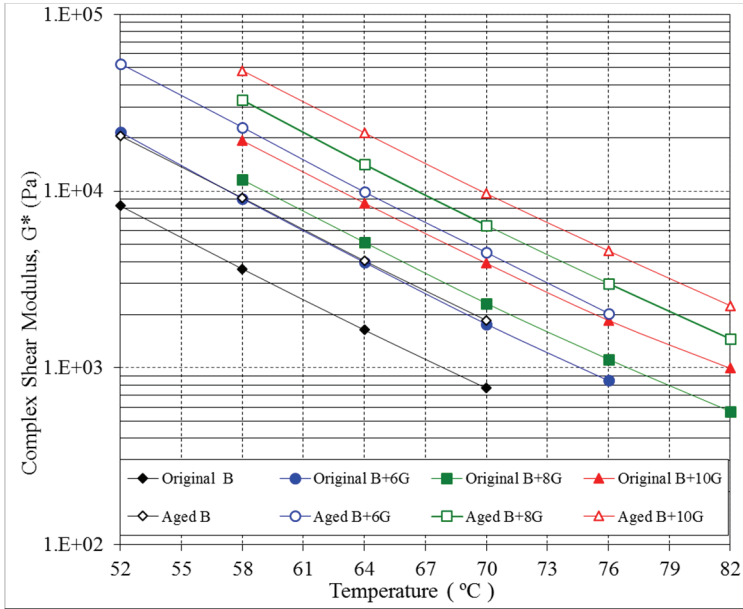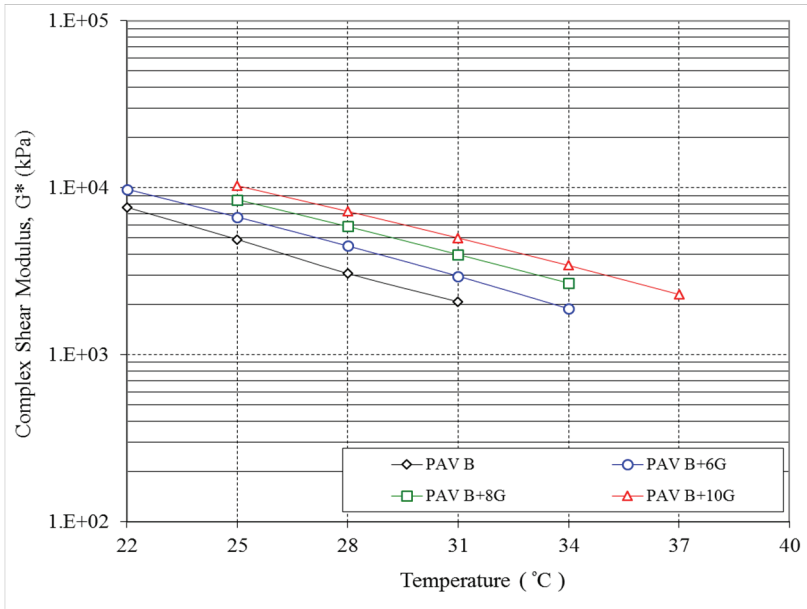

Figure 2 - Effect of Gilsonite on complex shear modulus (G) for original and RTFOT aged bitumens*
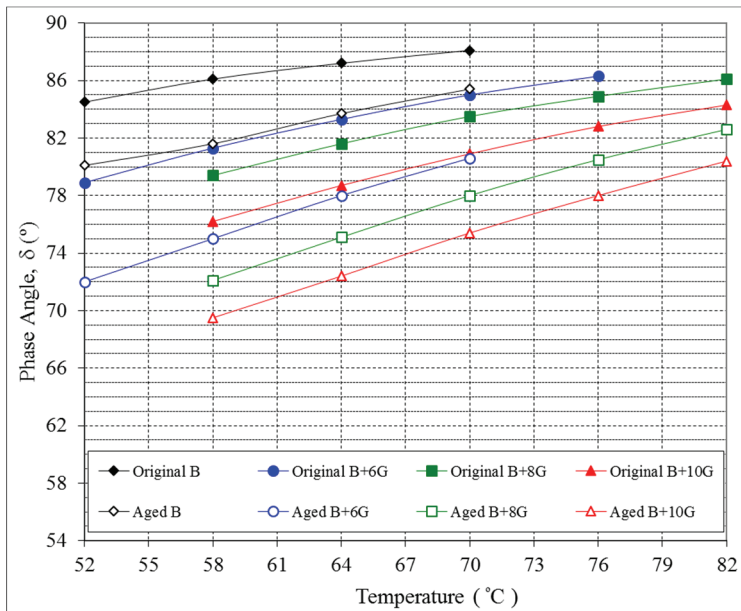
Figure 3 - Effect of Gilsonite on phase angle (δ) for original and RTFOT aged bitumens
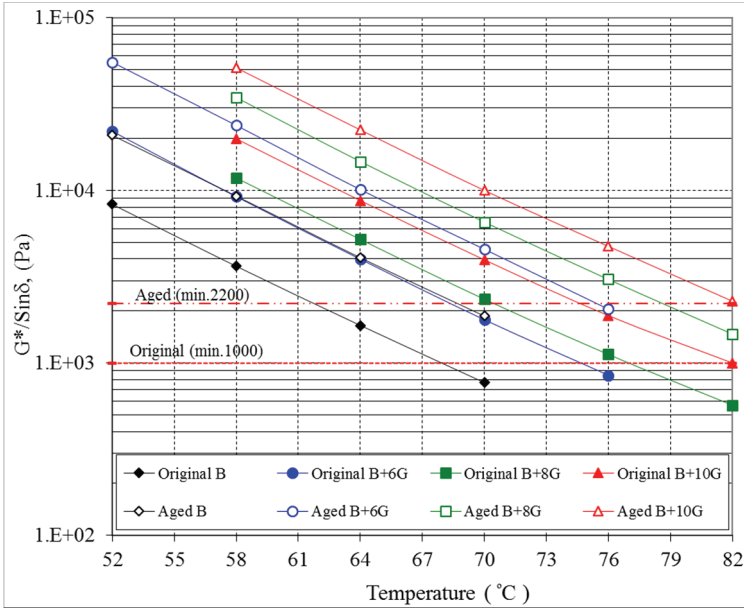
Figure 4 - Rutting performance of Gilsonite modified bitumens

Figure 4 showed the *G*/sinδ* of original and RTFOT aged samples. B+10G has the highest G*/sinδ value of 8.73 kPa compared to the rest of samples. This showed that the stiffness of bitumen increased as Gilsonite content increased. This result was compatible with conventional test data.

G*/sinδ of aged sample was higher than that of the original sample of the same bitumen type. For example, at 64 °C the *G*/sinδ* for original B was 1.65 kPa and for aged B was 4.07 kPa. At the same temperature, for original B+10G the *G*/sinδ* was also 8.73 kPa and for aged B+10G was 22.4 kPa.

G*/sinδ of the base and modified bitumens (seen in Figure 4) indicate that aged B+8G provides the maximum increase in stiffness between the samples which is around 182.7% compared to base bitumen, whereas the aged B, B+6G, and B+10G exhibited the increases of 146.7, 153.1, and 156.6% respectively. As expected, the increment in temperature leads to a decrease in *G** and an increase in *δ*. Moreover, the B+10G shows much more resistance against permanent deformation rather than B. As can be seen in Figure 4, B+10G achieved the specifications of rutting parameter in terms of both aged and unaged conditions up to 82°C, while B reaches only up to 64°C considering Superpave specifications.

To study the fatigue performance of Gilsonite-modified bitumen, complex shear modulus (*G**) and phase angle (*δ*) for PAV-aged bitumen at different temperatures and different Gilsonite contents were shown in Figure 5 and 6, respectively. The fatigue parameters (*G*sinδ*) for all bitumen types were calculated, and fatigue performance of Gilsonite modification was shown in Figure 7. The effects of the Gilsonite additive on the rheological properties of bitumen are summarized in Table 3.

Figure 5 - Effect of Gilsonite on complex shear modulus (G*) for PAV aged bitumens
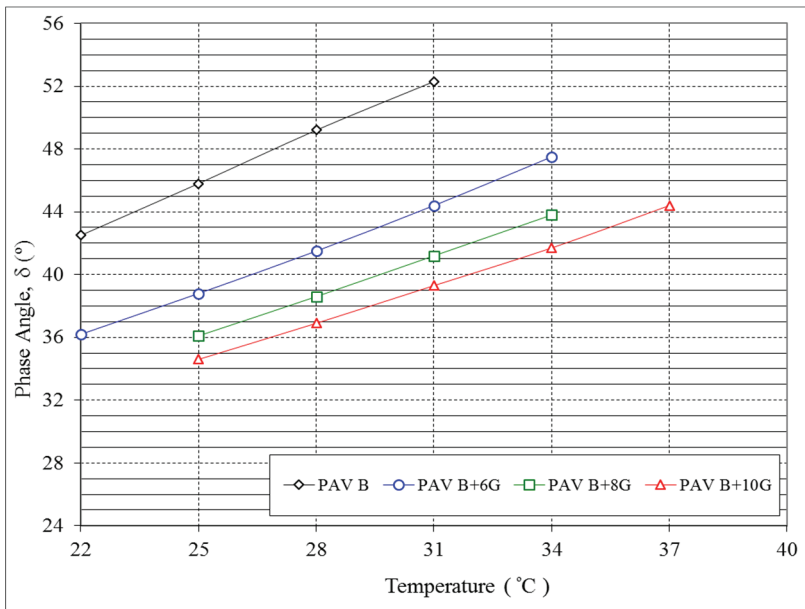
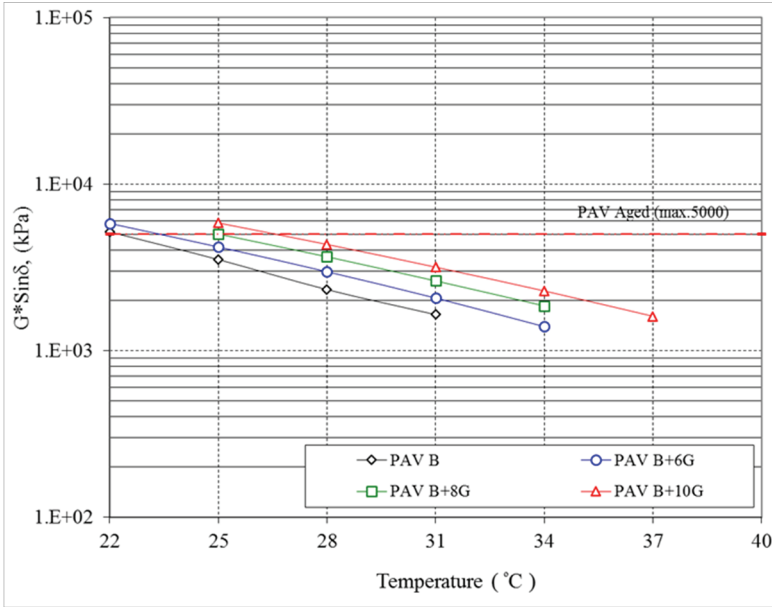*Figure 6 - Effect of Gilsonite on phase angle (δ) for PAV aged bitumens*

Figure 7 - Fatigue performance of Gilsonite modified bitumens

The fatigue parameters ($G*sin\delta$) of modified bitumens increased with increasing Gilsonite content compared to the base bitumen due to the increase of $G*$ and decrease in δ. It should be noted that fatigue parameter was determined at intermediate test temperature by adding the high-grade temperature to the low-grade temperature dividing the result by 2 and adding 4. Hence, the comparison between the base bitumen B and B+10G should be related to the PG grade of each bitumen since stiffness differs from one bitumen to another. The PG grade of B was PG 64-16, therefore, the intermediate test temperature of RTFOT+PAV aged bitumen used in DSR test was calculated as 28 °C (by using abovementioned formula which is correspond to (64-16)/2+4=28 in this case). Similarly, from Table 5 for B+10G which is PG 82-16 graded bitumen, the intermediate test temperature was found as 37 °C by using the same formula.

As can be seen in Figure 7, $G*sin\delta$ of B was found as 2327 kPa at 28 °C, 2070 kPa at 31 °C for B+6G, 1858 kPa at 34 °C for B+8G, and 1610 kPa for B+10G at 37 °C, which indicated that Gilsonite modified bitumen achieved the standard requirement of fatigue parameter ($G*sin\delta$<5000 kPa). On the other hand, by comparing the intermediate temperature (28 °C) of RTFOT+PAV aged bitumens to base bitumen (Fig. 6), there was an improvement in δ as it goes down from 49.2 °C to 36.9 °C which corresponds to 25% decrement in phase angle after the modification. This is also applicable for other test temperatures. The decrease in δ value while $G*$ value being increased by adding Gilsonite, caused the elastic behavior of Gilsonite-modified bitumens to prevail at the new achieved intermediate performance temperatures.

4.5. Bending Beam Rheometer (BBR) Test Results

Creep tests were performed at two different temperatures (-16 ºC and -22 ºC) to determine the performances of the bitumens at low temperatures. In Figures 8 and 9, the creep stiffness of all bitumens satisfied with the Superpave specification at -16 ºC, and all bitumens showed higher m-values than the required minimum at this temperature. The creep stiffness of B+10G was higher than that of B while its creep rate as *m-value* was lower. Furthermore, the stiffness of samples increased with decreasing temperature while *m-value* decreased. In addition to this, the creep stiffness and *m-values* of bitumens were failed to meet the Superpave specification at -22 ºC which means the low temperature PG grade of all bitumens was determined as PG X-16.

Ten percent addition of natural Gilsonite by weight of bitumen was enough for the beneficial use as it reaches to the highest (high temperature) performance grade of PG 82-16. Hence it is believed that the optimum usage of Gilsonite content is 10%, since the *m-value* of B+10G at -16 ºC was 0.324 which was very close to 0.300. On the other hand, the Gilsonite modification did not contribute an enhancement to the low temperature PG grade. For example, *m-value* for B+6G was 0.271, and for B+10G it was 0.260. This indicated that with adding Gilsonite, the creep rate decreased, and the bitumen was more brittle and stiffer. At the same time, the PG grade of base and Gilsonite modified bitumen were given in Table 3.
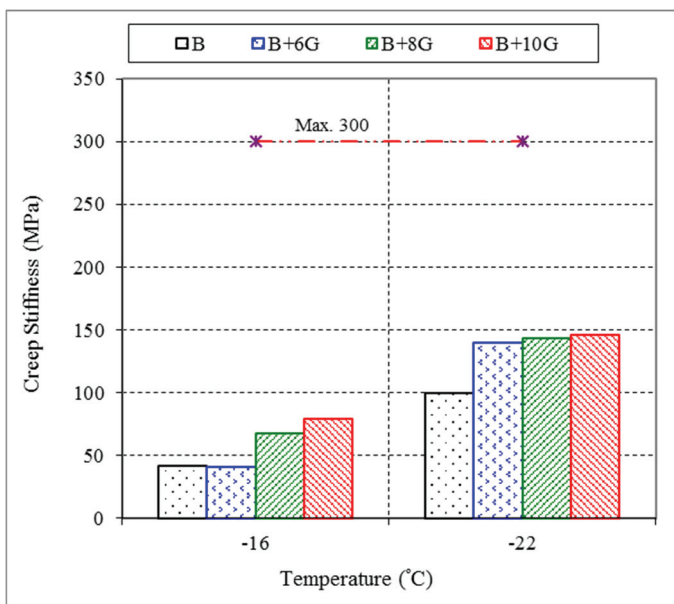
Figure 8 - Creep stiffness of the base and Gilsonite modified bitumens

Block cracking is a low temperature failure in flexible pavement similar to thermal cracking which develops in both longitudinal and transverse directions. Block cracking generally occurs when flexible pavement is old (aged) and traffic volume is low. A parameter named critical temperature (ΔT_c) is relatively up to date for the evaluation of low temperature

performance of binders against block cracking [39]. ΔT_c is obtained by means of the low continuous grade temperature for the stiffness criteria minus low continuous grade temperature for the m-value criteria (which are 10 °C lower than failure points determined in BBR test) and suggested to examine the ductility loss of aged bitumens leading to block cracking.

ΔT_c of the binders was calculated as -9.9 °C, -9.5 °C, -9.7 °C, -9.9 °C for the base, %6, %8, and %10 Gilsonite modified binders, respectively. Lower ΔT_c means that binder is vulnerable to cracking at low temperature region. Generally, it is suggested that ΔT_c should not be lower than -5 °C which means that ΔT_c of base and Gilsonite modified binders are not within the acceptable level. However, it should be noted that base and Gilsonite modified binders have very similar ΔT_c which signifies that Gilsonite has no positive or negative effect on the loss of ductility of binder.
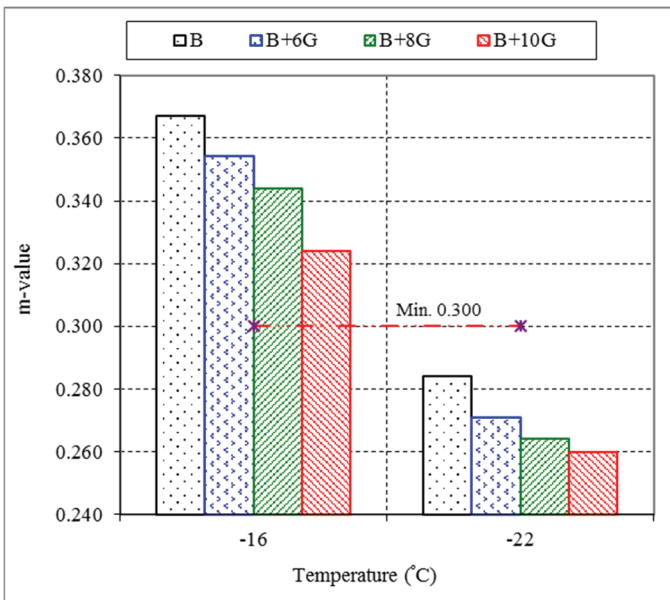
Figure 9 - The m-value of the base and Gilsonite modified bitumens

4.6. PG Grade and PMBs Requirements

The enhancement after Gilsonite modification was determined and mentioned in Section 4 as the base (B) is a PG64-16 graded bitumen (in Figs. 2-7) while grade of modified bitumens (B+6G, B+8G, and B+10G) are PG 70-16, PG 76-16, and PG 82-16, respectively.

Although the modified bitumens did not meet some of the specifications in TS EN 14023 standard, it is believed that the PG grade is a better indicator for bitumen performance, in which rheological parameters are taken into consideration, compared to penetration and softening point tests, in which only basic techniques are applied. Besides, the difference in softening point and penetration after storage stability tests indicated that all modified

bitumens with respect to their relative PG grades meet the requirements of storage stability in accordance with TS EN 14023 standard. This means that Gilsonite modification achieves the homogeneity and has no phase separation problems.

5. CONCLUSIONS

In this study, the effects of natural Gilsonite on the performance properties of bitumen were investigated, and the following conclusions were obtained.

1. The conventional test results showed that the addition of natural Gilsonite remarkably increased the viscosity and stiffness of the base bitumen. The RV results also confirm that Gilsonite had a stiffening effect on the bitumen. In spite of relatively high mixing and compacting temperature ranges of modified bitumens, it was assumed that using Gilsonite could be a suitable modifier taking into consideration the high cost of base bitumen and insufficient resources of this material.

2. The results obtained from elastic recovery showed a slight decrease in elastic recovery after the modification, yet it was considered acceptable.

3. The storage stability test showed that Gilsonite was fully compatible and highly stable with bitumen and had no phase separation in the bitumen during long time of storage process.

4. The natural Gilsonite has a considerable effect on G^* and δ of bitumen. Gilsonite modified bitumen had higher rutting parameter ($G^*/sin\delta$) than that of the base bitumen both before and after aging processes. In addition, Gilsonite modification had positive effect on fatigue resistance of bitumen. Moreover, the Gilsonite modification at three different levels of Gilsonite content (i.e, 6, 8, and 10%) provided high performance grade of bitumens of PG 70-Y, PG 76-Y, and PG 82-Y, respectively.

5. BBR test results showed that Gilsonite additive had no positive effect on low-temperature cracking resistance of bitumen and caused the creep rate decrease. The low performance grade at three levels of Gilsonite modification of 6, 8, and 10 % were found as PG X-16, PG X-16, and PG X-16, respectively. This was attributed to the stiffening effect of Gilsonite additive which is also compatible with elastic recovery results.

According to the findings, Gilsonite has positive effects on the physical properties of bitumen such as stiffening meaning that the pavements become more resistant to permanent deformation after the modification. Although the Gilsonite contributes no enhancement against low-temperature cracking, it provides a positive effect on high temperatures. The use of 10 % of Gilsonite improves the performance grade of base bitumen from PG 64-16 up to PG 82-16 which corresponds to an enhancement of three levels. For this reason, it is advised to use Gilsonite at high temperature regions and/or very heavy loaded flexible pavement projects up to 10%. It should also be noted that light modification of Gilsonite is recommended in cold regions since the modifier increases the stiffness of bitumen.

Symbols

DSR	: *Dynamic shear rheometer*
G*	: *Complex shear modulus*
m-value	: *Creep rate*
PAV	: *Pressure aging vessel*
PG	: *Performance grade*
PMB	: *Polymer modified bitumen*
RTFOT	: *Thin film oven test*
RV	: *Rotational viscometer*
s	: *Creep stiffness*
δ	: *Phase angle*
η_{base}	: *Viscosity of base bitumen*
$\eta_{modified}$	: *Viscosity of modified bitumen*

References

[1] Garcia, A., Schlangen, E., Ven, M., Sierra-Beltrana, G., Preparation of capsules containing rejuvenators for their use in asphalt concrete, Journal of Hazardous Materials, 11, 184-603, 2010.

[2] Lu, X.H., Isacsson, U., Chemical and rheological evaluation of ageing properties of SBS polymer modified bitumens, Fuel, 77:9, 961-972, 1998.

[3] Qadir, A., Rutting performance of polypropylene modified asphalt concrete, International Journal of Civil Engineering, 12:3, 304-312, 2014.

[4] Lu, X.H., Isacsson, U., Compatibility and storage stability of styrene-butadiene-styrene copolmer modified bitumens, Materials and Structures, 30:10, 618-626, 1997.

[5] Ma, T., Wang, H., Zhao, Y., Huang, X., Wang, S., Laboratory investigation of crumb rubber modified asphalt binder and mixtures with warm-mix additives, International Journal of Civil Engineering, doi:10.1007/s40999-016-0040-3, 2016.

[6] Sureshkumar, M.S., Filippi, S., Polacco, G., Kazatchkov, I., Stastna, J., Zanzotto, L., Internal structure and linear viscoelastic properties of EVA/asphalt nanocomposites, European Polymer Journal, 46, 621-633, 2010.

[7] Gad, Y.H., Magida, M.M., El-Nahas, H.H., Effect of ionizing irradiation on the thermal blend of waste low density polyethylene/ethylene vinyl acetate/bitumen for some industrial applications, Journal of Industrial and Engineering Chemistry, 16:6, 1019-1024, 2010.

[8] Ahmedzade, P., Fainleib, A., Gunay, T., Grygoryeva, O., Modification of bitumen by electron beam irradiated recycled low density polyethylene, Construction and Building Materials, 69, 1-9, 2014.

[9] Fu, H., Xie, L., Dou, D., Li, L., Yu, M., Yao, S., Storage stability and compatibility of asphalt binder modified SBS graft copolymer, Construction and Building Materials, 21, 1528-1533, 2007.

[10] Yilmaz, M., Yamaç, Ö.E., Evaluation of Gilsonite and styrene-butadiene-styrene composite usage in bitumen modification on the mechanical properties of hot mix asphalts, J. Mater. Civ. Eng., 29:9, 04017089, 2017.

[11] Kök, B.V., Yilmaz, M., Guler, M., Evaluation of high temperature performance of SBS + Gilsonite modified binder, Fuel, 90, 3093–3099, 2011.

[12] Bahia, H.U., Hanson, D.I., Zeng, M., Zhai, H., Khatri, M.A., Anderson, R.M., Characterization of modified asphalt binders in Superpave mix design (Project No. 9-10 FY'96), NCHRP, Washington, 2001.

[13] Nasrekani, A.A., Naderi, K., Nakhaei, M., Mahmoodinia, N., High-temperature performance of Gilsonite modified asphalt binder and asphalt concrete, Petroleum Science and Technology, 34:21, 1783-1789, 2016.

[14] Babagoli, R., Hasaninia, M., Namazi, N.M., Laboratory evaluation of the effect of Gilsonite on the performance of stone matrix asphalt mixtures, Road Materials and Pavement Design, 16:4, 889-906, 2015.

[15] Jahanian, H.R., Shafabakhsh, G., Divandari, H., Performance evaluation of Hot Mix Asphalt (HMA) containing bitumen modified with Gilsonite, Construction and Building Materials, 131, 156–164, 2017.

[16] Brown, S.F., Rowlett, R.D., Boucher, J.L., Asphalt modification, Proceedings of the conference, The United States strategic highway research program, London: Institute of Civil Engineers, London, 181–203, 1990.

[17] Ameri, M., Mansourian, A., Ashani, S.S., Yadollahi, G., Technical study on the Iranian Gilsonite as an additive for modification of asphalt binders used in pavement construction, Constr. Build. Mater., 25:3, 1379-1387, 2011.

[18] Nasrekani, A.A., Nakhaei, M., Naderi, K., Fini, E., Aflaki, S., Improving moisture sensitivity of asphalt concrete using natural bitumen (Gilsonite), Transportation Research Board 96th Annual Meeting, Washington DC, United States, http://amonline.trb.org/, 2017.

[19] Anderson, D.A., Maurer, D., Ramirez, T., Christensen, D.W., Marasteanu, M.O., Mehta, Y., Field performance of modified asphalt binders evaluated with superpave test methods: 1–80 test project, Transportation Research Record 1661, 60–68, 1999.

[20] Aflaki, S., Tabatabaee, N., Proposals for modification of Iranian bitumen to meet the climatic requirements of Iran, Construction and Building Materials, 23, 2141–2150, 2009.

[21] Tang, N., Huang, W., Zheng, M., Hu, J., Investigation of Gilsonite-, polyphosphoric acid- and styrene–butadiene–styrene-modified asphalt binder using the multiple stress creep and recovery test, Road Materials and Pavement Design, 18:5, 1084–1097, 2017.

[22] Widyatmoko, I., Elliott, R., Characteristics of elastomeric and plastomeric binders in contact with natural asphalts, Constr. Build. Mater., 22, 239–249, 2008.

[23] Quintana, H.A.R., Noguera, J.A.H., Bonells, C.F.U., Behavior of Gilsonite-modified hot mix asphalt by wet and dry processes, J. Mater. Civ. Eng., 28:2, 04015114, 2016.

[24] Zhi, S., Gun, W.W., Hui, L.X., Bo, T., Evaluation of fatigue crack behavior in asphalt concrete pavements with different polymer modifiers, Construction and Building Materials, 27, 117-125, 2012.

[25] Huang, B., Li, G., Shu, X., Investigation into three-layered HMA mixtures, Composites, 37, 679–690, 2006.

[26] Słowik, M., Bilski, M., An experimental study of the impact of aging on Gilsonite and trinidad epuré modified asphalt binders properties, Baltic Journal of Road & Bridge Engineering, 12:2, 71-81, 2017.

[27] TS EN 14023, Bitumen and bituminous binders - Framework specification for polymer modified bitumens, Turkish and European standard, 2006.

[28] EN 13399, Bitumen and Bituminous Binders - Determination of Storage Stability of Modified Bitumen, European standard, 2010.

[29] Anderson, D., Christensen, D.W., Bahia, H.U., Dongre, R., Sharma, M.G., Antle, C.E., Button, J., Strategic highway research program binder characterization: Physical properties. SHRP-A-369, Vol. 3, National Research Council, Washington, DC, 1994.

[30] Bahia, H.U., Anderson, D.A., Strategic highway research program binder rheological parameters: background and comparison with conventional properties, Transportation Research Record, TRB, National Research Council, 32-39, Washington, DC, 1995.

[31] AASHTO: AASHTO T 316- Viscosity determination of asphalt binder using rotational viscometer, Washington D.C., 2004.

[32] The Asphalt Institute, Superpave mix design: Superpave series no. 2, (SP-2), 2001.

[33] EN 12607-1, Bitumen and bituminous binders: Determination of the resistance to hardening under the influence of heat and air - Part 1: RTFOT method, European standard, 2003.

[34] AASHTO: AASHTO T 240- Effect of heat and air on a moving film of asphalt (Rolling Thin-Film Oven Test) standard test methods, Washington D.C., 2013.

[35] AASHTO: AASHTO R 28- Accelerated aging of asphalt binder using a pressurized aging vessel (PAV) standard test methods, Washington D.C., 2012.

[36] AASHTO: AASHTO T 315- Determining the rheological properties of asphalt binder using a dynamic shear rheometer (DSR) standard test methods, Washington D.C., 2012.

[37] AASHTO: AASHTO T 313- Determining the flexural creep stiffness of asphalt binder using the bending beam rheometer (BBR) standard test methods, Washington D.C., 2012.

[38] ASTM: ASTM D6373- Standard specification for performance graded asphalt binder, West Conshohocken, PA, 1999.

[39] Anderson, R. M., King, G. N., Hanson, D. I., Blankenship, P. B., Evaluation of the relationship between asphalt binder properties and non-load related cracking. Journal of the Association of Asphalt Paving Technologists, 80, 2011.

FE Analysis of FGM Plates on Arbitrarily Orthotropic Pasternak Foundations for Membrane Effects

Ülkü Hülya ÇALIK-KARAKÖSE[1]

ABSTRACT

In this study, the finite element analysis of sigmoid functionally graded material (S-FGM) plates resting on orthotropic Pasternak elastic foundations with different material angles is presented. For modelling, SAP2000 software package is used in which the required adjustments are made to obtain the expected behaviour of the plate-foundation system. The plate is modelled using both solid elements and layered shell elements by defining a number of solid elements and layers in the thickness direction having elastic properties equivalent to the properties of the S-FGM plate. The interaction between the plate and the foundation is provided by equalizing the vertical displacements of the plate and foundation nodal points. The orthotropic Pasternak foundation is modelled using plane strain elements with some adjustments to the elastic properties. The membrane effects of the simply supported S-FGM plate on Pasternak foundation are considered by defining the edge boundaries of the system as pinned supports. These effects are excluded by converting all boundary nodes into roller supports except for one of the corner nodes of the plate and the foundation due to the stability requirement. A number of verification examples are performed to demonstrate the convenience and robustness of the proposed model. This work can be easily extended to static and dynamic analyses of FGM plates with various geometries resting on arbitrarily orthotropic Pasternak elastic foundations for further studies.

Keywords: Functionally graded material plates, membrane effects, orthotropic Pasternak foundation, material angle.

1. INTRODUCTION

Functionally graded materials (FGMs) are heterogeneous materials in which the material properties are varied continuously in the thickness direction as presented by Suresh and Mortenson [1], and are used to improve the strength and stiffness of structural elements in many engineering applications. In laminated composites which are used to satisfy the desired high-performance demands, stress singularities may occur at the interface of two

different materials which may cause de-bonding or cracking. This problem is eliminated by the gradual change of the material properties of the functionally graded materials. Studies on FGMs were first made for thermal barriers by Koizumi [2] and thermal mechanical behaviour of FGMs was investigated in [3,4].

Reddy [5] presented theoretical formulation and finite element models of functionally graded rectangular plates based on the third-order shear deformation theory. Cheng and Batra [6] derived field equations for a functionally graded plate using both first-order and third-order shear deformation theories.

Three different homogenization methods are used to describe the variation of material properties; namely power law [7,8], exponential [9,10] and sigmoid functions. Since the material properties vary continuously but rapidly and stress concentrations appear in one of the interfaces in both the power-law and exponential functions, Chung and Chi [11] defined a new volume fraction proposing an S-FGM, which was composed of two power-law functions. It is demonstrated that the stress intensity factors of a cracked body are significantly reduced by Chi and Chung [12] through the use of an S-FGM,. Chi and Chung [13] derived theoretical formulations of a simply supported rectangular FGM plate of medium thickness subjected to transverse loading and numerical solutions were obtained by using the formulations derived by Chi and Chung [13], and also checked by the finite element method in Chi and Chung [14]. The coupling effect of extension and bending in functionally graded plates under transverse loading was investigated by Orakdöğen et.al.[15] using the finite element method. Zenkour [16] introduced the bending analysis of a simply supported functionally graded rectangular plate subjected to a transverse uniform load. Elishakoff et.al.[17] presented the static response of a three-dimensional functionally graded material rectangular plate with clamped boundary conditions and a power-law distribution of the mechanical properties is adopted in the modelling. Swaminathan et.al.[18] presented an extensive review of the various methods used in studying the static, dynamic and stability behaviours of FGM plates where analytical and numerical methods are both considered.

Plates resting on elastic foundations have been widely studied by many researchers to be used in modelling various engineering applications. The simplest elastic foundation model is the Winkler or one-parameter model by Winkler [19] in which the interaction between the plate and the foundation is represented by a series of independent vertical linear elastic springs. A more realistic representation of the elastic medium is made with two-parameter or Pasternak model by Pasternak [20] which has a second dependent parameter that introduces the shear interaction between springs avoiding the deflection discontinuity on the interacted surface of the plate.

There exist many studies performing the static analysis of isotropic rectangular plates resting on isotropic Pasternak foundations [21,22] and vibration analysis of this type of plate-foundation system [23-26]. Shen [27] carried out the post-buckling analysis of a simply supported, composite laminated rectangular plate resting on an isotropic two-parameter elastic foundation where the plate is subjected to in-plane loading. Huang et.al. [28] presented exact solutions for functionally graded thick plates based on the three-dimensional theory of elasticity and examined interactions between the Winkler-Pasternak elastic foundation and the plate demonstrating that elastic foundations have significant effect on the mechanical behaviour of functionally graded thick plates. Lee et.al. [29]

developed a refined higher order shear and normal deformation theory for the bending analysis of power law, exponential and S-FGM plates resting on isotropic Pasternak foundations. Vibration analysis of isotropic FGM plates on isotropic two-parameter foundations is also performed by many researchers, [30-33]. Mansouri and Shariyat [34] performed the analysis of orthotropic FGM plates on elastic foundations in their paper. In [35,36], seismic behaviour of a 3D structural system resting on a two-parameter elastic foundation was analysed using SAP2000. In the modelling of the foundation, the part of the governing equation that belongs to Winkler behaviour is represented by elastic springs and the part that belongs to elastic shear layer is taken into account by using four-noded quadrilateral finite elements with four degrees of freedom.

There are also studies in the literature on the analysis of homogeneous plates and FGM plates resting on orthotropic Pasternak foundations [37-42]. In this paper, the finite element analysis of S-FGM plates resting on orthotropic Pasternak elastic foundations with different material angles is presented and coupling effect of extension and bending is investigated. SAP2000 software package, [43] is used in the implementation process and some adjustments are made to the software for the expected behaviour of the plate-foundation system. S-FGM plate is first modelled using layered shell elements by defining a number of layers in the thickness direction having elastic properties equivalent to the properties of the S-FGM plate. The plate is also modelled using solid elements. The membrane force-bending moment coupling effect of the simply supported S-FGM plate is considered by assigning the edge boundary nodes as pinned supports.

The interaction between the plate and the foundation is provided by equalizing the plate and corresponding foundation nodal point vertical displacements. Orthotropic Pasternak foundation is modelled using plane strain elements with some adjustments to the elastic properties. After verifying the proposed model with a number of examples taken from the literature, the influence of the material properties, membrane effects, number of layers used for FGM plate and material angles of the orthotropic Pasternak foundation on deflections and stresses are examined with numerical examples.

2. MATERIAL PROPERTIES OF S-FGM PLATES

In Figure 1, an S-FGM plate example is shown where z axis is in the thickness direction and originated at the middle surface of the plate. The material properties vary continuously and functionally based on the volume fraction of the sigmoid distribution.
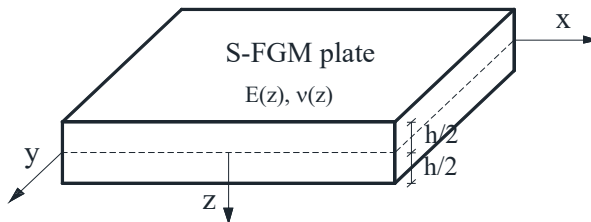

Figure 1 - An S-FGM plate example

The volume fraction for S-FGM is defined using two power-law functions to ensure smooth distribution of stresses among all interfaces of the plate, Chung and Chi [11]. The two power-law functions are defined by

$$V_1(z) = 1 - \frac{1}{2}\left(\frac{\frac{h}{2}-z}{\frac{h}{2}}\right)^p \qquad \text{for} \qquad 0 \leq z \leq \frac{h}{2} \tag{1}$$

$$V_2(z) = \frac{1}{2}\left(\frac{\frac{h}{2}+z}{\frac{h}{2}}\right)^p \qquad \text{for} \qquad -\frac{h}{2} \leq z \leq 0 \tag{2}$$

where p is the material exponent. The elastic modulus of the S-FGM can be calculated using

$$E(z) = V_1(z)(E_1 - E_2) + E_2 \qquad \text{for} \qquad 0 \leq z \leq \frac{h}{2} \tag{3}$$

$$E(z) = V_2(z)(E_1 - E_2) + E_2 \qquad \text{for} \qquad -\frac{h}{2} \leq z \leq 0 \tag{4}$$

Here, E_1 and E_2 are the elastic moduli of the bottom and top surfaces of the plate, respectively. The Poisson's ratio is assumed to be constant since it is stated by Delale and Erdogan [9] that its effect on deformation is much less than that of the elastic modulus.

3. FINITE ELEMENT MODELLING

3.1. S-FGM Plate Model

The S-FGM plate is first modelled using shell finite elements for which the section type is defined as "Shell-Layered/Nonlinear" in SAP2000, consisting of a number of layers in the thickness direction. Each layer has a constant elastic modulus value which is pre-calculated using the functions given in Eqs. [1]-[4] representing the continuous variation of the elastic modulus of the plate starting from the bottom surface. The distance parameter "z" in the functions indicates the ordinate of the middle section of each layer. In Figure 2, a segment of an S-FGM plate and its equivalent representation with 8 layers is shown.

The shell element in the software is a four-noded finite element and its formulation combines membrane and plate-bending behaviours. The element always activates all six degrees of freedom which are 3 translations and 3 rotations at each of its connected joints. When the element is used as a pure plate, it must be ensured that restraints or other supports are provided to the degrees of freedom for in-plane translations and the rotation about the normal.

The layered shell allows any number of layers to be defined in the thickness direction, each with an independent location, thickness, behaviour, and material. For bending, a Mindlin formulation is used which always includes transverse shear deformations. Membrane and plate behaviours will be coupled if the layering is not symmetrical in the thickness direction and the edge boundaries are assigned as pinned supports.

The S-FGM plate is also modelled using solid elements where the elastic modulus of each solid element in the thickness direction is equal to the elastic modulus of the corresponding layer of the shell element.

The solid element used is an eight-noded finite element with three translational degrees of freedom at each joint. Rotational degrees of freedom are not activated. This element contributes stiffness to all of these translational degrees of freedom.

The membrane effects appear in the simply supported S-FGM plate when the edge boundary nodes of the plate are assumed to be pinned supports (no horizontal displacement) whereas these effects are excluded by converting all boundary nodes into roller supports except at one of the corner nodes due to the stability requirement.
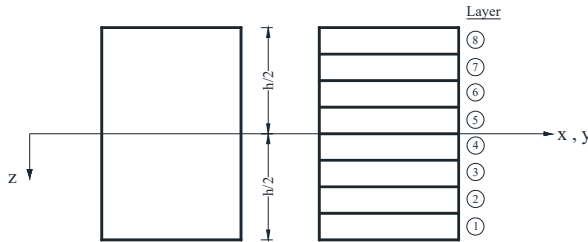
Figure 2 - A segment of an S-FGM plate and equivalent representation with 8 layers

3.2. Isotropic and Orthotropic Pasternak Foundation Models

Isotropic and orthotropic Pasternak foundations are also modelled using SAP2000. The material symmetry type of the isotropic soil element is selected as "orthotropic" so as to change the shear modulus values. All material properties are assigned to zero except the shear moduli G_{13} and G_{23} that represent the second parameter of the Pasternak foundation.

The finite element to be used in modelling the Pasternak foundation is defined as "shell" element, the section type is selected as "Plane-Strain" and the thickness is assigned a unit value, [44,45].

The plane strain element is one type of area objects and is used to model plane-strain behaviour in two-dimensional solids. It activates the three translational degrees of freedom at each of its joints. Rotational degrees of freedom are not activated. The plane-strain element models shear that is normal to the plane of the element, in addition to the in-plane behaviour. Thus, stiffness is created for all three translational degrees of freedom.

In the case of plane strain, when the elastic moduli and Poisson's ratios in three directions are defined as zero and the in-plane shear moduli in the two directions (G_{13} and G_{23}) are assigned to non-zero values, only shear stresses in the thickness direction of the element and end forces in the vertical direction appear. When the in-plane shear moduli are assigned to the shear moduli of the two-parameter foundation, the resulting element stiffness matrix is converted into the element stiffness matrix of the two-parameter orthotropic soil element. If the in-plane shear moduli of the soil element are assigned to the same values, the stiffness matrix of the isotropic soil element is obtained. The unknowns are only the deflections of the nodal points.

The first parameter of the Pasternak foundation which is represented by springs is taken into account as "area springs" assigned to the surface of the foundation.

For the orthotropic foundation model with different material angles, shear moduli G_{13} and G_{23} are assigned to different values and a desired material angle is selected.

3.3. Interaction between Plate and Pasternak Foundation

The plate-foundation interaction is provided by matching the vertical displacements of the plate and the corresponding foundation nodal points. "Equal constraint" property is used for this purpose where the number of constraints is equal to the number of nodes of the plate. Each constraint is then assigned to the respective plate and foundation nodes.

The S-FGM plate model of the system is created using both layered shell and solid elements as shown in Figure 3.

The membrane effects are excluded by releasing the in-plane translational degrees of freedom of both the plate and foundation edge nodes. Note that the in-plane translations of one of the corner nodes of the plate and the foundation are restrained for the stability requirement.

a)   b)
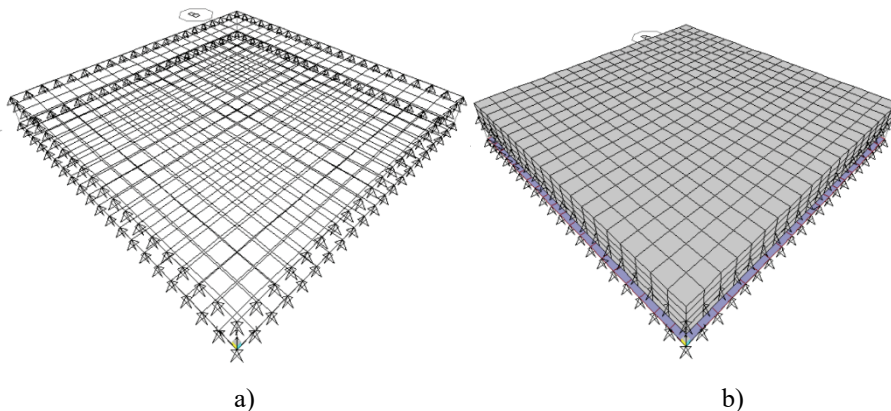
Figure 3 - Plate-foundation finite element model with membrane effects
a) using layered shell finite elements for the plate b) using solid finite elements for the plate

4. VERIFICATION EXAMPLES

4.1. Simply supported S-FGM Plate

A simply supported square S-FGM plate which has been solved both analytically by Chi and Chung [14] and numerically by [14,15] is analysed and the results are compared only with the results of Orakdöğen et.al.[15] because membrane effect analysis was not carried out by Chi and Chung [14]. The thickness of the plate is h =0.02 m, the length is a=1 m and the Poisson's ratio is υ= 0.3. The elastic modulus at the bottom surface is E_1=25x10^6 kN/m^2 and the material exponent is p=2. The plate is subjected to a uniformly distributed

load of q=100 kN/m². The problem is solved for two different elastic modulus ratios, $E_1/E_2=30$ and $E_1/E_2=2$ where E_2 indicates the elastic modulus of the top surface.

First, the plate is modelled using 8 layered shell finite elements and (4x4), (8x8) and (20x20) meshes for $E_1/E_2=30$, including membrane effects. This mesh refinement shows that convergence to the deflections along the x direction (at y=0.5 m) obtained by Orakdöğen et.al.[15] is achieved using an (8x8) mesh, Figure 4. However, due to one-to-one comparison of nodal values, the same mesh discretization with Orakdöğen et.al.[15] which is a (20x20) mesh has been used in the analyses.

The same example is also solved using 2 and 4 layered shell elements to see if the results change with the number of layers used in the modelling. It is observed that for the case $E_1/E_2=2$, the dimensionless deflections are almost the same for all number of layers both for the plate with and without membrane effects, Figure 5.
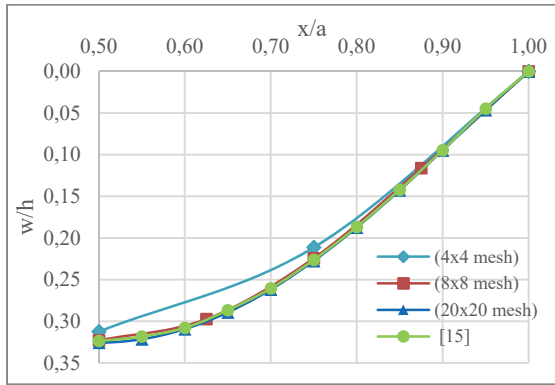
Figure 4 - Variation of dimensionless deflections with mesh refinement (membrane effects are included)
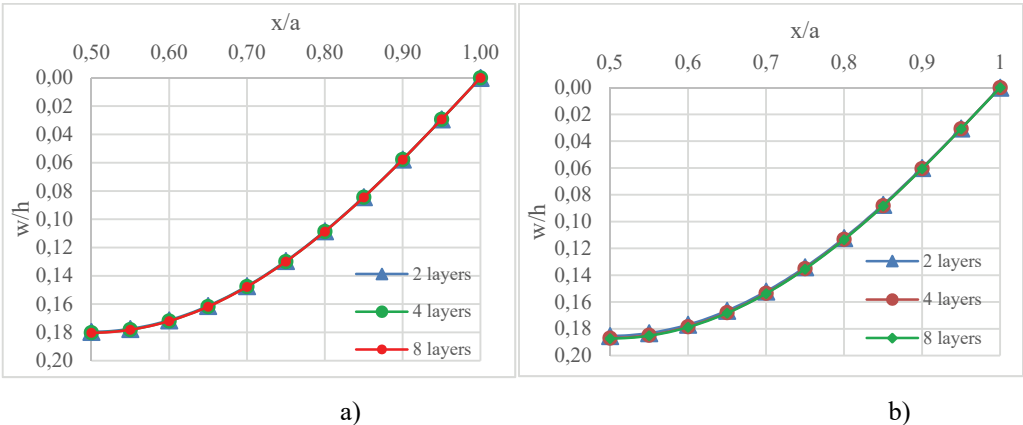

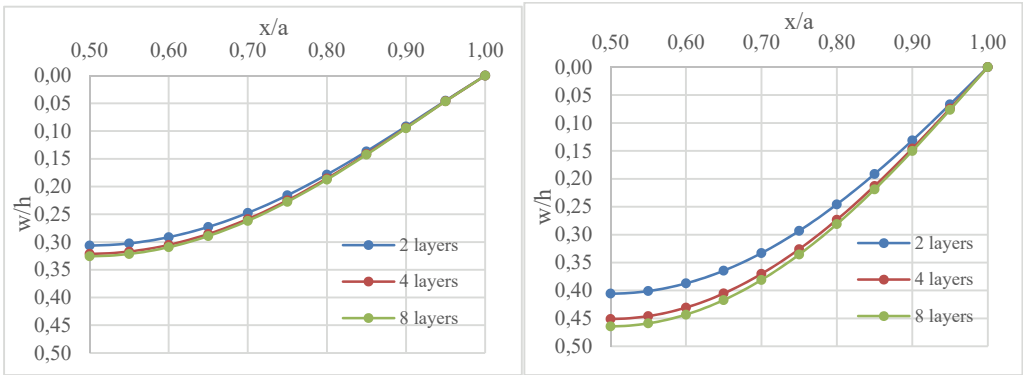a)   b)

Figure 5 - Comparison of dimensionless deflections for different number of layers
($E_1/E_2=2$)
a) membrane effects are included   b) membrane effects are excluded

On the other hand, the dimensionless deflections of the plate with elastic modulus ratio $E_1/E_2=30$ increase as the number of layers used increases and this difference becomes much larger when the membrane effects are excluded as shown in Figure 6.

The dimensionless deflections of the S-FGM plate along the x direction (at y=0.5 m) for the two elastic modulus ratios and for the cases with and without membrane effects (m.e.) are obtained and compared with the solution given by Orakdöğen et.al.[15], Figure 7. Note that 8 layers are used in the modelling while the number of layers used is 10 in Orakdöğen et.al.[15]. It is verified that the results obtained in this study have very good agreement with the reference solution.

Figure 6- Comparison of dimensionless deflections for different number of layers
($E_1/E_2=30$)
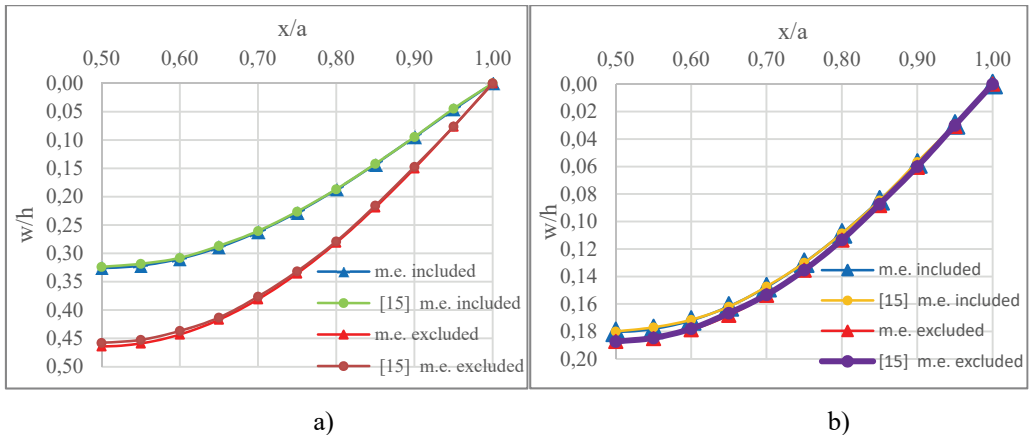*a) membrane effects are included   b) membrane effects are excluded*

Figure 7 - Comparison of dimensionless deflections   a) $E_1/E_2=30$ b) $E_1/E_2=2$

The example is modelled and solved using solid finite elements as well and the dimensionless deflections are compared with the values obtained using the model with layered shell elements. It is observed that solid elements can also be used for the modelling since all results match, Figure 8. It is also obtained that the mid-point deflections increase 1.8 times and 2.5 times for the cases with and without membrane effects, respectively as the elastic modulus decreases with a larger ratio from the bottom to the top surface of the plate.

a)   b)
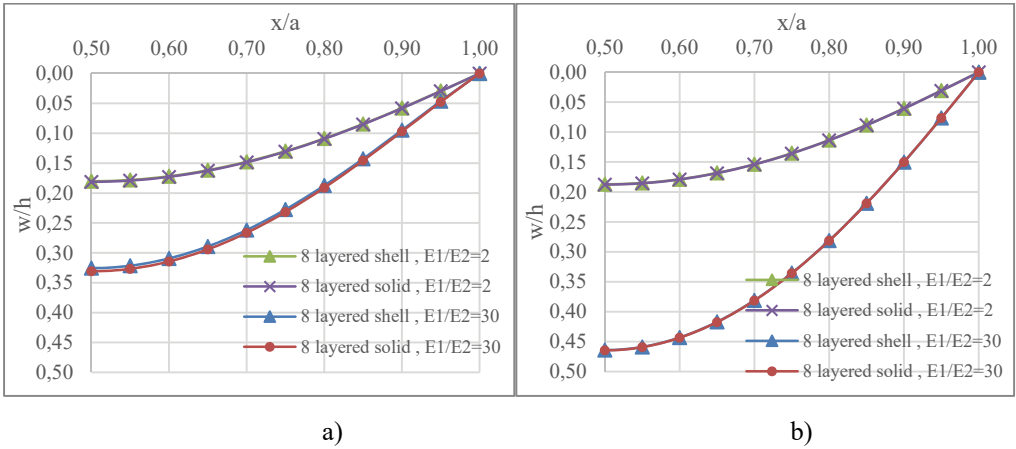
Figure 8- Comparison of dimensionless deflections using shell and 3D solid elements
a) membrane effects are included   b) membrane effects are excluded

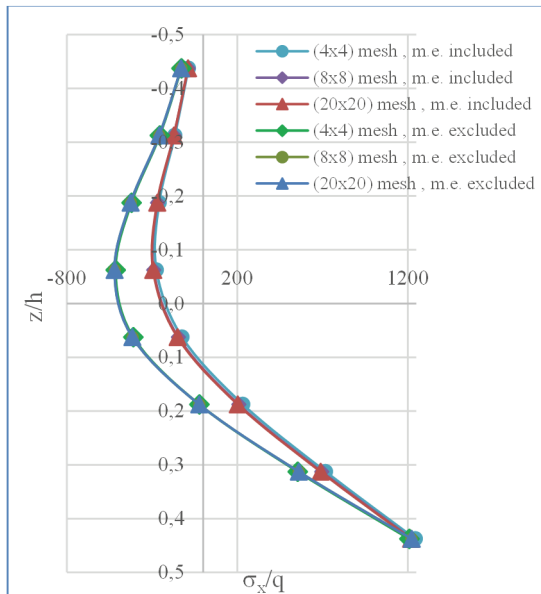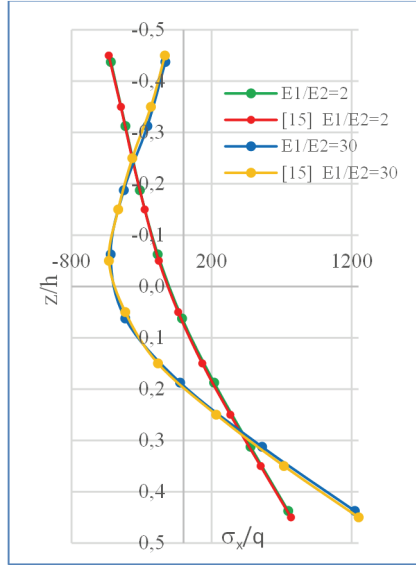*Figure 9 - Variation of dimensionless stresses with mesh refinement*

Figure 10- Comparison of dimensionless stresses (membrane effects are excluded)

a)   b)
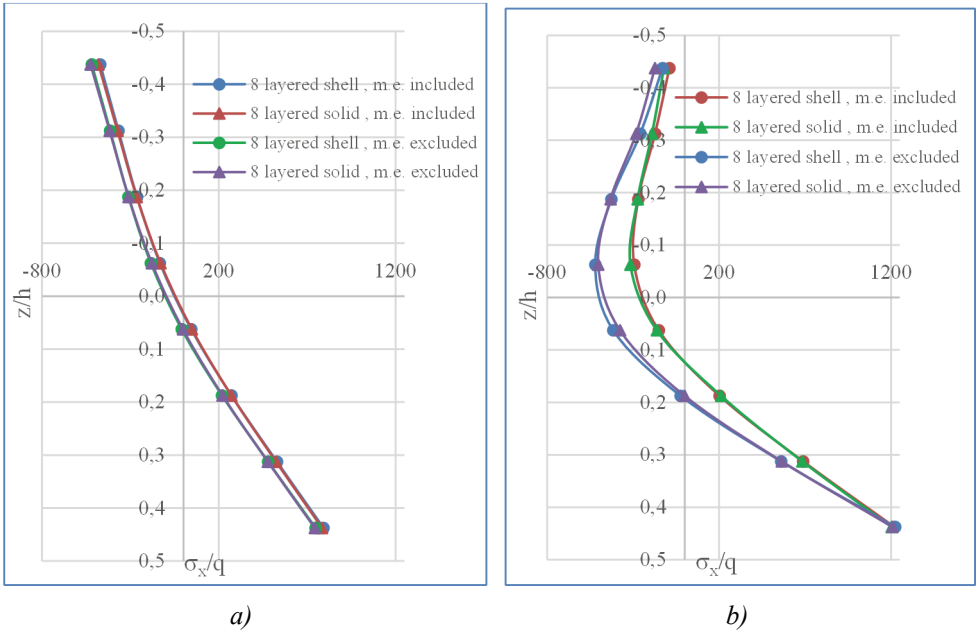
Figure 11- Comparison of dimensionless stresses using layered shell and 3D solid finite
elements a) $E_1/E_2=2$ b) $E_1/E_2=30$

A mesh refinement study using (4x4), (8x8) and (20x20) meshes is also carried out for the dimensionless σ_x stress distributions through the thickness of the plate centre and results are given comparatively in Figure 9. Note that 8 layered shell finite elements are used in the models and the elastic modulus ratio is $E_1/E_2=30$. It is observed that all values match except for (4x4) mesh where a negligible difference occurs when membrane effects are included.

The dimensionless σ_x stress distributions through the thickness of the plate centre are obtained using a (20x20) mesh and 8 layered shell finite elements for different elastic modulus ratios and compared with the values given in [15]. It is observed that the results have very good agreement with the reference solution, as shown in Figure 10.

The dimensionless stress distributions are also verified with the results obtained using the 3D plate model for the cases with and without membrane effects. It is observed that the dimensionless stress values decrease with the inclusion of membrane effects and this decrement is more apparent when E_1/E_2 ratio increases. It is also seen that the neutral axis moves towards the mid-section of the plate when membrane effects are included, as in Figure 11.

4.2. Homogeneous Plate on Isotropic Pasternak Foundation

Static analysis of a rectangular plate resting on an isotropic Pasternak foundation subjected to a uniform loading and a central point load is performed and compared with the reference solutions given in [21,22] to verify the proposed plate-foundation model. The geometrical and loading properties of the plate-foundation system are shown in Figure 12.
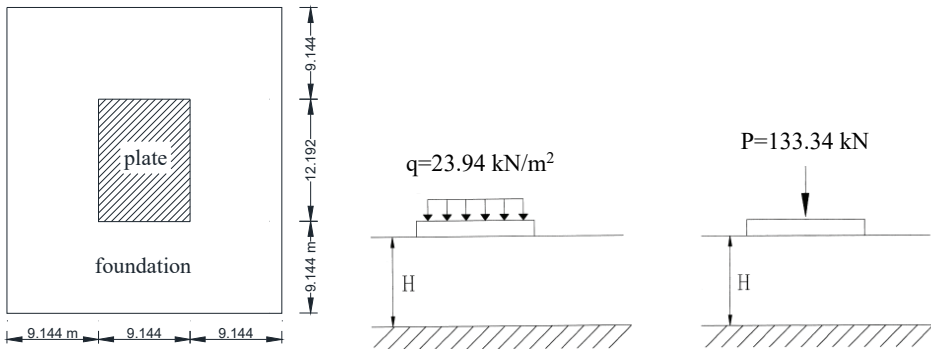

Figure 12 - Plan and vertical section of plate-foundation system

The plate thickness is h=0.1524 m and the material properties of the plate are; $E=2.0685 \times 10^6$ kN/m² and $\upsilon=0.2$. The foundation is extended in the in-plane directions and the plate rests freely on the foundation without assigning any boundary conditions to the edges. Here, the plate is modelled using thin plate finite elements.

The four-noded plate finite element used for modelling homogeneous plates has 3 degrees of freedom at each node, one translational degree of freedom in the direction normal to the plane of the element and 2 out-of-plane rotational degrees of freedom. In the thick plate

finite element formulation, the effects of transverse shear deformation are included whereas in the thin plate finite element formulation, transverse shearing deformation is neglected.

The midpoint deflections of the plate under uniformly distributed loading and under central point load for different soil depths are given in Table 1 and Table 2, respectively. Here, k_w is the first parameter (the coefficient of subgrade reaction), k_p is the second parameter (the shear modulus) of the Pasternak foundation.

The results are in good agreement with the reference solutions indicating that the proposed model fully represents the expected behaviour of the isotropic plate-foundation system.

Table 1 - Midpoint deflections of the plate under uniformly distributed loading for different soil depths

H(m)		3.048	6.096	9.144	15.24
k_w (kN/m³)		27206.59	13757.63	9377.96	5964.21
k_p (kN/m²)		26905.91	50410.87	70586.50	104664.46
w x10⁻²(m)	Ref.[22]	0.08720	0.15260	0.18930	0.22120
	Ref.[21]	0.08530	0.15240	0.18900	0.20700
	Present study	0.08713	0.15300	0.18900	0.22100

Table 2 - Midpoint deflections of the plate under central point load for different soil depths

H(m)		3.048	6.096	9.144	15.24
k_w (kN/m³)		31898.08	24256.05	23737.98	23710.59
k_p (kN/m²)		18913.08	23597.82	24035.56	24060.66
w x10⁻² (m)	Ref.[22]	0.08180	0.08450	0.08460	0.08460
	Ref.[21]	0.04800	0.09750	0.09750	0.09750
	Present study	0.07617	0.08052	0.08076	0.08077

4.3. Simply Supported Homogeneous Plate on Isotropic Pasternak Foundation

Example 1:

A simply supported homogeneous square plate resting on an isotropic Pasternak foundation given in [28,46] is modelled using thin plate finite elements and solved for different soil parameters. The plate is subjected to a uniformly distributed load of $q=E/10^5$ kN/m². Length to height ratio of the plate is a/h =100 and the Poisson's ratio is $\upsilon=0.3$.

Dimensionless central deflections are obtained and compared with the reference solutions as given in Table 3. Here, the dimensionless central deflection is defined as $w' = 10^3$ D w / qa^4 where $D = \frac{Eh^3}{12(1-\upsilon^2)}$, K_w and K_p are the soil parameters in non-dimensional form

expressed as $K_w = k_w a^4 / D$ and $K_p = k_p a^2 / D$. Results obtained in this study are very close to the reference values, and it is observed that the deflections decrease with increasing shear modulus as expected.

Table 3 - Dimensionless central deflections of a uniformly loaded square plate on Pasternak foundation

K_w	K_p	Dimensionless central deflection (w')		
		present	Ref. [28]	Ref. [46]
1	1	3.8536	3.8546	3.8530
1	81	0.7690	0.7630	0.7630
1	625	0.1162	0.1153	0.1150

Example 2:

A simply supported homogeneous square plate resting on two different foundation types, Winkler and isotropic Pasternak foundations, is modelled using thick plate finite elements and the deflection and moment values obtained at the plate centre are compared with those given in [24]. The plate is subjected to a uniformly distributed load of $q=30$ kN/m². Plate length is $a=10$ m and the thickness is $h=0.5$m. elastic modulus and Poisson's ratio are $E=200 \times 10^6$ kN/m² and $\nu=0.167$, respectively. The coefficient of subgrade reaction is $k_w=5620$ kN/m³ and the shear modulus of the Pasternak foundation is $k_p=120000$ kN/m². Note that the shear moduli of the soil element are assigned to zero values to represent the Winkler foundation.

The results given in Table 4 show that the central deflection and moment values obtained in this study are very close to the reference values where the relative errors are between 2.5 - 3 %.

Table 4 - Central deflections and moments of a uniformly loaded square plate on Winkler and Pasternak foundations

	Winkler		Pasternak	
	Ref.[24]	Present study	Ref.[24]	Present study
w x 10⁴ (m)	5.329	5.498	4.187	4.298
M (kNm/m)	120.250	124.125	92.730	95.281

4.4. Simply Supported Homogeneous Plate on Orthotropic Pasternak Foundation

The dimensionless angular frequencies of the first 5 modes of a square homogeneous plate resting on an orthotropic foundation with different material angles are obtained and compared with the solution given by Kutlu [37] to verify the orthotropic foundation model.

The plate is modelled using thick plate finite elements. Material and geometrical properties of the homogeneous plate are E=25x10⁶ kN/m², υ=0.3, a=10 m and h=1 m. The dimensionless coefficient of subgrade reaction and shear moduli are K_w=100, K_{px}=10 and K_{py} =70, respectively.

The coefficient of subgrade reaction of the soil is k_w =22893.773 kN/m³ and shear moduli of the soil are k_{px} = 228937.73 kN/m² and k_{py} =1602564.1 kN/m². Dimensionless angular

frequencies are calculated using $\omega' = \dfrac{\omega a^2}{\pi^2} \sqrt{\dfrac{\rho h}{D}}$ where $\rho = 2550$ kg/m³.

The dimensionless angular frequencies of the system obtained for 7 different material angles are given comparatively in Table 5. It is seen that the values are very close to each other which verifies the orthotropic Pasternak foundation model. Note that the dimensionless angular frequency values are the same for complementary angles due to the symmetry of the system in both geometry and loading.

Table 5 - Dimensionless angular frequencies of the first 5 modes for different material angles

		θ=0°	θ=15°	θ=30°	θ=45°	θ=60°	θ=75°	θ=90°
mode 1	Ref.[37]	3.5716	3.5616	3.5413	3.5310	3.5413	3.5616	3.5716
	Present study	3.5371	3.5276	3.5082	3.4984	3.5082	3.5276	3.5371
mode 2	Ref.[37]	5.7530	5.8207	5.9895	6.1075	5.9895	5.8207	5.7530
	Present study	5.6807	5.7510	5.9266	6.0514	5.9266	5.7510	5.6807
mode 3	Ref.[37]	7.1451	7.0716	6.8915	6.7678	6.8915	7.0716	7.1451
	Present study	7.0546	6.9811	6.7995	6.6716	6.7995	6.9811	7.0546
mode 4	[Ref.37]	9.0773	8.9905	8.8897	8.8529	8.8897	8.9905	9.0773
	Present study	8.7947	8.7332	8.6499	8.6178	8.6499	8.7332	8.7947
mode 5	Ref.[37]	9.5259	9.7388	10.1921	10.6600	10.1921	9.7388	9.5259
	Present study	9.4438	9.6309	10.0631	10.5428	10.0631	9.6309	9.4438

5. SIMPLY SUPPORTED S-FGM PLATE ON ORTHOTROPIC PASTERNAK FOUNDATION

The finite element analysis of a simply supported S-FGM square plate resting on an orthotropic Pasternak foundation is performed next, using layered shell finite elements. The elastic modulus at the bottom surface of the plate is E_1= 25 x10⁶ kN/m², the Poisson's ratio is υ=0.3, the thickness is h=1 m and the length is a=10 m. The plate is subjected to a uniformly distributed load of q=100 kN/m². The dimensionless coefficient of subgrade

reaction and shear moduli are $K_w=100$, $K_{px}=10$ and $K_{py}=70$, respectively where the material angle is 0°.

The deflections of the S-FGM plate along the x direction (at y=5 m) for the cases with and without membrane effects are obtained for $E_1/E_2=2$ and $E_1/E_2=30$. The plate is modelled with 2 and 8 layers in order to observe the effect of the number of layers used defining the variation of the elastic modulus of the S-FGM plate on deflections and it is seen that for all cases, the deflection values do not change with the number of layers used, Figures 13-14.

Comparison of the deflections according to the inclusion and exclusion of membrane effects is given in Figure 15 and it is observed that the deflection difference becomes more apparent as the elastic modulus ratio increases or in other words, as the elastic modulus decreases with a larger ratio from the bottom to the top surface of the plate.
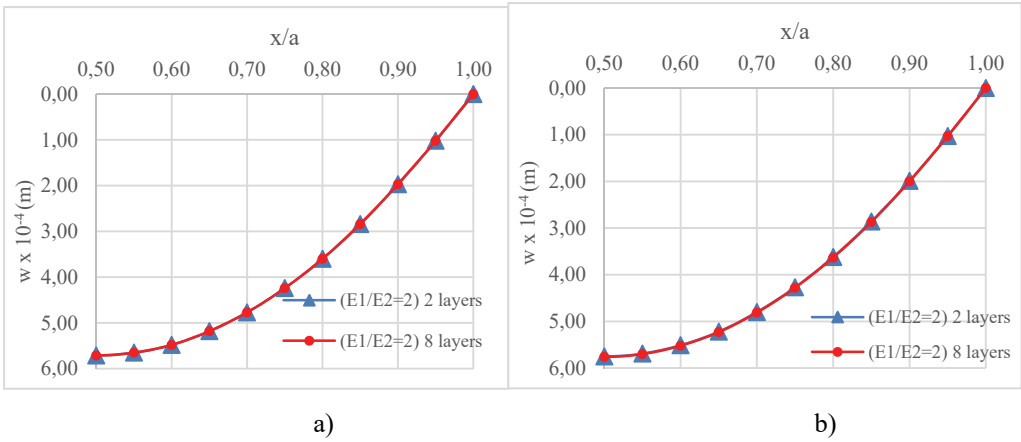

a)   b)

Figure 13 - Comparison of deflections for different number of layers ($E_1/E_2=2$)
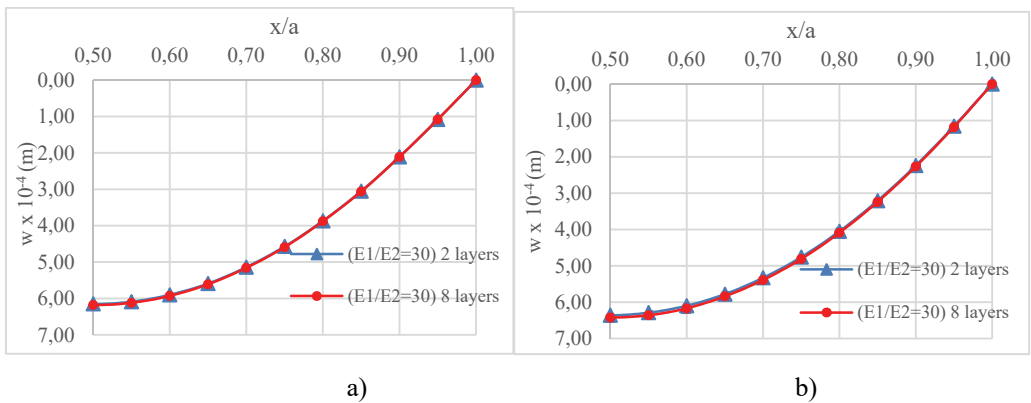*a) membrane effects are included   b) membrane effects are excluded*

a)   b)

Figure 14 - Comparison of deflections for different number of layers ($E_1/E_2=30$)
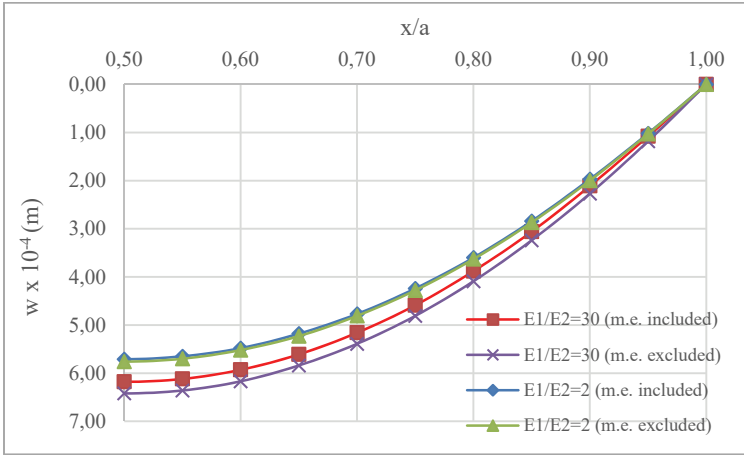*a) membrane effects are included   b) membrane effects are excluded*

Figure 15 - Comparison of deflections using 8 layers

The stress distributions through the thickness of the plate centre are investigated according to the elastic modulus ratio and membrane effects using two layers, Figure 16. σ_x and σ_y stresses are analogous but their magnitudes differ from each other due to the orthotropic property of the soil material. The stress distributions for $E_1/E_2=1$ corresponding to a homogeneous plate material are linear and the graphs for σ_x and σ_y gradually turn into curved shapes towards the top surface, as E_1/E_2 ratio increases. Besides, stress distributions diverge from each other for the cases with and without membrane effects as E_1/E_2 ratio increases. Note that the stress values are obtained at the top and bottom levels of each layer to be able to capture 3 stress values for the 2 layered solution.
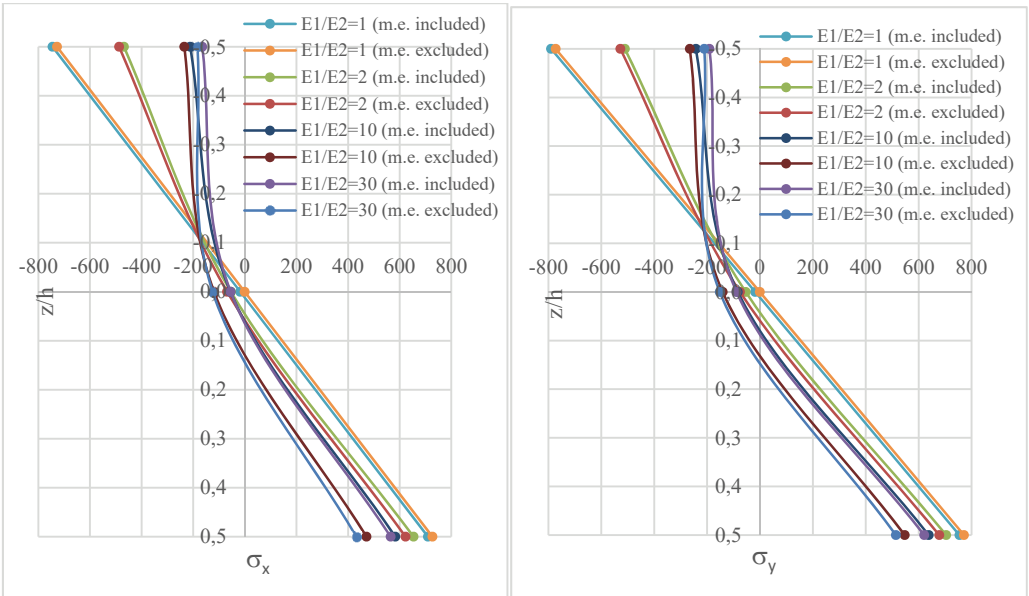

Figure 16 - σ_x and σ_y stress distributions for different E_1/E_2 ratios

Then, the stress distributions are recalculated for different number of layers used in modelling the S-FGM plate and shown comparatively in Figure 17. σ_x and σ_y stresses obtained for 4 and 8 layers are almost the same while they differ slightly near the top and bottom surfaces when 2 layers are used.
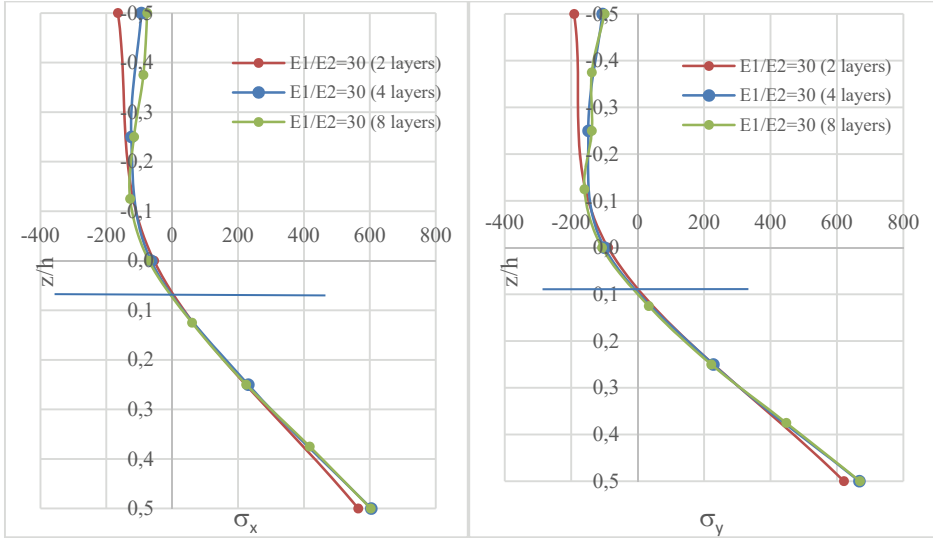

Figure 17 - σ_x and σ_y stress distributions for different number of layers (membrane effects are included)

In addition, two alternate arrangements of the S-FGM plate on the orthotropic Pasternak foundation are considered and solved for the stresses through the thickness of the plate for comparison. The σ_x and σ_y stress components in Figures 18a-19a belong to the arrangement where the surface with larger elastic modulus is attached to the elastic foundation whereas Figures 18b-19b indicate the stress distributions of the plate in the reverse arrangement. It is observed that σ_x and σ_y stresses start diverging towards the top surface as the elastic modulus decreases rapidly and this situation is the reverse for the other case, Figures 18-19. It is also obtained that zero σ_x and σ_y stresses which are at the mid-section of the homogeneous plate, are below and above the mid-section for the two arrangements, respectively due to the heterogeneity of the material.

σ_x and σ_y stress components are obtained for different material angles ranging from 0° to 90° at intervals of 15° and given comparatively in Figure 20. The elastic modulus ratio of the S-FGM plate is taken as $E_1/E_2=30$ and the system is analysed for the case where membrane effects are included. σ_x and σ_y stresses have the maximum divergence at the bottom surface and after converging, they reach the top surface almost with a constant difference.

Finally, the midpoint deflections are investigated for three different cases in which the non-dimensional soil parameters are; $K_w=100$ $K_{px}=10$ $K_{py}=70$ (case 1) ; $K_w=100$ $K_{px}=10$ $K_{py}=140$ (case 2) ; $K_w=100$ $K_{px}=10$ $K_{py}=280$ (case 3) . Coefficient of subgrade reaction and one of the shear moduli of the foundation are kept constant while the other shear modulus is doubled in each case.
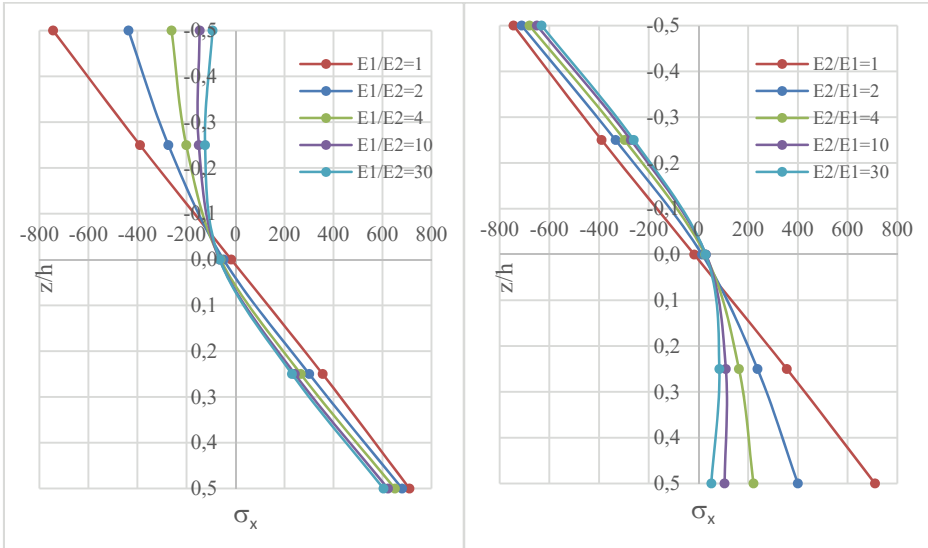
Figure 18 - σ_x stress distributions for different E_1/E_2 and E_2/E_1 ratios (membrane effects are included)
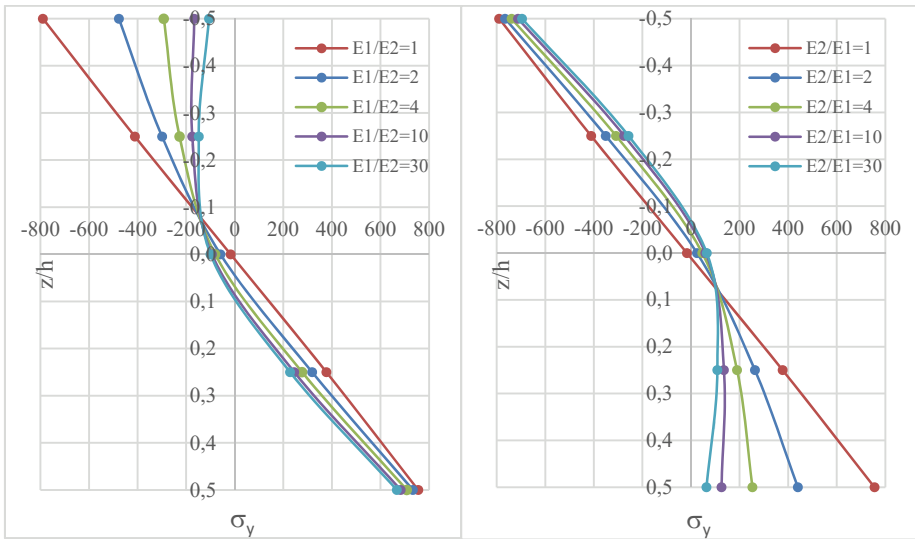

Figure 19 - σ_y stress distributions for different E_1/E_2 and E_2/E_1 ratios (membrane effects are included)

Two different elastic modulus ratios for the plate and seven material angles for the foundation are considered for all cases. It is observed in Figure 21 that the midpoint

deflections decrease with increasing shear modulus. The maximum midpoint deflection value is achieved when the material angle is 45° and the remaining values are in descending order and are the same for complementary angles. Besides, the midpoint deflections for $E_1/E_2=30$ are larger than the values obtained for $E_1/E_2=2$. In other words, midpoint deflections increase for "softer" top surfaces. This increment becomes more apparent when the membrane effects are excluded and with decreasing shear modulus, Figures 21-22.
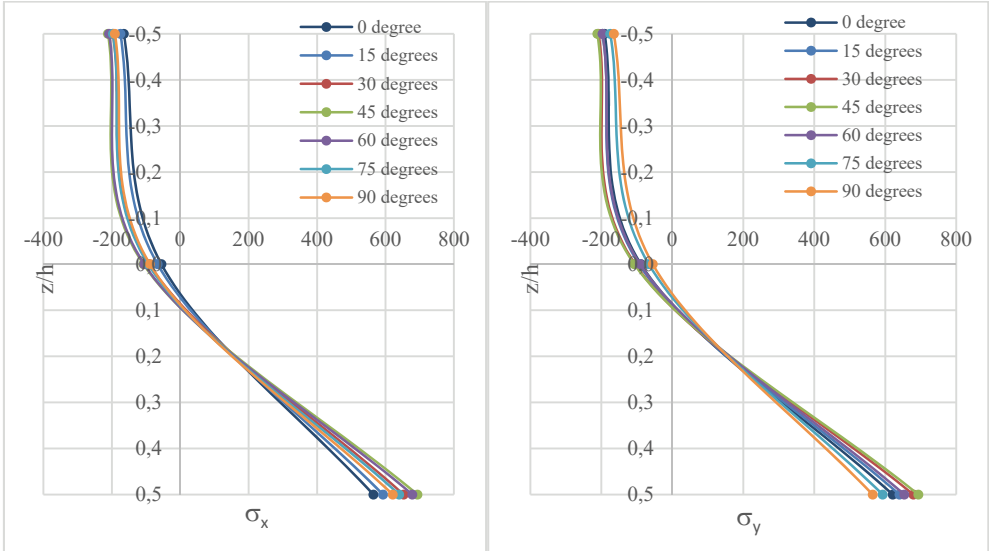

Figure 20 - σ_x and σ_y stress distributions for different material angles ($E_1/E_2=30$, membrane effects are included)
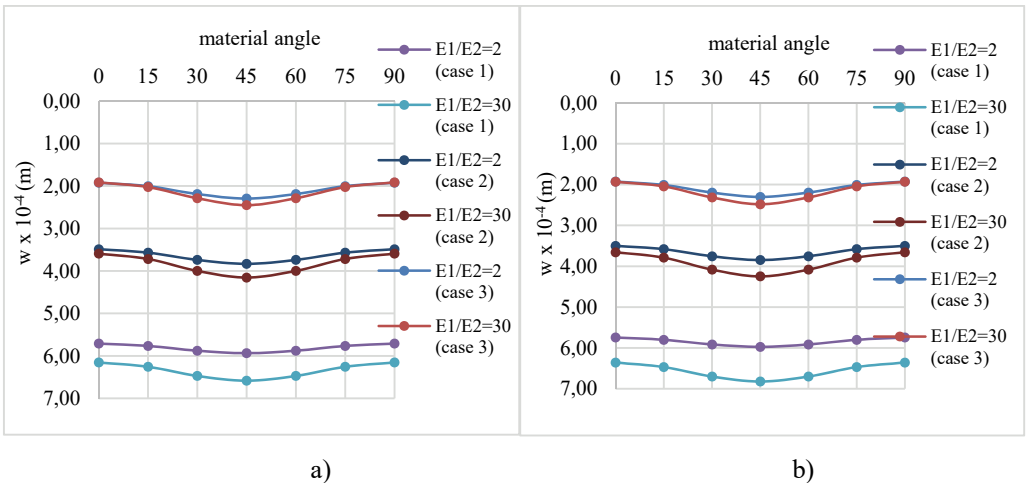

a)   b)

Figure 21 - Mid-point deflections for different material angles
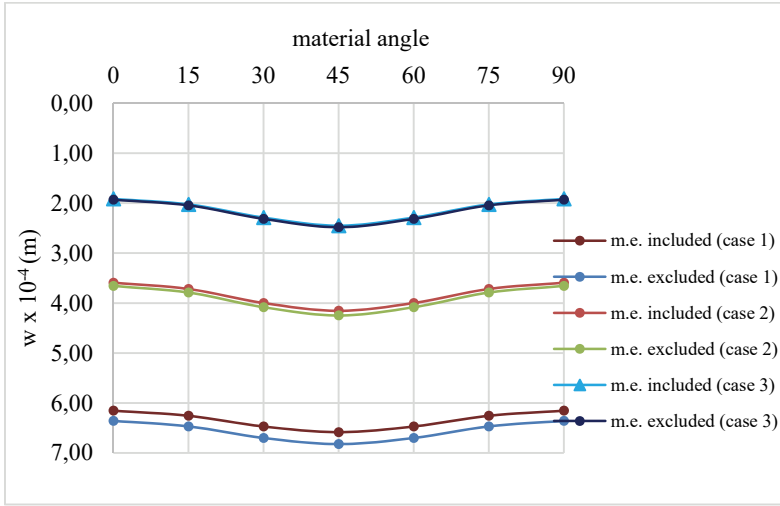a) membrane effects are included   b) membrane effects are excluded

Figure 22 - Mid-point deflections for different material angles (E$_1$/E$_2$=30)

6. CONCLUSIONS

In this study, the finite element analysis of S-FGM plates with and without membrane effects, resting on orthotropic Pasternak elastic foundations with different material angles is carried out using SAP2000 software package. It is demonstrated with the verification examples that the proposed model is convenient and robust. This work can be easily extended to static and dynamic analyses of FGM plates with various geometries resting on arbitrarily orthotropic Pasternak foundations for further studies.

The results obtained in the present study can be summarised as follows:

1) For small elastic modulus ratios (e.g. E$_1$/E$_2$=2), the deflections of the S-FGM plate both with and without Pasternak foundation do not change with the number of layers used for the plate.

2) For large elastic modulus ratios (e.g. E$_1$/E$_2$=30), the deflections of the plate on Pasternak foundation do not change with the number of layers used whereas the deflections of the plate without Pasternak foundation increase at a lower rate as the number of layers increases.

3) The deflections increase when the membrane effects are excluded and the deflection difference between the cases with and without membrane effects becomes more apparent as the elastic modulus decreases with a larger ratio from the bottom to the top surface of the plate.

4) Stresses σ$_x$ and σ$_y$ through the thickness of the plate centre are analogous but their magnitudes differ from each other due to the orthotropic property of the soil material. All stress distributions for a homogeneous plate material are linear while the distributions for σ$_x$ and σ$_y$ gradually turn into curved shapes towards the top surface as E$_1$/E$_2$ ratio increases.

5) The stress distributions diverge for the cases with and without membrane effects as E_1/E_2 ratio increases.

6) Stresses σ_x and σ_y obtained for 4 and 8 layers are almost the same while they differ slightly near the top and bottom surfaces when 2 layers are used.

7) Stresses σ_x and σ_y start diverging towards the top surface as the elastic modulus decreases with a larger rate for the arrangement of the S-FGM plate where the surface with larger elastic modulus is attached to the orthotropic Pasternak foundation. This divergence is towards the bottom surface for the opposite positioning of the plate. Zero σ_x and σ_y stresses which are at the mid-section of the homogeneous plate, are below and above the mid-section for the two arrangements, respectively due to the heterogeneity of the material.

8) For different material angles, σ_x and σ_y stresses have the maximum divergence at the bottom surface and after converging, they reach the top surface almost with a constant difference.

9) The midpoint deflections decrease with increasing shear modulus of the foundation. The maximum midpoint deflection value is achieved when the material angle is 45º and the remaining values are in descending order and are the same for complementary angles.

10) The midpoint deflections increase for softer top surfaces and this increment becomes more apparent with decreasing shear modulus and when the membrane effects are excluded.

Acknowledgements

References

[1] Suresh S., Mortenson A., Fundamentals of Functionally Graded Materials: Processing and Thermomechanical Behavior of Graded Metals and Metal-Ceramic Composites. IOM Communications Ltd, London, UK, 1998.

[2] Koizumi M., FGM activities in Japan. Composites Part B: Eng 28(1-2), 1-4, 1997.

[3] Tanigawa Y., Some basic thermoelastic problems for nonhomogeneous structural materials. Appl. Mech. Rev. 48(6), 287-300, 1995.

[4] Suresh S., Mortensen A., Functionally graded metals and metalceramic composites 2: thermomechanical behaviour. Int. Mater. Rev. 42(3), 85-116, 1997.

[5] Reddy J.N., Analysis of functionally graded plates. Int. J. Numer. Methods Eng., 47, 663-684, 2000.

[6] Cheng Z.Q., Batra R.C. Deflection relationships between the homogenous Kirchhoff plate theory and different functionally graded plate theories. Archives of Mechanics 52, 143-158, 2000.

[7] Bao G., Wang L., Multiple cracking in functionally graded ceramic/metal coatings. Int. J. Solids Struct., 32, 2853-2871, 1995.

[8] Jin Z.H., Paulino G.H., Transient thermal stress analysis of an edge crack in a functionally graded material. Int. J. Fracture, 107, 73-98, 2001.

[9] Delale F., Erdogan F., The crack problem for a nonhomogeneous plane. ASME J. Appl. Mech., 50, 609-614, 1983.

[10] Erdogan F., Wu B.H., Crack problems in FGM layers under thermal stresses. J. Therm. Stress., 19, 237-265, 1996.

[11] Chung Y.L., Chi S.H., The residual stress of functionally graded materials. J. Chin. Inst. Civ. Hydraul. Eng., 13, 1-9, 2001.

[12] Chi S.H., Chung Y.L., Cracking in sigmoid functionally graded coating. J. Mech., 18, 41-53, 2002.

[13] Chi S.H., Chung Y.L., Mechanical behavior of functionally graded material plates under transverse load-Part I: Analysis. Int. J. of Solids and Str., 43, 3657-3674, 2006a.

[14] Chi S.H., Chung Y.L., Mechanical behavior of functionally graded material plates under transverse load-Part II: Numerical results. Int. J. of Solids and Str., 43, 3675-3691, 2006b.

[15] Orakdöğen E., Küçükarslan S., Sofiyev A., Omurtag M.H., Finite element analysis of functionally graded plates for coupling effect of extension and bending. Meccanica, 45, 63-72, 2010.

[16] Zenkour A.M., Generalized shear deformation theory for bending analysis of functionally graded plates. Appl. Math. Model., 30, 67-84, 2006.

[17] Elishakoff I., Gentilini C., Viola E., Three-dimensional analysis of an all-round clamped plate made of functionally graded materials. Acta Mech., 180(1-4), 21-36, 2005.

[18] Swaminathan K., Naveenkumar D.T., Zenkour A.M., Carrera E., Stress, vibration and buckling analyses of FGM plates-A state-of-the-art Review. Composite Structures, 120, 10-31, 2015.

[19] Winkler E. Theory of Elasticity and Strength of Materials. Dominicus, Prague, 1867.

[20] Pasternak P.L., On a new method of analysis of an elastic foundation by means of two foundation constants. Cosudarstrennoe Izdatelstvo Literaturi po Stroitelstvu i Arkhitekture, Moscow, USSR, 1-56, 1954.

[21] Vallabhan C.V.G., Straughan W.T., Das Y.C., Refined Model of Analysis of Plates of Elastic Foundations. Journal of Engineering Mechanics, 117(12), 2830-2844, 1994.

[22] Celik M., Saygun A., A method for the analysis of plates on a two-parameter foundation. Int. J. of Solids and Str., 36, 2891-2915, 1999.

[23] Xiang Y., Wang C.M., Kitipornchai S., Exact vibration solution for initially stressed Mindlin plates on Pasternak foundation. Int. J. Mech. Sci., 36(4), 311-316, 1994.

[24] Omurtag M.H., Ozutok A., Akoz A.Y., Free vibration analysis of Kirchhoff plates resting on elastic foundation by mixed finite element formulation based on Gateaux differential. Int. J. Numer. Methods Eng., 40(2), 295-317, 1997.

[25] Matsunaga H. Vibration and stability of thick plates on elastic foundations. ASCE J. Eng. Mech., 126(1), 27-34, 2000.

[26] Zhou D., Cheung Y.K., Lo S.H., Au F.T.K., Three-dimensional vibration analysis of rectangular thick plates on Pasternak foundations. Int. J. Numer. Methods. Eng., 59(10), 1313-1334, 2004.

[27] Shen H.S., Postbuckling analysis of composite laminated plates on two-parameter elastic foundations. Int. J. Mech. Sci., 37(12), 1307-131, 1995.

[28] Huang Z.Y., Lü C.F., Chen W.Q., Benchmark solutions for functionally graded thick plates resting on Winkler–Pasternak elastic foundations. Composite Structures, 85, 95-104, 2008.

[29] Lee W.H., Han S.C., Park W.T., A refined higher order shear and normal deformation theory for E-,P-, and S-FGM plates on Pasternak elastic foundation. Composite Structures, 122, 330-342, 2015.

[30] Tajeddini V., Ohadi A., Sadighi M., Three-dimensional free vibration of variable thickness thick circular and annular isotropic and functionally graded plates on Pasternak foundation. Int. J. Mech. Sci., 53(4), 300-308, 2011.

[31] Baferani A.H., Saidi A.R., Ehteshami H., Accurate solution for free vibration analysis of functionally graded thick rectangular plates resting on elastic foundation. Composite Structures, 93(7), 1842-1853, 2011.

[32] Malekzadeh P., Golbahar Haghighi M.R., Atashi M.M., Free vibration analysis of elastically supported functionally graded annular plates subjected to thermal environment. Meccanica, 46, 893-913, 2011.

[33] Thai H.T., Choi D.H., A refined shear deformation theory for free vibration of functionally graded plates on elastic foundation. Composites Part B, 43, 2335-2347, 2012.

[34] Mansouri M.H., Shariyat M., Differential quadrature thermal buckling analysis of general quadrilateral orthotropic auxetic FGM plates on elastic foundations. Thin-Walled Structures, 112, 194-207, 2017.

[35] Hamarat M.A., Dynamic analysis of structures resting on two parameter elastic foundation. MSc Dissertation, Istanbul Technical University, Istanbul, 2012.

[36] Hamarat M.A., Çalık-Karaköse Ü.H., Orakdöğen E., Seismic Analysis of Structures Resting on Two Parameter Elastic Foundation. 15th World Conference on Earthquake Engineering. Lisbon, Portugal, September, 2012.

[37] Kutlu A., Analysis of free vibrations of Mindlin plates resting on arbitrarily orthotropic Pasternak foundation with mixed finite elements. MSc Dissertation, Istanbul Technical University, Istanbul, 2007.

[38] Kutlu A., Omurtag M.H., Large deflection bending analysis of elliptic plates on orthotropic elastic foundation with mixed finite element method, International Journal of Mechanical Sciences, 65, 64–74, 2012.

[39] Kutlu A., Ugurlu B., Omurtag M.H., Ergin A., Dynamic response of Mindlin plates resting on arbitrarily orthotropic Pasternak foundation and partially in contact with fluid. Ocean Engineering, 42,112-125, 2012.

[40] Kolahchi R., Safari M., Esmailpour M., Dynamic stability analysis of temperature-dependent functionally graded CNT-reinforced visco-plates resting on orthotropic elastomeric medium. Composite Structures, 150, 255-265, 2016.

[41] Heydari M. M., Bidgoli A. H., Golshani H. R., Beygipoor G., Davoodi, A., Nonlinear bending analysis of functionally graded CNT-reinforced composite Mindlin polymeric temperature-dependent plate resting on orthotropic elastomeric medium using GDQM. Nonlinear Dynamics, 79(2), 1425- 1441, 2015.

[42] Arani A. G., Cheraghbak A., Kolahchi R., Dynamic buckling of FGM viscoelastic nanoplates resting on orthotropic elastic medium based on sinusoidal shear deformation theory. Structural engineering and mechanics: An international journal, 60(3), 489-505, 2016.

[43] SAP2000, v18., Integrated Finite Elements Analysis and Design of Structures, Computers and Structures. p. Inc, Berkeley, CA, 2016.

[44] Elmacı Ş., Spectral analysis and determination of free vibration characteristics of quadratic plates resting on arbitrarily orthotropic two parameter elastic foundation. MSc Dissertation, Istanbul Technical University, Istanbul, 2019.

[45] Aykılıç B., Spectral analysis of circular and elliptic plates resting on arbitrarily orthotropic Pasternak type foundation. MSc Dissertation, Istanbul Technical University, Istanbul, 2019.

[46] Lam K.Y., Wang C.M., He X.Q., Canonical exact solution for Levy-plates on two parameter foundation using Green's functions. Eng. Struct., 22(4),364-378, 2000.

Causal Relationships of Readability Risks in Construction Contracts

Kerim KOC[1]
Asli Pelin GURGUN[2]

ABSTRACT

Issues related to readability risks in contracts could exacerbate conflict, claim and dispute occurrences in construction projects. Determination of root causes of readability risks by defining casual relationships in construction contracts is essential to improve contract documentation and enable successful risk management. This paper aims to differentiate net causes from net effect factors of readability risks in construction contracts. Most significant readability risks in construction contracts were analyzed using fuzzy decision-making trial and evaluation laboratory (DEMATEL) method, which is known for its wide implementation in similar problems. Root cause degree (RCD) diagram was drawn to illustrate the differentiation of these factors by adopting maximum mean de-entropy (MMDE) algorithm. Analysis results indicated that poor grammar use, legal terminology, visual representation, and negative language were the major underlying cause factors; while lengthy document, use of abbreviations, scope complexity, controversial uses, repetitions, and ambiguous words were the net effect factors. The results are expected to improve readability of contract documents, which would contribute to more effective risk management and better allocation of project resources.

Keywords: Construction projects, contract readability, contract drafting, construction conflicts, risk management.

1. INTRODUCTION

The adversarial nature, lack of trust, inherent risks and excessive time pressures of construction projects contribute to the germination of conflicts, claims and eventually disputes [1]–[4]. Cheung and Yiu [5] conceptualized construction disputes as having three main components: contract provisions, triggering events and conflicts. Contract incompleteness with inadequate contract documentation, poor understanding of contracts

---

1 Yildiz Technical University, Department of Civil Engineering, Istanbul, Turkey
  kerimkoc@yildiz.edu.tr - https://orcid.org/0000-0002-6865-804X

2 Yildiz Technical University, Department of Civil Engineering, Istanbul, Turkey
  apelin@yildiz.edu.tr - https://orcid.org/0000-0002-0026-4685

and improper contract administration processes [6]–[9] are leading factors contributing construction conflicts, as supported by a recent Arcadis report [10]. When the contract is incomplete, its provisions can be interpreted differently by involved parties, then a conflict and dispute is inevitable [11]. Maqsoom et al. [12] addressed that construction disputes could be considered as one of the keys for inefficient performance of construction projects. Therefore, improving contract documents could be regarded as a preventative approach to dispute occurrence prior to project execution process.

Contracts play a significant role in assisting to meet project objectives as a control and coordination mechanism [13], especially in construction projects due to their inherent uncertain, complex and project-specific natures [4], [14]. However, construction contracts are usually comprised of set of documents that contain numerous provisions, specifications and requirements, making their administrations difficult for project engineers and managers. Smooth functioning of contracts can be achieved only with high degree of readability, simplifying contract documents, reducing ambiguities in responsibilities, and increasing commonality in the interpretation [15]. Project parties could fail to understand their responsibilities if the draft of contract is hard to read. In addition, they may seek to find flaw of contracts to behave opportunistically particularly when conflicts arise [11]. Therefore, proper contract drafting and administration are essential elements for successful achievement of project objectives [15], [16]. This brought significant attention from both scholars and practitioners to contract design problems recently [17].

The readability of construction contracts can be improved prominently by exploring the root causes and causal relationships of readability problems. Poor readability of a document can be regarded as one of the root causes of contract incompleteness, which has also been regarded as one of the main root causes of construction disputes [2]. Root cause could be defined as the fundamental and underlying reason of an undesirable event, which, could prevent the problem from occurring recurrently, if eliminated properly [18]. In addition, readability risks leading to poor contract documentation are strongly associated with each other, highlighting the requirement of differentiating cause factors from effect factors. For instance, while decreasing the number of words, the structure of sentences could become more complex with grammatical errors [19], [20]. On the contrary, many scholars have also addressed that long sentences could make contract less readable [1], [21], [22]. Therefore, analysis of the most causal factors affecting contract readability is essential to improve construction contracts, which is the main legal instrument that connects various parties with a legal bond [23].

Readability risks of construction contracts are seldom examined and underlying causes are rarely analyzed in the existing literature [24]. In construction risk management literature, it is very common to focus on contractual risks affecting operations as part of a general risk management plan in projects. However, this approach mostly focuses on operational risks due to contractual provisions and requirements. This paper aims to further examine the risks identified by Koc and Gurgun [25] by investigating the causal relationships among the most significant readability risks to deliver more effective contract administration and risk management. Fuzzy decision-making trial and evaluation laboratory (DEMATEL) method was adopted to determine the causal relationships. Mean plus standard deviation (MPSD) and maximum mean de-entropy (MMDE) algorithms were both used to determine threshold values to indicate individual relationships between readability risks and draw the

root cause degree (RCD) diagram. By emphasizing the most effective measures to improve the quality of construction contracts, the findings of this study can be useful for contract drafters, dealing with traditional and standard contract forms such as the International Federation of Consulting Engineers (FIDIC) and New Engineering Contract (NEC), or contract modifications.

2. RELATED WORKS

Construction contracts are voluminous documents making it harder to read and extract required information whenever needed [26]. In fact, when any document is not readable hindering its intended meaning, there is just a little value of it [27]. High degree of comprehension can be achieved only when readability of the contract document is high [15]. Easy-to-read contract documentation is essential particularly with respect to construction contracts to minimize conflicts, claims, and disputes among involved parties [28].

In practice, traditional contracts are regarded to include more clarity issues compared to standard contract forms such as FIDIC or NEC [29]. Therefore, standard contract forms have been frequently used in the construction industry to reduce clarity and readability problems [30]. However, while adopting standard contract forms, various modifications in some clauses are made by clients to satisfy requirements of the projects [22]. Rameezdeen and Rodrigo [22] found that modifications to standard contract forms generally make the contracts more difficult to read. All these considerations require a thorough analysis of risk factors affecting readability of construction contracts for smooth contract administration. Existing literature mostly lacks systematic and overall assessment of readability risks and is not sufficiently contributing to the revelation of root causes regarding readability issues in standard forms and traditional contracts. Even studies that analyze readability of construction contracts are limited in the literature.

As examples of limited studies, Broome and Hayes [29] compared the clarity of traditional contracts and NEC, and found that while not being perfect, standard contract forms were more clear than traditional contracts. Rameezdeen and Rajapakse [15] investigated readability of FIDIC and NEC by using a readability formula to determine whether there was a relationship between readability and degree of commonality in interpretation and found a positive relationship. Chong and Zin [1] investigated the standard contract form in Malaysia, proposed measures to develop its language structure, and ranked those related to length of the sentences at top. Koc and Gurgun [25] investigated and prioritized readability risks in construction contracts based on their dispute potentials related to time, cost and quality criteria. Rameezdeen and Rodrigo [22] examined the impact of modification to standard contract forms on readability, and asserted that more than 50% of the original and modified contract clauses were still difficult to read. Besaiso et al. [2] compared the suitability of FIDIC and NEC standard forms in Palestine and addressed that NEC appears to be more capable than FIDIC to minimize disputes. Youssef et al. [31] assessed semantic risks of ad hoc and amended standard contract forms and found a strong correlation between contract risk rating and the magnitude of contingency included in the tender price of contractor. Lee et al. [32] proposed a proactive risk assessment model based on rule-based natural-language processing to detect missing contractor-friendly clauses in the

modified FIDIC conditions by clients, and included some of the readability factors in the proposed automated model. Previous studies show that there is a gap in the literature about root cause analysis of readability risks.

3. DETERMINATION OF READABILITY RISKS IN CONSTRUCTION CONTRACTS

Fundamentally, readability can be defined as a function of a text and a reader. It is the integration of the structure, characteristics, and context of a text with the information processing features and abilities of a reader [27]. In this study, readability risk of a contract is defined as structural and textual issues in a contract that hinder comfortability in reading and inevitably diversify the interpretation of contract clauses. A structure of a typical need for reading a construction contract is illustrated in Fig. 1. Contract management can be typically defined in three phases: pre-award, award and post-award phases. In pre-award phase, involved parties plan, prepare the scope, develop the contract to offer required services, define responsibilities and allocate risks to meet contract provisions. Then in the award phase, project parties negotiate and sign upon agreement of the contract terms. Finally, in post-award phase, project managers monitor the performance to meet the requirements according to contract provisions without any flaws until the end of the projects. In case of any flaw, conflicts may arise and the readability of the contract becomes more speculative. Parties usually seek evidence to justify events based on their interests referred in contract provisions. Such opportunistic approaches sometimes lead to conflicts that may jeopardize successful completion of projects [33] and hinder effective long-term relationships [34]. Therefore, acceptable degree of readability of construction contracts is essential from the initiation to the termination of construction projects.
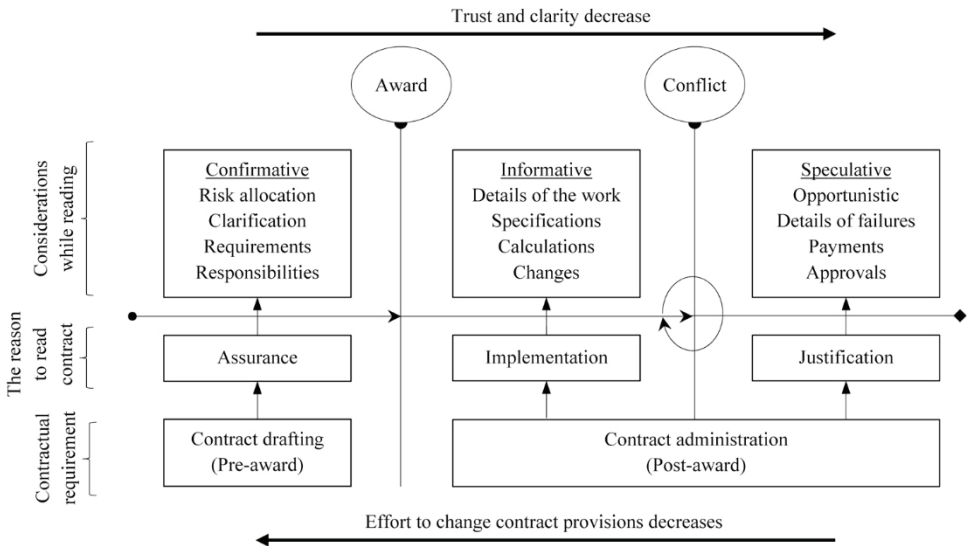

Fig. 1 - Generic structure of a typical need for reading construction contract.

There are numerous factors affecting the readability of construction contracts. Koc and Gurgun [25] performed a comprehensive literature review accompanied by a pilot study to unveil readability risks in construction contracts, which resulted in 18 readability risks. These risks mainly included ambiguity, specialized vocabulary, length-related, legalese, inconsistency, layout, and grammatical structure. The researchers analyzed and ranked these risks by using fuzzy VIKOR method to identify the most significant ones. Top ten risks which were identified in that study are shown in Table 1. These risks formed the basis of this research.

In this study, underlying facts of top ten risks are examined deeply and explained as follows:

R1) *Unnecessary length in the clauses, sentences, and words*: Construction contracts are mostly voluminous and complex documents. They contain a significant number of provisions with long sentences that nobody in the project could read with full attention, failing to comprehend project requirements [24]. It was addressed that putting accurate punctuation in long sentences could make the document easier to read [38]. The Flesch Reading Ease Score (FRES), which is one of the most widely used readability formula, considers two variables to estimate readability of documents as; average length of sentences and average number of syllabus per word [15]. Therefore, length in the clauses and sentences, and the number of words in construction contracts need to be minimized adequately to expedite reading and enable clear understanding. When construction contracts are drafted with long clauses, sentences and unnecessary words, then they are hardly read and understood by contractors during contract drafting process.

Table 1 - Most significant readability risks ([25]).

ID	Readability risks	References
R1	Unnecessary length in the clauses, sentences and words	Ameer Ali and Wilkinson [35], Besaiso et al [2], Broome and Hayes [29]
R2	Unnecessary complexity in the scope of work with complex noun phrases and improper use of referents	Chong and Oon [36], Rameezdeen and Rajapakse [15]
R3	Repetition of words and provisions	Ameer Ali and Wilkinson [35], Broome and Hayes [29], Chong and Oon [36]
R4	Use of negative style of language	Besaiso et al [2], Chong and Zin [1], Menches and Dorn [37]
R5	Controversial uses to legal terms and incoherence including other contracts in the projects	Chong and Zin [1], Murphy et al. [20], Rameezdeen and Rajapakse [15]
R6	Abstractness and ambiguity in word or sentence causing more than one meaning	Ameer Ali and Wilkinson [35], Besaiso et al [2], Broome and Hayes [29]
R7	Use of specialised vocabulary, legal terms and legal jargon	Rameezdeen and Rajapakse [15], Rameezdeen and Rodrigo [22], Broome and Hayes [29]
R8	Lack of visual representations	Schuhmann and Eichhorn [24]
R9	Poor grammar use including missing nouns, words formation	Ameer Ali and Wilkinson [35], Chong and Zin [1]
R10	Unnecessary use of abbreviations	Murphy et al. [20], Beaumont [19]

R2) *Unnecessary complexity in the scope of work with complex noun phrases and improper use of referents*: Construction contracts may contain complex and lengthy work descriptions including the scope of the work, responsible entities, the way requirements are handled etc., which could cause disagreements resulting with conflicts due to improper expressions. Scope of the intended works can be explicitly described without complex noun phrases and improper use of referents. Using verbs instead of noun phrases are recommended to increase the readability of construction contracts [1], [39]. Besides, using "he" or "she" could increase the complexity of the works since they can be used to indicate project manager, engineer or foreman [40]. This risk factor can also be associated with use of double negative phrases and "shall" [36]. For instance, Ameer Ali [41] highlighted the use of "shall" with reference to Malaysian Government design & build construction contract (Clause 42.1). "*... the Contractor shall (meaning: must) pay the Government a sum calculated at the rate ... such damages shall (meaning: may) be recoverable from the ...*". Additionally, the following sentence can be given as an example of a complexity of noun phrase "*the Government shall in no circumstances be liable to...*" [9].

R3) *Repetition of words and provisions*: This refers to the repetition of any information that has already been provided in other parts of the contracts. It was included in this study since particularly legalese language, with which construction contracts are heavily drafted, is criticized for being complicated and repetitive [42]. It also covers repetition of words with the same meaning to clarify contract documents [36], which is common in legal jargon. (e.g. "*claim by any and every...*" [9])

R4) *Use of negative style of language*: Contract clauses that contain negative language and expressions are usually associated with negative emotional reactions to the clauses [37]. The adopted way of expressions in contracts affect the readability of contracts, particularly emotional reactions during reading. Negative language in construction contracts could reduce trust and collaboration among parties [37], [43], which could increase the possibility of conflicts. The following clause component can be given as an example of negative style of language: "*…shall not be removed except for use upon the Works, unless the S.O. has consented...*" [1].

R5) *Controversial uses to legal terms and incoherence including other contracts in the projects*: This refers to all incoherent uses with respect to legal terms, other clauses in the contract and other contracts in the projects. Controversial expressions make it hard to interpret the actual meanings and intentions of the provisions [1], [36], [44]. This could result in opportunistic behaviors by contracting parties when things go wrong, thus conflicts. Resolution procedures of conflicts and disputes could be tedious in case of incoherence. When additional clauses or provisions are added, inconsistencies and mistakes need to be avoided to prevent further conflicts [20]. It was addressed that inconsistencies between modifications were one of the top causes of construction disputes in Australia [22].

R6) *Abstractness and ambiguity in word or sentence causing more than one meaning*: Contract ambiguity can be considered as one of the primary causes of conflicts and claims in construction projects [45]. A contract can be regarded as incomplete based on several factors such as ambiguity, deficiency, inconsistency and defectiveness [11]. Ambiguity can also contribute to possible opportunistic behaviors, thus leading

disagreement between parties. This factor includes words having double meanings by their nature and expressions such as "meaningful" or "reasonable", and considered in this study since their interpretations may differ based on parties with their incompatible interest [4], [46], [47]. In this context, "*inclement weather*" can be another example of ambiguous words [9]. When there is high ambiguity in construction contracts, then its readability can be regarded as low.

R7) *Use of specialized vocabulary, legal terms and legal jargon*: Presence of legalese language can be considered as one of the main causes of clarity and readability issues in construction contracts [22]. This factor refers to the use of too many legal terms and phrases, vocabulary deemed to legal jargon, making the contract difficult to read and understand [1]. It was addressed that minimizing legalese with plain language structure could increase the transparency of contracts [24]. In addition, FIDIC conditions have been criticized for containing many unnecessary legal expressions [2], [29]. It was addressed that drafters of NEC have taken a revolutionary step by abandoning legal language [2].

R8) *Lack of visual representations*: Visual representation of the contracts can increase the transparency of construction contracts, ensuring that the contracts are handled by project managers adequately [24]. It also includes inadequate presentation of technical documents, implementation details and work visualization that could reduce the clarity of the intended work and increase unwillingness of the employers to read the contracts.

R9) *Poor grammar use including missing nouns, words formation*: Missing nouns, complex words formation and poor grammar use can be related to clarity problems in construction contracts [1] eventually affecting its readability. For instance, NEC was regarded to promote clarity and simplicity within the contract, however, some researchers asserted that while decreasing the number of words in sentences, it failed to propose good grammar use with missing nouns [19], [20].

R10) *Unnecessary use of abbreviations*: Abbreviations are naturally used to prevent lengthy sentences and contexts. However, too many abbreviations in a single sentence, provision or clause can reduce their readability. Using abbreviations more than necessary in contracts can be pertained to poor grammatical structure of documents [19].

The following clause can be given as an example of a poorly drafted contract clause in several ways [41]: "*This Contract shall be deemed to be a Malaysian Contract and shall accordingly be construed according to the laws for the time being in force in Malaysia and the Malaysian Courts shall have exclusive jurisdiction to hear and determine all actions and proceedings arising out of this Contract and the Contractor hereby submits to the jurisdiction of the Malaysian Courts for the purposes of any such actions and proceedings.*" First, the sentence is too long (69 words, threefold of what has been suggested by Chong and Zin [1]), legalese and redundant [41]. In addition, the meaning of "Malaysian Contract" is not clear (whether it means that the contract is formed in Malaysia or based on Malaysian law). Separation of "hear" and "determine", and "actions" and "proceedings" could also be considered as clearer. Besides, the role of employer in jurisdiction is also not clear, such that only contractor is referred. For more detailed criticism of this clause (and many others), one may refer to the study of Ameer Ali [41].

4. RESEARCH METHODOLOGY

The main objective of this study is to reveal causal relationships of readability risks leading conflicts by determining their root causes in construction projects. Analysis of these relationships is important since in most cases, risks are found with inextricable cause-effect interrelations and identification of the most significant readability risks may not always be sufficient for proper risk management. Their cause-effect interrelations can exist in varying extents that may impose further elaboration. For instance, when shortening the long sentences as an improvement in the readability of a contract, the document can become poor in grammar with missing nouns and too many abbreviations, as NEC standard contract is criticized in this respect by some scholars [19], [20]. On the other hand, addition of redundant technical information that could be included in technical specifications would increase the length of the sentences, provisions and clauses. Such examples of cause-effect relationships need to be analyzed, which actually establish the major aim of this study. The research steps and adopted methods to analyze the causal relationships of the most significant readability risks are shown in Fig. 2.
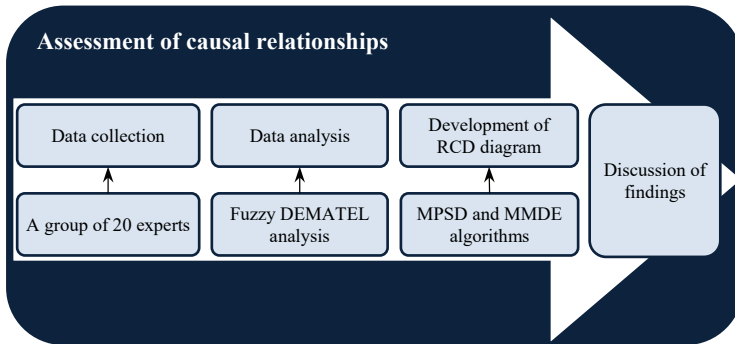

Fig. 2 - Research flow.

The first step of the assessment of causal relationships was to collect data in order to identify root causes of the most significant readability risks. A total number of 20 experts contributed to this study. Their professional backgrounds can be seen in Table 2. Past literature supports the sample sizes used in this study in terms of fuzzy DEMATEL method [48]–[50], since the quality of the data is regarded highly essential in a qualitative research as originally aimed in this study [48], [51]. In the data collection step, a decision framework was formed based on 10 readability risks (Table 1) leading to 10×10 decision matrix. Then, respondents were asked to provide their judgments using the linguistic variables (Table 3) regarding the influences of readability risks on each other. In other words, the influence of each readability risk on the others were inquired leading to 90 decisions (10×9) of each expert.

Table 2 - Professional background of experts.

ID	Proficiency	Education level	Role	Organization	Experience in construction industry (Year)	Experience in contract administration (Year)	Budget responsible (USD $)
E1	Civil engineering	Bachelor	Owner	Subcontractor	21	16	1 – 10 Million
E2	Civil engineering	MSc	Director	Contractor	24	12	1 – 10 Million
E3	Civil engineering	PhD	Senior executive director	Client	22	16	10 – 100 Million
E4	Civil engineering	Bachelor	Senior executive director	Client	25	17	10 – 100 Million
E5	Civil engineering	Bachelor	Owner	Contractor	32	27	≥ 100 Million
E6	Civil engineering	Bachelor	General manager	Client	17	13	≥ 100 Million
E7	Civil engineering	Bachelor	Project manager	Client	27	23	1 – 10 Million
E8	Civil engineering	Bachelor	Vice general director	Client	21	18	10 – 100 Million
E9	Civil engineering	Bachelor	Contract manager	Contractor	29	22	1 – 10 Million
E10	Architecture	MSc	Technical office architect	Contractor	7	4	≤1 Million
E11	Civil engineering	Bachelor	Senior executive director	Client	32	21	≥ 100 Million
E12	Civil engineering	Bachelor	Project coordinator	Contractor	20	13	10 – 100 Million
E13	Civil engineering	Bachelor	Site engineer	Subcontractor	5	5	≤1 Million
E14	Architecture	Bachelor	General manager	Client	24	20	1 – 10 Million
E15	Civil engineering	PhD	Contract manager	Contractor	21	21	1 – 10 Million
E16	Architecture	Bachelor	Project manager	Client	14	11	10 – 100 Million
E17	Architecture	MSc	Technical office manager	Client	11	8	1 – 10 Million
E18	Architecture	MSc	Design manager	Client	13	10	1 – 10 Million
E19	Architecture	Bachelor	Project coordinator	Client	28	20	10 – 100 Million
E20	Civil engineering	Bachelor	Technical office engineer	Client	8	6	1 – 10 Million

Table 3 - Fuzzy linguistic scales used in fuzzy DEMATEL method.

Linguistic variables	Influence score	Triangular fuzzy numbers
No influence	0	(0.00, 0.00, 0.25)
Very low influence	1	(0.00, 0.25, 0.50)
Low influence	2	(0.25, 0.50, 0.75)
High influence	3	(0.50, 0.75, 1.00)
Very high influence	4	(0.75, 1.00, 1.00)

The collected data was analyzed by a multi-criteria decision-making method, fuzzy DEMATEL. DEMATEL was selected particularly for its wide application as a practical method to underly root causes of various problems in the literature [52] such as labor productivity [53], intersection safety [54], waste management [55], and project performance [56]. This method has been used by many researchers, since it is powerful in separating net causes from net effects ensuring the underlying causes of the problems [54], drawing a root cause degree (RCD) diagram and aiding the development of countermeasures to the specific issues [57]. DEMATEL approach is very useful when critical and suitable

decisions for specific problems are sought [58], [59]. In addition, a network relation map can be constructed, which enables the observations of the correlated factors [60]. The method has been regarded as one of the most prominent methods to evaluate the importance of causal relationships among included criteria as well as having an ability to validate the interrelationships of evaluated criteria [48]. Since traditional DEMATEL method considers neither fuzziness, nor subjectivity in decision-making processes, fuzzy DEMATEL approach was adopted. Respondents, who participated in the questionnaire were chosen by judgment sampling based on their experiences and roles in construction contract administration [61]. At this point, a variety of participant features were considered to mark diversification in contract administration with respect to backgrounds of the participants. Interviews were performed through face-to-face individual discussion sessions. The objective of the research and fundamentals of DEMATEL analysis were explained to maximize the accuracy in their judgments for better representation.

For the initial step of the fuzzy DEMATEL method, direct relation matrix (T) was formed by experts through adopting pairwise comparisons between readability risks. Each element in T was converted to triangular fuzzy number (TFN) denoted as (l_{ij}, m_{ij}, r_{ij}) indicating the influences of risk i on risk j. Triangular fuzzy scale used in fuzzy DEMATEL method is presented in Table 3 [62].

Adopted fuzzy DEMATEL method included five main steps as follows [62]:

1) TFNs were converted into direct relation matrix (Z). For this preliminary step, normalization was performed by using Eqs. (1) – (3).

$$xr_{ij}^n = \frac{\left(r_{ij}^n - \min l_{ij}^n\right)}{\Delta_{min}^{max}} \tag{1}$$

$$xm_{ij}^n = \frac{\left(m_{ij}^n - \min l_{ij}^n\right)}{\Delta_{min}^{max}} \tag{2}$$

$$xl_{ij}^n = \frac{\left(l_{ij}^n - \min l_{ij}^n\right)}{\Delta_{min}^{max}} \tag{3}$$

where $\Delta_{min}^{max} = \max r_{ij}^n - \min l_{ij}^n$; $n = 1, 2, 3, …, h$ is the number of experts. Then, right (rs) and left (ls) normalized values were calculated as follows:

$$xrs_{ij}^n = \frac{xr_{ij}^n}{(1+xr_{ij}^n-xm_{ij}^n)} \tag{4}$$

$$xls_{ij}^n = \frac{xm_{ij}^n}{(1+xm_{ij}^n-xl_{ij}^n)} \tag{5}$$

Then, aggregated crisp values were calculated by using Eqs. (6) – (8).

$$x_{ij}^n = \frac{xls_{ij}^n\left(1-xls_{ij}^n\right)+xrs_{ij}^n\times xrs_{ij}^n}{\left(1-xls_{ij}^n+xrs_{ij}^n\right)} \tag{6}$$

$$Z_{ij}^n = \min l_{ij}^n + x_{ij}^n \times \Delta_{min}^{max} \tag{7}$$

$$Z_{ij} = \frac{(Z_{ij}^1 + Z_{ij}^2 + \cdots + Z_{ij}^h)}{h} \tag{8}$$

where x_{ij}^n is the total normalized crisp values; Z_{ij}^n is the computed crisp value for expert n.

2) Generalized direct relation matrix (S) was calculated by Eq. (9).

$$S = \frac{1}{max_{1 \leq i \leq n} \sum_{j=1}^n Z_{ij}} \times Z \tag{9}$$

3) Total relation matrix (M) was computed by using Eq. (10) as follows:

$$M = S(I - S)^{-1} \tag{10}$$

where, I is the identity matrix. Therefore, indirect effects of readability risks on each other were taken into account. The overall total relation matrix of readability risks is presented in Table 4.

Table 4 - Total relation matrix.

R	R1	R2	R3	R4	R5	R6	R7	R8	R9	R10
R1	0.78	0.92	0.85	0.85	0.93	0.90	0.78	0.62	0.81	0.72
R2	0.94	0.87	0.90	0.91	**0.99**	**0.97**	0.82	0.66	0.88	0.78
R3	0.89	0.93	0.79	0.89	<u>0.95</u>	0.93	0.79	0.64	0.84	0.75
R4	0.91	<u>0.96</u>	0.90	0.79	<u>0.95</u>	<u>0.96</u>	0.79	0.64	0.85	0.76
R5	0.94	**1.00**	0.93	0.91	0.89	**0.99**	0.83	0.67	0.88	0.78
R6	<u>0.95</u>	**1.00**	0.94	0.94	**1.00**	0.89	0.84	0.68	0.90	0.81
R7	0.86	0.91	0.85	0.85	0.91	0.90	0.68	0.62	0.80	0.71
R8	0.69	0.70	0.67	0.67	0.73	0.70	0.59	0.43	0.62	0.56
R9	**0.96**	**1.00**	**0.96**	<u>0.95</u>	**1.01**	**1.01**	0.84	0.67	0.80	0.79
R10	0.72	0.75	0.70	0.70	0.76	0.75	0.63	0.51	0.67	0.53

Note: Bold values are equal or higher than the MMDE, and underlined values are equal or higher than the MPSD thresholds.

In Table 4, the sum of rows and the sum of columns were then referred as D and R, respectively. D + R was denoted as the prominence (P_i), while D – R was the net effect (E_i). Prominence and net effects of readability risks are presented in Table 5. It is important to note that positive E value indicates that the corresponding risk is a net cause factor (influences others more than it is influenced by), while a negative E value indicates that the risk is a net effect factor (influenced by others more than it influences others).

Table 5 - Prominence and net effect.

ID	D	R	E_i	P_i
R1	8.14	8.64	-0.50	16.78
R2	8.72	9.05	-0.33	17.77
R3	8.40	8.49	-0.09	16.89
R4	8.50	8.46	0.04	16.96
R5	8.82	9.13	-0.31	17.96
R6	8.95	9.02	-0.07	17.97
R7	8.09	7.58	0.51	15.68
R8	6.39	6.14	0.24	12.53
R9	9.01	8.05	0.95	17.06
R10	6.74	7.19	-0.44	13.93

4) Since all readability risks have effects on others in a varying extent, an acceptable threshold value must be established to keep the complexity of the identified system manageable, so that the ones with smaller impacts in total relation matrix can be filtered out. It should be noted that only an acceptable degree of threshold value can provide meaningful information about the relation system [63]. Therefore, threshold values should be neither very high, nor very low. Two different approaches were addressed in the literature for threshold value determination as mean plus standard deviation (MPSD) approach and maximum mean de-entropy (MMDE) algorithm. In this study both threshold values were calculated.

Average and standard deviation of all elements in Table 4 were calculated in MPSD approach and their sum was set as a threshold value. 0.946 was computed as a threshold value by adopting MPSD approach through Eq. (11).

$$T^{MPSD} = SD + \bar{x} \tag{11}$$

where SD and $\bar{x}$ are the standard deviation and average values of all 100 elements in Table 4, and T^{MPSD} is the threshold value calculated by adopting MPSD approach.

As an alternative approach, the threshold value was also determined based on robust MMDE algorithm based on entropy approach proposed by Li and Tzeng [63]. This algorithm has been implemented in information science, in which entropy refers to the criterion used to determine the amount of uncertainty. MMDE algorithm used in fuzzy DEMATEL analysis involved the following steps [48], [63]–[65]:

    (i) Matrix M in Table 4 was converted to an ordered set M, which involves $\{m_{11}, m_{12}, \ldots, m_{21}, m_{22}, \ldots, m_{nn}\}$ where m_{nn} is an element of $n \times n$ total relation matrix. Then, each element in the matrix was rearranged from the highest to the smallest and converted into a M^* denoting an ordered triplet as (m_{ij}, x_i, x_j). In this triplet, m_{ij} is the influence value computed in the matrix M, x_i and x_j are the order of row and column numbers referred as dispatch

node and receive node, respectively. For simplification reasons, only dispatch node was considered in the steps (ii)-(iv).

(ii) The second element of M^* was obtained for each element of the total relation matrix, to generate new set of ordered dispatch node, M^{Di} as $(x_1, x_2, \ldots, x_n)$ with a corresponding probability of $P = (p_1, p_2, \ldots, p_n)$.

(iii) The first element of M^{Di} was taken as a new set M_t^{Di} to assign the probability of each element in the new set. Accordingly, H_D of the set M_t^{Di}, H_t^{Di} was computed by using Eq. (12).

$$H(p_1, p_2, \ldots, p_n) = -\sum p_i . \ln(p_i) \tag{12}$$

$$p_i = \frac{k}{m} \tag{13}$$

Subject to:

$$\sum_{i=1}^{n} p_i = 1 \tag{14}$$

$$p_i . \ln(p_i) = 0 \quad \text{if } p_i = 0 \tag{15}$$

$$H^D = H\left(\frac{1}{n}, \frac{1}{n}, \ldots, \frac{1}{n}\right) - H(p_1, p_2, \ldots, p_n) \tag{16}$$

where p_i is the probability of the variable x_i, m is the number of variables in M^{Di}, k is the observed frequency of variable x_i, and H^D is the de-entropy value.

(iv) The mean de-entropy was determined by using Eq. (17) as follows:

$$MDE_t^{Di} = \frac{H_t^{Di}}{N(M_t^{Di})} \tag{17}$$

where $N(M_t^{Di})$ is the number of variables with unique values. Maximum MDE_t^{Di} and its corresponding M_t^{Di} values were then chosen in a number of $C(M_t^{Di})$ mean de-entropy values, where $C(M_t^{Di})$ is the total number of variables. This dispatch node set was denoted as M_{max}^{Di}.

(v) An ordered receive node set M^{Re} and a MMDE set M_{max}^{Re} was computed by adopting the same steps (ii)-(iv).

(vi) First u elements in M^* was taken as the subset while having T^{Th}, which consists of M_{max}^{Di} and M_{max}^{Re}, the threshold value was determined from the minimum influence value in T^{Th}. After all the calculations made in Excel, MMDE value was calculated as 0.964.

Hence, threshold values calculated through MMDE (0.964) and MPSD (0.946) algorithms were used to highlight significant relationships between readability risks and indicated in Table 4 (with bolded and underlined values, respectively). It is important to

note the difference between significant relationships calculated through MMDE and MPSD algorithms. The relationships between readability risks were stronger regarding threshold value calculated through MMDE algorithm compared to one attained via MPSD method. In this study, both MMDE and MPSD threshold values were used to draw attention to the causal risks, while other researchers might consider relationships based on only MMDE method to focus on the more crucial causal relationships.

5) At the last step of fuzzy DEMATEL analysis, root cause degree (RCD) diagram was drawn by mapping the dataset of (D + R, D − R), where (D + R) was put at horizontal axis, and (D − R) was put at vertical axis. If $(D_x - R_x) > 0$, then the criterion x dispatches the impact on other factors more than it receives [66]. RCD diagram of readability risks is illustrated in Fig. 3. Calculated threshold values from both MPSD and MMDE approaches were used in the diagram to show the relationships between readability risks. RCD diagram (Fig. 3) drawn based on total relation matrix (Table 4) and threshold values shows that R9, R7, R8 and R4 were the cause factors (influences other risks more than influenced by others), while the rest of the readability risks were effect factors (affected by the factors rather than affecting the others). R9 was the most significant causal factor influencing majority of the readability risks apart from R7, R8 and R10, which were found to be independent readability risks. On the other hand, R1 was the most affected readability risk in the overall scheme, which was directly influenced by R9 (with respect to MMDE) and R6 (with respect to MPSD).
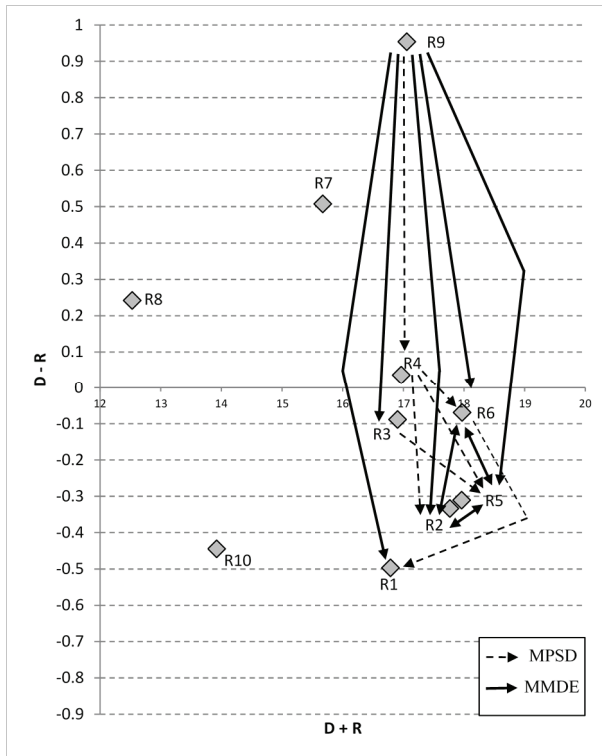

Fig. 3 - RCD diagram of readability risks.

5. DISCUSSIONS

Based on analysis results of Koc and Gurgun [25], the top five most significant readability risks were identified as "unnecessary complexity in the scope of work with complex noun phrases and improper use of referents (R2)", "abstractness and ambiguity in word or sentence causing more than one meaning (R6)", "unnecessary length in the clauses, sentences, and words (R1)", "lack of visual representations (R8)", and "controversial uses to legal terms and incoherence including other contracts in the projects (R5)". These findings may be of interest for decision makers and contract drafters during contract preparation and administration phases. With a closer look into the analysis of their causal relationships, further details and outcomes could be provided to understand their impacts on each other, which is actually the aim of this study. Findings of fuzzy DEMATEL were helpful to map out the root cause factors within the most significant risks based on their causal relationships. For example, "poor grammar use including missing nouns, words formation (R9)" and "use of specialized vocabulary, legal terms and legal jargon (R7)" were found to be the root causes of readability risks in construction contracts, with 0.95 and 0.51 net effect values, respectively. Other two cause factors (R8 and R4) were assessed with net effect values less than 0.25, separating top two from them. It can be noted that the results of prioritization solely may not always be adequate to develop effective measures, since improvements regarding them may not clarify the contract document as expected due to lack of understanding the causal relationships between them. Table 6 shows the most significant ten readability risks and their roles in causal hierarchy developed by using fuzzy DEMATEL approach.

Table 6 - The role of the most significant ten readability risks in causal hierarchy.

Risk factor	Rank in fuzzy VIKOR Koc and Gurgun, [25]	Causal rank in Fuzzy DEMATEL	Causal position	Influence on	Influenced by
R2	1	8	Net effect	R5, R6	R4, R5, R6, R9
R6	2	5	Net effect	R1, R2, R5	R2, R4, R5, R9
R1	3	10	Net effect	−	R6, R9
R8	4	3	Net cause	−	−
R5	5	7	Net effect	R2, R6	R2, R3, R4, R6, R9
R9	6	1	Net cause	R1, R2, R3, R4, R5, R6	−
R7	7	2	Net cause	−	−
R4	8	4	Net cause	R2, R5, R6	R9
R3	9	6	Net effect	R5	R9
R10	10	9	Net effect	−	−

Some additional highlights can be pointed out based on analysis findings. One of the most remarkable outcomes was that four of the top five readability risks, which were highlighted by Koc and Gurgun [25], were actually found to be net effect factors. The results may be of particular importance, since in fact improvements in effect factors may not be effective as much as expected, allowing related problems remain in the contract documents if

underlying causes are disregarded. For instance, despite reducing the length of the sentences could be regarded as one of the mostly recommended measures, this could lead poor grammatical structure with missing nouns [20], which was found to be the most significant causal factor in this study. A clear flow from R9 to R1 was found in this study (Fig. 3), which is on the contrary to what is generally believed [20]. The reason of this could be that poor grammatical structure and missing nouns could cause potential readers of construction contracts to perceive the sentences are unnecessarily long complicating its readability. That is probably why reducing sentence length was ineffective in facilitating the readability of sentences due to issues caused by poor grammatical structure [20]. As another example, excessive use of legal terminology could make contracts even harder to read since they are drafted by lawyers but used by engineers. It can be noted that abandoning legal terminology has been regarded as one of the revolutionary steps of NEC drafters [2], and use of specialized vocabulary, legal terms and legal jargon (R7) was found to be the second causal readability risk in this study. Five of the six net effect factors in Table 6 were influenced by "poor grammar use including missing nouns, words formation (R9)", making it the most significant causal factor affecting readability of construction contracts. In other words, even though problems about noun phrases, referents, ambiguous words and controversies could contribute to the poor contract document at most; using wrong grammatical structure with missing nouns and poor word formations could be the root causes of these problems. Fig 3. shows clear flows from R9 at the top, to the net effects in the middle and at the bottom. R7 was determined and shown as the second most significant causal factor in RCD diagram. Although it was not found to be the significant cause of any of the other risks, it was identified to be affecting all the others in some extent, without being influenced by them. One of the experts contributed to this study indicated that sometimes it was very difficult to incorporate the updated standards to contract provisions, thus increasing the readability risk of the corresponding clauses. Frequently updated conditions with legal terminology could decrease the quality and readability of contract documents [21].

According to the threshold values calculated by MPSD and MMDE approaches, "use of specialized vocabulary, legal terms and legal jargon" (R7), "lack of visual representations" (R8), and unnecessary use of abbreviations (R10) were found to be independent readability risks. In other words, when these risks emerged, then the readability of overall contract document was affected, more than due to emergence of other individual risks. Visual representation (R8) with respect to transparency [24], and use of abbreviations (R10) with respect to simplicity [20] were important readability factors, affecting and affected by others below the threshold values. The results are considered pertinent since R8 and R10 cannot easily be associated with other readability risks. Visualization could significantly supplement contract documents through diagrams, charts, timelines, images etc., which may appear inside a contract or alongside of it [67], making it harder to relate with other readability factors. Similarly, excessive use of abbreviation could paralyze the ability of the readers to think clearly [68], as a discriminating attribute of it from others. On the other hand, despite "use of specialized vocabulary, legal terms and legal jargon" (R7) was the second most causal factor in RCD diagram, it was determined as an independent readability risk. The reason of this could be that experts participated to fuzzy DEMATEL questionnaires kept the influences of R7 on the other risks in a large extent but just below the calculated threshold values. At the very bottom of the RCD diagram, "unnecessary

length in the clauses, sentences and words" (R1) was seen as a net effect factor influenced by "poor grammar use including missing nouns, words formation" (R9), with respect to MMDE and R6 with respect to MPSD. Despite R1 was the third most significant readability risk, amelioration of sentences in terms of length could not be as effective as expected since it was the most affected factor placed at the bottom of the RCD diagram. There were some other readability factors contributing to the length of the sentences, provisions and clauses, relatively less significant but underlying cause factors. Therefore, improvement of the length related risks should not be considered individually to improve the quality of construction contracts [20].

Interestingly, "unnecessary complexity in the scope of work with complex noun phrases and improper use of referents" (R2), "controversial uses to legal terms and incoherence including other contracts in the projects" (R5), "abstractness and ambiguity in word or sentence causing more than one meaning" (R6) triangle emerged with a dyadic nature such that all affected each other (Fig. 3). This can be another significant finding since it indicated that differentiating these three from each other during contract drafting process could be less effective, compared to the risk mitigation measures covering all three risks. The results implied that scope complexity with inadequate noun phrases, ambiguous expressions and words, and incoherence could be regarded as bound to each other in construction contracts. For instance, when the scope of the work is complex by using inadequate noun phrases, then its provisions relationally unclear. Correspondingly, when there are too many ambiguous words in the provisions, then the scope of the work would become more complex. Similar to this, when incoherence with controversial uses is high, then the scope of the work could become more complex. If the complexity of the scope of the work is apparent in different contracts in a project, then it is likely to include inconsistent expressions between other contracts in the project. This highlights that in some cases, considering group of measures could be more effective than treating them individually.

6. IMPLICATIONS FOR CONTRACT DRAFTERS

Poor contract documentation was considered by various scholars as major causal factors incurring construction conflicts [69], [70]. With the aim of increasing the ease of contract reading, this study further revealed the underlying causes of readability problems in construction contracts. Ranking the most significant readability risks could provide contract drafters a guideline for risk management; however, solely focusing on this might cause overlooking the fact that risk factors affecting readability of construction contracts are related to each other. With the butterfly effect in mind [71], estimating the consequences of any positive steps on the other readability risks is essential for improved contract drafting process. By managing underlying causes determined through fuzzy DEMATEL analysis [72], sub-optimality in the readability of construction contracts can be improved in a more effective manner, differentiating cause factors from effect factors.

While drafting contract and performing modifications, it can be difficult for contract drafters to consider the impacts of the modifications on the clarity and readability of documents [22]. Traditionally, reducing the number of syllables in words, words in sentences, and sentences in clauses are recommended [1], which are also considered in readability formulas [73], and adopted commonly by contract drafters to increase clarity

and ease of reading. This can be related to the fact that construction contracts are usually considered as voluminous documents, with long and complex sentences. However, despite regarded as one of the most significant readability risks, "unnecessary length in the clauses, sentences, and words" was found to be the most affected factor in this study, ranking last in the causal hierarchy. This finding entails particular attention, since it reveals that the efforts made by improving contract documents through length-related measures could be ineffective at some point if other causal risks that result in lengthy documents are not managed properly. Furthermore, "scope complexity with improper noun phrases and referents" was found to be the most significant factor affecting the readability of construction contracts, however, ranked eighth in causal hierarchy based on the fuzzy DEMATEL method outcomes. By looking into RCD diagram, poor grammar use, ambiguous words and sentences, and their incoherent uses should be avoided to reduce complexity of the scope of work. RCD diagram can also be used to develop countermeasures for some of the particular readability problems. Fig. 4 shows a framework for scope drafting in a construction contract developed based on RCD diagram, as a practical implication.
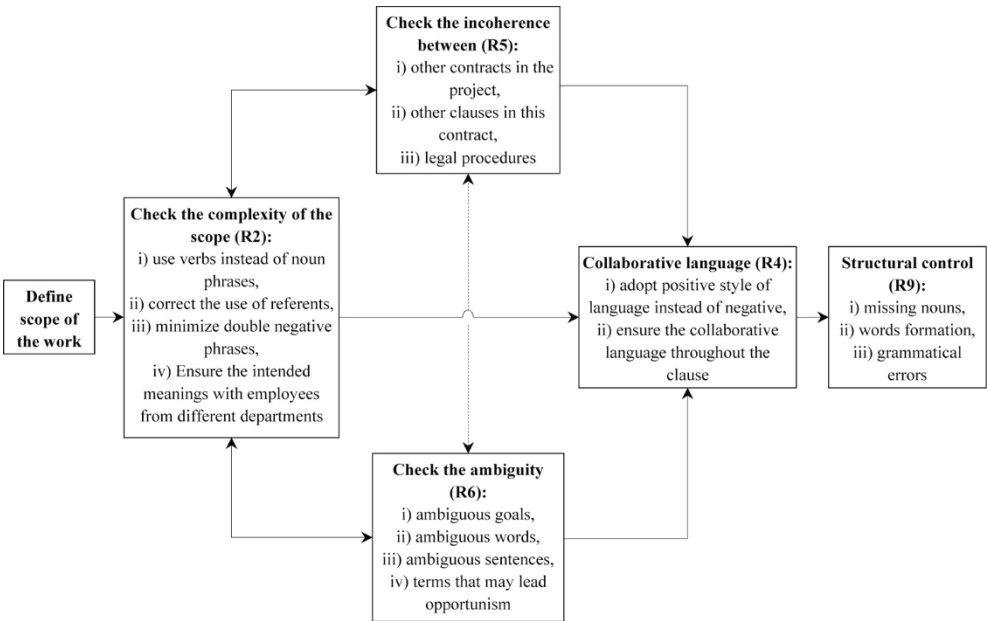

Fig. 4 - Example of a scope drafting based on proposed RCD diagram.

To perform useful improvements in overall contract readability to prevent contractual conflicts, four of the readability risks, which were determined as net causes require proper management. These factors are particularly important for contract drafters since effective measures should be adopted to minimize the negative impacts of the underlying cause factors, solving the readability problems in contracts immediately. These readability risks were identified as: poor grammar use including missing nouns, words formation; use of specialised vocabulary, legal terms and legal jargon; lack of visual representations; and use

of negative style of language. Therefore, while drafting construction contracts or modifications to standard contract forms, contract drafters should pay more attention to these four risks to increase clarity and readability of documents. Such a preventative approach against potential disputes can be considered as an effective strategy for construction projects since the conflicts between contracting parties can be avoided from emerging during project execution process, with the efforts made during contract drafting process.

7. CONCLUSION

This study aimed to reveal underlying root causes of readability risks in contraction contracts. In this context, the most significant readability risks were analyzed by fuzzy DEMATEL method to specify the cause-effect relationships among them. The adoption of fuzzy DEMATEL analysis contributes a lot to obtain the findings in this study since components of contracts have strong relationship with each other. Without focusing on the underlying cause factors, the intended measures could not be as effective as expected.

Some significant highlights can be implied from the findings of fuzzy DEMATEL analysis. First, four of the most significant five risks were found to be net effect factors, indicating the ineffectiveness of the traditionally suggested measures for smooth, readable, and clear contract documentation. "Poor grammar use including missing nouns, words formation" and "use of specialized vocabulary, legal terms and legal jargon" were determined as the most causal factors, while "unnecessary length in the clauses, sentences, and words" and "unnecessary use of abbreviations" were the most affected readability risks. Contract clarification strategies can be employed for proper grammar use, missing nouns, words formation, and specialized legal terms to improve the whole contract documents most effectively. Scope complexity, ambiguity, and incoherence were determined to be as a triangle with dyadic relationships with each other. Therefore, remediation in any of them could improve the conditions of others relationally. This can depict the picture of scope complexity in construction contracts.

The literature lacks the investigation of underlying causes of readability risks in construction contracts. Discovering the root causes of readability risks and developing countermeasures accordingly to improve the readability of construction contracts can establish the fundamentals of successful risk management. Without the proposed approach, the real facts of risks and their underlying causal relationships could be overlooked resulting without substantial benefits from risk management implementation. Therefore, these interrelationships need to be accounted for particularly during contract drafting phase. The root cause degree diagram can be used to develop countermeasures for some particular readability issues. The findings of this study are useful for contract drafters, dealing with traditional, standard contract forms such as FIDIC and NEC, or contract modifications, by emphasizing the most effective measures to improve the quality of contract documents. Modifications to the specific clauses in standard contract forms could be made based on RCD diagram proposed in this study, and the results can be investigated in a case study by interested researchers in the future.

References

[1] Chong, H. Y. and Zin, R. M., A case study into the language structure of construction standard form in Malaysia, *International Journal of Project Management* 28, 601–608 2010.

[2] Besaiso, H., Fenn, P., Emsley, M., and Wright, D., A comparison of the suitability of FIDIC and NEC conditions of contract in Palestine: A perspective from the industry, *Engineering, Construction and Architectural Management* 25, 241–256 2018.

[3] El-Sayegh, S. M. and Mansour, M. H., Risk assessment and allocation in highway construction projects in the UAE, *Journal of Management in Engineering* 31, 04015004 2015.

[4] Zhang, L., Fenn, P., and Fu, Y., To insist or to concede? Contractors' behavioural strategies when handling disputed claims, *Engineering, Construction and Architectural Management* 26, 424–443 2019.

[5] Cheung, S. O. and Yiu, T. W., Are construction disputes inevitable?, *IEEE Transactions on Engineering Management* 53, 456–470 2006.

[6] Saseendran, A., Bigelow, B. F., Rybkowski, Z. K., and Jourdan, D. E., Disputes in Construction : Evaluation of Contractual Effects of ConsensusDOCS, *Journal of Legal Affairs and Dispute Resolution in Engineering and Construction* 12, 04520008 2020.

[7] El-Adaway, I. H., Abotaleb, I. S., Eid, M. S., May, S., Netherton, L., and Vest, J., Contract Administration Guidelines for Public Infrastructure Projects in the United States and Saudi Arabia: Comparative Analysis Approach, *Journal of Construction Engineering and Management* 144, 04018031 2018.

[8] Love, P. E. D., Davis, P. R., Cheung, S. O., and Irani, Z., Causal discovery and inference of project disputes, *IEEE Transactions on Engineering Management* 58, 400–411 2011.

[9] Chong, H. Y. and Zin, R. M., Construction contract administration- an approach on clarity, *Clarity* 60, 6–10 2008.

[10] Arcadis, Global Construction Disputes Report: Collaborating to achieve project excellence, Amsterdam, Netherlands, 2020.

[11] Cheung, S. O. and Pang, K. H. Y., Anatomy of construction disputes, *Journal of Construction Engineering and Management* 139, 15–23 2013.

[12] Maqsoom, A., Wazir, S. J., Choudhry, R. M., Thaheem, M. J., and Zahoor, H., Influence of Perceived Fairness on Contractors' Potential to Dispute: Moderating Effect of Engineering Ethics, *Journal of Construction Engineering and Management* 146, 04019090 2020.

[13] Wang, Y., Chen, Y., Wang, W., Chen, Y., and Jin, M., Revisiting the Relationship Between Contract Governance and Contractors' Opportunistic Behavior in Construction Projects, *IEEE Transactions on Engineering Management* 1, 1–13 2019.

[14] Cevikbas, M. and Koksal, A., An Investigation of Litigation Process in Construction Industry in Turkey, *Teknik Dergi* 29, 8715–8729 2018.

[15] Rameezdeen, R. and Rajapakse, C., Contract interpretation: The impact of readability, *Construction Management and Economics* 25, 729–737 2007.

[16] Gunduz, M. and Elsherbeny, H. A., Operational Framework for Managing Construction-Contract Administration Practitioners ' Perspective through Modified Delphi Method, *Journal of Construction Engineering and Management* 146, 040191110 2020.

[17] Yao, M. *et al.*, Optimal Incentive Contract with Asymmetric Cost Information, *Journal of Construction Engineering and Management* 146, 04020054 2020.

[18] Yiu, T. W., Cheung, S. O., and Lok, C. L., A fuzzy fault tree framework of construction dispute negotiation failure, *IEEE Transactions on Engineering Management* 62, 171–183 2015.

[19] Beaumont, B., Dispute Resolution in NEC3—User Unfriendly?, *Construction Law Journal* 25, 591–613 2009.

[20] Murphy, S. E., Spillane, J. P., Hendron, C., and Bruen, J., NEC Contracting: Evaluation of the Inclusion of Dispute Review Boards in lieu of Adjudication in the Construction Industry in the United Kingdom, *Journal of Legal Affairs and Dispute Resolution in Engineering and Construction* 6, 04514002 2014.

[21] Raj, S., Hillig, J. B., and Hughes, W., Responsiveness to change by standard-form contract drafters in the construction industry: A case study of the FIDIC White Book, *International Journal of Law in the Built Environment* 1, 205–220 2009.

[22] Rameezdeen, R. and Rodrigo, A., Modifications to standard forms of contract: The impact on readability, *Australasian Journal of Construction Economics and Building* 14, 31–40 2014.

[23] Mitropoulos, P. and Howell, G., Model for Understanding, Preventing, and Resolving Project Disputes, *Journal of Construction Engineering and Management* 127, 223–231 2001.

[24] Schuhmann, R. and Eichhorn, B., Reconsidering contact risk and contractual risk management, *International Journal of Law and Management* 59, 504–521 2017.

[25] Koc, K. and Gurgun, A. P., Assessment of Readability Risks in Contracts Causing Conflicts in Construction Projects, *Journal of Construction Engineering and Management* 147, 04021041 2021.

[26] Hassan, F. U. and Le, T., Automated Requirements Identification from Construction Contract Documents Using Natural Language Processing, *Journal of Legal Affairs and Dispute Resolution in Engineering and Construction* 12, 04520009 2020.

[27] Zakaluk, B. L. and Samuels, S. J., *Readability, Its Past, Present, and Future*. Newark, Delaware: The International Reading Association, 1988.

[28] Abotaleb, I. S., El-Adaway, I. H., and Moussa, M. B., Guidelines for Administrating and Drafting Nonpayment Owners' Obligation Provisions under Design-Build Contracts, *Journal of Management in Engineering* 35, 04019010 2019.

[29] Broome, J. C. and Hayes, R. W., A comparison of the clarity of traditional construction contracts and of the New Engineering Contract, *International Journal of Project Management* 15, 255–261 1997.

[30] Lau, C. H., Mesthrige, J. W., Lam, P. T. I., and Javed, A. A., The challenges of adopting new engineering contract: a Hong Kong study, *Engineering, Construction and Architectural Management* 26, 2389–2409 2019.

[31] Youssef, A., Osman, H., Georgy, M., and Yehia, N., Semantic Risk Assessment for Ad Hoc and Amended Standard Forms of Construction Contracts, *Journal of Legal Affairs and Dispute Resolution in Engineering and Construction* 10, 04518002 2018.

[32] Lee, J., Ham, Y., Yi, J. S., and Son, J., Effective Risk Positioning through Automated Identification of Missing Contract Conditions from the Contractor's Perspective Based on FIDIC Contract Cases, *Journal of Management in Engineering* 36, 05020003 2020.

[33] Shi, L., He, Y., Onishi, M., and Kobayashi, K., Double Moral Hazard and Risk-Sharing in Construction Projects, *IEEE Transactions on Engineering Management* 1, 1–11 2019.

[34] Zeng, W., Wang, H., Li, H., Zhou, H., Wu, P., and Le, Y., Incentive Mechanisms for Supplier Development in Mega Construction Projects, *IEEE Transactions on Engineering Management* 66, 252–265 2019.

[35] Ameer Ali, N. A. N. and Wilkinson, S., Modernising Construction Contracts Drafting – A Plea for Good Sense, 2010.

[36] Chong, H. Y. and Oon, C. K., A practical approach in clarifying legal drafting: Delphi and case study in Malaysia, *Engineering, Construction and Architectural Management* 23, 610–621 2016.

[37] Menches, C. L. and Dorn, L., Emotional Reactions to Variations in Contract Language, *Journal of Legal Affairs and Dispute Resolution in Engineering and Construction* 5, 97–105 2013.

[38] Cutts, M., *Oxford Guide to Plain English*. New York: Oxford University Press, 2004.

[39] Chong, H. Y., Balamuralithara, B., and Chong, S. C., Construction contract administration in Malaysia using DFD: A conceptual model, *Industrial Management and Data Systems* 111, 1449–1464 2011.

[40] Clough, R. H., Sears, G. A., and Sears, S. K., *Construction project management*. New York: John Wiley & Sons, 2000.

[41] Ameer Ali, N. A. N., Modern Plain English Drafting and Construction: the Malaysian Subcontract Model Terms, *Society of Construction Law* D90, 1–67 2008.

[42] Candlin, C. N., Bhatia, V. K., and Jensen, C. H., Developing legal writing materials for English second language learners: Problems and perspectives, *English for Specific Purposes* 21, 299–320 2002.

[43] Argyres, N. and Mayer, K. J., Contract Design as a Firm Capability: An Integration of Learning and Transaction Cost Perspectives, *The Academy of Management Review* 32, 1060–1077 2007.

[44] Azghandi-Roshnavand, A., Evaluation of construction contract documents to be applied in modular construction focusing ambiguities; A text processing approach, Concordia University, 2019.

[45] Kumaraswamy, M. M., Consequences of Construction Conflict: A Hong Kong Perspective, *Journal of Management in Engineering* 14, 66–74 1998.

[46] Acharya, N. K., Dai Lee, Y., and Man im, H., Conflicting factors in construction projects: Korean perspective, *Engineering, Construction and Architectural Management* 13, 543–566 2006.

[47] El-adaway, I. H., Vance, R. A., and Abotaleb, I. S., Understanding Extension of Time under Different Standard Design-Build Forms of Contract, *Journal of Legal Affairs and Dispute Resolution in Engineering and Construction* 12, 04519031 2020.

[48] Costa, F., Denis Granja, A., Fregola, A., Picchi, F., and Portioli Staudacher, A., Understanding Relative Importance of Barriers to Improving the Customer-Supplier Relationship within Construction Supply Chains Using DEMATEL Technique, *Journal of Management in Engineering* 35, 04019002 2019.

[49] Liu, H. and Long, H., Identification of critical factors in construction and demolition waste recycling by the grey-DEMATEL approach: a Chinese perspective, *Environmental Science and Pollution Research* 27, 8507–8525 2020.

[50] Negash, Y. T. and Hassan, A. M., Construction Project Success under Uncertainty: Interrelations among the External Environment, Intellectual Capital, and Project Attributes, *Journal of Construction Engineering and Management* 146, 1–13 2020.

[51] Chileshe, N., Rameezdeen, R., and Hosseini, M. R., Drivers for adopting reverse logistics in the construction industry: A qualitative study, *Engineering, Construction and Architectural Management* 23, 134–157 2016.

[52] Zhang, X., Zhang, W., Jiang, L., and Zhao, T., Identification of Critical Causes of Tower-Crane Accidents through System Thinking and Case Analysis, *Journal of Construction Engineering and Management* 146, 04020071 2020.

[53] Nasirzadeh, F., Rostamnezhad, M., Carmichael, D. G., Khosravi, A., and Aisbett, B., Labour productivity in Australian building construction projects: a roadmap for improvement, *International Journal of Construction Management* 1, 1–10 2020.

[54] Zhou, S., Sun, J., Li, K., and Yang, X., Development of a Root Cause Degree Procedure for measuring intersection safety factors, *Safety Science* 51, 257–266 2013.

[55] Kumar, A. and Dixit, G., An analysis of barriers affecting the implementation of e-waste management practices in India: A novel ISM-DEMATEL approach, *Sustainable Production and Consumption* 14, 36–52 2018.

[56] Wang, D., Wang, X., Liu, M., Liu, H., and Liu, B., Managing public – private partnerships: a transmission pattern of underlying dynamics determining project performance, *Engineering, Construction and Architectural Management* 2020.

[57] Chen, C.-A., Using DEMATEL method for medical tourism development in Taiwan, *American journal of tourism research* 1, 26–32 2012.

[58] Lin, C. L. and Tzeng, G. H., A value-created system of science (technology) park by using DEMATEL, *Expert Systems with Applications* 36, 9683–9697 2009.

[59] Ghoddousi, P., Nasirzadeh, F., and Hashemi, H., Evaluating Highway Construction Projects' Sustainability Using a Multicriteria Group Decision-Making Model Based

on Bootstrap Simulation, *Journal of Construction Engineering and Management* 144, 2018.

[60] Charkhakan, M. H. and Heravi, G., Risk Manageability Assessment to Improve Risk Response Plan: Case Study of Construction Projects in Iran, *Journal of Construction Engineering and Management* 144, 2018.

[61] Hasan, A., Elmualim, A., Rameezdeen, R., and Marshall, A., An exploratory study on the impact of mobile ICT on productivity in construction projects, *Built Environment Project and Asset Management* 8, 320–332 2018.

[62] Chang, B., Chang, C. W., and Wu, C. H., Fuzzy DEMATEL method for developing supplier selection criteria, *Expert Systems with Applications* 38, 1850–1858 2011.

[63] Li, C. W. and Tzeng, G. H., Identification of a threshold value for the DEMATEL method using the maximum mean de-entropy algorithm to find critical services provided by a semiconductor intellectual property mall, *Expert Systems with Applications* 36, 9891–9898 2009.

[64] Alzahrani, A. I., Al-Samarraie, H., Eldenfria, A., and Alalwan, N., A DEMATEL method in identifying design requirements for mobile environments: students' perspectives, *Journal of Computing in Higher Education* 30, 466–488 2018.

[65] Lee, P. T. W. and Lin, C. W., The cognition map of financial ratios of shipping companies using DEMATEL and MMDE, *Maritime Policy and Management* 40, 133–145 2013.

[66] Tzeng, G. H., Chiang, C. H., and Li, C. W., Evaluating intertwined effects in e-learning programs: A novel hybrid MCDM model based on factor analysis and DEMATEL, *Expert Systems with Applications* 32, 1028–1044 2007.

[67] Barton, T., Berger-walliser, G., and Haapio, H., Visualization: Seeing Contracts for What They Are, and What They Could Become, *Journal of Law, Business & Ethics* 19, 47–64 2013.

[68] Siegel, A. I., Lambert, J. V, and Burkett, J. R., Techniques for Making Written Material More Readable/Comprehensible, Texas, 1974.

[69] Yildizel, S. A., Dogan, E., Kaplan, G., and Ergut, A., Major Constructional Dispute Causes in Turkey, *Archives of Civil Engineering* 62, 193–204 2016.

[70] Jagannathan, M., Santosh, V., and Delhi, K., Litigation in Construction Contracts: Literature Review, *Journal of Legal Affairs and Dispute Resolution in Engineering and Construction* 12, 03119001 2020.

[71] Coyle, J. F., The Butterfly Effect in Boilerplate Contract Interpretation, *Law and Contempopary Problems* 82, 1–13 2019.

[72] Singh, R. and Bhanot, N., An integrated DEMATEL-MMDE-ISM based approach for analysing the barriers of IoT implementation in the manufacturing industry, *International Journal of Production Research* 58, 2454–2476 2020.

[73] Rameezdeen, R. and Rodrigo, A., Textual complexity of standard conditions used in the construction industry, *Australasian Journal of Construction Economics and Building* 13, 1–12 2013.

TECHNICAL NOTE

Applying the Hierarchical Gray Relational Clustering Method to Municipal Water Use in Turkey

Mehmet Şamil GÜNEŞ[1]
Coşkun PARİM[2]
Doğan YILDIZ[3]
Ali Hakan BÜYÜKLÜ[4]

ABSTRACT

This study aims to compare the municipal water distribution performance and classify the municipal water distribution systems in the provinces of Turkey using the Gray Relational Hierarchical clustering method for both 2006 and 2016. A correlation analysis was used to determine the variables affecting the distributed water. The Hierarchical gray clusters and the changes during the decade are presented with spatial distribution maps using statistically significant variables. Consequently, the findings reveal that the municipalities of Istanbul, Izmir, Bursa, Gaziantep, and Kocaeli managed water distribution effectively, whereas the municipalities of Konya, Şanlıurfa, Diyarbakır, Samsun, Trabzon, and Sakarya managed it poorly.

Keywords: Climate change, municipal water use, water management, sustainability.

1. INTRODUCTION

The importance of water distribution systems has increased gradually in recent years due to direct or indirect factors such as increasing population, water consumption, industrialization, seasonal conditions, and climate change [1, 2]. Currently, a critical concern is to ensure urban water sustainability and to improve the decision-making processes for sustainable development planning [3]. Water distribution modelling is used to predict what the future water consumption and requirements depend on, based on various socio-economic and

---

1 Department of Statistics, Yıldız Technical University, Istanbul, Turkey - msgunes@yildiz.edu.tr - https://orcid.org/0000-0001-5842-5181

2 Department of Statistics, Yıldız Technical University, Istanbul, Turkey - cparim@yildiz.edu.tr - https://orcid.org/0000-0002-6412-1325

3 Department of Statistics, Yıldız Technical University, Istanbul, Turkey - dyildiz@yildiz.edu.tr - https://orcid.org/0000-0001-7430-2368

4 Department of Statistics, Yıldız Technical University, Istanbul, Turkey - hbuyuklu@yildiz.edu.tr - https://orcid.org/0000-0002-4174-4538

climatic factors that affect water use. Domestic water consumption is the most significant component of municipal water use, and precise estimation techniques are required to accurately predict future water needs with appropriate methodologies [4].

Gray Relational Analysis (GRA) is a method that has been used recently in cases where the data set is small and contains insufficient information. Missing and insufficient information is very common in hydrological data in water research [5]. GRA was initially developed to be used for interval analysis in cases of insufficient information [6, 7]. Deng [8-10], on the other hand, produced the gray system theory, which can formally deal with small samples using fuzziness. GRA and its simple concept can be observed in many analyses that exhibit excellent performance when there is a small sample and insufficient information. In this study, Hierarchical Gray Relation Clustering (HGRC), a combination of GRA and Hierarchical Cluster Analysis, is applied to the distribution water model.

This study aims to compare the water distribution performance of the municipalities for 2006 and 2016 and to classify the provinces using HGRC. One of the main goals of the study is to use the HGRC method to determine the variables and regions that affect municipal water distribution.

This study is structured as follows. First, the scientific literature on water distribution systems and the basis of applying the method to municipal water distribution models is reviewed. Then, the study area and data are presented, followed by a discussion of the calculation procedure for hierarchical relation gray clustering analysis. Next, HGRC is applied to the variables that explain the distributed water, and the results are visualized with three spatial distribution maps. The cluster results in this study are then discussed, and the changes in the variables affecting the water distribution during the decade of study are determined. Additionally, the contribution of this analysis to water distribution management is discussed. Finally, suggestions are made for future steps by determining the levels of water management for the provinces and regions.

2. STUDY AREA AND DATA

Turkey is a country with a total geographical area of 780,000 km^2, comprising 81 provinces. Its municipalities are units with a population of over 2000. According to UN estimates, Turkey has a population of about 84 million, and 75.7% of its population lives in urban centers. Municipal water statistics are published by Turkstat [11] every two years and cover Turkey and its provinces. Therefore, instead of using a time series method, data from this source are analyzed separately for both 2006 and 2016 to illustrate changes, and the variables used are presented in Table 1. Municipal water statistics have been published in Turkey since 2003 (biennially after 2004) and the two years with complete data are 2006 and 2016. The study includes the annual data for 81 provinces.

Previous studies have shown that streamflow has a significant effect on the main variables (river, dam, lake, well, etc.) affecting water distribution [12, 13]. The streamflow is not included in this study due to the lack of data and discontinuities.

The variables used in the study and their correlations are presented in Table 1. The analysis in this study was concluded on the basis of 81 provinces, reflecting the general characteristics of the data, and the total values for Turkey are displayed in Table 1.

Mehmet Şamil GÜNEŞ, Coşkun PARİM, Doğan YILDIZ, Ali Hakan BÜYÜKLÜ

The amount of distributed water is the most convenient variable to represent the municipal water distribution system in Turkey. Therefore, the aspects that explain the amount of distributed water are also described in the water distribution system. Existing literature has revealed that there are many variables that directly or indirectly affect the amount of water distributed [14-16]. Correlation analysis was thus used to determine whether all the data received from Turkstat [11] are related to the amount of water distributed. These variables, their definitions, and the correlation table are presented in Table 1. As can be observed in this table, the variables that have a significant correlation with the amount of water distributed are TNM, RPSD, NS, WIN, TAWA, LAKE, RIV, DAM, WAPC, NTP, TC, and AWT, while the variables whose correlations with the AWD are insignificant are TNM, SPR, and WELL. The variables that were not significant in the correlation analysis were removed, and only the significant variables were used in the HGRC analysis.

Table 1 - Variables used in the study (with descriptives for 2006 and 2016) and their correlations.

Municipal Water Use Indicators, 2006-2016			
Variable Codes	**Definition of Variables**	**2006**	**2016**
AWD	Amount of water distributed (m³)	2375043	3732875
TNM	Total number of municipalities	3225	1397
TMP	Total municipal population	58581515	74911343
RPSD	Rate of the population served by drinking water treatment plants in total municipal population (%)	41	55
NS	Number of subscribers	19358951	27486201
WIN	Water income (Turkish Lira)	3096377755	14217798093
TAWA	Total amount of water abstracted (Thousand m³)	5163500	5838561
SPR	Spring (Thousand m³)	1380057	1000205
LAKE	Lake (Thousand m³)	232621	104354
RIV	River (Thousand m³)	305271	552624
DAM	Dam (Thousand m³)	1843736	2618225
WELL	Well (Thousand m³)	1401815	1563154
WAPC	Water abstraction per capita in municipalities (liters/capita-day)	245	217
NTP	Total number of treatment plants	139	519
TC	Total capacity	3994060	6592863
AWT	The total amount of water treated	2426639	3350389

Source: Turkish Statistical Institute [21]

		TNM	TMP	RPSD	NS	WIN	TAWA	SPR	LAKE	RIV	DAM	WELL	WAPC	NTP	TC	AWT
AWD	*Correlation Coefficient*	0.20	0.99	0.37	0.99	0.91	0.98	0.01	0.44	0.84	0.92	0.25	-0.11	0.41	0.90	0.95
	P - Value	p ≤ 0.05		p > 0.05				p ≤ 0.05		p > 0.05		p ≤ 0.05		p > 0.05		

HGRC analysis was then applied to examine the municipal water distribution system and yearly changing state of water management for all provinces in Turkey. Excel for HGRC was used to perform the analysis. Variables found to be significant through the correlation analysis in explaining the amount of water distributed were used in HGRC, and their spatial distribution maps are presented with the help of maps.

3. METHODS

3.1. Hierarchical Gray Relational Clustering

Deng [17] first proposed the gray system theory in 1982. Gray means that a system provides partially known and partially unknown information; thus, it basically is an attempt to model uncertainty. Gray systems theory is used to examine systems that analyze relationships between systems, make predictions and decisions, and create models [18]. In 1987, Deng [19] first proposed gray cluster analysis (GCA). A new method has been developed known as gray relational clustering (GRC), which combines gray relational analysis and clustering to capture the complex factors and mixed structure in gray cluster analysis. The GRC method cannot use a tree diagram for classification without recalculation [20]. Hence, Wu et al. [20] combined the GRC method with hierarchical cluster analysis.

The calculation procedure for hierarchical gray relation clustering analysis proceeds as follows for the data set used in our study.

Let x_{jk} specify the kth coordinate axis of the jth province, and let x_j represent the indices for the jth province. It may be written as follows:

$$x_j = (x_{j1}, x_{j2}) \tag{1}$$

Step 1. Compute the difference series:

$$\Delta_{ij}(k) = \left| x_i(k) - x_j(k) \right| \tag{2}$$

Step 2. Compute the minimum and maximum of the difference series:

$$\Delta_{max} = \max_{\forall j \in i} \max_{\forall k} \left| x_i(k) - x_j(k) \right|$$
$$\Delta_{min} = \min_{\forall j \in i} \min_{\forall k} \left| x_i(k) - x_j(k) \right| \tag{3}$$

Step 3. Compute the gray relation coefficient:

$$\gamma(x_i(k), x_j(k)) = \frac{\Delta_{min} + \varsigma \, \Delta_{max}}{\Delta_{ij}(k) + \varsigma \, \Delta_{max}} \quad \varsigma = 0.1 \; i = 1, 2, ..., m, \tag{4}$$

The value of ς is used to expand or compress the range of the gray relation coefficient; it is called the distinguishing coefficient and represents the significance of Δ_{max} [21, 22]. If the

difference between the analyzed data is large, the ς value should be determined to be close to 0 [23]. Therefore, the value of ς is taken as 0.1.

Step 4. Compute the gray relation grade to develop the matrix R $(R=(\Gamma_{ij}), \ i,j=1,2,...,m)$:

$$\Gamma_{ij} = \frac{1}{k}\sum_{k=1}^{k}\gamma(x_i(k),x_j(k)) \quad i=1,2,....,m, j \in i, \ k=1,2 \tag{5}$$

Step 5. Develop the matrix $G\left(g_{ij} = (\Gamma_{ij} + \Gamma_{ij})/2\right)$ (known as the gray similar matrix, this is the crucial output for gray relational clustering):

$$G = \left[g_{ij}\right], \quad i,j = 1,2,....,m \tag{6}$$

Step 6. Determine the two points (province) of the most near.

Step 7. Repeat steps 1–6 until all data are in one cluster [20].

4. RESULTS AND DISCUSSION

4.1. Hierarchical Gray Relational Clustering for 2006 and 2016 and Changes during the Ten-Year Period

In this study, the distances of the cluster centers to each other are calculated. Provinces are then divided into five classes to demonstrate the data's general structure and facilitate interpretation. As a result of the evaluations made based on the variables, clusters are named according to their characteristics from very poor to very high for both 2006 and 2016.

When the results of the HGRC analysis were evaluated for 2006 (Figure 2), Istanbul, which is Turkey's most populous city, emerged as the city with the best water management. Furthermore, it is notable that the provinces neighboring Istanbul were at poor and very poor levels. While the capital Ankara had medium-level management, the water management level of Izmir, which is another high-population province, was very poor. It was observed that Konya, Eskişehir, and Antalya followed a well-distributed water policy for 2006 in the Central Anatolia region. The provinces in the eastern and southeastern regions apart from Şanlıurfa and Diyarbakır showed a poor level, and only the province of Balıkesir performed well in the Aegean region.

Turning to 2016 (Figure 3), while Istanbul maintains a well-distributed water management system, it may be observed that Ankara, the capital city, remained at the same level. Contrary to its poor level in 2006, Izmir improved to a medium level in 2016, while its surrounding provinces dropped to a very poor level. It can be clearly seen from Figure 3 that there were severe problems in distributed water management system in the Mediterranean and Black Sea coastal regions. While Gaziantep continued to have a high standard of water management approach, the management approach of the other municipalities in the Southeastern Anatolia region in 2016 had deteriorated. It was determined that the distributed water management of Turkey had deteriorated in 2016 compared to 2006.

Figure 4 shows how the management of the distributed water changed over 10 years. This figure illustrates the general structure of the long-term change result of the HGRC spatial distribution maps depicted earlier in Figures 2 and 3. It demonstrates that Izmir, Bursa, Kocaeli, and Gaziantep Provinces displayed positive developments in distributed water management over the decade. The Aegean region, on the other hand, is the region where water management generally worsened. It was also determined that in the Central Anatolia region, Eskişehir and Konya managed to distribute water poorly. Figure 4 shows that in the Eastern Anatolian region, water distribution in Erzurum, Şanlıurfa, and Diyarbakır has deteriorated. On the other hand, the provinces colored white showed no change in distributed water management level between 2006 and 2016.

Figure 2 - Municipal water distribution model results for 2006 according to Hierarchical Gray Relational Clustering

Figure 3 - Municipal water distribution model results for 2016 according to Hierarchical Gray Relational Clustering
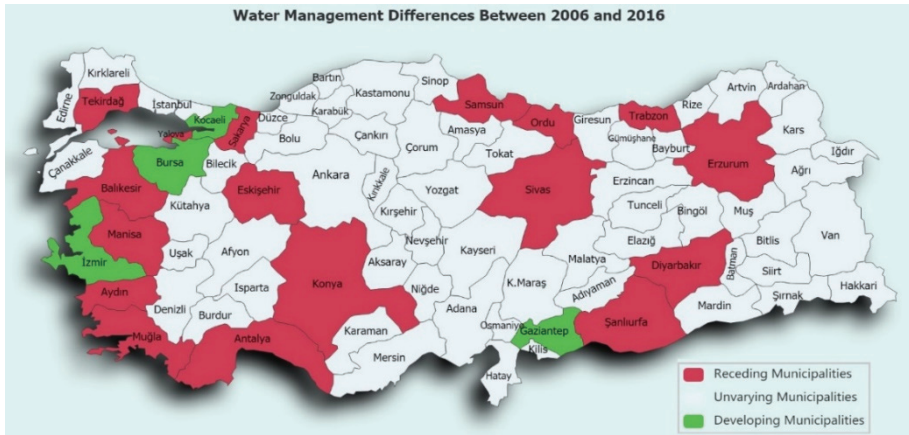
Figure 4 - Municipal water management results according to Hierarchical Gray Relational Clustering for a ten-year period

5. CONCLUSIONS

This study presented a comparative analysis of the relationships between such variables as water withdrawal, dams, lakes, wells, and treated water affecting the distributed water systems in Turkey over a decade (2006 and 2016). Population, water income, dams, streams, wells, and treated water can be considered as studied factors affecting water distribution, since their respective correlation coefficients are statistically significant.

According to the results of Hierarchical Gray Relational Clustering, we conclude that the municipalities of Izmir, Bursa, Gaziantep, and Kocaeli displayed an improved water management system over ten years. In contrast, the municipalities of Konya, Şanlıurfa, Diyarbakır, Samsun, Trabzon, and Sakarya experienced challenges in managing the water distribution. For example, the main reason for the shift in water management in Sakarya is the water withdrawal project for Istanbul. Istanbul, which is a megacity, is able to directly affect the environment in the distributed water management system and is part of the source of the distributed water from the surrounding municipalities. Large withdrawal water projects like the Melen River Project [24] can provide a valuable water source for Istanbul from the provinces of Düzce and Sakarya. The project is outlined for water withdrawal from the Melen River, which is located 180 kilometers east of Istanbul in Düzce Province in the Black Sea region [25]. For instance, in the province of Sakarya, water distribution management was in a poor condition in 2006, and this situation continued in 2016. It has been observed that the large amount of water withdrawal for the megacity of Istanbul affected Sakarya and the provinces surrounding Sakarya (this can be observed in Figures 2, 3, and 4). The amount of distributed water in the province of Düzce has doubled in 10 years (5,393,040 m^3 in 2006 and 11,293,906 in 2016 according to TUIK, Municipal Water Statistics [11]). When we consider the province of Düzce, whose current water management is poor, it can be expected that the withdrawal of large amounts of water will have a major effect on water management. One of the external factors affecting water distribution during this period was migration. Gaziantep, Şanlıurfa, Istanbul, and İzmir were some of the major cities witnessing immigration.

Migration was one of the factors in Şanlıurfa's deterioration in 2016, which had a good water management system in 2006. A reverse trend can be observed in Gaziantep [26]. Additionally, the province of Konya was one of the municipalities that witnessed the greatest groundwater withdrawal, which was responsible for the formation of a large number of sinkholes and the disappearance of groundwater resources [27]. For the surrounding provinces and the Central Anatolian region, this problem raises the problem of water scarcity, and this problem will worsen in the future if the distributed water is not managed well.

Most importantly, this study revealed that the distributed water management system was in a poor condition and that the number of provinces showing deterioration have been increasing.

From the study results, we note that the efficient management of the municipal water distribution is highly dependent on the environmental policy of the distributed water management, and this dependence reveals the necessity for an integrated water management system. Provinces sharing the same water basin and its source should thus follow a common distributed water policy. The results of this study will have a significant impact on research and analysis of distributed water system management in Turkey, which is an important contribution, due to the use of the Gray Relational Hierarchical clustering method.

Conflicts of Interest

The authors declare no conflicts of interest.

Reference

[1]   Mayer, P. W., DeOreo, W. B., Opitz, E. M., Kiefer, J. C., Davis, W. Y. Dziegielewski, B., & Nelson, J. O., *Residential end uses of water,* 1999.

[2]   Corbella, H. M., & i Pujol, D. S. What lies behind domestic water use?: a review essay on the drivers of domestic water consumption. *BAGE: Boletín de la Asociación de Geógrafos Españoles,* (50), 297-314, 2009.

[3]   Childers, D. L., Pickett, S. T., Grove, J. M., Ogden, L., & Whitmer, A. Advancing urban sustainability theory and action: Challenges and opportunities. *Landscape and urban planning, 125, 320-328, 2014.*

[4]   Firat, M., Yurdusev, M. A., & Turan, M. E. Evaluation of artificial neural network techniques for municipal water consumption modeling. Water resources management, 23(4), 617-632, 2009.

[5]   Ip, W. C., Hu, B. Q., Wong, H., & Xia, J. Applications of grey relational method to river environment quality evaluation in China. *Journal of Hydrology,* 379(3-4), 284-290, 2009.

[6]   Moore, R.E., Methods and applications of interval analysis. *SIAM*, 1979.

[7]   Huang, Y. P., & Huang, C. C. The integration and application of fuzzy and grey modeling methods. *Fuzzy sets and Systems,* 78(1), 107-119, 1996.

[8]   Julong, D. Introduction to grey system theory. *The Journal of grey system,* 1(1), 1-24, 1989.

[9]   Deng, J. L. Grey Prediction and Decision*, Huazhong University of Science and Technology*, 1986.

[10] Deng, J., Introduction to grey system theory. *The Journal of Grey System vol,* 1989.

[11] TUIK. Turkish Statistical Institue. Available from: http://www.turkstat.gov.tr/, 2020.

[12] Piccolroaz, S., Calamita, E., Majone, B., Gallice, A., Siviglia, A., & Toffolon, M. Prediction of river water temperature: a comparison between a new family of hybrid models and statistical approaches. *Hydrological Processes,* 30(21), 3901-3917, 2016.

[13] Zhu, S., Heddam, S., Nyarko, E. K., Hadzima-Nyarko, M., Piccolroaz, S., & Wu, S. Modeling daily water temperature for rivers: comparison between adaptive neuro-fuzzy inference systems and artificial neural networks models. *Environmental Science and Pollution Research*, 26(1), 402-420, 2019.

[14] Villarín, M. C. Methodology based on fine spatial scale and preliminary clustering to improve multivariate linear regression analysis of domestic water consumption. *Applied Geography,* 103, 22-39, 2019.

[15] House-Peters, L., Pratt, B., & Chang, H. Effects of urban spatial structure, sociodemographics, and climate on residential water consumption in hillsboro, oregon 1. *JAWRA Journal of the American Water Resources Association,* 46(3), 461-472, 2010.

[16] Griffin, R. C., & Mjelde, J. W. Distributing water's bounty. *Ecological Economics*, 72, 116-128, 2011.

[17] Ju-Long, D. Control problems of grey systems. *Systems & control letters,* 1(5), 288-294, 1982.

[18] Tsai, M. T., Hsiao, S. W., & Liang, W. K. Using grey theory to develop a model for forecasting the demand for telecommunications. *Journal of Information and Optimization Sciences,* 26(3), 535-547, 2005.

[19] Deng, J. Wuhan, China, *Basic method of grey system.* 1987.

[20] Wu, W. H., Lin, C. T., Peng, K. H., & Huang, C. C. Applying hierarchical grey relation clustering analysis to geographical information systems–A case study of the hospitals in Taipei City. *Expert Systems with Applications,* 39(8), 7247-7254, 2012.

[21] Hinduja, A., & Pandey, M. (2017). Multicriteria recommender system for life insurance plans based on utility theory. Indian Journal of Science and Technology, 10(14), 1-8.

[22] Yildirim, B. F., Hepsen, A., & Onder, E. (2015). Grey Relational Analysis Based Ranking of Latin American and Caribbean Economies. Journal of Economics Finance and Accounting, 2(3).

[23] Yıldırım, B. F. (2015). Gri ilişkisel analiz. Çok Kriterli Karar Verme Yöntemleri, 229-236.

[24] Islar, M., & Boda, C. Political ecology of inter-basin water transfers in Turkish water governance. *Ecology and Society,* 19(4), 2014.

[25] DSI, *The General Directorate of State Hydraulic Works*, Ankara, Turkey, 2020.

[26] Doganay, M., & Demiraslan, H. (2016). Refugees of the Syrian civil war: impact on reemerging infections, health services, and biosecurity in Turkey. Health security, 14(4), 220-225.

[27] Günay, G., Çörekçioğlu, İ., & Övül, G. Geologic and hydrogeologic factors affecting sinkhole (obruk) development in Central Turkey. *Carbonates and evaporites*, 26(1), 3-9, 2011.

TEKNİK DERGİ MANUSCRIPT DRAFTING RULES

1. The whole manuscript (text, charts, equations, drawings etc.) should be arranged in Word and submitted in ready to print format. The article should be typed on A4 (210 x 297 mm) size paper using 10 pt (main title 15 pt) Times New Roman font, single spacing. Margins should be 40 mm on the left and right sides and 52.5 mm at the top and bottom of the page.

2. Including drawings and tables, articles should not exceed 25 pages, technical notes 10 pages.

3. Your contributed manuscript must be sent over the DergiPark system. (http://dergipark.gov.tr/tekderg)

4. The text must be written in a clear and understandable language, conform to the grammar rules. Third singular person and passive tense must be used, and no inverted sentences should be contained.

5. Title must be short (10 words maximum) and clear, and reflect the content of the paper.

6. Sections should be arranged as: (i) abstract and keywords, (ii) title, abstract and keywords in the other language, (iii) main text, (iv) symbols, (v) acknowledgements (if required) and (vi) references.

7. Both abstracts should briefly describe the object, scope, method and conclusions of the work and should not exceed 100 words. If necessary, abstracts may be re-written without consulting the author. At least three keywords must be given. Titles, abstracts and keywords must be fitted in the first page leaving ten line space at the bottom of the first page and the main text must start in the second page.

8. Section and sub-section titles must be numbered complying with the standard TS1212.

9. Symbols must conform to the international rules; each symbol must be defined where it appears first, additionally, a list of symbols must be given in alphabetic order (first Latin, then Greek alphabets) at the end of the text (before References).

10. Equations must be numbered and these numbers must be shown in brackets at the end of the line.

11. Tables, drawings and photographs must be placed inside the text, each one should have a number and title and titles should be written above the tables and below the drawings and photographs.

12. Only SI units must be used in the manuscripts.

13. Quotes must be given in inverted commas and the source must be indicated with a reference number.

14. Acknowledgement must be short and mention the people/ institutions contributed or assisted the study.

15. References must be numbered (in brackets) in the text referring to the reference list arranged in the order of appearance in the text. References must include the following information:

    If the reference is an article: Author's surname, his/her initials, other authors, full title of the article, name of the journal, volume, issue, starting and ending pages, year of publication.

    > Example : Naghdi, P. M., Kalnins, A., On Vibrations of Elastic Spherical Shells. J. Appl. Mech., 29, 65-72, 1962.

    If the reference is a book: Author's surname, his/her initials, other authors, title of the book, volume number, editor if available, place of publication, year of publication.

    > Example : Kraus. H., Thin Elastic Shells, New York. Wiley, 1967.

    If the reference is a conference paper: Author's surname, his/her initials, other authors, title of the paper, title of the conference, location and year.

    If the source is a thesis: Author's surname, his/her initials, thesis title, level, university, year.

    If the source is a report: Author's surname, his/her initials, other authors, title of the report, type, number, institution it is submitted to, publication place, year.

16. Discussions to an article published in Teknik Dergi should not exceed two pages, must briefly express the addressed points, must criticize the content, not the author and must be written in a polite language. Authors' closing remarks must also follow the above rules.

17. A separate note should accompany the manuscript. The note should include, (i) authors' names, business and home addresses and phone numbers, (ii) brief resumes of the authors and (iii) a statement "I declare in honesty that this article is the product of a genuinely original study and that a similar version of the article has not been previously published anywhere else" signed by all authors.

18. Copyright has to be transferred to UCTEA Turkish Chamber of Civil Engineers. The standard copyright form signed by the authorised author should therefore be submitted together with the manuscript.

CONTENTS